UNIVERSIDAD NACIONAL AUTÓNOMA DE MÉXICO

UNAM POSGRADO

FACULTAD DE QUÍMICA

PROGRAMA DE MAESTRÍA Y DOCTORADO EN CIENCIAS BIOQUÍMICAS

Control de la síntesis de tripanotión de *Trypanosoma cruzi*. Modelado cinético de la vía metabólica.

T E S I S

QUE PARA OBTENER EL GRADO DE:

DOCTOR EN CIENCIAS (BIOQUÍMICAS)

P R E S E N T A:

Q.A. MARÍA VIRIDIANA OLIN SANDOVAL

Tutora: DRA. EMMA C. SAAVEDRA LIRA

MÉXICO, D. F. 2012

MÉXICO D.F. 2012

CONTROL DE LA SÍNTESIS DE TRIPANOTIÓN DE *Trypanosoma cruzi*.
MODELADO CINÉTICO DE LA VÍA METABÓLICA

RECONOCIMIENTOS

Esta tesis doctoral se realizó bajo la dirección de la Dra. Emma Cecilia Saavedra Lira en el Departamento de Bioquímica del Instituto Nacional de Cardiología “Ignacio Chávez”. México D.F. México

El Comité Tutoral que asesoró el desarrollo de esta tesis estuvo formado por:

Dra. Emma C. Saavedra Lira	Departamento de Bioquímica, INCICh
Dr. Wilhelm Hansberg Torres	Instituto de Fisiología Celular, UNAM
Dr. Juan Pablo Pardo Vázquez	Facultad de Medicina, UNAM

Se reconoce la colaboración de la Dra. Bertha Espinoza Gutiérrez, del Departamento de Inmunología del Instituto de Investigaciones Biomédicas, UNAM y a la Dra. Ingeborg Becker del Departamento de Inmunoparasitología de la Facultad de Medicina, UNAM, en cuyos laboratorios se cultivaron los parásitos que se utilizaron durante el proyecto.

Se reconoce la asesoría técnica del M. en C. Ignacio Martínez y la Dra. Miriam Berzunza en los cultivos de epimastigotes utilizados en este proyecto.

Se reconoce la asesoría del Dr. Rafael Moreno Sánchez

El proyecto de investigación fue apoyado parcialmente por el donativo de Ciencia Básica CONACyT 83084.

Agradezco al CONACyT por otorgarme una beca (no. 176966) para la realización de mis estudios de doctorado.

La defensa de esta tesis de doctorado se realizó el día…….

El Jurado de Examen Doctoral estuvo constituido por:

Presidente	Dr. Armando Gómez Puyou Instituto de Fisiología Celular, UNAM
Vocal	Dr. Roberto Hernández Fernández Instituto de Investigaciones Biomédicas, UNAM
Vocal	Dra. María Guadalupe Ortega Pierres CINVESTAV, Unidad Zacatenco
Vocal	Dra. Rebeca Manning Cela CINVESTAV, Unidad Zacatenco
Secretario	Dra. Paz María Salazar Schettino Facultad de Medicina, UNAM

INDICE

INDICE DE TABLAS Y FIGURAS

RESUMEN

El tripanotión [$T(SH)_2$] es un análogo del glutatión (GSH) presente principalmente en tripanosomátidos. El $T(SH)_2$ junto con la tripanotión reductasa (TryR) y las enzimas desintoxicantes de peróxidos que dependen de este metabolito reemplazan las funciones que lleva a cabo el sistema GSH/glutatión reductasa/GSH peroxidasas en células humanas. Debido a esto, se han propuesto a las enzimas del metabolismo del $T(SH)_2$ como sitios de intervención terapéutica. En *Trypanosoma cruzi* no se han validado blancos terapéuticos por ninguna estrategia; sin embargo, diversos estudios en *Trypanosoma brucei* y *Leishmania* en los cuales se disminuyó el 50-90% la actividad de las enzimas de esta vía por métodos genéticos demostraron que todas las enzimas son esenciales para la sobrevivencia y manejo del estrés oxidante de los parásitos por lo que se concluyó que todas las enzimas de la vía son blancos terapéuticos validados. Desde el punto de vista metabólico, que todas las enzimas hayan resultado esenciales por este método de validación genética no son resultados inesperados, ya que la inhibición en altos grados de cualquier enzima de cualquier vía metabólica tendrá el mismo efecto de disminuir el funcionamiento de la vía y por lo tanto afectará la función celular del parásito. Es por ello que consideramos que se tienen que aplicar criterios adicionales a los de esencialidad validada genéticamente para poder identificar a las enzimas con un mayor potencial terapéutico, es decir, se tienen que identificar a las enzimas cuya inhibición farmacológica sea moderada pero que tenga un efecto negativo importante sobre la función de la vía metabólica. Esta estrategia de inhibir a las enzimas que controlan de manera principal a la vía metabólica puede ayudar a disminuir las dosis de los fármacos a utilizar, disminuyendo los efectos colaterales adversos por el uso de altas concentraciones de inhibidores que tienen como blancos enzimas que tienen poco control sobre la vía.

Tomando en consideración los fundamentos básicos de la regulación del metabolismo celular, en esta tesis se propone que las enzimas con mayor potencial terapéutico deben ser aquella(s) que además de ser esenciales controlan de manera prioritaria el flujo o la concentración de intermediarios de la vía. En este contexto, el

análisis del control metabólico (MCA) ha demostrado que el control de una vía metabólica está distribuido en diferentes grados entre todas las enzimas que la componen y por lo tanto descarta la existencia de un único paso limitante ("rate-limiting step") como se describe en los libros de texto de bioquímico. Mediante estrategias experimentales definidas a través del MCA se puede cuantificar el grado de control que cada enzima tiene sobre la vía metabólica. Por lo tanto, el objetivo de esta tesis fue determinar el grado de control que tiene cada una de las enzimas sobre la síntesis y la concentración de $T(SH)_2$ en el parásito *T.cruzi*, mediante la construcción de un modelo cinético de la vía metabólica. Para construir el modelo se requirió determinar los siguiente parámetros experimentales: i) producción de las enzimas recombinantes γ-glutamilcisteína sintetasa (γECS), glutatión sintetasa (GS), tripanotión sintetasa (TryS) y TryR y su caracterización cinética en condiciones cercanas a las fisiológicas; ii) las actividades enzimáticas, concentración de intermediarios y flujos de la vía metabólica en los parásitos en condiciones basales y de estrés oxidante. Los datos cinéticos se utilizaron para construir el modelo empleando para ello el programa de modelado metabólico COPASI (Complex Pathway Simulator) y los datos de concentraciones de intermediarios y flujos metabólicos en los parásitos se utilizaron para validar el modelo comparando sus predicciones con el comportamiento de la vía *in vivo*. Después de un proceso iterativo de experimentación-modelado-experimentación, el modelo refinado al que se llegó pudo predecir de manera cercana el comportamiento de la vía observada *in vivo*. Las predicciones del modelo indican que la γECS, la TryS y el transporte de espermidina (SpdT) ejercen el principal control sobre el flujo de síntesis de $T(SH)_2$. Por otro lado, la concentración de $T(SH)_2$ está controlada esencialmente por la demanda de este metabolito (estrés oxidante) y por la TryR; sin embargo, la γECS y la TryS también participan en el control de la concentración de $T(SH)_2$ cuando éstas se inhiben más del 70%. El modelo también permitió predecir el comportamiento de la vía al disminuir las actividades de cada una de las enzimas (individual o en grupos) de una manera análoga a la disminución de la expresión proteica por métodos genéticos. Así por ejemplo, para inhibir en un 50% el flujo de la vía sería necesario inhibir a la γECS y a la TryS en un 58% y 63% respectivamente o simultáneamente

en un 50% lo cual sugiere el uso de una terapia multisitio. La conclusión de esta tesis es que de las 11 reacciones que componen la vía metabólica, la γECS, la TryS y el SpdT pueden ser las enzimas con mayor potencial terapéutico debido a que además de que son esenciales, son las que controlan la homeostasis del sistema antioxidante del parásito al determinar los flujos de síntesis y la concentración del $T(SH)_2$.

ABSTRACT

Trypanothione [$T(SH)_2$] is a glutathione (GSH) analogue present in trypanosomatids. $T(SH)_2$ together with trypanothione reductase (TryR) and the peroxide detoxifying enzymes that depend on this metabolite, replaces all the functions that the GSH/glutathione reductase/glutathione peroxidases system carry out in human cells. Thus, the participating enzymes of the $T(SH)_2$ metabolism have been proposed as targets for therapeutic intervention. Despite no drug target validation studies have been reported for *Trypanosoma cruzi*, in *Trypanosoma brucei* and *Leishmania,* in which the enzymes of this pathway were inhibited by genetic strategies in a 50-90% have demonstrated that they are essential for survival and for oxidative stress management and therefore, they have been proposed as validated drug targets. From a metabolic regulation point of view, the fact that all the enzymes that were genetically validated resulted in essential steps of the pathway are not unexpected results. This is because inhibiting any enzyme of a pathway in those high degrees, will affect in the same way in all cases, and the cellular function of the parasite will be compromised. Thus, we consider that additional criteria to the genetic validation has to be applied for identifying the enzymes with the highest therapeutic potential i.e. it is necessary to identify those enzymes in which a moderate pharmacological inhibition has an important negative effect on the pathway functions. The strategy of inhibiting the enzymes that mainly control a metabolic pathway can help in decreasing the drug doses that have to be used, reducing the adverse side effects produced by using high concentrations of inhibitors that target enzymes with low control in the pathway.

Considering the basics of the regulation of cellular metabolism, this thesis proposes that the enzymes with the highest therapeutic potential are those that besides being essential, they mainly control the pathway flux or their intermediary concentrations. In this regard, Metabolic Control Analysis (MCA) has demonstrated that the control of a pathway is distributed to different degrees amongst all the participating enzymes and rules out the presence of a single “rate- limiting step” as it has been described in the biochemistry text books. Through its experimental

approaches, the MCA allows to quantitatively determine the degree of control that each enzyme has on the metabolic pathway. Thus, the aim of this thesis was to determine the degree of control that each enzyme exerts on the synthesis and concentration of $T(SH)_2$ in the parasite *Trypanosoma cruzi* by constructing a kinetic model of the pathway. For this purpose, it was required to determine the following experimental parameters: i) production of the recombinant enzymes γ-glutamylcysteine synthetase (γECS), glutathione synthetase (GS), trypanothione synthetase (TryS) and trypanothione reductase (TryR) and carry out their kinetic characterization under near physiological conditions and; ii) the enzyme activities, intermediary concentrations and fluxes of the metabolic pathway in the parasites subjected to basal and oxidative stress conditions. These kinetic data were used to construct the model using the metabolic simulator COPASI (Complex Pathway Simulator) and the *in vivo* data were used to validate the predictions of the model. After an iterative experimental- modeling- experimental process, the refined model can closely predict the pathway behavior in the parasite. The main predictions of the model indicated that γECS, TryS and the spermidine transporter (SpdT) exerted primary control on the $T(SH)_2$ synthesis flux . The $T(SH)_2$ concentration was controlled by the reactions that consume it (oxidative stress) and by TryR. However, γECS and TryS also exerted control on the $T(SH)_2$ concentration when they were inhibited more than 70%. The model also allowed the prediction of the pathway behavior by decreasing the enzyme activity (alone or by groups) in a similar way to the diminution of the protein expression by genetic methods. For example, in order to decrease by 50% the $T(SH)_2$ synthesis flux it was necessary to inhibit γECS and TryS at 58% and 63% of their original levels, respectively or simultaneously by 50%, highlighting the importance of a therapeutic multi-target strategy. The conclusion of this thesis was that from the 11 reactions composing the pathway, γECS, TryS and SpdT might be the enzymes with the highest therapeutic potential due to the fact that, besides being essential, they control the homeostasis of the antioxidant system by determing the $T(SH)_2$ synthesis flux and concentration.

ABREVIATURAS

AdoMet	S-adenosil metionina
AdoMetDC	S-adenosil metionina descarboxilasa
Apx	ascorbato peroxidasa
Asc	ascorbato
BNZ	benznidazol
BSO	butionina sulfoximina
Cad	cadaverina
COPASI	Complex Pathway Simulator
Cys	cisteína
DHA	dehidroascorbato
γEC	γ-glutamilcisteína
γECS	γ-glutamilcisteína sintetasa
Glu	glutamato
Gly	glicina
GSH	glutatión
GSSG	disulfuro de glutatión
GS	glutatión sintetasa
HK	hexocinasa
H_2O_2	peróxido de hidrógeno
LDH	lactato deshidrogenasa
MCA	Análisis de Control Metabólico (Metabolic Control Analysis)
NFX	nifurtimox
nsGPx	glutatión peroxidasa no dependiente de selenio
$O_2^{\cdot -}$	superóxido
ODC	ornitina descarboxilasa
PK	piruvato cinasa

Put	putrescina
RNAi	RNA de interferencia
R-NHOH	intermediario hidroxilamina
R-NO	intermediario nitroso
$R\text{-}NO_2^{\cdot -}$	radical nitro
SB	Biología de Sistemas (Systems Biology)
SOD	superóxido dismutasa
Spd	espermidina
SpdT	transportador de Spd
$T(SH)_2$	tripanotión reducido
TS_2	disulfuro de tripanotión
TryS	tripanotión sintetasa
TryR	tripanotión reductasa
TXN	triparredoxina
TXN-Px	2-Cys peroxirredoxina

1. INTRODUCCIÓN

1.1 *Trypanosoma cruzi*

Trypanosoma cruzi es el agente causal de la enfermedad de Chagas o tripanosomiasis americana. Este organismo es un protista unicelular perteneciente al phylum *Euglenozoa*, orden *Kinetoplastida*, familia *Trypanosomatidae* (Flisser y Pérez-Tamayo, 2006). En este grupo también se encuentran los tripanosomátidos de importancia médica *Trypanosoma brucei* que causa la enfermedad del sueño o tripanosomiasis africana y especies de *Leishmania* las cuales causan diferentes formas de leishmaniasis.

Los organismos pertenecientes al orden Kinetoplastida se caracterizan por tener una sola mitocondria que ocupa la mayor parte del volumen celular. En la matriz mitocondrial, cerca de la parte adyacente del flagelo, se encuentra el DNA mitocondrial el cual forma una estructura llamada cinetoplasto (k-DNA). Éste está formado por 20-30 mil mini círculos de DNA (con un tamaño de 0.45 µm cada uno) los cuales están estrechamente unidos por varias docenas de maxi círculos con un diámetro de 10 µm que son análogos del DNA mitocondrial de eucariontes superiores (De Souza, 2002; De Souza, 2009).El k-DNA codifica para proteínas tales como la topoisomerasa tipo II, DNA polimerasa β, la proteína de unión al origen del minicírculo, proteínas de condensación y unión al k-DNA así como las proteínas de resistencia a estrés por calor (HSP) mitocondriales. En el caso de epimastigotes de *T. cruzi*, el k-DNA representa el 20- 25% del DNA total de la célula (De Souza, 2002).

Trypanosoma cruzi tiene tres estadios de desarrollo (Fig. 1) distribuidos en hospederos invertebrados (Orden *Hemíptera;* Familia *Reduviidae;* Subfamilia *Triatominae*) y vertebrados (humanos, armadillos, perros, roedores). Algunos de los estadios son replicativos y pueden identificarse dependiendo de la ubicación del cinetoplasto con respecto al núcleo (De Souza, 2002) y por diferentes aspectos morfológicos (Salazar, 2011). Los estadios de desarrollo son:

a. Epimastigotes: esta forma es replicativa y se encuentra presente en los hospederos insectos de los géneros *Triatoma, Paratriatoma, Rhodnius,*

Dipetalogaster, Eratyrus y *Panstrongylus*. Este estadio tiene una estructura en forma de huso con un tamaño de 16-18 µm de largo. El cinetoplasto se encuentra ubicado sobre el núcleo o en la parte anterior a éste (Fig. 1A). En los medios de cultivo son móviles y forman estructuras tipos rosetas.

b. Tripomastigotes: este estadio es infectivo pero no es proliferativo y se presenta en tejidos y en la sangre del hospedero vertebrado (tripomastigote sanguíneo) y en la parte posterior del intestino, heces y orina del hospedero invertebrado (tripomastigote metacíclico). Esta forma tiene un tamaño de 18-21 µm de largo y 1-4 µm de ancho, es alargado, con forma de "S" o "C", el flagelo se extiende por toda la célula además que el cinetoplasto se encuentra en la parte posterior al núcleo (Fig. 1B). En medios de cultivo son móviles debido a su flagelo.

c. Amastigotes: este estadio es la forma replicativa e intracelular en el hospedero vertebrado. Tienen una estructura esférica de 2-4 µm de diámetro y son organismos aflagelados aunque ya se ha reportado la presencia de un pequeño flagelo (Fig 1C).

A. Epimastigote **B. Tripomastigote** **C. Amastigote**

Fig 1. Estadios de desarrollo de *Trypanosoma cruzi*. La identificación de los estadios de desarrollo se basa en la morfología del parásito así como en la ubicación del cinetoplasto con respecto al núcleo. La figura muestra parásitos teñidos con giemsa (tinción de núcleos y cinetoplasto). Modificado de De Souza, 2002

1.2 Ciclo de vida de Trypanosoma cruzi

El ciclo de vida de ese parásito (Fig. 2) inicia cuando el insecto vector se alimenta de la sangre del hospedero vertebrado infectado con tripomastigotes sanguíneos (fase infectiva). Al llegar al estómago del insecto se transforman en epimastigotes, y en el intestino se duplican por fisión binaria y se pueden adherir a las células intestinales. Los epimastigotes que llegan al recto del insecto se transforman en tripomastigotes metacíclicos los cuales se depositan junto con las heces durante una segunda alimentación de sangre. Los tripomastigotes metacíclicos ingresan al hospedero a través de mucosas o de una herida en la piel. Una vez en el hospedero vertebrado, los tripomastigotes interactúan con células del sistema fagocítico mononuclear transformándose en amastigotes los cuales se dividen por fisión binaria y se transforman en tripomastigotes sanguíneos que son liberados al torrente sanguíneo. Los tripomastigotes sanguíneos invaden células del tejido liso, estriado y fibroblastos repitiendo el ciclo tripomastigote-amastigote (De Souza, 2002; Salazar-Schettino y Marín y López, 2006).

Las interacciones hospedero-parasito se llevan a cabo mediante proteínas expuestas en la superficie celular del parásito y el hospedero como las trans-sialidasas; las glicoproteínas de membrana tales como gp30, gp63, gp82, gp90; proteasas como la cruzipaína, así como con azúcares tales como la galactosa, manosa y N-acetilglucosamina (De Souza, 2002; Epting *et al*, 2010). Posteriormente, existen dos mecanismos a través de los cuales los tripomastigotes se internalizan en las células del hospedero vertebrado. Una es mediada por vías de señalización activadas por calcio, en donde se promueve el reclutamiento de lisosomas del hospedero en el sitio de entrada del tripomastigote fusionándose gradualmente con la membrana plasmática y formando un compartimento vacuolar (vacuola parasitófora); el otro mecanismo es mediante la invaginación de la membrana plasmática que genera una vacuola la cual posteriormente se fusiona con lisosomas. La liberación de los parásitos hacia el citoplasma depende de los lisosomas y del pH, de tal manera que al acidificarse esta vacuola, los parásitos secretan moléculas conocidas como Tc-Tox y LYT1, las cuales promueven la lisis de la membrana

facilitando la salida del parásito de la vacuola. Una vez que se encuentran en el citoplasma, el tripomastigote se transforma en amastigote y prolifera hasta alcanzar una alta densidad y se transforma en tripomastigote sanguíneo. Estas formas del parásito al encontrarse en gran número en la célula hospedera promueven su rompimiento por mecanismos no bien descritos liberando los tripomastigotes a la sangre. Puede existir un ciclo intracelular alternativo en donde los amastigotes, los cuales también son infectivos, son liberados e invaden otras células de la misma manera (Andrade y Andrews, 2005; Epting *et al*, 2010). Al estar en el torrente sanguíneo del hospedero vertebrado, los parásitos pueden ser ingeridos por otro insecto, cerrándose así el ciclo de vida de este organismo (De Souza, 2002).

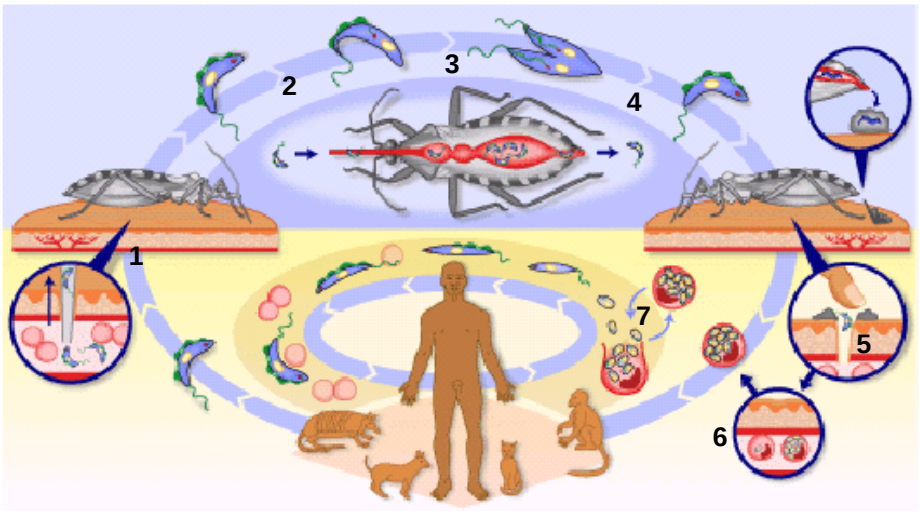

Fig. 2. Ciclo de vida de *Trypanosoma cruzi*.1. El triatómino ingiere tripomastigotes sanguíneos. **2.** En el estómago, los tripomastigotes se transforman en epimastigotes. **3.** En el intestino los epimastigotes se duplican.**4.** Los epimastigotes que llegan al recto del triatómino se transforman en tripomastigotes metacíclicos los cuales salen junto con las heces del insecto. **5.** Los tripomastigotes metacíclicos entran al hospedero mamífero por mucosas y heridas en la piel. **6.** En el mamífero, los tripomastigotes se introducen en las células transformándose en amastigotes los cuales se multiplican por fisión binaria y se transforman en tripomastigotes sanguíneos. **7.** Estos últimos son liberados al torrente sanguíneo en donde podrán diseminarse e infectar otras células, o bien, ser ingeridos por otro insecto vector. Modificado de www.who.int/tdrold/diseases/chagas/lifecycle.htm

1.3 Enfermedad de Chagas

La enfermedad de Chagas afecta a millones de personas principalmente en Latinoamérica. En 2006 se reportó que existían 12 500 muertes anuales causadas por esta enfermedad, 15 millones de casos de individuos infectados y 28 millones de personas en riesgo de contraer la enfermedad en regiones distribuidas en 21 países (WHO, 2007). A pesar de que esta enfermedad es endémica de Latinoamérica, en los últimos años se han reportado casos en zonas no endémicas como son Estados Unidos, Europa y África, como consecuencia de los patrones migratorios de la población humana, al trasplante de órganos, donación de sangre así como al transporte de los vectores triatóminos en el equipaje (Clayton, 2010).

En el caso de México, las dos terceras partes del territorio son consideradas áreas endémicas. Se han reportado casos de infección en toda la República Mexicana, encontrándose una seroprevalencia de 1.6%. Los estados con la mayor prevalencia son Hidalgo, San Luis Potosí, Veracruz y Tamaulipas (Guzmán-Bracho, 2001).

Los principales mecanismos de transmisión de esta enfermedad son:

a) Transmisión por vector. Esta es la forma más importante de transmisión. Como ya se mencionó anteriormente, el vector de esta enfermedad son los insectos de la subfamilia *Triatominae*, la cual es conocida como chinche besucona o vinchuca, aunque el nombre depende en gran parte de la región en la que se encuentren estos insectos. En México, las principales especies que resaltan por su capacidad de transmisión vectorial de la enfermedad son *Triatoma barberi*, *T. dimidiata*, *T. pallidipennis*, *Rhodnius prolixus* entre otras (Salazar-Schettino y Marín y López, 2006).

b) Transfusión sanguínea. La WHO estima que el riesgo de transmisión por esta vía está entre 12-20% (WHO, 2007) debido a la falta de monitoreo exhaustivo de la sangre de donadores provenientes de regiones endémicas.

c) Vía congénita. El riesgo relacionado a esta vía de transmisión es de alrededor del 5% y se ha determinado que está limitada a las zonas rurales o en ciudades a donde migran las mujeres infectadas (WHO, 2007).

La enfermedad de Chagas presenta dos fases (http://www.who.int/neglected_diseases/diseases/chagas/en/index.html; Rodrigues, Borges-Pereira, 2010):

Fase aguda. Se caracteriza por presentar una parasitemia alta poco tiempo después de la infección, la cual tiene una duración de aproximadamente 2 meses. El 70% de las personas infectadas son asintomáticas y menos del 5% presentan síntomas tales como fiebre, edemas en el ojo (signo de Romaña- Mazza) y nódulos subcutáneos (Chagoma de inoculación) los cuales indican el área de entrada del parásito. En casos más severos, se presentan síntomas como adenopatía, edema, hepatoesplenomegalia, miocarditis y meningoencefalitis.

Fase crónica. En esta etapa se presentan las siguientes formas clínicas:

a) Indeterminada. Es asintomática y generalmente se presenta al inicio de la fase crónica. Se ha observado que el 40-90% de los pacientes permanecen asintomáticos toda su vida. En esta etapa los electrocardiogramas así como las radiografías en corazón, esófago y colon son normales. Sin embargo los pacientes son seropositivos al parásito.

b) Cardiaca. Se presenta hasta en el 30% de los pacientes. Aparece en la segunda a cuarta década de vida, después de 5-15 años de que el paciente fue infectado. Las cardiopatías se caracterizan por arritmias, falla cardiaca, tromboembolias, cardiomegalia.

c) Lesiones digestivas. Se presenta en el 10% de los pacientes. Esta se caracteriza por los mega síndromes caracterizados por mega esófago y megacolon.

También pueden presentarse formas clínicas mixtas (cardiacas más digestivas).

1.4 Tratamiento de la enfermedad de Chagas

Los fármacos utilizados para el tratamiento de la enfermedad de Chagas son el nifurtimox [dióxido de 5- nitrofurano 3-metil-4-(5'-nitrofurfurildeneamina) tetrahidro-4H-1,4-tiazina-1,1] (NFX) y el benznidazol [2 nitro-imidazol (N-bencil-2-nitroimidazol acetamida] (BNZ) conocidos comercialmente como Lampit y Rochagan, respectivamente (WHO, 2007) (Fig. 3A).

A pesar de que el mecanismo de acción de estos fármacos es diferente (Fig. 3B), ambos compuestos se activan al reducirse sus grupos nitro por la acción de nitroreductasas del parásito y pasando por la formación de metabolitos electrofílicos. En el caso del BNZ, los intermediarios reducidos generados por la nitroreductasa tipo I son del tipo nitroso (R-NO) e hidroxilamina (R-NHOH) los cuales forman el ion nitrenio, que es precursor del compuesto más estable, 4,5-dihidro-4,5-dihidroxi imidazol, el cual se va disociando lentamente liberando glioxal (Hall y Wilkinson, 2012). Estos metabolitos se pueden unir a proteínas, ácidos nucleicos, lípidos y tioles solubles tales como GSH y $T(SH)_2$ (revisado por Maya *et al*, 2007; Hall y Wilkinson, 2012). Por otro lado, diversos estudios han demostrado que la reducción del NFX lleva a la formación del anión radical nitro ($R\text{-}NO_2^{\bullet -}$) el cual puede formar metabolitos electrofílicos o bien, puede reaccionar con el O_2 regenerando la molécula de NFX y formando el anión superóxido ($O_2^{\bullet -}$). Este último puede formar peróxido de hidrógeno (H_2O_2) por la acción de la superóxido dismutasa (SOD) generando más especies reactivas de oxígeno (EROs) por medio de la reacción de Haber-Weiss (Maya *et al*, 2007).Sin embargo, en contraste con lo anterior, recientemente se ha determinado que el NFX se activa también por la nitroreductasa tipo I, la cual no genera el radical $R\text{-}NO_2^{\bullet -}$ y por lo tanto EROS. De esta manera, el mecanismo tripanocida que se ha propuesto para el NFX es que su reducción genera un nitrilo de cadena abierta (el cual se ha detectado por HPLC) que junto con sus precursores (metabolitos nitrosos) generan los efectos observados por este fármaco (Hall *et al*, 2011). Sin embargo este último mecanismo aún no está bien caracterizado.

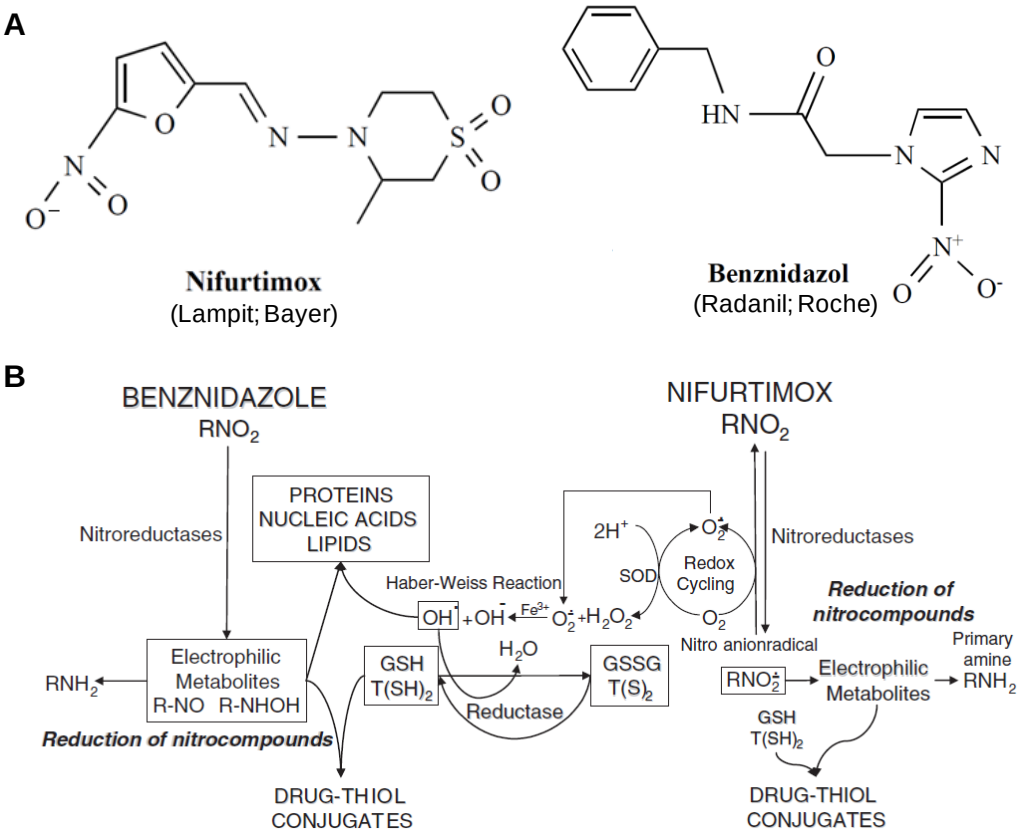

Fig. 3 Nifurtimox y Benznidazol

A. Estructuras de los fármacos y sus nombres comerciales. B. Mecanismo de acción: los fármacos son activados por nitroreductasas y su mecanismo de acción común es generar estrés oxidante debido a la unión a moléculas antioxidantes como GSH y $T(SH)_2$. Además el BNZ se une a macromoléculas mientras que el NFX genera especies reactivas de oxígeno (EROS). Tomado de Maya *et al*, 2007.

Sin embargo, el uso de estos compuestos para el tratamiento actual de la enfermedad de Chagas tiene varias desventajas. Una de ellas es que los efectos secundarios del NFX y BNZ son muy severos ya que son hepatotóxicos y nefrotóxicos http://www.who.int/neglected_diseases/diseases/chagas/en/index.html). Además, en el caso del primero genera anorexia, pérdida de peso, nauseas, alucinaciones, vómito, convulsiones, entre otros; los efectos del segundo son dermatitis, edema general, depleción de la médula ósea y polineuropatía periférica (Rodrigues, 2009).Por otro lado, estos fármacos son efectivos en la fase aguda ya que en un tratamiento completo de 60 días, el 80% de los pacientes se cura; sin embargo, la eficacia en la fase crónica varía de acuerdo al área geográfica, edad del paciente y dosis prescrita (Muñoz et al, 2011). Por ejemplo, se ha observado que el uso de BNZ en la fase temprana de la etapa crónica tiene una eficacia del 60% en niños de 6 a 12 años de edad (Estani *et al*, 2012). Aunado a estas inconveniencias, la falta de interés por parte de la industria farmacéutica de sintetizarlos ha afectado de manera importante la disponibilidad de estos fármacos para su uso clínico. De hecho, la producción comercial de NFX ya se encuentra descontinuada y el BNZ no se encuentra disponible en México excepto por las donaciones humanitarias solicitadas a través de la Organización Mundial de la Salud (OMS). Además, los gobiernos de las zonas endémicas invierten muy poco en investigación e infraestructura para esta enfermedad. La Fundación Global de Innovación para Enfermedades Marginadas (G-FINDER) solo invierte el 11.8% de sus recursos a la investigación en enfermedades causadas por tripanosomátidos, siendo principalmente ciencia básica y no enfocada en diagnóstico, desarrollo de fármacos y vacunas (Clayton, 2010).

Debido a los inconvenientes anteriores, se continúa la búsqueda de nuevos blancos o estrategias terapéuticas. Dentro de los blancos de intervención terapéutica que se han propuesto se encuentran las enzimas de la vía de síntesis de esteroles, la proteasa de cisteína cruzipaína, la hipoxantina-guanina fosforibosiltransferasa, topoisomerasas de ADN, hidrofolato reductasa, inhibidores del metabolismo del pirofosfato, de la entrada de purinas, así como las enzimas pertenecientes a la vía de

síntesis, consumo y regeneración del $T(SH)_2$ (WHO, 2007; Mansour, 2002; Rodrigues-Coura 2002). Esta última vía fue motivo de estudio en el trabajo de tesis.

1.5 Metabolismo del $T(SH)_2$ como blanco terapéutico

El TSH_2 es un conjugado de dos moléculas de GSH y una de espermidina (Spd) el cual está presente en todos los estadios de los tripanosomátidos (Krauth-Siegel y Comini, 2008) y en otros organismos tales como *Euglena gracilis* y *Entamoeba histolytica* (Montrichard *et al,* 1999; Tamayo *et al*, 2005). En los tripanosomátidos, el $T(SH)_2$ junto con su enzima reductora tripanotión reductasa (TryR) y las enzimas desintoxicantes dependientes de $T(SH)_2$ reemplazan las funciones que el sistema GSH/GSH reductasa/GSH peroxidasas lleva a cabo en otras células (Fairlamb y Cerami, 1992). El metabolismo del $T(SH)_2$ se muestra en la (Fig. 4).

El $T(SH)_2$ es sintetizado por la tripanotión sintetasa (TryS) a partir de dos moléculas de GSH y una de espermidina (Spd). A su vez, la síntesis de GSH es catalizada por dos enzimas: la γECS que une Cys y Glu formando γEC; y la GS la cual le agrega una Gly, formando el GSH. Por otro lado, la Spd puede sintetizarse *de novo* por la espermidina sintasa (SpdS) a partir de putrescina (Put) y S-adenosil metionina descarboxilada (dAdoMet); este último metabolito es a su vez sintetizado por la S-adenosil metionina descarboxilasa (AdoMetDC). Además la Spd y la Put pueden transportarse del medio extracelular a través de transportadores de alta afinidad. El $T(SH)_2$ cede sus equivalentes reductores a metabolitos oxidados tales como dehidroascorbato (DHA), triparedoxina oxidada (TXNox) y disulfuro de glutatión (GSSG) los cuales, en su forma reducida, son sustratos de las enzimas antioxidantes ascorbato peroxidasa (APx), 2-Cys peroxirredoxina (TXN-Px), enzimas tipo glutatión peroxidasa no dependiente de selenio (nsGPxA y nsGPxB) y de la tripanotión-glutatión tiol transferasa (p52). El disulfuro de tripanotión formado (TS_2) es reducido por la tripanotión reductasa (TryR) en una reacción dependiente de NADPH (Olin-Sandoval *et al*, 2010).

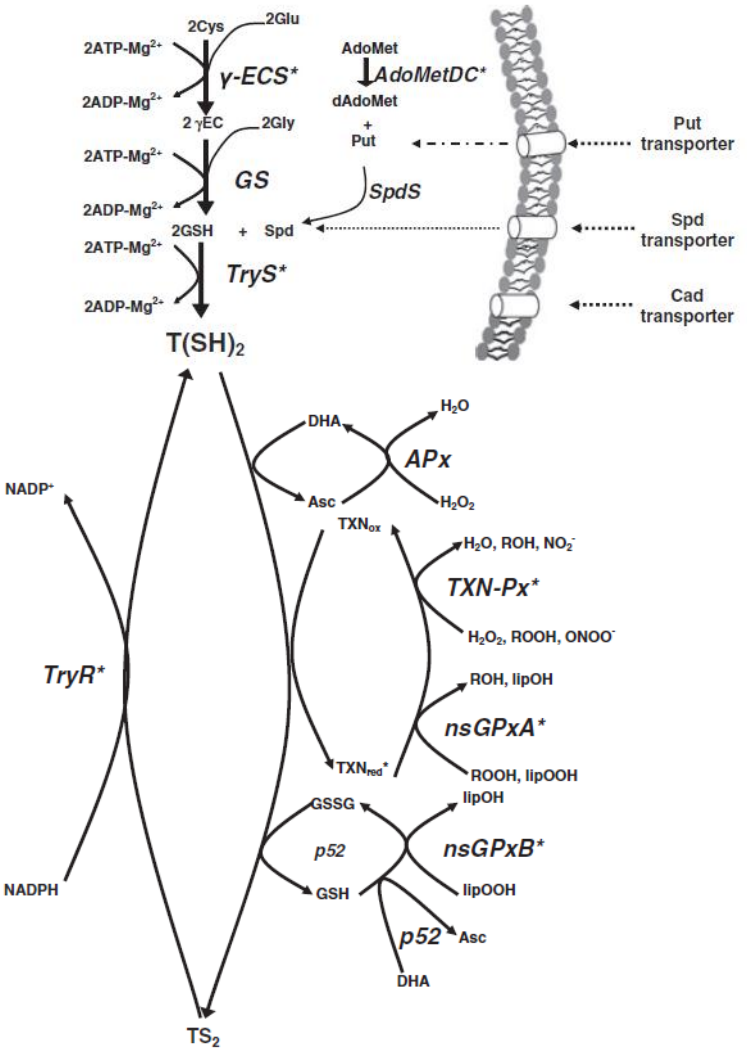

Fig. 4. Metabolismo de $T(SH)_2$ en *Trypanosoma cruzi*.

El $T(SH)_2$ se sintetiza por la tripanotión sintetasa (TryS) a partir de GSH y Spd. A su vez, la vía de síntesis de GSH está formada por la γ- glutamilcisteína sintetasa (γECS) y la glutatión sintetasa (GS) mientras que el suministro de Spd proviene de la vía de síntesis *de novo* formada por la espermidina sintasa (SpdS), la S-adenosil metionina descarboxilasa (AdoMetDC) y el transportador de putrescina (Put) o por su transporte del medio extracelular a través de un transportador de Spd. Este parásito también puede sintetizar análogos de tripanotión que contienen cadaverina (Cad) la cual se transporta del medio extracelular. El $T(SH)_2$ reduce al dehidroascorbato (DHA), a la triparredoxina oxidada (TXN_{ox}) y el disulfuro de glutatión (GSSG) los cuales, en su forma reducida son sustratos de las enzimas antioxidantes ascorbato peroxidasa (APx), 2-Cys peroxirredoxina (TXN-Px), enzimas tipo glutatión peroxidasas no dependientes de selenio (nsGPxA y nsGPxB) y la tripanotión-glutatión tiol transferasa (p52). El disulfuro de tripanotión (TS_2) es reducido por la tripanotión reductasa (TryR). Las enzimas marcadas con asterisco, son aquellas que han sido inhibidas por métodos genéticos en *T. brucei* y *Leishmania.*

Debido a que el GSH no puede reemplazar al $T(SH)_2$ como el principal metabolito antioxidante y a que las enzimas de este sistema antioxidante son exclusivas de tripanosomátidos se propuso desde el descubrimiento de la molécula en 1985 (Fairlamb *et al*, 1985; Fairlamb y Cerami, 1992) y con la descripción posterior de la vía metabólica en la década de los 90s, que las enzimas de esta vía pueden ser sitios potenciales de intervención terapéutica.

En la siguiente revisión publicada en 2010 en la revista *Current Drug Targets* (factor de impacto 2009: 3.93; en 2010: 3.06) se realizó una recopilación de la información cinética reportada de cada una de las enzimas participantes en esta vía, además se realizó un análisis crítico de su valoración como blancos terapéuticos mediante el uso de la estrategia genética de la inhibición *in vivo* de su expresión.

Desde su aparición en diciembre del 2010, esta revisión ha sido citada 4 veces en los siguientes trabajos:

-Walter Rivarola H, Paglini-Oliva P (2011) Mal de Chagas-Mazza: Fisiopatogenia y nuevas propuestas de tratamientos. Revista Facultad de Ciencias Médicas 68 (4) 154-163.

-Duschak V (2011) A decade of targets and patented drugs for chemotherapy of Chagas disease. *Rec Pat on Anti-Inf Drug Disc* 6 (3) 216-259.

-Krauth-Siegel L and Leroux AE (2012) Low molecular mass antioxidants in parasites. *Antiox Red Sign*. doi:10.1089/ars.2011.4392.

-Teixeira SM, Cardoso de Paiva RM, Kangussu-Marcolino MM, DaRocha WD (2012) Trypanosomatid comparative genomics: contributions to the study of parasite biology and different parasitic diseases. *Genet Mol Biol* ahead of print.

1614 *Current Drug Targets*, 2010, *11*, 1614-1630

Targeting Trypanothione Metabolism in Trypanosomatid Human Parasites

Viridiana Olin-Sandoval, Rafael Moreno-Sánchez and Emma Saavedra*

Departamento de Bioquímica, Instituto Nacional de Cardiología, México D.F., 14080, México

Abstract: The diseases caused by the trypanosomatid parasites *Trypanosoma brucei, Trypanosoma cruzi* and *Leishmania* are widely distributed throughout the world. Because of the toxic side-effects and the economically unviable cost of the currently used pharmaceutical treatments, the search for new drug targets continues. Since the antioxidant metabolism in these parasites relies on trypanothione [$T(SH)_2$], a functional analog of glutathione, most of the pathway enzymes involved in its synthesis, utilization and reduction have been proposed as drug targets for therapeutic intervention. In the present review, the antioxidant metabolism and the phenotypic effects of inhibiting by genetic (RNA interference, knock-out) or chemical approaches, the $T(SH)_2$ and polyamine pathway enzymes in the parasites are analyzed. Although the genetic strategies are helpful in identifying essential genes for parasite survival/infectivity, they are less useful for drug-target validation. The effectiveness of targeting each pathway enzyme was evaluated by considering (i) the enzyme kinetic properties and antioxidant metabolite concentrations and (ii) the current knowledge and experimental approaches to the study of the control of fluxes and intermediary concentrations in metabolic pathways. The metabolic control analysis indicates that highly potent and specific inhibitors have to be designed for trypanothione reductase and the peroxide detoxification system, and hence other enzymes emerge (γ-glutamylcysteine synthetase, trypanothione synthetase, ornithine decarboxylase, S-adenosylmethionine decarboxylase and polyamine transporters) as alternative more suitable and effective drug targets in the antioxidant metabolism of trypanosomatids.

Keywords: *Leishmania*, *Trypanosoma*, trypanothione, drug-targeting, microbial antioxidant metabolism.

1. INTRODUCTION

The trypanosomatid parasites *Trypanosoma brucei*, *Trypanosoma cruzi* and *Leishmania* are the causal agents of three deadly diseases that affect millions of people around the world: sleeping sickness (*African trypanosomiasis*), Chagas' disease (American trypanosomiasis), and leishmaniasis (cutaneal, visceral and mucosal). The treatments for these pathologies include the administration of difluoromethylornithine (DFMO), pentamidine, suramin and melarsoprol for *T. brucei*; nifurtimox and benznidazol for *T. cruzi*; and amphotericin B, sodium stibogluconate, pentamidine, miltefosine and meglumine antimoniate for *Leishmania* [1] (see Fig. **1A** for drug chemical structures). The treatments with these compounds have several disadvantages: most of them are highly toxic for the patient; usually they are not easily affordable for the sick people who live in poor communities; administration of some drugs requires hospitalization; they usually act only in a particular stage; and resistant strains have emerged [2]. Hence, there is a public health demand for alternative therapeutic strategies.

Drug-targets have been searched and drugs have been designed for enzymes of glycolysis, purine salvage and pyrimidine metabolism, nucleoside transport, sterol biosynthesis, protein prenylation and degradation, and antioxidant pathways [3, 4]. The enzymes that synthesize, use or recycle trypanothione [$T(SH)_2$] have been considered potential targets for drug intervention because of their absence in the human host [3-7].

2. TRYPANOTHIONE IS THE MAIN ANTIOXIDANT METABOLITE IN TRYPANOSOMATIDS

All living organisms are exposed to reactive oxygen and nitrogen species (ROS and RNS, respectively) such as superoxide anion ($\bullet O_2^-$), hydrogen peroxide (H_2O_2), hydroxyl radical ($HO\bullet$), nitric oxide ($\bullet NO$) and peroxynitrite (NOO^-). These compounds can be generated inside the cells by basal metabolic function, oxidative or nitrosative stresses, and drug metabolism. Alternatively, $\bullet O_2^-$, $\bullet NO$ and NOO^- can be generated by the host's immune system as a first line of defense against the parasite infection [8].

In most living cells, the enzymatic antioxidant machinery primarily relies on reduced glutathione (GSH) (Fig. **2**) as a source of electrons to reduce and inactivate ROS and RNS. GSH, together with glutathione reductase (GR), which reduces oxidized glutathione (GSSG) at expense of NADPH oxidation, represents the principal cellular mechanism to cope with oxidant and nitrosative stresses. Furthermore, GSH can non-enzimatically reduce the oxidized forms of cellular antioxidant molecules such as ascorbate (Asc) and vitamin E due to its higher redox potential (Table **1**) [8, 9]; the relative slow rates of these non-enzymatic reactions may be a shortcoming for contending against severe oxidative stress.

Despite the presence in trypanosomatid parasites of significant amounts of GSH, their antioxidant enzymatic machinery uses its functional analog $T(SH)_2$ (N^1, N^8- bis-glutathionylspermidine; Fig. **2**) as the predominant reducing agent. Thus, $T(SH)_2$, together with its reducing enzyme,

*Address correspondence to this author at the Departamento de Bioquímica, Instituto Nacional de Cardiología. Juan Badiano No. 1 Col. Sección XVI, Tlalpan, México D.F. 14080, México; Tel: (+5255) 5573-2911, Ext. 1298; E-mail: emma_saavedra2002@yahoo.com

1389-4501/10 $55.00+.00

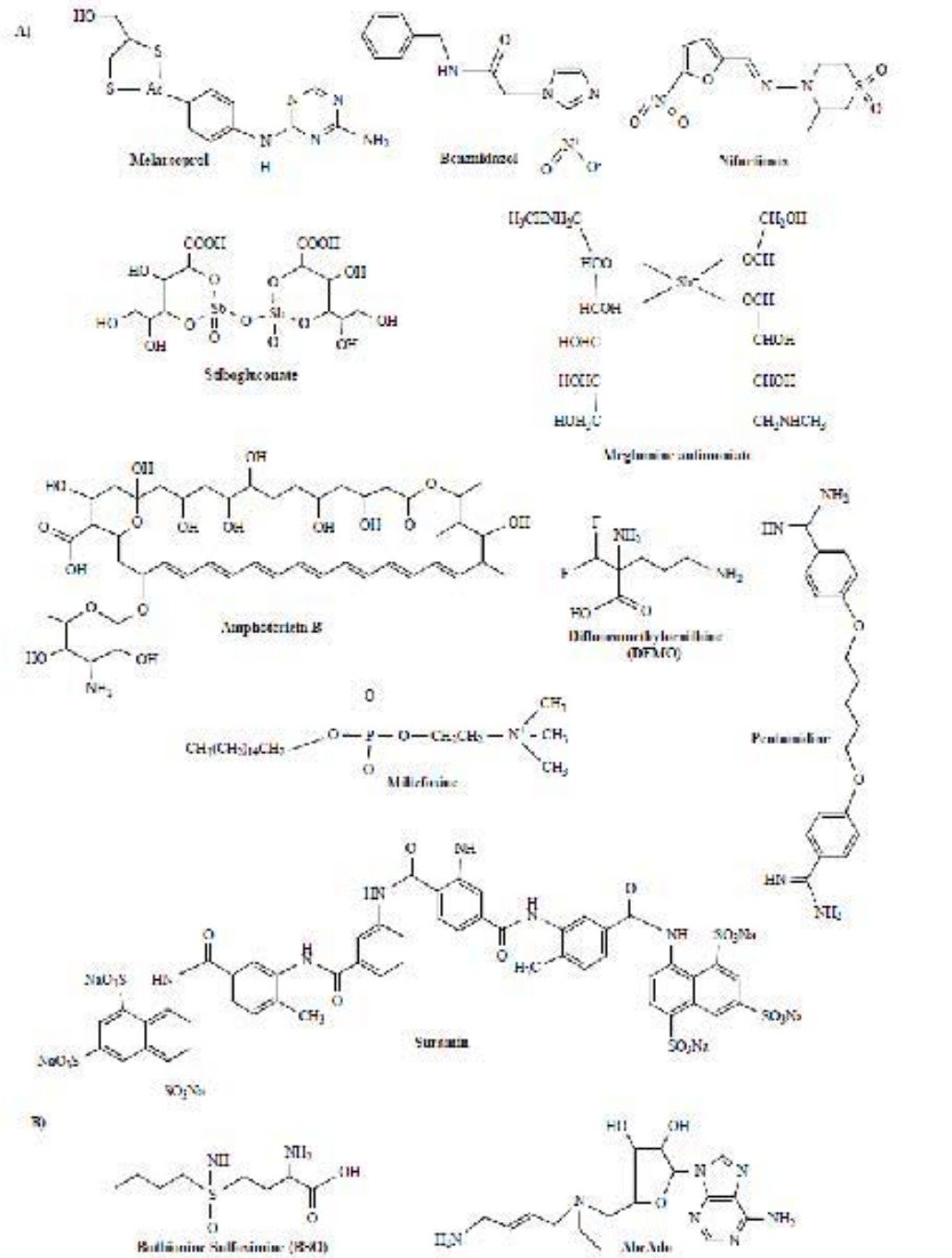

Fig. (1). Drugs against trypanosomatid caused human diseases. A. Agents commonly used for trypanosomatid diseases treatment. B. Agents with targets in $T(SH)_2$/polyamine metabolism

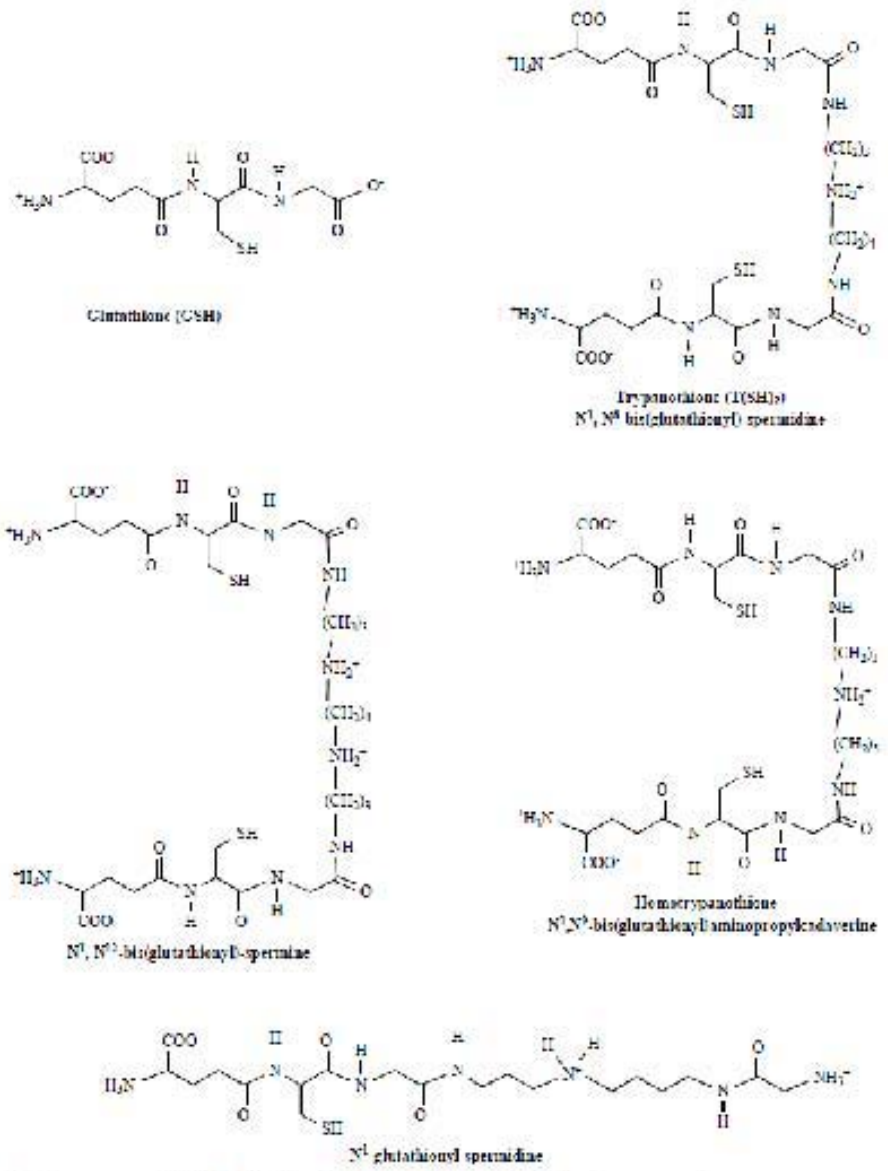

Fig. (2). Thiols in trypanosomatids. GSH, $T(SH)_2$ and $T(SH)_2$- analogues in which the polyamine moiety varies.

trypanothione reductase (TryR), replaces all the functions that the GSH/GR system has in other organisms [3, 5]. In fact, the activities and genes of GR and thioredoxin reductases (TrxR) have not been detected in trypanosomatids (for recent reviews see [6, 7, 10, 11].

$T(SH)_2$ is constituted by two GSH molecules bound to one spermidine (Spd) molecule, however, $T(SH)_2$ analogues have also been described in *T. cruzi* containing other polyamine moieties such as spermine (Spm) or cadaverine (bis-glutathionyl-spermine and homotrypanothione, respectively) (Fig. 2) [12]. Despite the close redox potential values of $T(SH)_2$ and GSH (Table 1), the dithiol conjugate of $T(SH)_2$ displays other physico-chemical properties that confer functional advantages. The reason is that being a dithiol, the formation of the intramolecular thiol disulphide bond is faster in $T(SH)_2$ than the intermolecular disulphide bond formation between two GSH molecules [10].

Moreover, the positively charged amino group in the Spd moiety (Fig. 2) confers $T(SH)_2$ a SH pK value near 7.4, becoming more reactive than GSH (–SH pK – 8.66) at physiological pH [10]. Although the antioxidant enzymatic machinery relies on $T(SH)_2$ as reducing equivalent donor, the concentrations of $T(SH)_2$ and GSH in trypanosomatids are remarkably similar (0.1 - 2.1 mM and 0.03 -2.1 mM, respectively), however, the $T(SH)_2$/GSH concentration ratio can vary among different trypanosomatids, stages or growing phases [11].

Table 1. Redox Potential Values for Antioxidant Molecules Involved in $T(SH)_2$ Metabolism

Pair	E° (mV)	References
$T(SH)_2$ / TS_2	-340	[10]
GSH / GSSG	-230	[10]
TXN_{red} / TXN_{ox}	-240	[56]
Trx_{red} / Trx_{ox}	-261	[26]
Asc / DHA	66	[9]

Although $T(SH)_2$ was previously considered exclusive of trypanosomatids, it has also been found in the free living, unicellular, flagellated protist *Euglena gracilis*, a close taxonomical relative of trypanosomatids [13], and in the human parasite *Entamoeba histolytica* [14], however, the $T(SH)_2$ function in these microorganisms has not been clearly established.

3. TRYPANOTHIONE BIOSYNTHESIS

The precursors for $T(SH)_2$ biosynthesis are supplied by two major pathways in the parasites: the GSH and polyamine syntheses (Fig. 3). The importance of these pathways in providing precursors are analyzed, emphasizing the control that they might have on the steady-state concentration of $T(SH)_2$, when the parasites are under control conditions, or oxidative or nitrosative stresses.

3a. Glutathione Synthesis in Trypanosomatids

The first reaction in the GSH biosynthetic pathway (Fig. 3) is catalyzed by γ-glutamylcysteine synthetase (γECS, EC 6.3.2.2), which forms a peptide linkage between the γ-carboxyl group of glutamate (Glu) and the α-amino group of cysteine (Cys) to produce γ-glutamylcysteine (γEC) in an ATP consuming reaction. In most organisms, γECS is a dimer constituted of a catalytic and a regulatory subunit [15]. The function of the regulatory subunit is to increase the affinity for Glu, for instance, the recombinant catalytic subunit of the rat enzyme displays a Km_{Glu} value of 18.2 mM compared to the 1.4 mM *Km* value of the recombinant holoenzyme [15]. The *T. brucei* recombinant enzyme has been purified and characterized [16]. The monomeric enzyme does not require a regulatory subunit due to its natural high affinity for Glu (0.24 mM) [16]. The *T. brucei* γECS contains an insertion of 60 amino acid residues starting at position 242, which has been suggested to replace the functions of the regulatory subunit in the enzyme from rat [16].

γECS from mammalian cells is considered the rate limiting step of GSH synthesis because it is competitively inhibited by GSH (versus Glu), the end-product of the pathway, at physiological levels of the metabolite (Ki_{GSH} 3.3 and 2.3 mM for the human and rat enzymes, respectively) [17, 18]. This assumption has been extended to the *T. brucei* enzyme because it is also *in vitro* inhibited by GSH (Ki_{GSH} of 1.1 mM, [16]). However, whether this inhibitory mechanism physiologically operates in the parasites has not yet been determined. It is recalled that *in vitro* enzyme inhibition also depends on the concentration of the substrates, particularly for competitive (and mixed-type) inhibitors such as GSH. Then, for a quantitative first approximation on the assessment of the expected inhibitory effect of GSH on γECS under physiological conditions, the [GSH]/Ki_{GSH} ratio should be compared with that of [Glu]/Km_{Glu}: if the inhibitor ratio is higher than the substrate ratio, then strong inhibition of activity can be predicted.

Glutathione synthetase (GS, EC 6.3.2.3) catalyzes the second reaction in GSH synthesis (Fig. 3). It covalently binds an γEC molecule to glycine (Gly), consuming one ATP molecule per mole of GSH synthesized. The enzyme has been scarcely studied in trypanosomatids probably because it has been considered a non rate limiting step in GSH synthesis. However, recent studies in antimony-resistant strains of *Leishmania tarentolae* and their revertants indicate that the higher resistance is related to their increased $T(SH)_2$ levels, and to the up-regulation of the γECS (*gsh1*), GS (*gsh2*) and ABC transporter (*pgpc*) genes in the resistant strains [19-21]. Although the changes were only monitored at the mRNA levels, which do not necessarily translate into increased protein content or enzyme activity, these observations suggest a possible contribution also of GS to $T(SH)_2$ synthesis. The *T. brucei* GS crystal structure has been recently described at 3.15 Å of resolution [22]. The authors concluded that, because of its high similarity at the amino acid sequence and structural levels with the human enzyme, trypanosomal GS is not an adequate drug target. However, this has not been demonstrated in live parasites.

Recently, we have characterized the biochemical properties of recombinant *T. cruzi* GS (*Tc*GS) (Olin-Sandoval V & Saavedra E, manuscript in preparation). The enzyme has a dimeric structure displaying *Km* values similar to those reported for the GS from *Plasmodium falciparum* [23]. However, in contrast to the cooperative binding for γEC observed in the enzyme from rat [24], *Tc*GS displays typical hyperbolic kinetics for this substrate. Furthermore, *T. cruzi* parasites challenged with H_2O_2 does not display changes in GS activity and GSH concentration with respect to control parasites. These results suggest that GS is indeed a non-limiting step in GSH synthesis.

3b. Polyamine Sources in Trypanosomatids

Polyamine *de novo* synthesis or transport from the extracellular milieu are the pathways supplying the second precursor for $T(SH)_2$ synthesis (Fig. 3).

Spermidine is the polyamine present in $T(SH)_2$. Spd is synthesized by spermidine synthase (SpdS, EC 2.5.1.16) that covalently binds a putrescine molecule to decarboxylated S-adenosylmethionine (dAdoMet). In turn, putrescine is

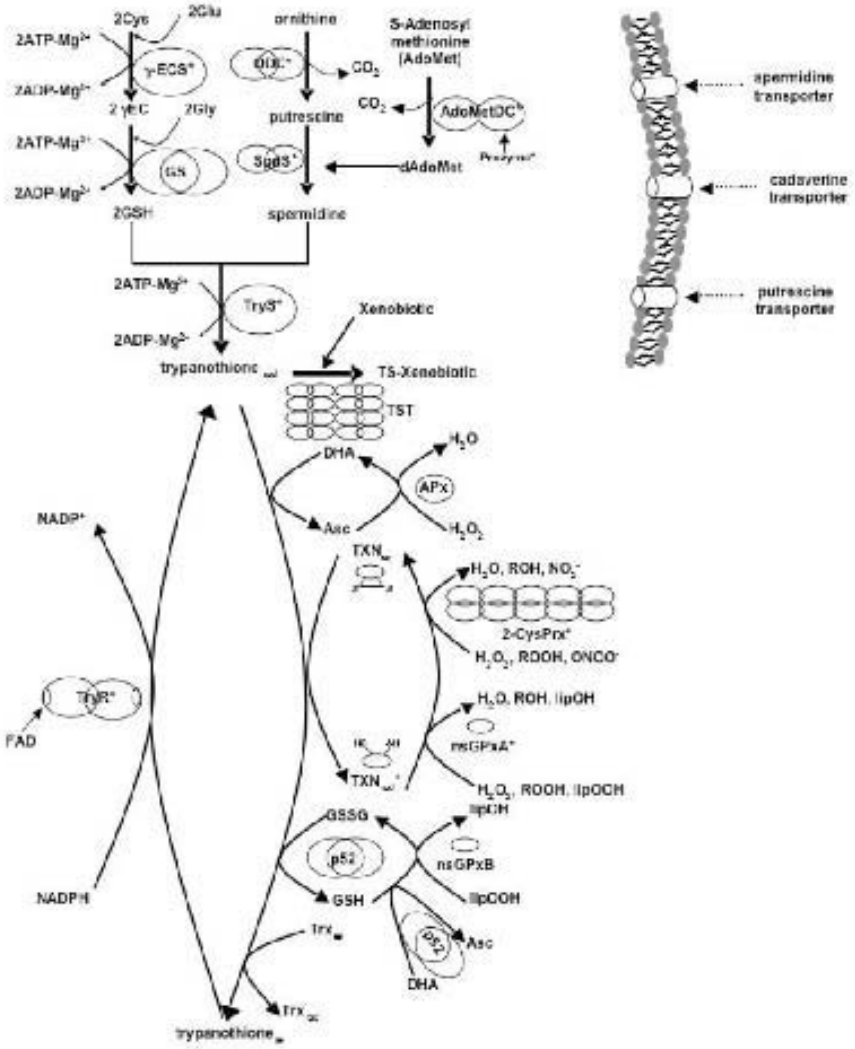

Fig. (3). Trypanothione and polyamine metabolism in trypanosomatids. Two ways supply the precursors for T(SH)$_2$ synthesis: the glutathione and the polyamine synthesis/transport pathways. T(SH)$_2$ is the reducing molecule for several metabolites and oxido-reductase enzymes which in turn are substrates of different antioxidant enzymes that use the electrons derived from NADPH to reduce peroxides. Ornithine decarboxylase (ODC; EC 4.1.1.17) in *T. cruzi* is absent and polyamine transporters in *T. brucei* have not been identified. γ-glutamyl cysteine synthetase (γ-ECS; EC 6.3.2.2); glutathione synthetase (GS; EC 6.3.2.3); S-adenosyl methionine decarboxylase (AdoMetDC; EC 4.1.1.50); spermidine synthase (SpdS; EC 2.5.1.16); trypanothione synthetase (TryS; EC 6.3.1.9), ascorbate peroxidases (APx; EC 11.1.11); tryparedoxin (TXN); 2-Cys peroxiredoxins (2-Cys-Prx; EC 1.11.1.15); non-selenium glutathione peroxidase A and B types (nsGPxA, nsGPxB; EC 1.11.1.9), trypanothione-S-transferase (TST); trypanothione reductase (TryR; EC 1.8.1.12), trypanothione-glutathione thiol transferase (p52). The enzymes are shown in proportional sizes. Their oligomeric states have been described in [10, 16, 22, 25, 32, 42-44, 67, 68, 71, 72, 82, 84, 119, 120]. * Indicates enzymes that have been studied as drug targets.

synthesized by ornithine decarboxylation in a reaction catalyzed by ornithine decarboxylase (ODC; EC 4.1.1.17) whereas dAdoMet is synthesized by S-adenosylmethionine decarboxylase (AdoMetDC; EC 4.1.1.50) through S-adenosyl methionine decarboxylation.

To our knowledge, SpdS has only been characterized in *T. brucei* [25, 26]. The enzyme displays *Km* values for putrescine and dAdoMet of 200 - 205 and 0.09- 0.1 μM, respectively [25, 26]. The reported concentrations for these metabolites in the parasite are 0.25 and 0.5 pmol/10^8 cells [25, 27], which correspond to 1.8 mM and 0.15 μM, respectively, by considering that $1x10^8$ *T. brucei* procyclic forms are equivalent to 0.5 mg cellular protein [28] in 3.5 μL of intracellular water volume [29]. Thus, it seems that this enzyme might be non limiting for polyamines synthesis under *in vivo* conditions. Unfortunately, no enzyme activities in the parasites have been assessed to determine whether the enzyme is controlling *de novo* spermidine synthesis.

AdoMetDC has been characterized from several trypanosomatids (reviewed in [30]). The enzymes from the parasites are slightly higher in size than the mammalian enzyme (42-44 *versus* 38 kDa, respectively). Interestingly, the parasitic enzymes also contain the conserved motif Gly Ser Ser where the mammalian proenzyme is processed to produce the activated heterotetrameric enzyme [30]. In a similar fashion to the human enzyme, putrescine is a non-essential activator of the trypanosomatid enzymes [30-32]. However, a high $Ka_{putrescine}$ value of 4.3 mM has been reported for the *T. cruzi* enzyme [32], whereas a putrescine level of 0.01 mM has been found in this parasite [33], suggesting a minor effect on the activity under physiological conditions. In fact, AdoMetDC in *T. brucei* cell extracts is activated by only 50% with 10 mM putrescine [32] suggesting that this regulatory mechanism does not operate in trypanosomatids. Interestingly, it has been documented that *Tb*AdoMetDC forms a heterodimer with an inactive paralog (termed prozyme) which increases its catalytic efficiency (k_{cat}/Km) from 35 $M^{-1}s^{-1}$ (in the presence of only putrescine) to 1.2 $x10^4$ $M^{-1}s^{-1}$ in the oligomeric form with the prozyme [34]. The latter value is similar to that determined for the human activated enzyme in the presence of putrescine (4.4 $x10^7$ $M^{-1}s^{-1}$) [35]. This prozyme regulatory mechanism is parasite specific and has been proposed as a target for therapeutic intervention. In fact, the enzyme activity is low in long slender *T. brucei* parasites (11 pmol min^{-1} mg cellular $protein^{-1}$) [31]; hence low inhibitor concentration might indeed be required. However, the presence of polyamine transporters (discuss below) precludes AdoMetDC to be an appropriate drug target for *T. cruzi* and *Leishmania*.

ODC is a homodimeric enzyme that catalyzes the first step of the polyamine biosynthetic pathway transforming ornithine into putrescine. Low enzyme activities of 0.1 and 0.05 nmol min^{-1} mg cellular $protein^{-1}$ in *T. brucei* and *T. rangeli* have been determined [36, 37]. The *Km* value for ornithine of *Tb*ODC is 0.28 mM [36] indicating that *in vivo* this enzyme is kinetically inefficient (k_{cat}/Km = 0.0014 min^{-1} mg^{-1}) suggesting that it might indeed be a rate-controlling step of polyamine synthesis.

Remarkably, in human cells ODC undergoes a rapid turnover, with half lives of less than one hour, in contrast, in *T. brucei* and *Leishmania* the turnover is much slower, conferring a high ODC stability within the cell [10]. The ODC suicide irreversible inhibitor DFMO (Fig. 1A) is highly effective in the treatment of sleeping sickness caused by *T. brucei gambiense* [38]. Although the human enzyme is also sensitive to the drug, the slower protein turnover of the enzyme in the parasite makes it more susceptible to DFMO inhibition and thus polyamine depletion. Interestingly, this drug is not an efficient inhibitor of *Leishmania donovani* and *T. brucei rhodesiense* ODCs despite being also very stable within the cells, which suggests different post-translational regulatory mechanisms of the enzyme activity among parasites. An explanation based on phylogenetic analyses has suggested that *T. brucei gambiense* ODC derives from a horizontal gene transfer event from a vertebrate species, both having high susceptibility to the inhibitor [30]. So far, ODC activity in *T. cruzi* has not been detected [30].

In parallel to *de novo* synthesis, highly active transporters for polyamines have been found in several *Leishmania* species. For *L. mexicana* amastigotes, the *Km* values for putrescine and Spd were 7.8 μM and 0.9 μM with *Vmax* values of 54 and 24 nmol min^{-1} (mg cellular $protein)^{-1}$, respectively [39, 40]. Since *T. cruzi* lacks ODC, it has developed high affinity transport systems for putrescine, cadaverine and Spd with *Km* values of 0.16 - 2, 4-18 and 0.8 μM and *Vmax* of ~0.1 – 6.6, 7.7 and 2.7 nmol min^{-1} (mg cellular $protein)^{-1}$, respectively determined for mid log phase epimastigotes [33, 41] and considering the protein converting values described in [28]. Thus, depending on the trypanosomatid species and the environmental conditions, polyamine biosynthesis may or may not be involved in the control of parasite $T(SH)_2$ synthesis.

3c. $T(SH)_2$ Synthesis

$T(SH)_2$ is synthesized by trypanothione synthetase (TryS, EC 6.3.1.9) by conjugating two GSH molecules to a Spd molecule in an ATP-consuming reaction (Fig. 3). TryS is a monomer present in the trypanosomatid genera *Crithidia*, *Leishmania* and *Trypanosoma* [42-45]. Although in *in vitro* experiments the enzyme displays amidase activity [42, 43], the high negative $\Delta G^{0'}$ value for the ATP hydrolysis reaction (-7.3 kcal/mol multiplied by 2, see Fig. (3) for stoichiometric relationships) makes this reaction essentially irreversible under physiological conditions. It is worth noting that $T(SH)_2$ synthesis is energetically costly, as six ATP molecules are consumed *per* $T(SH)_2$ synthesized from the single amino acid and polyamine components (Fig. 3).

Trypanosoma cruzi TryS (*Tc*TryS) can use other physiological polyamines such as Spm, aminopropylcadaverine, N-acetylspermine, N^8 acetylspermidine and N^1 acetylspermidine with different affinities. *Tc*TryS shows higher affinity for Spm compared to Spd (*Km* values of 0.13 and 0.65 mM, respectively), indicating a lower catalytic efficiency (k_{cat}/Km) with Spd. However, the levels of bis-glutathionyl-spermine in *T. cruzi* epimastigotes and amastigotes are lower (0.002- 0.05 nmoles/10^8 cells or 0.6-15 μM according to [29]) compared to those of $T(SH)_2$ [12], which suggests lower physiological activityof *Tc*TryS with Spm.

4. TRYPANOTHIONE DEPENDENT ANTIOXIDANT METABOLISM

$T(SH)_2$ cannot efficiently reduce peroxides, instead, it is able to reduce the oxidized electron donor substrates of several enzymes of the antioxidant machinery such as GSH and Asc and the oxidized forms of the dithiol redox proteins tryparedoxin (TXN) and thioredoxin (Trx), the latter being

reduced by thioredoxin reductase (TrxR) in other cell types [8], but not in trypanosomatids. Moreover, $T(SH)_2$ can form complexes with heavy metals or drugs for their detoxification (Fig. 3). Despite the presence in several parasite stages of similar contents of $T(SH)_2$ and GSH (the latter also serving as an electron donor to Asc and TXN), the superior physicochemical properties of $T(SH)_2$ that facilitate the interaction with its respective substrates as well as the absence of GR and TrxR in the parasites [10, 46], make the antioxidant system exclusively dependent on $T(SH)_2$ [47].

4a. Tryparedoxin (TXN) is the Link between $T(SH)_2$ and Several Antioxidant Enzymes in Trypanosomatids

Trypanosomatid TXNs are part of the peroxide detoxification system in which electrons are transferred, in sequence, from NADPH to $T(SH)_2$, TXN and then, to two types of TXN-dependent antioxidant enzymes, the 2-Cys peroxiredoxins (2-Cys-Prx) and the non-selenium glutathione peroxidase type A (nsGPxA), which are the main enzymes responsible for reducing peroxides (Fig. 3).

TXNs are dithiol proteins, until now only described in trypanosomatids, displaying functions similar to those of glutaredoxins (Grx) or Trx from other organisms; however, TXNs are considered distant relatives of members of the Trx superfamily due to their low percentage of homology (15%). Trypanosomatid TXNs are small proteins of 144 amino acids in length (15 kDa) and their active sites contain the sequence WCPPCR, instead of the WCGPCK(R) signature present in most Trxs. TXN is highly abundant in *C. fasciculata* and *T. cruzi* epimastigotes, accounting for 3-5 % of the total soluble protein [47] (or 0.3-0.5 mM, according to the conversion values described above and reported in [28, 29] for *T. brucei* and assuming that the intracellular volumes are similar among all trypanosomatids species and stages).

The electron transfer from $T(SH)_2$ to TXN reduces the disulfide bridge in oxidized TXN. The vicinal sulfhydryl groups generated from this reduction are in turn used to reduce the disulfide bridges from oxidized TXN-dependent peroxidases (TXNPx). The reduction of oxidized TXN by $T(SH)_2$ has been postulated as the rate-limiting step in the TXN-dependent hydroperoxide reduction pathway based on its lower specificity constant ($k_{cat_{TXN}}/Km_{TXN}$: 7.6×10^5 $M^{-1}s^{-1}$) in comparison to those of the other TXN dependent antioxidant reactions ($k_{cat_{TXN}}/Km_{GSH} = 2.4 \times 10^7$ $M^{-1}s^{-1}$, $k_{cat_{GSH}}/Km_{cumene\ hydroperoxide} = 3.5 \times 10^6$ $M^{-1}s^{-1}$) [18]. However, considering that the intracellular concentration of $T(SH)_2$ is high (0.1-2.1 mM), the $T(SH)_2$ -TXN reduction couple is saturated with the dithiol ($Km = 41$ µM); thus, the high intracellular abundance of TXN and $T(SH)_2$ may compensate for the lower specificity constant. In addition, a more physiological comparison of kinetic properties should consider the catalytic efficiencies (V_{max}/Km) rather than the specificity constants of the antioxidant reactions, because the former involves the determination of the active enzyme content expressed inside the cell, whereas the latter makes inferences with the turnover catalytic constant (k_{cat}) determined in purified (native or recombinant) enzymes. It remains to be determined whether *in vivo* TXN reduction by $T(SH)_2$ is in fact a controlling step in the antioxidant system in the parasites.

The importance of TXN in the trypanosomatid redox metabolism and its absence in the human host makes it a suitable drug target, as previously suggested [18, 19]. The crystal structure of the oxidized *C. fasciculata* TXN [50] may allow for using drug design approaches. However, due to the high levels of TXN found in the parasites, one should be aware that almost complete inhibition (>95%) in the expression of this protein has to be achieved in order to affect the parasite's redox metabolism. Thus, TXN is not an appropriate target for drug-design studies.

4b. TXN-Dependent Antioxidant Enzymes

Reduced TXN is the electron donor of two main types of TXN-dependent antioxidant enzymes: the 2-Cys-Prx (EC 1.11.1.15) and the non-selenium glutathione-peroxidase type A TXN peroxidase (nsGPXA, EC 1.11.1.9) (Fig. 3).

The trypanosomatid 2-Cys-Prxs contain two conserved Cys residues in VCP motifs, which are typical of Prxs from several organisms [51]. The parasitic active enzymes are homo-decamers of 22 kDa per subunit. The H_2O_2 reductive reaction involves the oxidation of Cys 52, producing a sulfenic acid derivative (R-SOO-R) and yielding 2 H_2O molecules. The modified Cys residue further reacts with Cys173 of another subunit in the oligomer, establishing an inter-subunit disulfide bridge which is further reduced by TXN [47]. In addition to H_2O_2, the 2-Cys Prxs are able to detoxify short chain organic peroxides and peroxynitrite [52, 53]. Due to the low Km values of 2-Cys-Prxs for TXN (2.1 and 1.1 µM for *L. donovani* and *T. cruzi*, respectively) [51, 55] and the high concentration of TXN in the parasites, the 2-Cys Prxs are expected to be saturated with TXN. Moreover, *T. brucei* Trx can also reduce 2-Cys-Prxs with a specificity constant of 2.0×10^5 $M^{-1}s^{-1}$, an order of magnitude lower efficient reduction compared with that displayed with *C. fasciculata* TXN (2.9×10^6 $M^{-1}s^{-1}$) [56]. The efficient transfer of reductive equivalents between TXN and 2-CysPrxs and the high catalytic efficiency of the latter, ensure a non limiting peroxide detoxification system.

Functional variations depending on subcellular location have been found for 2-Cys-Prxs. In *T. cruzi*, a cytosolic isoenzyme (*Tc*CPX) appears to be a TXNPx homologue with probable general peroxide scavenging function. In turn, the mitochondrial isoenzyme (*Tc*MPX), localized in the vicinity of the kinetoplast, apparently has a protective function against peroxide-mediated damage to the mitochondrial genome [57].

The second main TXN-dependent antioxidant enzyme is the nsGPXA, named as *Tc*GPXI in *T. cruzi*, peroxiredoxin III in *T. brucei* and TDPX1 in *L. major*. These trypanosomatid enzymes differ from the classical GSH dependent peroxidases found in humans or plants in containing a Cys instead of a selenocysteine residue in their active sites [47]. The trypanosomal enzymes display a high Km_{TXN} (> 5 mM) [58, 59], a value higher than the physiological concentration found in the parasites, and do not show activity using $T(SH)_2$ as electron donor [58]. It has been further established that the true electron donor of these GSH-peroxidase type enzymes is in fact TXN [48], but not GSH (see Fig. 3).

*Tc*GPXI does not exhibit activity with H_2O_2; instead, it shows activity with short-chain fatty acid and phospholipid

peroxides, having a specificity constant (*kcat/Km*) for cumene hydroperoxide of 3.5×10^6 M^{-1} s^{-1} [48, 58]. This *T. cruzi* enzyme shows glycosomal and cytosolic locations [48]. The *T. brucei* Px III is 72% identical to *Tc*GPxI, however, it is able to also reduce hydrogen, thymine and linoleic peroxides with specificity constants of 8.7×10^4, 7.6×10^4 and 7×10^4 M^{-1} s^{-1} respectively [60]. Interestingly, *Tb*PxIII can use either TXN or Trx as electron donors (*kcat/Km* constants of 2×10^7 and 5×10^6 M^{-1} s^{-1}, respectively) being more efficient with TXN [59]. This enzyme is localized in the cytosol as well as in the mitochondria [60]. On the other hand, the cytosolic *Lm*1DPX1 is 60% identical to the *Tb*PxIII, and similarly it reduces hydrogen and cumene peroxides with a similar specificity constant value of 0.8×10^7 $M^{-1}s^{-1}$ [61].

The two TXN-dependent peroxidases together with TXN, $T(SH)_2$ and TryR (see section 5) constitute the main system for peroxide detoxification in trypanosomatids.

4c. Non-Selenium Glutathione Peroxidases Type B (nsGPXB) Not Dependent on TXN

The nsGPxB (Fig. 3) shows only 30% of identity with the nsGPXA; it uses GSH instead of TXN as electron donor, but with very low affinity (Km_{GSH} of 5 mM), suggesting that other molecule or protein, probably Trx, is the physiological electron donor [47]. This enzyme has only been characterized in *T. cruzi* and it has been localized in the endoplasmic reticulum (ER). The enzyme has high affinities for long chain fatty acid peroxides such as linoleic peroxide (*Km* of 0.67 µM, *kcat/Km* of 1.8×10^3 M^{-1} s^{-1}) [62].

4d. Thioredoxin

In most organisms, Trx has many biological activities functioning as growth factor, antioxidant, and as a source of electrons for ribonucleotide reductase, which catalyzes the reduction of ribonucleoside diphosphates to deoxyribonucleoside diphosphates, the precursors for DNA synthesis. The oxidized Trx is, in turn, reduced by TrxR at expenses of NADPH [63]. TrxR has not been detected in trypanosomatids, although an unusual Trx has been found in the three developmental stages (procyclic culture form, long slender and short stumpy bloodstream parasites isolated from mice) of *T. brucei* [64]. This protein displays 56% identity with a putative Trx of *T. major* whereas they both show 21-33% identity percentages with the Trxs from *E. coli* and *S. cerevisiae*. The trypanosomal Trxs have a basic iso electric point (pI of 8.5) in contrast to the acidic one (pI of 4.5-5) of other Trxs [64]. Interestingly, although the trypanosomal Trxs can be used as substrates of TrxR and as electron source for ribonucleotide reductase from human sources, the trypanosomal TryR cannot reduce Trx; instead, it is directly reduced by $T(SH)_2$ with a second order rate constant of 14 M^{-1} s^{-1} [56] (Fig. 3). As mentioned above, the *Tb*Trx can be used as a source of electrons by 2 Cys Prxs and nsGPXI.

4e. Ascorbate/Ascorbate Peroxidases (APx) System

Activities of APx (EC 1.11.1.11) (Fig. 3) have been detected in *T. cruzi and L. major* [65-67]. The amino acid sequences of both enzymes contain an amino terminal segment of 22-24 residues with a putative trans-membrane domain, which is reminiscent of the signal sequences targeting to ER or plasma membrane. Accordingly, *Tc*APX has an ER location [66]. The recombinant mature APXs show high affinity for H_2O_2 in the presence of Asc (*Km* values of 3.1 and 25 µM in *T.cruzi* and *L. major*, respectively) and high V_{max} values (9.8 and 15 µmoles min^{-1} mg^{-1}) [66, 67]. The dehydroascorbate (DHA) product of the reaction is non enzymatically reduced by $T(SH)_2$ [65] with a second order rate constant of 1300 M^{-1} s^{-1}, which is 2-3 orders of magnitude higher than the reduction rate attained by using GSH as substrate [65]. Thus, although Asc can be reduced by both thiol-molecules, which are present in similar amounts, the predominant physiological reductant agent is most likely $T(SH)_2$ due to its higher rate constant.

4f. p52 from *T. cruzi* is a Trypanothione-Glutathione Thiol Transferase

GSSG can be non enzymatically reduced by $T(SH)_2$. However, Montiel *et al.* [68] purified a $T(SH)_2$ GSH thiol transferase (also named p52) from *T. cruzi*, which is a homodimer that reduces GSSG (*Km* of 70 µM) by using $T(SH)_2$ (*Km* of 67 µM) as electron donor (Fig. 3). These *Km* values are well within the physiological concentrations reported for both metabolites, which suggests that this other GSH regenerating system may truly operate under physiological conditions. In addition, the enzyme shows an *in vitro* DHA reductase activity (Km_{DHA} = 0.67 mM) exclusively dependent on GSH (Km_{GSH} = 2.6 mM) as electron donor [68]. Considering the reported average content of DHA in *T. cruzi* epimastigotes of 2.4 nmol/mg protein [70] and the parasite intracellular water volume [29] the DHA concentration in epimastigotes reaches 0.16 mM. Hence, it seems that the DHA reductase activity displayed by p52 is low under physiological conditions. Thus, TryR and p52 may constitute a system for maintaining the GSH and $T(SH)_2$ pools in their reduced state (but probably not the Asc pool) to better cope with the environmental oxidative stress.

4g. Trypanothione-S-transferase (TST)

Glutathione-S- transferases (GSTs) are responsible for xenobiotic detoxification in many organisms and due to the high concentration of $T(SH)_2$, a $T(SH)_2$ S transferase (TST) activity in trypanosomatids may be expected. However, no full –length GSTs or TST genes can be identified in the three main trypanosomatid genomes. A Blast analysis of the trypanosome genomes against GSH S transferases from several fungi and protozoan organisms yielded short-segments of amino acid sequence with low percentages of identity and similarity (30 and 50-60 %, respectively). Such analysis also showed higher and more significant percentage values of similarities with the gamma subunit of the ribosomal eukaryotic elongation factor 1B (eEF1B). In fact, TST activities have been detected in these subunits from the *C. fasciculata* and *T. major* eEF1Bs [71, 72]. The TST activities are specific for $T(SH)_2$ with *Km* values of 159 and 140 µM, respectively, which are well within the physiological concentration range. *Cf*TST and *Lm*TST do not show activity with H_2O_2 or tert-butyl-hydroperoxide, but they can use CDNB (1-chloro-2,4-dinitrobenzene) as substrate [71, 72]. Although *In vitro Lm* TST can reduce cumene hydroperoxide, the high *Km* value for this substrate (7.1 mM) rules out a physiological significance for this

activity. Instead, this enzyme shows high peroxidase activity with linoleic hydroperoxide (1 μmol min^{-1} mg $protein^{-1}$). The leishmanial TST is localized on the surface of the ER probably to protect the membrane from oxidative damage [72].

5. TRYPANOTHIONE REDUCTASE (TRYR), THE REGENERATING ENZYME

TryR (EC 1.8.1.12) is a flavoenzyme that catalyzes the reduction of trypanothione disulphide (TS_2) at expenses of NADPH oxidation (Fig. **3**). Hence, TryR is the main link between the cellular reductive power and the antioxidant system.

TryR from several trypanosomatids has been characterized. The enzyme is particularly abundant in *T. cruzi*, reaching an intracellular concentration of 1.25 μM [73]. TryR activity values of 60 and 220 nmoles min^{-1} (mg cellular $protein)^{-1}$ and 130 nmoles min^{-1} $(10^8$ $cells)^{-1}$ (which is equivalent to 260 nmoles min^{-1}(mg cellular $protein)^{-1}$ assuming the converting values described above) have been determined in *L. donovani*, *T. cruzi* and *T. brucei* cellular extracts, respectively [74, 75]. These activities are high compared to those of the GSH- and $T(SH)_2$- synthesis pathway enzymes found in *L. tarentolae* [19]. Purified TryR (native or recombinant) shows *Km* values for oxidized TS_2 and NADPH of 18-50 μM and 1–20 μM, respectively [76-79] and *Vmax* for the recombinant *L. donovani* and *T. cruzi* enzymes of 112.7 and 143.2 μmoles min^{-1}(mg $protein)^{-1}$, respectively [80, 81]. No allosteric properties have been described for this enzyme. The low *Km* values for its substrates and the high TryR concentration in the parasites ensures the maintenance of $T(SH)_2$ in its reduced state, especially when parasites are under oxidative stress conditions.

TryR crystal structures from *C. fasciculata and T. cruzi* have been described [82, 83]. TryR is a homodimer of 100 kDa (50 kDa per subunit); each subunit is constituted of three or four domains [82-84] in which domains I and II bind FAD and NADPH, respectively. The active site is formed by Cys 53, Cys 58 and His 461 which are situated in a cleft found in the interface between domain I of one subunit and domain III of the partner subunit [83, 84]. These cysteine residues in *T. cruzi* TryR are essential for catalysis, with Cys 53 directly interacting with TS_2 and the thiolate of Cys 58 interacting with FAD [80, 85].

Trypanosomatid TryRs not only have low identities (~35%) at the primary sequence level with human GR, but they also display great structural differences mainly at the Spd moiety binding site, which results in a high specificity for their respective substrates. With the aim of understanding the molecular basis of these differences, site directed mutagenesis analyses have been conducted to obtain GR mutants with TryR activity and *vice versa* [86-88]. The main difference between both enzymes resides in the charge of the active site. TS_2 is a positively charged and bulkier molecule than GSSG (Fig. **2**); hence TryR active site is wider, hydrophobic and negatively charged than the GR active site. Therefore, GSSG has more conformational mobility freedom in the TryR active site which decreases the binding energy available for catalysis [89]. Because TryR is only present in trypanosomatid parasites and has multiple structural differences with human GR, it has been the drug-target of choice for structure-based drug design studies.

6. TRYPANOTHIONE METABOLISM AS A POTENTIAL THERAPEUTIC TARGET FROM A METABOLIC REGULATION POINT OF VIEW

Since $T(SH)_2$ metabolism is unique in trypanosomatid parasites, all enzymes involved in its synthesis and utilization have been considered as suitable targets for therapeutic intervention. In addition to studies where specific inhibitors have been designed and tested, the *in vivo* effects of down-regulating several enzymes of this antioxidant metabolism have been analyzed by using either chemical or genetic tools such as targeted gene replacement, gene disruption or RNA interference (RNAi), the latter being only available for *T. brucei*. In this section we describe and analyze the available data on inhibition of $T(SH)_2$ metabolism enzymes and related proteins (Table **2**) aiming to its potential as drug targets based on what is known about the control of metabolic pathways.

6a. γECS Inhibition

Gene knockdown by using RNAi of γECS in *T. brucei* promotes cell death after 4-6 days of interference induction, condition under which the parasites display 80% decrease in the GSH and $T(SH)_2$ pools [90] (Table **2**). However, addition of 80 μM GSH to transformed cells allows for cell growth recovery. This result indicates that the parasites are able to transport GSH from the medium, thus circumventing the lack of *de novo* GSH synthesis [90]. A potent inhibitor of γECS is buthionine sulfoximine (BSO; Fig. **1B**). When BSO (30-120 μM) is added to *T. brucei* uninduced γECS RNAi cells, the thiol-molecule pools diminish at a similar extent to that shown in the RNAi induced parasites; however, in the latter case, cell growth is not reverted by GSH supplementation. This suggests that BSO may also affect the plasma membrane GSH transporter or other enzymes involved in GSH synthesis [90].

Heterozygous mutants lacking one allele copy of γECS in *Lesihmania infantum* showed 50% decreased GSH and $T(SH)_2$ pools making the parasites highly susceptible to oxidative stress damage caused by H_2O_2 and pentostam as well as decreased survival in activated macrophages [118].

A similar 70-80% decrease in thiol-molecules content is obtained by treating any of the three *T. cruzi* stages with 500 μM BSO, a decrease which correlates with a slightly higher susceptibility of the parasites to nifurtimox and benznidazole [91] (Fig. **1A**). Moreover, the combination of BSO and nifurtimox increases the survival rate of treated *versus* control mice, although parasitaemia levels are not significantly different between BSO alone and BSO *plus* nifurtimox treated mice [92]. This suggests that the treatment with BSO may diminish the toxic effects of nifurtimox. However, severe side-effects on the host physiology by administration of this combination of drugs might develop. The combined therapy might induce potentiated side-effects by decreasing the thiol-molecules content in the patient, as BSO also inhibits human γECS (and maybe other GSH-related enzymes). Nonetheless, a promising observation is that BSO

Table 2. Phenotypic Effects of Decreased Expression/Inhibition of $T(SH)_2$ and Polyamine Pathway Enzymes

Enzyme	Remaining activity (% of the control)	Free thiol content (% of the control)		Polyamine and its precursors contents (% of the control)			Biological effects	Refs.
		GSH	$T(SH)_2$	Spd	Putrescine	AdoMet/ dAdoMet		
γ-ECS	20-50	17-50	8-50	*	*	*	Cell death in culture and in Vero infected cells. Decrease survival in macrophages. Higher susceptibility to oxidative stress.	[90-92, 118]
TryS	15	483	14	110	91	*	Cell death in culture; sensitivity to oxidative stress and drugs	[29,98]
TryR	10-50	100	100	*	*	*	Loss of parasite virulence in mice and viability in culture	[75,99-101]
nsGPxI	27	*	*	*	*	*	Growth inhibition in culture; no susceptibility to hydrogen peroxide	[103]
2-$CysPrx_{cytosol}$	14	*	*	*	*	*	Growth inhibition in culture; increased susceptibility to H_2O_2	[103]
TXNI	3	200	500	*	*	*	Increased sensitivity to H_2O_2 in cell culture	[104]
ODC	0-10	50-175	5-50	11-50	0	100/400-4000	Cell death in culture. Growth inhibition by DFMO treatment.	[27,107, 109,110]
AdoMetDC	10-20	80	<5	40	600	150-2000	Cell death in culture. Over-expression of ODC and AdoMetDC prozyme (7 and 25 fold, respectively). Decreased parasitemia in rats. Improper methylation or hypermethylation of proteins and DNA	[27, 111, 112]
AdoMetDC prozyme	0	30-50	<5	<5	1000	*	Cell death in culture. Five-fold overexpression of ODC	[27, 111]
SpdS	<10	125	<5	20	30	100/18,000	Cell death probably by dAdoMet accumulation	[27]

*Not determined.

has been also used to potentiate the effect of antineoplastic drugs for cancer treatment [93].

Because γECS is assumed to be the rate-limiting step of GSH synthesis due to its feed-back inhibition by GSH, drug targeting of this step seems appropriate for therapeutics. However, according to Metabolic Control Analysis (MCA) studies [94, 95] the degree of control (control coefficient) over the pathway flux or metabolite concentration is not a permanent, intrinsic property of a pathway enzyme; instead, it is a systemic property which depends on the functioning of all the pathway enzymes and how they respond to the metabolite concentration and environmental changes under a specific cellular steady-state condition [95]. Two important implications of the MCA framework is that all the participating enzymes share the pathway control in different degrees and that an enzyme may exert significant flux control under an experimental or *in vivo* condition whereas it might not be a controlling step under other conditions [95]. Such case has been observed for γECS in a model of metal resistance in plants, where γECS has high control on GSH concentration under non-stressing conditions, but its degree of control diminishes under oxidative stress conditions, where GSH content is low and thus, feedback inhibition on γECS is not an efficient regulatory mechanism [96]. Moreover, as GSH inhibition over γECS is of the competitive type against Glu [17], the higher levels of the latter under oxidative stress conditions also attenuates the effect of the feed–back inhibition [96]. Remarkably, under both conditions, the GSH-consuming processes have an important control on the rate of GSH synthesis and its concentration [96]. This is in agreement with other analyses made by MCA which indicate that the steady-state flux of any metabolic pathway depends not only on the processes involved in its synthesis, but also on the processes that consuming it (supply-demand theory) [97].

Other considerations have to be taken into account when selecting γECS as drug-target. For instance, alternative sources of GSH supply may exist such as extracellular GSH transport, as documented for *T. brucei* [90], which would make γECS an inadequate target. However, because of the low levels of γECS activity in the parasites, it might still be advantageous to tackle this enzyme, which would require the design of potent and specific inhibitors mainly targeting parasite´s γECS or GSH- metabolism enzymes but not the host enzymes.

6b. TryS Inhibition

A 10-fold decrease in TryS by RNAi in *T. brucei* induces 14-fold increase in free GSH and 5-10 times decrease in $T(SH)_2$ and glutathionyl-spermidine levels (Table **2**) [29, 98]. Remarkably, Western blot analysis reveals 3-fold increase in γECS and TryR and 2-fold decrease in ODC protein levels in such transformants. These results suggest the onset of a compensatory mechanism that increases GSH concentration and TS_2 reduction rate to preserving $T(SH)_2$ levels (Fig. **3**). Since TryS is not completely absent in the transformed parasites as analyzed by Western blot (in fact, no complete absence of the protein is a common result in RNAi down-

regulation experiments), the increased TryR activity warrants that the fewer $T(SH)_2$ molecules synthesized remain in their reduced state. As expected, $T(SH)_2$ lower content in the transformed parasites causes higher susceptibility to the trypanocidal compounds nifurtimox and eflagenol, significantly decreasing their IC_{50} values from 3.6 to 1.6 μM and from 0.2 to 0.06 μM, respectively [29, 98].

Interestingly, the greatest changes in GSH and $T(SH)_2$ levels have been obtained by inhibiting TryS activity (Table 2). Since the antioxidant machinery in the parasites ultimately relies on $T(SH)_2$, it is clear from the TryS RNAi experiment that GSH accumulation (Table 2) does not suffice to overcome the $T(SH)_2$ deficiency. Moreover, relatively low levels of TryS activity have been observed in trypanosomatids indicating a main role for this enzyme in the pathway control. These results suggest that TryS might be an appropriate drug-target because its uniqueness and low levels of activity in the parasites, with its inhibition having marked impact on antioxidant metabolic concentrations. However, few studies have been focused in designing inhibitors for this enzyme.

6c. TryR Inhibition

TryR has been extensively studied as a drug-target because it is the enzyme responsible for the maintenance of $T(SH)_2$ and thus, it is involved in the redox homeostasis of the entire antioxidant pools in the parasites [4, 11]. At the same time, this physiological function is very likely the main reason why TryR has the highest activity in the antioxidant system including the enzymes of the $T(SH)_2$-synthetic and -consuming pathways (Fig. 3). This excess of activity ensures the presence of a constant and high $T(SH)_2$ concentration under a wide variety of environmental fluctuations. In fact, TS_2 concentrations are usually in the order of 1.6 μM compared to 0.1-2 mM for $T(SH)_2$ [11]. Hence, TryR appears to have a similar function to that of adenylate kinase which maintains the balance of the intracellular adenine nucleotide pools.

The effect of TryR inhibition by genetic approaches has been evaluated in several trypanosomatid parasites [75, 99-101] (Table 2). However, a 50-90% decrease of cellular TryR activity does not significantly affect the reduced thiol-molecule pools. These results strongly suggest that in principle, only 10% of endogenous TryR may suffice to maintaining the cellular redox homeostasis. However, this TryR shortage causes an increased sensitivity to oxidative stress generated by activated macrophages, and loss of infectiveness [75, 99]. These observations suggest that under *in vitro* conditions, where low oxidant stress challenges prevail, TryR activity is not a rate- and concentration-controlling step. Furthermore, during the infection stages in the host, in which severe and long-term oxidative stress conditions surge, a constantly active and efficient system to maintaining $T(SH)_2$ in their reduced state is required for survival. The intrinsically high TryR activity in the parasites indicates that this enzyme does not exert significant flux control on $T(SH)_2$ synthesis and then, the main controlling steps of this pathway very likely reside somewhere else. In this regard, in the TryR knock-down studies it has not been evaluated whether other enzymes of the antioxidant systems are indeed modified.

Notwithstanding the previous data, historically TryR has been the target of choice for therapeutic intervention and several efforts have been made in designing and discovering new inhibitors [102]. However, for most of the inhibitors tested against trypanosomal TryR their K_i, IC_{50} or EC_{50} values are still in the micromolar range, a threshold concentration that might yield undesirable side effects in the host.

From the metabolic point of view, TryR appears to be the most challenging target among all the enzymes constituting the full antioxidant system of the parasites because its properties demand, not partial but full inhibition. (i) from the perspective of enzyme activity, it is one of the most abundant enzymes in the parasites; (ii) from the kinetic point of view, TryR is by far the most catalytically efficient enzyme of the pathway (see section 5), and (iii) no allosteric modulators have been described for this enzyme. Hence, none of the criteria used to identifying flux or metabolite concentration controlling- steps in metabolic pathways [94, 95] are fulfilled by TryR. Thus, under oxidative stress conditions, other enzymes are most likely flux controlling steps before TryR become limiting.

6d. Antioxidant Enzymes

The trypanosomal peroxide detoxification enzymes (Tab. 3) have also been considered as potential therapeutic targets because of its dependence on $T(SH)_2$ and because their peculiarities that make them different from those in the human host. Thus, inhibition studies on these enzymes have been undertaken to evaluate their relative importance in coping with oxidative stress challenges.

Down-regulation by RNAi (73% inhibition) of the mGPx I in the bloodstream form of *T. brucei* causes a decrease in cell growth [103]. No increased susceptibility to H_2O_2 is observed in these transformants, however, other hydroperoxides have not been assayed, which could explain the failure in cellular growth. On the other hand, the RNAi inhibition (86%) of the cytosolic 2-Cys Prx renders the parasites highly susceptible to H_2O_2 [103]. Since thiol molecule concentrations were not reported, it is not known whether the $T(SH)_2$ pool is modified in the transformants.

The high redundancy of the GPX-type and Prx enzymes in trypanosomatids (Fig. 3) complicates the identification of the best drug targets within this block of the trypanosomatid antioxidant machinery. Few studies have been focused on these enzymes for therapeutic intervention. To our knowledge, no inhibitors for these enzymes have been designed.

On the other hand, down regulation of *T. brucei* TXN by 97% induced a 5 fold increased susceptibility to H_2O_2 [104]. Remarkably, GSH and $T(SH)_2$ levels increased by 2- and 5-fold, respectively (Table 2). The authors suggested that the elevation in thiol molecules concentration might represent a compensating mechanism for the deficiency in TXN [104]. However, it might also be possible that $T(SH)_2$ accumulates because it is not used for the reduction of the remaining TXN molecules after the RNAi induction (Fig. 3). Furthermore, the extremely high percentage of TXN inhibition required to attain an oxidative-sensible phenotype suggests a TXN overcapacity for the antioxidant system, which is in agreement with the high abundance of this protein in the

trypanosomatids [17]. In consequence, to consider TXN as drug target, highly potent inhibitors have to be developed to fully abolish its activity.

6e. Polyamine synthesis

The polyamine *de novo* synthesis in trypanosomatids has been considered a potential pathway for drug intervention [102]. The advantage of inhibiting enzymes in this pathway is that in addition to affecting $T(SH)_2$ metabolism, Spd and Spm are also necessary for cellular differentiation as well as DNA stability [156]. However, as contribution to $T(SH)_2$ synthesis is variable because of the diversity of polyamine sources used by different trypanosomatid species as discussed above. On the other hand, targeting parasite polyamine synthesis may also affect the pathway's host.

The common biochemical strategy to studying polyamine metabolism enzymes has been the use of DFMO to inhibit ODC. DFMO is used for the treatment of *T. brucei* sickness (200 and 400 mg/Kg/day during 6 weeks for the early and late stages of infection, respectively [107]), but it brings about severe non-desired effects on the patients. As discussed above (section 3b), this inhibitor is effective because of the low ODC turnover in *T. brucei* compared to the human enzyme [108]. However, for leishmanial parasites, DFMO treatment is only effective at elevated concentrations (>10 mM) [109]. In *L. mexicana*, 50% ODC inhibition by DFMO produces significant diminution of the Spd levels (from 17.4 to 4.4 nmol 10^8 parasites) [109]. However, even the Spd lower level gives a value of 1.1 mM, which is a concentration 1.4-fold above the *Km* value of *Lm*TryS for this polyamine [34], suggesting that *Lm*TryS may still be active, and might be not a controlling step under such a diminution in the polyamine pool.

Metabolic changes when knocking-out the ODC gene have been described for *L. donovani* [110]. Null mutants are able to grow in medium supplemented with putrescine, spermidine, cadaverine and 1,3 diamino propane. When these mutants are transferred to a medium lacking putrescine, they show a significant decrease in putrescine, GSH and $T(SH)_2$ levels (17, 45 and 34 % the initial values, respectively) after 1 day of culture, whereas the Spd levels remain unchanged but at a very low level (2.4 nmol 10^8 cells grown in cadaverine which corresponds to 11% the level found in wild type parasites grown with no polyamine supplements). After 9 days of culture in the putrescine-deficient medium, putrescine levels continue decreasing, $T(SH)_2$ and Spd remain constant at their inhibited state levels, but remarkably, GSH level progressively increases up to 7.5 fold above its initial value [110]. The authors concluded that the increment in GSH seems to compensate the cellular redox status. In addition, it might be also possible that the decreased $T(SH)_2$ synthesis is caused by the limited amount of Spd present in the ODC null parasites, a value equivalent to 0.12 mM which is a concentration below the *Km* of TryS for this polyamine (0.94 mM) [44]. Thus, inhibition of $T(SH)_2$ synthesis in the null mutants leads to accumulation of GSH, its direct precursor. On the other hand, when only one of the alleles was deleted, ODC activity in the mutants diminishes by 50% (from 13 to 5 nmol min^{-1} (mg protein)$^{-1}$), but very interestingly, the third and poly-amine concentrations do not change compared to the wild type cells [110]. This result indicates that ODC inhibition to an extent higher than 50% is necessary to effectively perturb putrescine synthesis in *T. donovani*.

RNAi silencing of ODC in *T. brucei*, resulting in 90 % decrease in enzyme content in the parasites, promotes depletion of putrescine, 40-50% decreased Spd concentration, fourfold accumulation of dAdoMet and > 90% decrease level of $T(SH)_2$, whereas GSH remains unchanged [29]. Restoration of the $T(SH)_2$ and polyamine pools can be attained when cultures in medium supplemented with putrescine and Spd, however, the mutant cells are no longer viable after two days, suggesting that ODC depletion has pleiotropic effects on other functions involved in parasite survival [29]. On the other hand, ODC inhibition by DFMO in the parasites, promotes decreased contents of Spd and $T(SH)_2$, but also of GSH (all by approximately 40%). The authors hypothesized that the unexpected decrease in GSH concentration might be caused by GSH oxidation due to accumulation of TS_2. Although no changes are observed by Western blot analysis on other enzymes of the GSH and $T(SH)_2$ synthetic pathways and TryR [32], it might still be possible that the inhibitor also affects the activity of the GSH producing pathway enzymes. Interestingly, a 40 fold accumulation of dAdoMet with no significant change in AdoMet level is also observed after the DFMO treatment [29]. The authors suggested that S-adenosylmethionine synthase may decrease its activity in response to dAdoMet accumulation, to maintaining the AdoMet levels unchanged. Alternatively, it may be that AdoMetDC is not sensitive to the accumulation of its product (caused by putrescine depletion because of the absence of ODC), supporting that the enzyme can maintain a non-limiting steady-state precursor concentration for Spd synthesis.

The comprehensive study of AdoMetDC and its prozyme undertaken by Willert and Phillips [111] revealed that RNAi silencing of AdoMetDC in *T. brucei* promotes cell death after 10 days from induction, however at day 6, decreased levels of Spd, glutathionyl spermidine, $T(SH)_2$ and GSH (10, 5, 10 and 80% the levels in the un-induced parasites, respectively) and 6 fold increased putrescine are observed [111, 29], the latter effect most probably resulting from the lack of dAdoMet for Spd synthesis. Addition of Spd to the culture medium restores polyamine and thiol-molecule pools to 60-80% the levels found in the control parasites. The silencing also promotes over-expression of both ODC (7 fold the control and 8-11 fold the activity) and the prozyme responsible for AdoMetDC activation (25 fold) with no effect on TryS, TpdS and TryR contents [111]. It can be hypothesized that the higher expression of the prozyme might compensate the lower expression of AdoMetDC to allowing an increased enzyme activity level, but apparently it does not suffice to maintaining the steady state concentration of dAdoMet necessary for Spd and $T(SH)_2$ synthesis.

In the same study, a conditional prozyme knockout (KO) cell line was generated [111]. The non-expression of the prozyme causes growth arrest after two days and cell death after six days. In contrast to what occurs when AdoMetDC was knocked down, addition of exogenous Spd does not allow for growth cell recovery. In the prozyme KO parasites, putrescine levels increase by 10 fold as expected, whereas Spd, GSH, spermidine, $T(SH)_2$ and GSH decrease to 10, 5, 5,

5 and 40% the levels found in the parasites expressing the prozyme, respectively [111]. Moreover, similar AdoMetDC and a slightly higher ODC protein contents are attained. In addition, these authors demonstrated that prozyme is an efficient AdoMetDC activator, increasing by 5 fold the activity present in parasite lysates (from 0.3 to 5 pmol min^{-1} (mg protein)$^{-1}$. These results conclusively demonstrate that the prozyme is essential for parasite survival and AdoMetDC activity.

On the other hand, AdoMetDC chemical inhibition with the suicide inhibitor 5'-{[(Z)-4-amino-2-hexenyl](methyl-amino)}-5'-deoxyadenosine (AbcAdo; Fig. 1B) is highly effective to perturbing polyamine metabolism, causing AdoMet and dAdoMet build up, which leads to improper methylation or hypermethylation of proteins and DNA [112].

Spermidine synthase knock-down in *T. brucei* promotes a decrease of 80 and 95% in Spd and $T(SH)_2$ content and 25% accumulation of GSH [27]. As for the other enzymes, addition of Spd to the culture medium restores the thiol molecule and polyamine levels [27].

It has been assumed in most of the above-mentioned studies that each of the enzymes involved in polyamine biosynthesis are potential drug targets; however, in most of them it has also been demonstrated that the almost complete depletion of these enzymes can be readily overcome by supplementing with exogenous polyamines. It is well documented that *Leishmania* has transporters for putrescine and Spd with similar affinities to those displayed by *T. cruzi*, but with higher rates [33, 39, 41]. Thus, since high affinity polyamine transporters have been identified in *T. cruzi* and in different leishmanial species, targeting *de novo* polyamine biosynthesis appears difficult for treatment of these diseases. Moreover, *T. cruzi* lacks ODC. Then, searching for inhibitors against polyamine transporters in these two trypanosomatid species might be an alternative target for therapeutic intervention. However, these transporters have been scarcely studied.

This section has analyzed the phenotypic effects of the inhibition of the enzymes involved in $T(SH)_2$ and polyamine metabolism. By using the genetic approach (RNAi, KO) where percentages of >80% decreased activity are generally obtained, it is not unexpected from a metabolic control point of view to find that all the evaluated enzymes have proved to be essential for parasite survival or infection capabilities. Such high percentages of decreased function of a given enzyme in any metabolic pathway will bring about the conversion of a non controlling into a highly controlling step [94, 95]. These genetic experimental results also imply that, to attain a similar effect on parasite growth, susceptibility to oxidative stress and infection capacity, by applying pharmacological specific inhibitors against a particular enzyme, extremely high inhibition (> 70-80%) is required to be achieved. Moreover, cellular compensatory mechanisms may be turned on to overcome inhibition of a particular enzyme; thus, the enzyme activity and metabolite concentration patterns seen under a specific metabolic steady state (in this case under the RNAi induction) may not be the same when the parasites are infecting the host. Hence, it is clear that, although the genetic approach is very useful to investigate the effects of an almost full blockade of enzyme activity (with the consequent shutting-down of the metabolic pathway) to identifying essential/non essential enzymes, this strategy does not help to identifying the enzyme(s) with the highest therapeutic potential, particularly when similar biological effects are obtained for most of the enzymes analyzed in the same pathway. Instead, the question that needs to be addressed for a proper drug target identification in the $T(SH)_2$ and polyamine pathways should be...*How much is the pathway flux or $T(SH)_2$ or polyamine concentration perturbed when a pathway enzyme is partially inhibited?* The answer to the last question involves the determination of the degree of control (control coefficient) that each pathway enzyme exerts under both basal and oxidative stress conditions. Thus, an integral, dynamic and quantitative analysis of the complete $T(SH)_2$ and polyamine pathways involving the synthesis (GSH and Spd synthesis pathways, TryS), consumption (antioxidant enzymatic machinery and $T(SH)_2$ demand *i.e.* oxidative stress) and regeneration (TryR) can be depicted. This can be achieved by applying the basic principles of MCA [94, 95] and network-based analyses as has been already done for other metabolic pathways in parasites [113-115] and human cancer (reviewed in [116, 117]; Marin Hernández A., Gallardo Pérez JC, Rodríguez-Enríquez S, Encalada R, Moreno-Sánchez R & Saavedra E. Modeling cancer glycolysis. Submitted).

7. CONCLUDING REMARKS

The presence of $T(SH)_2$ based antioxidant metabolism exclusively in trypanosomatid parasites of medical importance makes its pathway enzymes, including those of the polyamine biosynthetic pathway, potential drug targets for therapeutic intervention. In this regard, the results of genetic experiments, by down-regulating the pathway enzymes show that high percentages of inhibition (50-90%) have to be attained to achieve a significant decrease in the parasite's antioxidant capabilities. In terms of MCA these results can be interpreted as that most of the enzymes have overcapacity over the antioxidant cellular requirements. In consequence, highly specific and very potent inhibitors for the enzymes are required to attain significant diminution in parasite growth by affecting their antioxidant abilities through inhibiting just one specific enzyme. In order to identifying the enzymes/proteins with the highest control over $T(SH)_2$ and polyamine pathway fluxes and metabolite concentrations, and hence the steps with the highest therapeutic potential, the enzyme activities have to be progressively modulated (for example by using tunable promoters), together with parasite growth and/or oxidative stress susceptibility monitoring. On the other hand, analysis of metabolite contents in parasites when only one allele is deleted during the KO procedure can help to define whether within these levels of enzyme inhibition (in principle 50%) there are metabolic changes which may help to identifying the enzyme with the lowest overcapacity for the pathway fluxes. These strategies might help to pinpoint the enzymes whose inhibition does not have to be total to thus be able to attain a significant decay in the parasite antioxidant defense. Such enzymes can be further studied with a rational drug-design approach. In addition, multi-target drugs against several specific trypanosomatid enzymes might be also a promising alternative.

However, some encouraging conclusions can be drawn from the experiments described above. The genetic and kinetic analyses and the patterns of metabolite changes strongly suggest that γ-ECS and TryS are the main controlling steps in $T(SH)_2$ synthesis; in turn, the control of the steady-state concentration of the metabolite is shared between the cellular $T(SH)_2$ synthesis and consuming processes [95-97], the degree of control of these two systems will depend on the prevailing oxidant conditions. On the other hand, ODC and AdometDC enzyme/prozyme as well as polyamine transporters seem also appropriate targets for drug design studies. Finally, negligible control contribution of TryR on the rate of synthesis and minor control on the steady-state concentration of $T(SH)_2$ can be predicted because of its high abundance and no allosteric properties whereas the redundant enzymatic antioxidant machinery has overcapacity to contend against oxida-tive stress damage; thus, the latter two components of the $T(SH)_2$ metabolism are difficult targets for therapeutic intervention.

ACKNOWLEDGEMENTS

The present work was partially supported by CONACyT Mexico grants No. 83084 (ES) and 80534 (RMS), and also by PICS08-5 grant from the Instituto de Ciencia y Tecnologia del Distrito Federal.

ABBREVIATIONS

AdoMetDC	–	S-adenosyl methionine decarboxylase
Apx	–	Ascorbate peroxidase
Asc	–	Ascorbate
BSO	–	Buthionine sulfoximine
Cys	=	Cysteine
2-CysPrx		2-Cysteine peroxiredoxin
dAdoMet		Decarboxylated S-adenosyl methionine
DFMO	=	Difluoromethylornithine
DHA	=	Dehydroascorbate
ER	–	Endoplasmic reticulum
γEC	–	γ-Glutamylcysteine
γECS	–	γ-Glutamylcysteine synthetase
Glu	–	Glutamate
Gly	=	Glycine
GR	–	Glutathione reductase
nsGPX	–	Non-selenium glutathione peroxidase
Grx	–	Glutaredoxin
GSH	–	Glutathione
GSSG	=	Glutathione disulphide
GS	=	Glutathione synthetase
GSpS		Glutathionyl spermidine synthetase
GST		Glutathione S-transferase
ODC	=	Ornithine decarboxylase
RNS	=	Reactive nitrogen species
ROS	–	Reactive oxygen species
Spd	–	Spermidine
SpdS	–	Spermidine synthase
Spm	–	Spermine
TryR	=	Trypanothione reductase
Trx	–	Thioredoxin
TrxR	–	Thioredoxin reductase
TryS	–	Trypanothione synthetase
$T(SH)_2$	–	Trypanothione
TS_2	=	Trypanothione disulphide
TST	=	Trypanothione-S-transferase
TXN		Tryparedoxin
TXNPx		Tryparedoxin peroxidases

REFERENCES

[1] Croft SL, Barrett MP, Urbina JA. Chemotherapy of trypanosomiases and leishmaniasis. Trends Parasitol 2005; 21: 508-12.

[2] Stuart K, Brun R, Croft S, *et al.* Kinetoplastids: related protozoan pathogens, different diseases. J Clin Invest 2008; 118: 1301-10.

[3] Mansour TE. In: Chemotherapeutic Targets in Parasites. UK, The Press Syndicate of the University of Cambridge 2002; 90-101.

[4] Linares GE, Ravaschino EL, Rodriguez JB. Progresses in the field of drug design to combat tropical protozoan parasitic diseases. Curr Med Chem 2006; 13: 335-60.

[5] Fairlamb AH, Cerami A. Metabolism and functions of trypanothione in the Kinetoplastida. Annu Rev Microbiol 1992; 46: 695-729.

[6] Schmidt A, Krauth-Siegel RL. Enzymes of the trypanothione metabolism as targets for antitrypanosomal drug development. Curr Top Med Chem 2002; 2: 1239-59.

[7] Jaeger T, Flohe L. The thiol-based redox networks of pathogens: unexploited targets in the search for new drugs. Biofactors 2006; 27: 109-20.

[8] Valko M, Leibfritz D, Moncol J, Cronin MT, Mazur M, Telser J. Free radicals and antioxidants in normal physiological functions and human disease. Int J Biochem Cell Biol 2007; 39: 44-84.

[9] Borsook H, Keighley G. Oxidation-Reduction Potential of Ascorbic Acid (Vitamin C). Proc Natl Acad Sci USA 1933; 19: 875-8.

[10] Krauth-Siegel LR, Comini MA, Schlecker T. The trypanothione system. Subcell Biochem 2007; 44: 231-51.

[11] Krauth-Siegel RL, Comini MA. Redox control in trypanosomatids, parasitic protozoa with trypanothione-based thiol metabolism. Biochim Biophys Acta 2008; 1780: 1236-48.

[12] Ariyanayagam MR, Oza SL, Mehlert A, Fairlamb AH. Bis(glutathionyl)spermine and other novel trypanothione analogues in *Trypanosoma cruzi*. J Biol Chem 2003; 278: 27612-9.

[13] Montrichard F, Le Guen F, Laval-Martin DL, Davioud-Charvet E. Evidence for the co-existence of glutathione reductase and trypanothione reductase in the non-trypanosomatid Euglenozoa: Euglena gracilis Z. FEBS Lett 1999; 442: 29-33.

[14] Tamayo EM, Iturbe A, Hernandez E, *et al.* Trypanothione reductase from the human parasite *Entamoeba histolytica*: a new drug target. Biotechnol Appl Biochem 2005; 41: 105-15.

[15] Griffith OW, Mulcahy RT. The enzymes of glutathione synthesis: gamma-glutamylcysteine synthetase. Adv Enzymol Relat Areas Mol Biol 1999; 73: 209-67, xii.

[16] Lueder DV, Phillips MA. Characterization of *Trypanosoma brucei* gamma-glutamylcysteine synthetase, an essential enzyme in the biosynthesis of trypanothione (diglutathionylspermidine). J Biol Chem 1996; 271: 17485-90.

[17] Richman PG, Meister A. Regulation of gamma-glutamyl-cysteine synthetase by nonallosteric feedback inhibition by glutathione. J Biol Chem 1975; 250: 1422-6.

[18] Misra I, Griffith OW. Expression and purification of human gamma-glutamylcysteine synthetase. Protein Expr Purif 1998; 13: 268-76.

[19] Grondin K, Haimeur A, Mukhopadhyay R, Rosen BP, Ouellette M. Co-amplification of the gamma-glutamylcysteine synthetase gene gsh1 and of the ABC transporter gene pgpA in arsenite-resistant Leishmania tarentolae. EMBO J 1997; 16: 3057-65.

[20] Haimeur A, Brochu C, Genest P, Papadopoulou B, Ouellette M. Amplification of the ABC transporter gene PGPA and increased trypanothione levels in potassium antimonyl tartrate (SbIII) resistant Leishmania tarentolae. Mol Biochem Parasitol 2000; 108: 131-5.

[21] Guimond C, Trudel N, Brochu C, *et al.* Modulation of gene expression in Leishmania drug resistant mutants as determined by targeted DNA microarrays. Nucleic Acids Res 2003; 31: 5886-96.

[22] Fyfe PK, Alphey MS, Hunter WN. Structure of *Trypanosoma brucei* glutathione synthetase: domain and loop alterations in the catalytic cycle of a highly conserved enzyme. Mol Biochem Parasitol 2010; 170: 93-9.

[23] Meierjohann S, Walter RD, Müller S. Glutathione synthetase from *Plasmodium falciparum*. Biochem J 2002; 363: 833-8.

[24] Luo JL, Huang CS, Babaoglu K, Anderson ME. Novel kinetics of mammalian glutathione synthetase: characterization of gamma-glutamyl substrate cooperative binding. Biochem Biophys Res Commun 2000; 275: 577-81.

[25] Bitonti AJ, Kelly SE, McCann PP. Characterization of spermidine synthase from *Trypanosoma brucei brucei*. Mol Biochem Parasitol 1984; 13: 21-8.

[26] Taylor MC, Kaur H, Blessington B, Kelly JM, Wilkinson SR. Validation of spermidine synthase as a drug target in *African trypanosomes*. Biochem J 2008; 409: 563-9.

[27] Xiao Y, McCloskey DE, Phillips MA. RNA interference-mediated silencing of ornithine decarboxylase and spermidine synthase genes in *Trypanosoma brucei* provides insight into regulation of polyamine biosynthesis. Eukaryot Cell 2009; 8: 747-55.

[28] Hereld D, Krakow JL, Bangs JD, Hart GW, Englund PT. A phospholipase C from *Trypanosoma brucei* which selectively cleaves the glycolipid on the variant surface glycoprotein. J Biol Chem 1986; 261: 13813-9.

[29] Ariyanayagam MR, Oza SL, Guther ML, Fairlamb AH. Phenotypic analysis of trypanothione synthetase knockdown in the *African trypanosome*. Biochem J 2005; 391: 425-32.

[30] Persson L. Ornithine decarboxylase and S-adenosylmethionine decarboxylase in trypanosomatids. Biochem Soc Trans 2007; 35: 314-7.

[31] Selzer PM, Hasne F, Hamm-Künzelmann B, Mühlstädt K, Schulz H, Duszenko M. Down regulation of S-adenosyl-L-methionine decarboxylase activity of *Trypanosoma brucei* during transition from long slender to short stumpy-like forms in axenic culture. Eur J Cell Biol 1996; 69: 173-9.

[32] Kinch LN, Scott JR, Ullman B, Phillips MA. Cloning and kinetic characterization of the *Trypanosoma cruzi* S-adenosylmethionine decarboxylase. Mol Biochem Parasitol 1999; 101: 1-11.

[33] Le Quesne SA, Fairlamb AH. Regulation of a high-affinity diamine transport system in *Trypanosoma cruzi* epimastigotes. Biochem J 1996; 316 (Pt 2): 481-6.

[34] Willert EK, Fitzpatrick R, Phillips MA. Allosteric regulation of an essential trypanosome polyamine biosynthetic enzyme by a catalytically dead homolog. Proc Natl Acad Sci USA 2007; 104: 8275-80.

[35] Beswick TC, Willert EK, Phillips MA. Mechanisms of allosteric regulation of *Trypanosoma cruzi* S-adenosylmethionine decarboxylase. Biochemistry 2006; 45: 7797-807.

[36] Phillips MA, Coffino P, Wang CC. *Trypanosoma brucei* ornithine decarboxylase: enzyme purification, characterization, and expression in *Escherichia coli*. J Biol Chem 1988; 263: 17933-41.

[37] Haimeur A, Guimond C, Pilote S, *et al.* Elevated levels of polyamines and trypanothione resulting from overexpression of the ornithine decarboxylase gene in arsenite-resistant Leishmania. Mol Microbiol 1999; 34: 726-35.

[38] Burri C, Brun R. Eflornithine for the treatment of human *African trypanosomiasis*. Parasitol Res 2003; 90 (Suppl 1): S49-52.

[39] Basselin M, Coombs GH, Barrett MP. Putrescine and spermidine transport in Leishmania. Mol Biochem Parasitol 2000; 109: 37-46.

[40] Hasne MP, Ullman B. Identification and characterization of a polyamine permease from the protozoan parasite *Leishmania major*. J Biol Chem 2005; 280: 15188-94.

[41] Hasne MP, Coppens I, Soysa R, Ullman B. A high-affinity putrescine-cadaverine transporter from *Trypanosoma cruzi*. Mol Microbiol 2010; 76: 78-91.

[42] Oza SL, Tetaud E, Ariyanayagam MR, Warnon SS, Fairlamb AH. A single enzyme catalyses formation of Trypanothione from glutathione and spermidine in *Trypanosoma cruzi*. J Biol Chem 2002; 277: 35853-61.

[43] Oza SL, Ariyanayagam MR, Aitcheson N, Fairlamb AH. Properties of trypanothione synthetase from *Trypanosoma brucei*. Mol Biochem Parasitol 2003; 131: 25-33.

[44] Oza SL, Shaw MP, Wyllie S, Fairlamb AH. Trypanothione biosynthesis in *Leishmania major*. Mol Biochem Parasitol 2005; 139: 107-16.

[45] Comini M, Menge U, Wissing J, Flohe L. Trypanothione synthesis in crithidia revisited. J Biol Chem 2005; 280: 6850-60.

[46] Irigoín F, Cibils L, Comini MA, Wilkinson SR, Flohé L, Radi R. Insights into the redox biology of *Trypanosoma cruzi*: Trypanothione metabolism and oxidant detoxification. Free Radic Biol Med 2008; 45: 733-42.

[47] Castro H, Tomas AM. Peroxidases of trypanosomatids. Antioxid Redox Signal 2008; 10: 1593-606.

[48] Wilkinson SR, Meyer DJ, Taylor MC, Bromley EV, Miles MA, Kelly JM. The *Trypanosoma cruzi* enzyme TcGPXI is a glycosomal peroxidase and can be linked to trypanothione reduction by glutathione or tryparedoxin. J Biol Chem 2002; 277: 17062-71.

[49] Romao S, Castro H, Sousa C, Carvalho S, Tomas AM. The cytosolic tryparedoxin of Leishmania infantum is essential for parasite survival. Int J Parasitol 2009; 39: 703-11.

[50] Alphey MS, Leonard GA, Gourley DG, Tetaud E, Fairlamb AH, Hunter WN. The high resolution crystal structure of recombinant *Crithidia fasciculata* tryparedoxin-I. J Biol Chem 1999; 274: 25613-22.

[51] Hofmann B, Hecht HJ, Flohe L. Peroxiredoxins. Biol Chem 2002; 383: 347-64.

[52] Nogoceke E, Gommel DU, Kiess M, Kalisz HM, Flohe L. A unique cascade of oxidoreductases catalyses trypanothione-mediated peroxide metabolism in *Crithidia fasciculata*. Biol Chem 1997; 378: 827-36.

[53] Trujillo M, Budde H, Pineyro MD, Stehr M, Robello C, Flohe L, Radi R. *Trypanosoma brucei* and *Trypanosoma cruzi* tryparedoxin peroxidases catalytically detoxify peroxynitrite via oxidation of fast reacting thiols. J Biol Chem 2004; 279: 34175-82.

[54] Guerrero SA, Lopez JA, Steinert P, *et al.* His-tagged tryparedoxin peroxidase of *Trypanosoma cruzi* as a tool for drug screening. Appl Microbiol Biotechnol 2000; 53: 410-4.

[55] Flohe L, Budde H, Bruns K, *et al.* Tryparedoxin peroxidase of *Leishmania donovani*: molecular cloning, heterologous expression, specificity, and catalytic mechanism. Arch Biochem Biophys 2002; 397: 324-35.

[56] Schmidt H, Krauth-Siegel RL. Functional and physicochemical characterization of the thioredoxin system in *Trypanosoma brucei*. J Biol Chem 2003; 278: 46329-36.

[57] Wilkinson SR, Temperton NJ, Mondragon A, Kelly JM. Distinct mitochondrial and cytosolic enzymes mediate trypanothione-dependent peroxide metabolism in *Trypanosoma cruzi*. J Biol Chem 2000; 275: 8220-5.

[58] Wilkinson SR, Meyer DJ, Kelly JM. Biochemical characterization of a trypanosome enzyme with glutathione-dependent peroxidase activity. Biochem J 2000; 352 Pt 3: 755-61.

[59] Hillebrand H, Schmidt A, Krauth-Siegel RL. A second class of peroxidases linked to the trypanothione metabolism. J Biol Chem 2003; 278: 6809-15.

[60] Schlecker T, Schmidt A, Dirdjaja N, Voncken F, Clayton C, Krauth-Siegel RL. Substrate specificity, localization, and essential role of the glutathione peroxidase-type tryparedoxin peroxidases in *Trypanosoma brucei*. J Biol Chem 2005; 280: 14385-94.

[61] König J, Fairlamb AH. A comparative study of type I and type II tryparedoxin peroxidases in *Leishmania major*. FEBS J 2007; 274: 5643-58.

[62] Wilkinson SR, Taylor MC, Touitha S, Mauricio IL, Meyer DJ, Kelly JM. TcGPXII, a glutathione-dependent *Trypanosoma cruzi* peroxidase with substrate specificity restricted to fatty acid and

phospholipid hydroperoxides, is localized to the endoplasmic reticulum. Biochem J 2002; 364: 787-94.
[63] Powis G, Montfort WR. Properties and biological activities of thioredoxins. Annu Rev Biophys Biomol Struct 2001; 30: 421-55.
[64] Reckenfelderbaumer N, Ludemann H, Schmidt H, Steverding D, Krauth-Siegel RL. Identification and functional characterization of thioredoxin from *Trypanosoma brucei brucei*. J Biol Chem 2000; 275: 7547-52.
[65] Krauth-Siegel RL, Ludemann H. Reduction of dehydroascorbate by trypanothione. Mol Biochem Parasitol 1996; 80: 203-8.
[66] Wilkinson SR, Obado SO, Mauricio IL, Kelly JM. *Trypanosoma cruzi* expresses a plant-like ascorbate-dependent hemoperoxidase localized to the endoplasmic reticulum. Proc Natl Acad Sci USA 2002; 99: 13453-8.
[67] Adak S, Datta AK. *Leishmania major* encodes an unusual peroxidase that is a close homologue of plant ascorbate peroxidase: a novel role of the transmembrane domain. Biochem J 2005; 390: 465-74.
[68] Moutiez M, Aumercier M, Schoneck R, *et al.* Purification and characterization of a trypanothione-glutathione thioltransferase from *Trypanosoma cruzi*. Biochem J 1995; 310 (Pt 2): 433-7.
[69] Moutiez M, Quemeneur E, Sergheraert C, Lucas V, Tartar A, Davioud-Charvet E. Glutathione-dependent activities of *Trypanosoma cruzi* p52 makes it a new member of the thiol:disulphide oxidoreductase family. Biochem J 1997; 322 (Pt 1): 43-8.
[70] Clark D, Albrecht M, Arevalo J. Ascorbate variations and dehydroascorbate reductase activity in *Trypanosoma cruzi* epimastigotes and trypomastigotes. Mol Biochem Parasitol 1994; 66: 143-5.
[71] Vickers TJ, Fairlamb AH. Trypanothione S-transferase activity in a trypanosomatid ribosomal elongation factor 1B. J Biol Chem 2004; 279: 27246-56.
[72] Vickers TJ, Wyllie S, Fairlamb AH. *Leishmania major* elongation factor 1B complex has trypanothione S-transferase and peroxidase activity. J Biol Chem 2004; 279: 49003-9.
[73] Krauth-Siegel RL, Enders B, Henderson GB, Fairlamb AH, Schirmer RH. Trypanothione reductase from *Trypanosoma cruzi*. Purification and characterization of the crystalline enzyme. Eur J Biochem 1987; 164: 123-8.
[74] Kelly JM, Taylor MC, Smith K, Hunter KJ, Fairlamb AH. Phenotype of recombinant *Leishmania donovani* and *Trypanosoma cruzi* which over-express trypanothione reductase. Sensitivity towards agents that are thought to induce oxidative stress. Eur J Biochem 1993; 218: 29-37.
[75] Krieger S, Schwarz W, Ariyanayagam MR, Fairlamb AH, Krauth-Siegel RL, Clayton C. Trypanosomes lacking trypanothione reductase are avirulent and show increased sensitivity to oxidative stress. Mol Microbiol 2000; 35: 542-52.
[76] Shames SL, Fairlamb AH, Cerami A, Walsh CT. Purification and characterization of trypanothione reductase from *Crithidia fasciculata*, a newly discovered member of the family of disulfide-containing flavoprotein reductases. Biochemistry 1986; 25: 3519-26.
[77] Jockers-Scherubl MC, Schirmer RH, Krauth-Siegel RL. Trypanothione reductase from *Trypanosoma cruzi*. Catalytic properties of the enzyme and inhibition studies with trypanocidal compounds. Eur J Biochem 1989; 180: 267-72.
[78] Sullivan FX, Shames SL, Walsh CT. Expression of *Trypanosoma congolense* trypanothione reductase in *Escherichia coli*: overproduction, purification, and characterization. Biochemistry 1989; 28: 4986-92.
[79] Cunningham ML, Fairlamb AH. Trypanothione reductase from *Leishmania donovani*. Purification, characterisation and inhibition by trivalent antimonials. Eur J Biochem 1995; 230: 460-8.
[80] Borges A, Cunningham ML, Tovar J, Fairlamb AH. Site-directed mutagenesis of the redox-active cysteines of *Trypanosoma cruzi* trypanothione reductase. Eur J Biochem 1995; 228: 745-52.
[81] Mittal MK, Misra S, Owais M, Goyal N. Expression, purification, and characterization of *Leishmania donovani* trypanothione reductase in *Escherichia coli*. Protein Expr Purif 2005; 40: 279-86.
[82] Bailey S, Fairlamb AH, Hunter WN. Structure of trypanothione reductase from *Crithidia fasciculata* at 2.6 A resolution; enzyme-NADP interactions at 2.8 A resolution. Acta Crystallogr D Biol Crystallogr 1994; 50: 139-54.
[83] Zhang Y, Bond CS, Bailey S, Cunningham ML, Fairlamb AH, Hunter WN. The crystal structure of trypanothione reductase from the human pathogen *Trypanosoma cruzi* at 2.3 A resolution. Protein Sci 1996; 5: 52-61.
[84] Krauth-Siegel RL, Schoneck R. Flavoprotein structure and mechanism. 5. Trypanothione reductase and lipoamide dehydrogenase as targets for a structure-based drug design. FASEB J 1995; 9: 1138-46.
[85] Bond CS, Zhang Y, Berriman M, Cunningham ML, Fairlamb AH, Hunter WN. Crystal structure of *Trypanosoma cruzi* trypanothione reductase in complex with trypanothione, and the structure-based discovery of new natural product inhibitors. Structure 1999; 7: 81-9.
[86] Henderson GB, Murgolo NJ, Kuriyan J, *et al.* Engineering the substrate specificity of glutathione reductase toward that of trypanothione reduction. Proc Natl Acad Sci USA 1991; 88: 8769-73.
[87] Sullivan FX, Sobolov SB, Bradley M, Walsh CT. Mutational analysis of parasite trypanothione reductase: acquisition of glutathione reductase activity in a triple mutant. Biochemistry 1991; 30: 2761-7.
[88] Stoll VS, Simpson SJ, Krauth-Siegel RL, Walsh CT, Pai EF. Glutathione reductase turned into trypanothione reductase: structural analysis of an engineered change in substrate specificity. Biochemistry 1997; 36: 6437-47.
[89] Hunter WN, Bailey S, Habash J, *et al.* Active site of trypanothione reductase. A target for rational drug design. J Mol Biol 1992; 227: 322-33.
[90] Huynh TT, Huynh VT, Harmon MA, Phillips MA. Gene knockdown of gamma-glutamylcysteine synthetase by RNAi in the parasitic protozoa *Trypanosoma brucei* demonstrates that it is an essential enzyme. J Biol Chem 2003; 278: 39794-800.
[91] Faundez M, Pino L, Letelier P, *et al.* Buthionine sulfoximine increases the toxicity of nifurtimox and benznidazole to *Trypanosoma cruzi*. Antimicrob Agents Chemother 2005; 49: 126-30.
[92] Faundez M, Lopez-Munoz R, Torres G, *et al.* Buthionine sulfoximine has anti-*Trypanosoma cruzi* activity in a murine model of acute Chagas' disease and enhances the efficacy of nifurtimox. Antimicrob Agents Chemother 2008; 52: 1837-9.
[93] Maeda H, Hori S, Ohizumi H, *et al.* Effective treatment of advanced solid tumors by the combination of arsenic trioxide and L-buthionine-sulfoximine. Cell Death Differ 2004; 11: 737-46.
[94] Fell D. In: Understanding the control of metabolism. London: Portland Press 1997.
[95] Moreno-Sanchez R, Saavedra E, Rodriguez-Enriquez S, Olin-Sandoval V. Metabolic control analysis: a tool for designing strategies to manipulate metabolic pathways. J Biomed Biotechnol 2008; 2008: 597913.
[96] Mendoza-Cozatl DG, Moreno-Sanchez R. Control of glutathione and phytochelatin synthesis under cadmium stress. Pathway modeling for plants. J Theor Biol 2006; 238: 919-36.
[97] Hofmeyr JS, Cornish-Bowden A. Regulating the cellular economy of supply and demand. FEBS Lett 2000; 476: 47-51.
[98] Comini MA, Guerrero SA, Haile S, Menge U, Lunsdorf H, Flohe L. Validation of *Trypanosoma brucei* trypanothione synthetase as drug target. Free Radic Biol Med 2004; 36: 1289-302.
[99] Dumas C, Ouellette M, Tovar J, *et al.* Disruption of the trypanothione reductase gene of *Leishmania* decreases its ability to survive oxidative stress in macrophages. EMBO J 1997; 16: 2590-8.
[100] Tovar J, Wilkinson S, Mottram JC, Fairlamb AH. Evidence that trypanothione reductase is an essential enzyme in Leishmania by targeted replacement of the tryA gene locus. Mol Microbiol 1998; 29: 653-60.
[101] Tovar J, Cunningham ML, Smith AC, Croft SL, Fairlamb AH. Down-regulation of *Leishmania donovani* trypanothione reductase by heterologous expression of a trans-dominant mutant homologue: effect on parasite intracellular survival. Proc Natl Acad Sci USA 1998; 95: 5311-6.
[102] Spinks D, Shanks EJ, Cleghorn LA, *et al.* Investigation of trypanothione reductase as a drug target in *Trypanosoma brucei*. ChemMedChem 2009; 4: 2060-9.
[103] Wilkinson SR, Horn D, Prathalingam SR, Kelly JM. RNA interference identifies two hydroperoxide metabolizing enzymes

that are essential to the bloodstream form of the african trypanosome. J Biol Chem 2003; 278: 31640-6.
[104] Comini MA, Krauth-Siegel RL, Flohe L. Depletion of the thioredoxin homologue tryparedoxin impairs antioxidative defence in *African trypanosomes*. Biochem J 2007; 402: 43-9.
[105] Muller S, Coombs GH, Walter RD. Targeting polyamines of parasitic protozoa in chemotherapy. Trends Parasitol 2001; 17: 242-9.
[106] Thomas T, Thomas TJ. Polyamines in cell growth and cell death: molecular mechanisms and therapeutic applications. Cell Mol Life Sci 2001; 58: 244-58.
[107] Van Nieuwenhove S, Schechter PJ, Declercq J, Bone G, Burke J, Sjoerdsma A. Treatment of gambiense sleeping sickness in the Sudan with oral DFMO (DL-alpha-difluoromethylornithine), an inhibitor of ornithine decarboxylase; first field trial. Trans R Soc Trop Med Hyg 1985; 79: 692-8.
[108] Heby O, Persson L, Rentala M. Targeting the polyamine biosynthetic enzymes: a promising approach to therapy of African sleeping sickness, Chagas' disease, and leishmaniasis. Amino Acids 2007; 33: 359-66.
[109] Carrillo C, Cejas S, Cortes M, *et al.* Sensitivity of trypanosomatid protozoa to DFMO and metabolic turnover of ornithine decarboxylase. Biochem Biophys Res Commun 2000; 279: 663-8.
[110] Jiang Y, Roberts SC, Jardim A, *et al.* Ornithine decarboxylase gene deletion mutants of *Leishmania donovani*. J Biol Chem 1999; 274: 3781-8.
[111] Willert EK, Phillips MA. Regulated expression of an essential allosteric activator of polyamine biosynthesis in *African trypanosomes*. PLoS Pathog 2008; 4: e1000183.
[112] Byers TL, Bush TL, McCann PP, Bitonti AJ. Antitrypanosomal effects of polyamine biosynthesis inhibitors correlate with increases in *Trypanosoma brucei brucei* S-adenosyl-L-methionine. Biochem J 1991; 274 (Pt 2): 527-33.
[113] Hornberg JJ, Bruggeman FJ, Bakker BM, Westerhoff HV. Metabolic control analysis to identify optimal drug targets. Prog Drug Res 2007; 64: 171, 3-89.
[114] Saavedra E, Marin-Hernández A, Encalada R, Olivos A, Mendoza-Hernández G, Moreno-Sánchez R. Kinetic modeling can describe *in vivo* glycolysis in *Entamoeba histolytica*. FEBS J 2007; 274: 4922-49.
[115] Moreno-Sanchez R, Encalada R, Marin-Hernandez A, Saavedra E. Experimental validation of metabolic pathway modeling. An illustration with glycolytic segments from *Entamoeba histolytica*. FEBS J 2008; 275: 3454-69.
[116] Hornberg JJ, Bruggeman FJ, Westerhoff HV, Lankelma J. Cancer: a Systems Biology disease. Biosystems 2006; 83: 81-90.
[117] Moreno-Sánchez R, Saavedra E, Rodriguez-Enriquez S, Gallardo-Pérez JC, Quezada H, Westerhoff HV. Metabolic Control Analysis indicates a change of strategy in the treatment of cancer. Mitochondrion 2010. DOI: 10.1016/j.mito.2010.06.002
[118] Mukherjee A, Roy G, Guimond C, Ouellette M. The γ-glutamylcysteine synthetase of Leishmania is essential and involved in response to oxidants. Mol Microbiol 2009; 74:914-927
[119] Alphey MS, Bond CS, Tetaud E, Fairlamb AH, Hunter WN. The structure of reduced tryparedoxin peroxidase reveals a decamer and insight into reactivity of 2Cys-peroxiredoxins. J Mol Biol 2000; 300: 903-16.
[120] Grishin NV, Osterman AL, Brooks HB, Phillips MA, Goldsmith EJ. X-ray structure of ornithine decarboxylase from *Trypanosoma brucei*: the native structure and the structure in complex with alpha-difluoromethylornithine. Biochemistry 1999; 38: 15174-84.

Received: February 15, 2010 Revised: August 05, 2010 Accepted: August 05, 2010

Conclusiones principales de la revisión

Después del análisis de la literatura reportada sobre esta vía metabólica llegamos a la conclusión de que con los ensayos de inhibición genética se pudo determinar que todas las enzimas de la vía son esenciales para la supervivencia o manejo del estrés oxidante de los parásitos *T. brucei* y *Leishmania*. Sin embargo, como todas las enzimas resultaron esenciales, consideramos que se deben de aplicar criterios adicionales para identificar, de entre todas las enzimas, aquellas que no tienen que inhibirse en alto grado como la inhibición genética para tener un efecto negativo en el funcionamiento de la vía metabólica. A qué me refiero con esto. Si se analiza la estructura de cualquier vía metabólica, disminuir la expresión en más del 80% de cualquiera de sus enzimas crea una interrupción en el flujo de la vía por lo que en tales condiciones cualquier enzima será esencial para el parásito. Sin embargo, las enzimas tienen diferentes grados de participación en el funcionamiento de la vía metabólica; esto es, existen enzimas líderes que son capaces de determinarla velocidad a la que trabaja la vía; mientras que otras enzimas simplemente van a catalizar su reacción a la velocidad que les marcan las primeras. Algunas características de las enzimas líderes es que tienen inhibidores metabólicos (son reguladas alostéricamente) o son poco abundantes en las células o catalizan reacciones irreversibles; ejemplos de las segundas son enzimas abundantes en las células, catalizan reacciones cercanas al equilibrio y son muy eficientes catalíticamente. En el caso de la inhibición genética, los porcentajes de inhibición de la expresión de la proteína son tan altos que alcanzan el umbral de inhibición en que todas las enzimas, tanto las líderes como las que no lo son, se convierten en pasos limitantes. Por lo tanto, además de los criterios de esencialidad determinada genéticamente se deben de considerar la abundancia de las enzimas en el parásito (*Vm*), sus afinidades por sus sustratos, productos y efectores lo cual determina su eficiencia catalítica (*Vm*/*Km*) en la célula, así como las concentraciones intracelulares de los metabolitos pertenecientes a la vía metabólica. Esto quiere decir que si queremos disminuir el flujo de una vía metabólica se deben de inhibir principalmente aquellas enzimas que tienen esa función de líder ya que probablemente se requiera menor concentración de un inhibidor que al tratar de inhibir una enzima que en la

célula es muy abundante o muy eficiente catalíticamente. Desde el punto de vista del control del metabolismo, las enzimas catalíticamente menos eficientes de la vía determinarán o controlarán la velocidad de síntesis del metabolito de interés.

Considerando las características cinéticas de las enzimas, su contenido de enzima activa en el parásito y analizando las concentraciones de metabolitos reportados en las células propusimos en este artículo que la γECS, la TryS, y el suministro de poliaminas (constituido por la ornitina descarboxilasa (ODC), la S-adenosilmetionina descarboxilasa (AdoMetDC) y los transportadores de poliaminas) podrían ser las enzimas que predominantemente controlan la síntesis de $T(SH)_2$ en los tripanosomátidos. Por lo anterior, se consideró que estas enzimas tienen un mayor potencial terapéutico y por lo tanto su inhibición puede afectar esta vía metabólica esencial para el parásito.

Por otro lado, después de este análisis metabólico consideramos que la TryR y las enzimas del sistema reductor de hidroperóxidos, aún cuando pueden considerarse blancos terapéuticos, su inhibición puede no ser tan efectiva en disminuir el flujo de la vía debido a que estas enzimas son muy abundantes y catalíticamente muy eficientes en el parásito. Por ejemplo, a pesar de que se pudo disminuir en altos porcentajes la actividad de la TryR en *T. brucei* y *Leishmania*, las pozas de GSH y $T(SH)_2$ permanecieron constantes, lo que sugiere que la enzima tiene una gran capacidad para contender con el estrés oxidante y que solamente un 10% de la actividad es necesaria para la sobrevivencia del parásito. A pesar de este último hallazgo, la TryR es la que más se estudia para el desarrollo de fármacos, ya sea por diseño racional o por la identificación de compuestos inhibidores a través de cribados de librerías de un alto número de compuestos (“high-throughput screenings”) (Martyn *et al*, 2007; Holloway *et al*, 2007; Holloway *et al*, 2009). A la fecha se han reportado más de 100 trabajos al respecto y en promedio se publican alrededor de un artículo de investigación al mes en los que se describen inhibidores para esta enzima. Sin embargo, a pesar de que se han logrado diseñar o identificar inhibidores altamente potentes y específicos para esta enzima, muchos de ellos afectan el crecimiento de parásitos en cultivo a concentraciones micromolares o

tienen poco efecto para contrarrestar la infección en modelos animales. Nosotros sugerimos que debido a la gran abundancia de la enzima en los parásitos y a su alta capacidad catalítica esta enzima es un blanco terapéutico que presenta dificultades para ser considerada como tal.

La conclusión del análisis cinético y la propuesta que se hizo en el artículo de revisión fue que deberían buscarse inhibidores de aquellas enzimas que de antemano son limitantes en los parásitos. Además se enfatizó que para la validación de blancos terapéuticos en el metabolismo antioxidante de los tripanosomátidos se requieren aplicar criterios adicionales a los de validación genética, es decir, que aunque las enzimas sean esenciales, deben de tener una función principal en controlar la vía metabólica.

1.6. Estrategias actuales de validación de blancos terapéuticos

Desde la descripción inicial de las vías metabólicas y hasta la fecha, algunos de los criterios para seleccionar blancos de intervención terapéutica para combatir enfermedades tales como el cáncer o algunas generadas por organismos patógenos se basan en diseñar fármacos contra las enzimas que se reportan como las enzimas "marcapaso", "cuello de botella" o "paso limitante". De manera alternativa se considera a las enzimas particulares de parásitos que no están presentes en el hospedero humano o aquellas que están modificadas en el proceso patológico o, en último caso, a las enzimas modelo de estudio del investigador. Además de los problemas de accesibilidad del fármaco al blanco y de problemas de toxicidad para el hospedero, la selección de un blanco terapéutico inadecuado puede llevar al fracaso a una buena estrategia terapéutica farmacológica. Debido a esto, es necesario realizar una validación y caracterización adecuada de los blancos terapéuticos con lo cual se podrán diseñar fármacos que cumplan con las características requeridas para que un fármaco sea clínicamente exitoso (TPPs; Target Product Profile) (Wyatt *et al*, 2011).

De acuerdo con la Unidad de Descubrimiento de Fármacos de la Universidad de Dundee, Reino Unido, la valoración de enzimas para el diseño de fármacos debe cumplir con las siguientes características:

1) una estructura potencialmente adecuada para la unión de un inhibidor (druggability) o bien que ya existan inhibidores de esa enzima.

2) que no exista un homólogo en el hospedero o que en su caso no sea esencial para el mismo.

3) que no tenga isoformas que puedan no ser inhibidas (potencial de resistencia).

4) que se cuente con información estructural de las proteínas (cristales a una resolución de <2.3 Å).

5) que se tenga la validación genética y química de que esa enzima es esencial para el crecimiento y la supervivencia del organismo.

Sin embargo, en cuanto a este último requerimiento existen varias desventajas ya que existen pocos inhibidores altamente específicos que afecten solamente un blanco. Así mismo, desde el punto de vista genético, esta estrategia no permite identificar blancos que no sean genes, no distingue entre requerimientos estructurales y catalíticos, pueden existir genes multicopia, así como tener mutaciones compensatorias. Además en algunos organismos no existen las técnicas necesarias para realizar este tipo de ensayos genéticos tales como knock-out o knock-down (Wyatt *et al*, 2011).

Considerando esto, el análisis de control metabólico (MCA por las siglas en inglés de Metabolic Control Analysis) es un enfoque bioquímico que puede ser adicional a la validación genética para la búsqueda de blancos terapéuticos ya que permite resaltar de entre todas las enzimas consideradas esenciales genéticamente, a aquellas que son líderes en la vía metabólica y que por lo tanto requerirán ser inhibidas en menor grado para obtener un efecto negativo en la vía. Además, es una alternativa de validación de blancos terapéuticos en organismos en donde los ensayos genéticos son limitados, tales como *T. cruzi* y tiene la ventaja adicional que no requiere *a priori* la utilización de inhibidores específicos para cada enzima.

1.6.1 Estudio de redes metabólicas para la identificación de blancos terapéuticos

En el marco de un enfoque metabólico, las enzimas con mayor potencial terapéutico en una vía metabólica deben ser aquéllas que tienen un control importante sobre su funcionamiento, es decir en el caso que nos ocupa en esta tesis del metabolismo del $T(SH)_2$, son aquellas que controlan el flujo de síntesis y la concentración del metabolito. Por lo tanto, en lugar de analizar el potencial terapéutico estudiando las enzimas aisladas, se requieren análisis sistémicos, es decir, enfoques en los que se evalúa la participación de cada enzima en el control de la red metabólica completa. Por lo tanto, se decidió aplicar el MCA el cual es un enfoque de la Bioquímica actual que estudia el control del metabolismo de tal manera que permite determinar *cuantitativamente* la importancia relativa de cada enzima en el funcionamiento de la vía completa, además de que ayuda a identificar los mecanismos por los cuales una enzima controla o no controla una vía metabólica.

1.6.2 Fundamentos del MCA

La teoría del control metabólico (MCA) cuyos fundamentos se establecieron formalmente desde finales de 1970 ha demostrado experimentalmente que el control de una vía no reside únicamente en una enzima (el rate-limiting step) sino que está distribuido en diferentes grados en todas las enzimas de la vía, incluyendo a las reacciones que suministran y consumen un metabolito. Así, este enfoque descarta la existencia de una única enzima o paso limitante en las vías metabólicas y el control del metabolismo lo analiza de una manera más dinámica (Fell, 1997; ver artículo por Moreno-Sánchez et al, 2008 del cual soy coautora en el anexo de esta tesis para una explicación más detallada del MCA).

El MCA permite determinar de manera cuantitativa el grado de control que ejerce cada una de las enzimas de una vía metabólica sobre su flujo o sobre la concentración de un intermediario. El grado de control que una enzima tiene sobre el flujo de la vía se denomina coeficiente de control de flujo (C_{Ei}^{J}) mientras que el que tiene sobre la concentración de un intermediario es el coeficiente de control de concentración (C_{Ei}^{X}) donde C es coeficiente, *J* es flujo, *X* es la concentración del

metabolito y *Ei* es la actividad de la enzima/transportador/proceso celular *i* de la vía metabólica.

El C_{Ei}^{J} se define matemáticamente (Ecuación 1) como la variación en el flujo *J* de una vía metabólica cuando la actividad de una enzima se modifica infinitesimalmente (*dJ/dEi*). Para que el coeficiente carezca de unidades, se multiplica por el factor escalar (E_{i0}/J_0) el cual representa la actividad enzimática de la reacción metabólica y el flujo de la vía en condiciones control previo a la manipulación de la actividad enzimática.

$$C_{Ei}^{J} = \frac{dJ}{dEi} \cdot \frac{Eio}{Jo} \qquad \textit{(Ec. 1)}$$

La suma de los coeficientes de control de flujo de todas las enzimas de la vía debe de ser igual a 1 (Teorema de la sumatoria). Esto quiere decir que el 100% del control recae solamente en las reacciones de la vía metabólica (Fell, 1997; Moreno-Sánchez *et al*, 2008). Por ejemplo, en una vía metabólica lineal, una enzima que tenga un coeficiente de control de flujo de 1 (esto es, un verdadero paso limitante) será aquella enzima que al variar en la célula en un 1% su actividad, el flujo metabólico variará en un 1%.

Por otro lado, el C_{Ei}^{X} se define como el cambio en la concentración de un intermediario de la vía al variar la actividad de una enzima de la vía metabólica, multiplicado por el factor escalar

$$C_{Ei}^{X} = \frac{dX}{dEi} \cdot \frac{Eio}{Xo} \qquad \textit{(Ec. 2)}$$

La suma de los coeficientes de control de concentración de las enzimas sobre un metabolito particular debe ser 0, debido a que van a existir enzimas que lo producen pero también otras que lo consumen (Moreno-Sánchez *et al*, 2008). Es necesario enfatizar que los C_{Ei}^{J} y C_{Ei}^{X} son propiedades sistémicas de las enzimas, es decir que solamente pueden determinarse cuando las enzimas están trabajando en la vía metabólica, por lo que sus valores no pueden deducirse estudiando las enzimas aisladas.

Para determinar experimentalmente el C_{Ei}^{J} de una enzima en la vía se debe variar la actividad de ésta en la célula, manteniendo constantes la actividad de las demás enzimas de la vía. La gráfica teórica que se puede obtener se muestra en la Figura 5. El C_{Ei}^{J} se calcula de la pendiente de la recta tangente (la derivada) en la actividad fisiológica de enzima (100% de actividad). La figura 5 muestra la titulación de dos enzimas con diferente grado de control. Cerca del punto de interés del 100% de actividad enzimática es claro que la variación en la actividad de la enzima E1 tiene grandes cambios en el flujo de la vía; por otro lado, la enzima E2 es saturante para el flujo metabólico ya que si se disminuye su actividad no se producen decrementos significativos en el flujo. En el ejemplo sencillo de la figura, la enzima E1 tiene mayor control de flujo que la enzima E2. Cabe mencionar que el 100% de actividad de cada enzima en la célula puede ser muy diferente; en el caso del ejemplo anterior, la actividad enzimática de E2 debe ser por lo menos un orden de magnitud mayor que la de E1, de tal manera que ésta ultima es la que esencialmente controla el flujo de la vía.

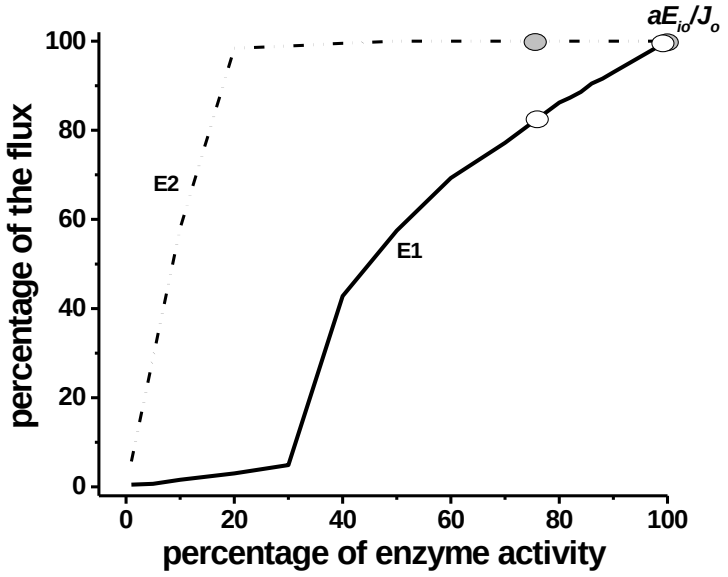

Fig. 5. Determinación experimental del coeficiente de control de flujo Este coeficiente se determina modificando la actividad de una enzima y midiendo el flujo de la vía metabólica en cada condición. El C_{Ei}^{J} será la pendiene de la recta tangente en las condiciones control (100%). La enzima 1 (E1) tiene un control mayor que la enzima 2 (E2) (Modificado de Saavedra *et al*, 2011)

Los C_{Ei}^{J} y C_{Ei}^{X} de las enzimas están directamente relacionados con sus propiedades cinéticas individuales a través del coeficiente de elasticidad (ε_X^{vi}), el cual se define como la variación en la velocidad *v* de una enzima *i* de la vía cuando uno de sus ligandos (sustratos, productos o moduladores alostéricos; X) varía en proporciones infinitesimales.

$$\varepsilon_X^{vi} = \frac{dvi}{dX} \cdot \frac{Xo}{vio} \qquad \textit{(Ec. 3)}$$

Es necesario distinguir que a diferencia de la gráfica de una cinética enzimática clásica en la que se varía el sustrato y se mide la velocidad parcial de la enzima en el ensayo, en el caso del coeficiente de elasticidad la *vi* se refiere a la velocidad *v*a la que trabaja la enzima *i* en la vía metabólica completa. Por ejemplo, para el caso de una vía lineal, la *vi* correspondería al flujo total de la vía metabólica ya que en el estado estacionario metabólico, todas las enzimas de la vía están trabajando a la misma velocidad parcial. Los ε_X^{vi} pueden ser positivos si el ligando incrementa la

velocidad de la enzima en la vía y son negativos si el ligando disminuye la velocidad. En otras palabras, el $\mathcal{E}_X^{vi}$ describe la capacidad de respuesta de cada enzima a cambios en la concentración de los metabolitos en el estado estacionario metabólico. Por ejemplo, si al variar la concentración de uno de sus sustratos en la célula la enzima no incrementa su velocidad (por ejemplo cuando ésta ya se encuentra saturada por el ligando) la enzima tiene una elasticidad cercana a 0 ($\mathcal{E}_X^{vi} = 0$) y pone un freno al flujo de la vía. Al contrario, si la enzima puede responder satisfactoriamente a los cambios en las concentraciones de sus ligandos en la célula, la enzima tendrá una elasticidad alta ($\mathcal{E}_X^{vi} = 1$) y no representa una limitación al flujo de la vía. Esto quiere decir que el C_{Ei}^J de una enzima con una elasticidad baja hacia el sustrato, tendrá un coeficiente de control alto sobre el flujo de una vía debido a que ya no puede variar su velocidad al presentarse un cambio en sus ligandos; por otro lado, una enzima con elasticidad alta tendrá un control bajo sobre el flujo de la vía ya que podrá ajustar su velocidad a los cambios en la concentración de sus ligandos dependiendo de las necesidades (Fell, 1997; Moreno-Sánchez *et al*, 2008).

A partir de los coeficientes de elasticidad y aplicando el Teorema de la conectividad que dice que la suma de la multiplicación de los coeficientes de control por la elasticidades es igual a cero, se pueden obtener los C_{Ei}^J de cada enzima de la vía metabólica.

$$\frac{C_{E1}^J}{C_{E2}^J} = -\frac{\varepsilon_X^{v2}}{\varepsilon_X^{v1}} \qquad \textit{(Ec. 4)}$$

Para determinar estos coeficientes de control se requiere de un gran esfuerzo intelectual para poder diseñar los experimentos de manipulación de las actividades enzimáticas en la célula y llevar a cabo el experimento que se muestra en la Fig. 5 o para diseñar la estrategia experimental para determinar los coeficientes elasticidad para poder calcular los coeficientes de control de cada una de las enzimas de una vía metabólica. Sin embargo, el desarrollo de herramientas bioinformáticas poderosas y la evolución del MCA como un enfoque de Biología de Sistemas

(Systems Biology) ha permitido poder construir modelos cinético-matemáticos que pueden replicar el comportamiento de la vía *in vivo*.

1.6.3 Biología de Sistemas y Análisis de Control Metabólico

La Biología de Sistemas (SB; o Systems Biology) es la ciencia que se enfoca en estudiar las funciones biológicas que emergen de las interacciones entre los componentes de un sistema que no se puede dilucidar cuando se estudian de manera aislada (Westerhoff, 2011). Por ejemplo, cuando las enzimas trabajan en una vía metabólica emergen propiedades regulatorias entre ellas las cuales no se pueden dilucidar fácilmente cuando se analizan las propiedades cinéticas individuales de cada enzima.

Se puede considerar que la biología de sistemas es la fusión de dos ramas del conocimiento científico, la biológica y la matemática. La rama biológica inició con el desarrollo de la biología molecular, desde el descubrimiento del código genético y se fue desarrollando hasta llegar a la secuenciación de genomas de diversos organismos (Westerhoff y Palsson, 2004). Esta rama se desarrolló posteriormente hasta la genómica funcional (Westerhoff *et al*, 2007). Por otro lado, la parte sistémica o matemática de SB ha evolucionado desde sus bases, la termodinámica alejada del equilibrio (la cual buscaba explicar y cuantificar la interacción entre sistemas acoplados) y la cinética enzimática, hasta el desarrollo de modelos matemáticos que buscan integrar y analizar a la célula como un sistema y de esta manera entender por qué las macromoléculas funcionan diferente cuando se encuentran aisladas y cuando funcionan en un sistema complejo como lo es una vía metabólica o una vía de señalización (Westerhoff y Palsson, 2004; Westerhoff *et al*, 2007). Este tipo de análisis se basa en enfoques tales como el MCA (Westerhoff y Palsson, 2004). Actualmente, la SB une estas dos ramas para poder analizar al sistema completo (Westerhoff y Palsson, 2004) y no solamente analizar al sistema desde un punto de vista de biología molecular o del control de una vía metabólica sino entender los

mecanismo de regulación que subyacen en el funcionamiento de una célula (Westerhoff *et al*, 2010).

Existen dos tipos de enfoques de SB a través de las cuales se pueden estudiar los sistemas biológicos. El primero es conocido como el "top –down systems biology", el cual busca patrones de comportamiento a partir de un todo (de lo general) y busca desarrollar leyes empíricas y relaciones causa-efecto (Westerhoff, 2011). De esta manera, el enfoque "top-down" es un método que caracteriza células utilizando sistemas provenientes de los "omics" (por ejemplo, transcriptómica y metabolómica) combinados con modelos matemáticos (Bruggeman *et al*, 2007). El otro enfoque es el "bottom-up systems biology" el cual estudia las propiedades individuales de los componentes más básicos, es decir las enzimas y las propiedades que emergen al interaccionar unas con otras, es decir al formar parte de vías metabólicas o de señalización (Westerhoff, 2011). Por lo tanto, el enfoque bottom-up construye un modelo matemático detallado basado en las propiedades moleculares de los componentes individuales del sistema; este enfoque permite realizar un estudio cuantitativo y predictivo así como entender los mecanismos de regulación y control que subyacen en los diferentes procesos celulares (Bruggeman *et al*, 2007). La construcción de modelos cinéticos de vías metabólicas como el que se desarrolló en este proyecto de tesis de doctorado es parte del enfoque bottom-up SB el cual integra la información obtenida de enzimas individuales en un programa de cómputo para producir un modelo matemático que pueda predecir el comportamiento de una vía bajo ciertas condiciones fisiológicas.

1.6.4. Modelado metabólico y MCA para la identificación de nuevos blancos terapéuticos

Una manera de determinar la distribución de control (coeficientes de control) de las enzimas de una vía metabólica es a través de la construcción de un modelo matemático que pueda predecir el comportamiento de la vía. Estos modelos permiten analizar un sistema que es difícil de entender debido a la magnitud o grado de complejidad (Wildermuth, 2000). Los modelos cinético-matemáticos que pueden

realizar MCA consideran la estequiometria de cada una de las reacciones, las *Km*, *Ki* y *Kp* de cada una de las enzimas por sustratos, productos y efectores, las ecuaciones de velocidad de cada una de las enzimas, las *Keq* así como las velocidades de las enzimas, concentración de intermediarios intracelulares y flujos metabólicos en la misma célula y en un estado metabólico específico (Moreno-Sánchez *et al*, 2008). De estos datos, los parámetros individuales de las enzimas (cinéticos y termodinámicos) así como los valores de *Vmax* en el extracto se utilizan para la construcción del modelo, mientras que los flujos y la concentración de intermediarios se utilizan para su validación. Una vez que se cuenta con esta información experimental se utilizan programas de computación de modelado metabólico tales como Metamodel (Cornish-Bowden y Hofmeyr, 1991), WinScamp (Sauro, 1993) (http://www.sys-bio.org/) PysCES (http://pysces.sourceforge.net) (Olivier *et al*, 2005). Uno de los más utilizados es el GEPASI (http://www.gepasi.org/ ; Mendes 1993) y su actualización COPASI (Complex Pathway Simulator (http://www.copasi.org; Hoops *et al*, 2006).

Las ventajas que presentan la construcción de estos modelos es que pueden describir el comportamiento de una vía en un estado estacionario evaluado experimentalmente y permiten analizar la respuesta de todo el sistema a diferentes perturbaciones hipotéticas (Moreno-Sánchez *et al*, 2008; Wildermuth, 2000). El modelado metabólico permite identificar propiedades nuevas del sistema que no se pueden determinar estudiando a las enzimas de manera aislada (Westerhoff, 2011; Kolodkin *et al*, 2011). Por otro lado, un modelo cinético validado, puede ser utilizado como un laboratorio virtual en el que se pueden integrar concentraciones de metabolitos y actividades enzimáticas intracelulares determinadas en otros estados estacionarios para poder predecir el comportamiento de la vía metabólica en esa nueva condición. Uno de los objetivos más ambiciosos del modelado metabólico es construir células virtuales (“silicon cells”) de modelos biológicos que ayuden a entender los mecanismos de regulación metabólica o de transducción de señales que subyacen en el comportamiento celular y aplicar estos modelos a la biotecnología y a la medicina (Snoep, 2005).

Una de las aplicaciones más importantes del MCA y de SB es la identificación de blancos terapéuticos. Los coeficientes de control de cada enzima permiten determinar qué enzimas/transportadores o procesos celulares ejercen un control importante en el sistema de tal manera que nos pueden permitir establecer prioridades de blancos terapéuticos en una vía metabólica para su intervención farmacológica. Por lo tanto, los mejores blancos terapéuticos son aquellas enzimas que tengan los coeficientes de control más altos ya que será necesario inhibirlas poco para obtener un efecto importante en el flujo o en la concentración de un metabolito (Fig. 5) (Moreno-Sánchez *et al*, 2008; Saavedra *et al*, 2011). Así, inhibiendo a las enzimas que mayoritariamente controlan la vía se pueden utilizar menores concentraciones del inhibidor o del fármaco, lo que puede disminuir los efectos secundarios adversos así como la inespecificidad. Además, comparando las diferencias entre la distribución de control de una vía por ejemplo, entre el hospedero y un parásito, o bien entre células tumorales y no tumorales, se pueden identificar a las enzimas que pueden ser explotadas como blancos terapéuticos (Hornberg *et al*, 2007). Debido a su naturaleza de análisis integral de las vías metabólicas, este enfoque resalta la importancia de una terapia combinatoria para diferentes enfermedades (Cascante *et al*, 2002; Saavedra *et al*, 2007; Marín-Hernández *et al,* 2011; Kolodkin *et al*, 2011). Así, un enfoque diferente de validación de blancos terapéuticos es el de la vía de glioxilasa en *Leishmania infantum*, en el cual el modelado descartó a las enzimas de esta vía como blancos terapéuticos adecuados ya que se determinó que la concentración de metilglioxal está determinada por la concentración de $T(SH)_2$ y su síntesis y que las enzimas del sistema de la glioxalasa no participan en el control de la concentración del metilglioxal (Sousa *et al*, 2005).

Debido a que se requiere de una gran cantidad de datos experimentales para la construcción de modelos cinéticos, existen pocos reportados en la literatura de los cuales la mayoría son de la glucólisis en diversos organismos (para una base de datos consultar http://jjj.biochem.sun.ac.za/database/). En el caso de parásitos que infectan humanos, solamente se han reportado tres modelos cinéticos: para la glucólisis en *T. brucei* (Bakker *et al,* 1999*;* Albert *et al*, 2005); un modelo sencillo del sistema de la glioxalasa en *Leishmania* (Sousa *et al*, 2005) y el modelo cinético de la

glucólisis en *Entamoeba histolytica* construido por el grupo de investigación en el que realicé esta tesis (Saavedra *et al*, 2007).

Actualmente existe la iniciativa para la construcción de la célula virtual de *T. brucei* cuya finalidad es construir un modelo multi-escala de la fisiología del parásito (Bakker *et al*, 2010; http://silicotryp.ibls.gla.ac.uk/wiki/Main_Page). En dicho proyecto están involucrados siete laboratorios localizados en el Reino Unido, Holanda y Alemania. A partir del modelo de la glucólisis de *T. brucei*, la idea de este consorcio es agregar los modelos de la vía de las pentosas y el metabolismo del $T(SH)_2$ (Bakker, *et al*, 2010). Aunque ya existen avances con respecto a la adición de la vía de las pentosas (http://silicotryp.ibls.gla.ac.uk/wiki/Main_Page#Current_model_and_extensions), la vía del metabolismo del $T(SH)_2$ no la han podido modelar debido a la falta de una gran cantidad de información cinética y metabólica (tesis de doctorado Gu,Xu, 2010;Universidad de Glasgow; http://theses.gla.ac.uk/1618). Por lo tanto el modelo que se construyó durante este trabajo de tesis de doctorado es hasta el momento el primero reportado para el metabolismo del $T(SH)_2$, lo que resalta la originalidad y relevancia del proyecto.

2. PLANTEAMIENTO DEL PROBLEMA

La validación de blancos terapéuticos en el metabolismo del $T(SH)_2$ de *T. brucei* y *Leishmania* empleando la estrategia genética de inhibición de la expresión en las células permitió establecer que TODAS las enzimas de la vía analizadas son esenciales para el manejo del estrés oxidante, y es muy común que esta información la apliquen también al metabolismo antioxidante de *T. cruzi*. Debido a lo anterior es necesario aplicar criterios adicionales a los de esencialidad determinada genéticamente para priorizar e identificar aquella(s) enzimas de la vía que pudieran tener el mayor potencial terapéutico. Aunado a lo anterior, esta estrategia de validación genética no se ha podido utilizar para *T. cruzi* debido a que las herramientas de manipulación genética en este parásito son aún limitadas.

La evaluación cuantitativa de la distribución del control entre cada una de las enzimas permitirá identificar aquellas que tienen una función primordial para su funcionamiento. Desde el punto de vista metabólico, las enzimas que principalmente controlan la vía tendrán el mayor potencial terapéutico ya que su inhibición leve o moderada afectarán más el funcionamiento de la vía metabólica que la inhibición de una enzima que controla poco la vía. El enfoque que se decidió seguir en este proyecto fue determinar la estructura de control del metabolismo del $T(SH)_2$ en *T. cruzi* a través de la construcción de un modelo cinético (enfoque bottom-up Systems Biology) y la aplicación de los fundamentos del MCA que permita predecir el comportamiento de la vía metabólica en el parásito y poder determinar los coeficientes de control de cada una de las enzimas de la vía metabólica.

3. HIPÓTESIS

El control del flujo y de la concentración de $T(SH)_2$ recaerá principalmente en la γECS y la TryS debido a su baja eficiencia catalítica (*Vm*/*Km*) en los parásitos mientras que el sistema de desintoxicación de peróxidos y la TryR no ejercerán un control significativo sobre la vía debido a su alta eficiencia catalítica en el parásito.

4. OBJETIVO GENERAL DEL PROYECTO

Determinar cuantitativamente el grado de control que cada enzima tiene sobre la síntesis y la concentración de $T(SH)_2$ a través de modelado cinético y la aplicación del análisis del control metabólico.

5. OBJETIVOS PARTICULARES

- Clonar los genes, sobre-expresar en bacterias y purificar a la γECS, GS, TryS y TryR de *Trypanosoma cruzi*
- Caracterizar cinéticamente *in vitro* a estas enzimas en condiciones de pH y temperatura cercanas a las fisiológicas (7.4/37°C) y bajo las mismas condiciones experimentales.
- Determinar los parámetros de actividades enzimáticas, concentración de intermediarios y flujos de la vía en epimastigotes de *T. cruzi* para construir la base de datos experimentales en la misma cepa y bajo las mismas condiciones experimentales.
- Construir el modelo cinético en el programa de modelado metabólico GEPASI/COPASI.
- Validar las predicciones del modelo comparando con la respuesta de la vía en parásitos sometidos a diferentes estados estacionarios.

6. ESTRATEGIA EXPERIMENTAL

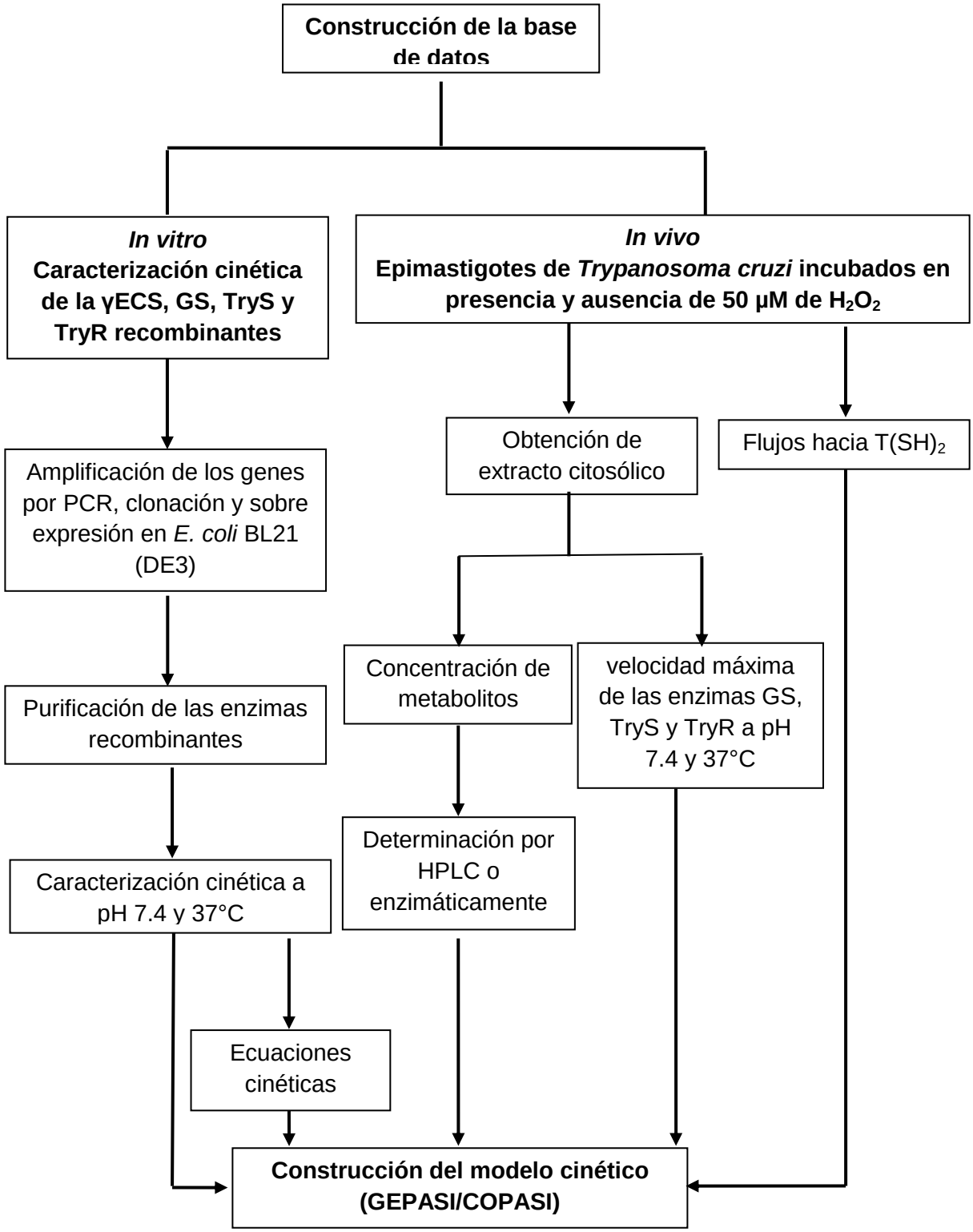

7. METODOLOGÍA

7.1 Determinación de los parámetros necesarios para la construcción del modelo cinético.

La mayor parte de la metodología utilizada en este proyecto se encuentra descrita de manera detallada en el artículo titulado “Drug target validation of the trypanothione pathway enzymes through metabolic modeling” que se incluye en la sección de resultados. A continuación se describe un resumen de la metodología.

La construcción de este modelo requirió la determinación de parámetros cinéticos de las enzimas involucradas en la vía así como de la determinación de la concentración de metabolitos, actividades enzimáticas y flujos de síntesis de $T(SH)_2$ en los parásitos.

Para llevar a cabo la caracterización cinética de la γECS, GS, TryS y TryR se obtuvieron a las enzimas recombinantes. Los genes que codifican para estas proteínas se amplificaron a partir de DNA genómico de *T. cruzi* de la cepa Ninoa, se clonaron y sobre expresaron en bacterias *E.coli* BL21 (DE3) fusionadas a una etiqueta de histidinas. Posteriormente, las enzimas se purificaron por cromatografía de afinidad a cobalto y se caracterizaron cinéticamente en condiciones cercanas a las fisiológicas (pH 7.4 y 37°C).

Las concentraciones de metabolitos, actividades enzimáticas de la vía y flujos de síntesis de $T(SH)_2$ se determinaron en epimastigotes de *T. cruzi* de la cepa Querétaro en tres condiciones experimentales : parásitos sin incubar (condición basal) e incubados durante 10 minutos en buffer PBS con 20 mM de glucosa en ausencia (condición control) o en presencia de 50 µM de H_2O_2 (condición de estrés).

Para determinar la concentración de metabolitos se obtuvo el extracto citosólico y desproteinizado de los parásitos. Los tioles solubles totales, Cys, γEC, GSH y $T(SH)_2$, se separaron por HPLC, se derivatizaron post-columna con el reactivo de Ellman (ácido 5,5’-ditio-bis(2-nitrobenzoico); DTNB) y se cuantificaron espectrofotométricamente . Los metabolitos Glu, Gly y Spd primero se derivatizaron

con ortho-pthalaldehído (OPA) para los dos primeros y con cloruro de dansilo para el tercero, se separaron por HPLC y se cuantificaron por fluorescencia. El ATP, TS_2 y $NADP^+$ se determinaron enzimáticamente utilizando ensayos acoplados con hexocinasa más glucosa-6-fosfato deshidrogenasa (G6PDH), TryR o G6PDH, respectivamente.

Uno de los aportes más importantes en cuanto a la metodología desarrollada en este trabajo fue haber establecido protocolos para la medición de las actividades de la GS y TryS **en extractos de los parásitos.** Los extractos citosólicos de los tripanosomátidos tienen una actividad de consumo de ATP contaminante muy alto que dificulta cuantificar la producción de ADP de las enzimas de interés utilizando el ensayo acoplado de la piruvato cinasa y lactato deshidrogenasa (PK/LDH). La determinación de este parámetro de velocidad enzimática es crítico para la construcción de un modelo cinético. La falta de estos datos experimentales ha sido el principal impedimento por el cual el grupo que está construyendo la célula virtual de *T. brucei* no ha podido construir el bloque correspondiente al metabolismo del $T(SH)_2$. Además, los diversos grupos que estudian esta vía metabólica desde hace décadas no han podido medir las actividades de estas enzimas en parásitos. Las actividades de GS y TryS en extractos del parásito se determinaron en ensayos de punto final en donde la reacción se incuba durante 30 minutos, se para con ácido perclórico al 3% y se neutraliza con KOH y Tris. Posteriormente se cuantifica el ADP producido utilizando el ensayo enzimático de PK/LDH. Para cada ensayo se prepararon dos reacciones, la reacción control no contenía a uno de los sustratos específicos (Gly o Spd); la segunda reacción contenía los tres sustratos de la GS o TryS. De esta manera la actividad específica de la GS y TryS se calculó de la resta de los nmoles de ADP presentes en la reacción con todos los sustratos menos los nmoles de ADP en la reacción control. En el caso de la TryS, la diferencia se dividió entre dos debido a que la enzima produce 2 ADPs por cada $T(SH)_2$ sintetizado. Como control del ensayo enzimático, siempre se aseguró que la actividad específica de cada enzima fuera lineal con respecto a la cantidad de proteína del extracto lo que nos aseguraba que la reacción que se estaba midiendo era específica de las enzimas de interés. Algo importante de resaltar es que este protocolo se puede

utilizar para medir estas enzimas en extractos de los otros estadios del parásito de otros tripanosomátidos siempre y cuando el ensayo se realice en condiciones de velocidad inicial.

Por otro lado, la actividad de la TryR se determinó monitoreando espectrofotométricamente la oxidación de NADPH en presencia de TS_2.

Los flujos hacia $T(SH)_2$se determinaron incubando a los parásitos en buffer PBS con 20 mM de glucosa en ausencia o en presencia de 50 µM de H_2O_2 durante 0, 5 y 10 minutos. Posteriormente, se cuantificó el $T(SH)_2$ presente en cada una de estas condiciones. El flujo se calculó a partir de la pendiente de la gráfica obtenida al graficar los datos obtenidos.

Para construir el modelo se utilizó el programa GEPASI y su versión actualizada COPASI. Para esto, se introdujeron los parámetros cinéticos de las enzimas recombinantes (valores de *Km*, *Ki* para los ligandos) y la *Vmax* de las enzimas en el extracto así como las concentraciones iniciales de metabolitos en los parásitos. Las reacciones que se incluyeron en el modelo fueron las de síntesis de GSH (γECS, GS); síntesis de $T(SH)_2$ por la TryS, el suministro de poliaminas (transportador de Spd); la demanda de $T(SH)_2$ (estrés oxidante) y su regeneración por la TryR; las fugas de metabolitos (Spd, GSH y $T(SH)_2$) que se observaron experimentalmente. Además se incluyó el sustrato H_2O_2 en la reacción de demanda de $T(SH)_2$ y la fuga de GSH para poder simular condiciones de ausencia y presencia de estrés. A cada una de las reacciones se le asignó una ecuación de velocidad que está relacionada con su mecanismo cinético de reacción.

Para validar el modelo se compararon las concentraciones de intermediarios y de flujos metabólicos que predecía el modelo con las determinadas experimentalmente en los parásitos en las distintas condiciones.

7.2 Metodología de los resultados no incluidos en el artículo

7.2.1 Determinación de la actividad de la GS y la TryS en extractos del parásito utilizando diferentes inhibidores de ATPasas.

A continuación se describen experimentos posteriores a la publicación del artículo para mejorar el método de medición de dichas actividades. Esto se debió a que los revisores del artículo criticaban el hecho de que la actividad de la enzima fuera de solamente el 8-11% del consumo total de ADP por el extracto. Con el objetivo de disminuir la actividad contaminante de ATPasa, se utilizó una mezcla de inhibidores de ATPasas que se agregó al medio de reacción enzimático. La mezcla contenía los siguientes inhibidores: 5 mM azida y 0.01 mg/mL oligomicina para las F-ATPasas; 5 mM molibdato y 0.2 mM vanadato para las P-ATPasas. Los extractos clarificados se prepararon de la siguiente manera: los epimastigotes de *T. cruzi* de la cepa Querétaro se cosecharon a 4500 x g y se lavaron dos veces con buffer PBS (137 mM NaCl, 2.7 mM KCl, 10 mM Na_2HPO_4, 2 mM KH_2PO_4 pH 7.4). Las células se resuspendieron en 0.1 mL de buffer de lisis (20 mM HEPES pH 7.4, 1 mM EDTA, 0.15 mM KCl, 1 mM DTT y 1 mMfluoruro de fenil metil sulfonilo (PMSF)) y se rompieron por tres ciclos de congelación/descongelación. El lisado total se centrifugó a 20 817 x g durante 10 min y la actividad de las enzimas se determinó inmediatamente en el clarificado.

Las reacciones se hicieron de la siguiente manera: en 0.5 ml de buffer 40 mM HEPES-1 mM EDTA pH 7.4 se mezclaron 10 mM de $MgCl_2$, 2 mM de ATP, 0.4 mM de γEC y 8 mM de Gly para la GS; y 10 mM de $MgCl_2$, 2 mM de ATP, 11 mM de Spd y 8 mM de GSH para la TryS y se inició la reacción con 0.1-0.2 mg de proteína del extracto. En paralelo, se hizo una mezcla de reacción similar sin incluir Gly para la GS y sin Spd para la TryS las cuales se utilizaron como controles de la actividad de ATPasa; además se realizaron las mismas mezclas de reacción en presencia de la mezcla de inhibidores. La reacción se incubó durante 15 ó 30 minutos a 37 °C y se detuvieron con ácido perclórico al 3% (v/v) y se centrifugaron a 20 817 x g a 4°C durante 10 minutos para eliminar la proteína precipitada. Los extractos se neutralizaron con diferentes volúmenes de 3M KOH/0.1 M Tris. El ADP se cuantificó

espectrofotométricamente usando el ensayo acoplado a la PYK/LDH. La cantidad de nmoles producidos por la reacción de GS o TryS se obtuvieron de la diferencia entre la reacción que contenía todos los sustratos y su control.

7.2.2 Polimorfismos del gen de GS en diferentes cepas de Trypanosoma cruzi

Debido a que no existían reportes para la GS en ningún tripanosomátido, se caracterizó tanto genéticamente como cinéticamente a esta enzima en *T. cruzi* y se preparó un artículo para su publicación. Sin embargo, debido a la exigencia de los revisores, los datos cinéticos se tuvieron que incluir en el artículo "Drug target validation of the trypanothione pathway enzymes through metabolic modeling" y la caracterización genética ya no se incluyó. A continuación se describe la metodología utilizada para determinar cuántos genes de GS están presentes en las cepas Ninoa y Querétaro, las cuales se utilizaron para la obtención de las enzimas recombinantes y para la determinación de actividades en el parásito, respectivamente. Así mismo, se comparó con lo que ocurre en el genoma de la cepa CL Brener en el que existen dos marcos de lectura abiertos que codifican para esta enzima.

Southern Blot

El DNA genómico se aisló de epimastigotes de *T. cruzi* de las cepas CL Brener, Ninoa y Querétaro como se describió en Berzunza-Cruz *et al*, (2002). El DNA se digirió con las enzimas de restricción *Hind* III o *Pst* I y los fragmentos se separaron por electroforesis en geles de agarosa y se realizó el análisis tipo Southern blot como se describió en Palma-Gutiérrez *et al* (2008) usando como sonda el gen de TcGS de la cepa Ninoa el cual teníamos clonado y secuenciado.

Expresión del mRNA de GS en las cepas Ninoa, Querétaro y CL Brener de T. cruzi

a) Aislamento de RNA

Se cosecharon $2x10^8$ epimastigotes a 4500 x g por 15 min y se lavaron dos veces con buffer PBS. Se eliminó el sobrenadante y se mantuvo el precipitado en hielo. Se agregó 1 mL de Trizol (Sigma) se agitó por 1 min, se incubó por 10 min a 4°C y después 5 min a temperatura ambiente. Se adicionaron 200 µL de cloroformo, se mezcló por inversión y se incubó por 3 min a temperatura ambiente. Pasado este

tiempo, la mezcla se centrifugó a 12 800 g durante 15 min a 4°C y se recuperó la fase acuosa. Se adicionó 1 volumen de alcohol isopropílico, se mezcló por inversión y se incubó por 10 min a temperatura ambiente. Se centrifugó a 12 800 g durante 15 min a 4°C y se decantó el sobrenadante. El precipitado se lavó con 1 mL de etanol al 75% frío, se mezcló por inversión con mucho cuidado, sin agitar, sólo se lavó por la superficie. Posteriormente, se centrifugó a 12 800 x g durante 15 min a 4°C; se decantó el sobrenadante se dejó secar la pastilla por 10 min y posteriormente se resuspendió en agua tratada con DEPC y se cuantificó el RNA.

Se trataron 18 µg de RNA con 1U de DNAsa incubando durante 15 min a temperatura ambiente. Se agregó EDTA a una concentración final de 2.5 mM y se calentó por 10 min a 65°C.

b) Síntesis de cDNA y amplificación del gen de la GS

En un volumen de 20 µl se mezcló lo siguiente: 5.5 mM $MgCl_2$, 0.5 mM de desoxiribonucleótidos (dNTPs), 2.5 µM de random hexamers, 250 ng oligo dT_{16}, 0.4 U de inhibidor de RNasa y 1.25 U de transcriptasa reversa. La síntesis de cDNA se llevó a cabo por incubaciones seriadas de 10 min a 25 °C, 30 min a 48ºC y 5 min a 95ºC. Se tomaron 5 µL de la reacción anterior y se realizó una reacción en cadena de la polimerasa (PCR) utilizando los cebadores diseñados para la GS descritos en el artículo (Olin-Sandoval *et al*, 2012). Los productos de PCR se separaron por electroforesis, se purificaron del gel y se digirieron con la enzima de restricción *Hind* III. Los productos de la digestión se separaron por electroforesis para verificar el resultado. En paralelo, se amplificó el gen de la GS a partir de DNA genómico y se procesaron de manera similar a los amplificados de GS a partir de cDNA.

8. RESULTADOS

8.1 Validación a través de modelado metabólico de algunas de las enzimas de la vía de síntesis de $T(SH)_2$ como blancos terapéuticos

Los resultados de este trabajo se publicaron en el siguiente artículo:

> Olin-Sandoval V, González-Chávez Z, Berzunza-Cruz M, Martínez I, Jasso-Chávez R, Becker I, Espinoza B, Moreno-Sánchez R, Saavedra E (2012) Drug target validation of the trypanothione pathway enzymes through metabolic modelling *FEBS J* 279, 1811-1833

A continuación se describe un resumen de los resultados.

Con el objetivo de validar a algunas de las enzimas del metabolismo del $T(SH)_2$ como blancos terapéuticos desde un enfoque de control metabólico aplicando los preceptos del MCA, se construyó un modelo cinético de la vía utilizando el programa de computadora GEPASI/COPASI. Para la construcción y validación del modelo se determinaron experimentalmente los parámetros cinéticos (*Km* y *Ki)* de las enzimas en su forma recombinante (γECS, GS, TryS, TryR); así como la *Vmax,* concentraciones de intermediarios y flujos de síntesis de $T(SH)_2$ en epimastigotes de *T. cruzi.*

Para la caracterización cinética de las enzimas fue necesario primero obtener a las enzimas recombinantes por lo que se amplificaron y clonaron cada uno de los genes y las proteínas se sobre expresaron en *E. coli* BL21 (DE3). Las proteínas se purificaron y caracterizaron cinéticamente bajo las mismas condiciones de pH y temperatura (pH 7.4 y 37°C) (Tabla 1). Es importante mencionar que la caracterización cinética de la GS que se realizó en este trabajo es la primera que se reporta para tripanosomátidos.

Como parte de la caracterización de las enzimas de la vía también se determinó si algún metabolito de la vía diferente a sus sustratos o productos ejercía algún efecto sobre su actividad (Tabla 1). La retro-inhibición de la γECS por GSH, el metabolito final de la síntesis de GSH, fue el único tipo de inhibición con relevancia fisiológica debido a que el valor de *Ki* se encontraba cercano al intervalo de concentración fisiológica.

Por otro lado, se determinaron las concentraciones de metabolitos, las actividades enzimáticas y los flujos de la vía en epimastigotes en tres condiciones diferentes: sin incubar (condición basal) e incubados en ausencia (condición control) y presencia de 50 µM de H_2O_2 (condición de estrés). Los metabolitos que cambiaron de manera estadísticamente significativa entre las condiciones experimentales fueron la Spd, la cual disminuyó en un 80% debido a la incubación; y el GSH, el cual disminuyó 48% en presencia de estrés con respecto a la condición control. En el caso del $T(SH)_2$, a pesar de no tener un cambio significativo en las diferentes condiciones, en la mayoría de los experimentos su concentración mantuvo una tendencia a disminuir en presencia de estrés con respecto a las condiciones basal y control (Tabla 2, columnas 2, 4 y 6).

Este trabajo reporta los primeros valores de actividades enzimáticas de GS y TryS en tripanosomátidos los cuales se encuentran entre 4-8 mU/mg de proteína celular. Estos valores de actividad son un orden de magnitud menores con respecto a la actividad de la TryR, la cual se encuentra entre 200-300 mU/ mg de proteína celular. Desafortunadamente, no se pudo determinar de manera confiable la actividad de γECS en el extracto debido a que su actividad debe de ser más baja que la de la GS y TryS y a la alta actividad contaminante de consumo de ATP en el extracto citosólico, aunado a que la enzima es catalíticamente poco eficiente.

Tabla 1. Caracterización cinética de las enzimas recombinantes de la vía de síntesis y regeneración de $T(SH)_2$

Enzima	*Tiol*			*Co-sustrato*	*Co-sustrato/coenzima*	*Efecto por otros metabolitos de la vía***
	Vmax*	***Kmapp****	***kcat/Kmapp*****	***Kmapp****	***Kmapp****	
γECS	0.37 ± 0.1 (3)	Cys 0.21 ± 0.1 (3)	$2.4x10^3$	Glu 0.13 ± 0.04 (3)	ATP 0.04 ± 0.012 (3)	K_{iGSH} 1.6 (2) $K_{iγEC}$ 0.43 (2) GSSG > 0.003
GS	2.04 ± 0.7 (3)	γEC 0.04 ± 0.01 (3)	$1.1x10^5$	Gly 1.2 ± 0.3 (3)	ATP 0.03 ± 0.01 (3)	$K_{iGSH\ versus\ Gly}$ 12 ± 0.6 $K_{iGSH\ versus\ ATP}$ 11 ± 1 $K_{iGSH\ versus\ γEC}$ 14.6 ± 5.6 TS_2>0.005 GSSG > 0.003 Spd, Spm > 2
TryS	1.04 ± 0.5 (3)	GSH 0.76 ± 0.21 (3)	$1.6x10^3$	Spd 0.86 ± 0.095 (3)	ATP 0.07 ± 0.04 (3)	GSSG > 0.003 $T(SH)_2$> 1 TS_2> 0.005
TryR	531 ± 137 (3)	TS_2 0.023 ± 0.006 (3)	$4.3x10^7$		NADPH 0.009 ± 0.005 (3)	$T(SH)_2$> 1

*U/mg proteína ** mM ***$M^{-1}s^{--1}$

Los flujos de síntesis de$T(SH)_2$ se determinaron en las condiciones control y de estrés. Se observó que el estrés oxidante promueve un incremento en el flujo hacia $T(SH)_2$ de casi el doble, de 1 a 1.9 nmol/min mg de proteína (Tabla 2, columnas 4 y 6). La velocidad de flujo tan baja hacia $T(SH)_2$ se debe principalmente a la baja actividad de las enzimas de síntesis de este metabolito.

Para la construcción del modelo se utilizaron los parámetros cinéticos de las enzimas recombinantes (valores de *Km*, *Ki* para los ligandos) y la *Vmax* de las enzimas en el extracto así como las concentraciones iniciales de metabolitos en los parásitos. Después de un extenso proceso iterativo de experimentación y modelado, el modelo se refinó comparando las concentraciones de intermediarios y de flujos metabólicos que predecía el modelo con aquéllas determinadas experimentalmente en los parásitos en las distintas condiciones. Las predicciones del modelo final dieron valores muy similares a los observados *in vivo* al variar la concentración de H_2O_2 (2.5 a 20 µM) así como el valor de la constante de velocidad de la fuga de GSH, Spd y demanda de $T(SH)_2$ (Tabla 2). La fidelidad de las predicciones del modelo con el comportamiento de la vía *in vivo* es un parámetro de validez que se aplica a los modelos cinéticos.

Predicciones del modelo validado

El modelo final al que se llegó es robusto ya que aumentando o disminuyendo los valores de *Km* y *Vmax* de cada enzima el modelo pudo predecir un estado estacionario estable. En dichas simulaciones la distribución de control de la vía permaneció en las mismas reacciones, aunque como cabe de esperarse, los valores absolutos de los coeficientes de control variaron. Sin embargo, el modelo no fue tan robusto a la variación en la concentración del H_2O_2 ya que a concentraciones mayores de 20 µM, la demanda de $T(SH)_2$ agotaba las pozas de este metabolito. A pesar de este inconveniente, las predicciones del modelo utilizando10 µM del peróxido eran similares a las que se habían determinado experimentalmente en parásitos expuestos a 50 µM del peróxido. Esto podría sugerir que *in vivo* los parásitos pudieran haber estado expuestos a concentraciones menores a los del bolo inicial y el resto del H_2O_2 reaccionó con el medio de incubación.

Coeficientes de control de las enzimas de la vía

Este modelo validado y robusto determinó que el flujo de síntesis de $T(SH)_2$ está controlado principalmente por la γECS, la TryS y el SpdT (Tabla 3) debido a la baja actividad y eficiencia catalítica de las enzimas en los parásitos; mientras que la concentración de $T(SH)_2$ está controlada principalmente por la demanda (estrés oxidante) y la TryR (Tabla 4) debido a la abundancia de estas enzimas y a que son las que directamente lo consumen o regeneran.

Experimentación virtual

El modelo permitió hacer el experimento virtual de “inhibir” la actividad de las enzimas de la vía de manera individual o combinada. Este tipo de experimentos no son posibles de realizar en *T. cruzi* porque no hay inhibidores específicos para cada enzima y los ensayos de manipulación genética son limitados y, aunque es factible de realizarse en *T. brucei* y *Leishmania,* se requeriría de un gran esfuerzo experimental.

Tabla 2. Metabolómica de la vía del $T(SH)_2$ en parásitos y concentraciones de metabolitos predichos por el modelo

condición	basal		control		+ estrés	
(min)	t=0		t=10		t=10 50 μM H_2O_2	
Metabolito (mM)*	*In vivo*	Modelo[#]	*In vivo*	Modelo[§]	*In vivo*	Modelo[&]
Cys	0.3 ± 0.14 (3)	**	0.4 ± 0.1(3) [d]	**	0.3 ± 0.07(3) [d,e]	**
γEC	0.15 ± 0.09 (3)	0.076	0.13 ± 0.08(3)	0.082	0.1 ± 0.04 (3)	0.09
GSH_{tot}	0.8 ± 0.26(4)	0.68	0.77 ± 0.3 (3)	0.92	0.4 ± 0.05 (3) [d, e]	0.5
$T(SH)_2$	3.8 ± 1.6(4)	6.7	5.9 ± 2.5(4)	7.1	4.2 ± 1.8 (4) [d]	1.7
TS_2	0.5± 0.24(3)	0.58	0.4±0.22(3)	0.47	0.6 ±0.12(4)	0.34
$NADP^+$	0.039±0.02(3)	0.026	0.026±0.012(3)[f]	0.026	0.012±0.004(3)[g,h]	0.025
NADPH	0.12[a]	0.08	0.084[a]	0.084	0.04[a]	0.085
Spd_{int}	1.2 ± 0.06 (3)	0.8	0.2 ± 0.08 (3)[c]	0.33	0.2 ± 0.13 (3)[c]	0.35
Spd_{ext}	0.0011[b]	**	0.0011[b]	**	0.0011[b]	**
ATP	4 ± 0.6 (3)	NI	4.6 ± 0.9(3)	NI	3.4 ± 1.1(3)	NI
J_{TryS} * **		0.88	1(2)	0.7	1.9(2)	0.5
$J_{TryR/\ demanda\ T(SH)2}$		252		248		246

considerando que 10^8 epimastigotes de *T. cruzi* corresponden a 3 µL. Los valores son el promedio ± SD. ** Metabolitos considerados fijos en el modelo. *** Flujos (J) en nmol min^{-1} mg proteína^{-1}. NI, no incluidos en el modelo. GSH_{tot} indica la concentración de GSH reducido y oxidado. [a] recalculado considerando que la proporción de NADP/NADPH es igual a 0.31 en epimatigotes de *T.cruzi* de la cepa CL Brener. [b] concentración de Spd en suero. Estadística t-student: [c] $p<0.01$ *vs* t=0; [d] $p<0.05$ *vs* t=0; [e] $p<0.05$ *vs* t=10; [f] $p<0.5$ *vs* t=0; [g] $p<0.2$ *vs* t=0; [h] $p<0.2$ *vs* t=10.

Tabla 3. Coeficientes de control de las enzimas sobre el flujo de síntesis de $T(SH)_2$

condición	basal	control	+ estrés
enzima/ proceso (Ei)		C^J_{Ei}*	
γECS	0.84	0.58	0.7
GS	0.0011	6.5×10^{-4}	9.8×10^{-4}
TryS	0.14	0.49	0.58
SpdT	0.016	0.24	0.22
TryR	-0.0029	-0.012	-0.0095
demanda de $T(SH)_2$	0.003	0.012	0.0095
suministro de NADPH	-3×10^{-5}	-1.6×10^{-4}	-5.5×10^{-5}
fuga de Spd	-1.5×10^{-4}	-0.17	-0.17
fuga de GSH	-8.2×10^{-5}	-0.14	-0.35
fuga deTS_2	1.5×10^{-4}	7.7×10^{-4}	6.9×10^{-4}

*El flujo que se consideró fue el de la reacción de la TryS. El signo negativo en el coeficiente de control de flujo indica que esas actividades no favorecen la síntesis de $T(SH)_2$ porque consumen precursores para su síntesis, o son responsables de su regeneración.

Tabla 4. Coeficientes de control de las enzimas sobre la concentración de $T(SH)_2$

condición	basal	control	+ estrés
enzima/ proceso (E_i)		$C^{[T(SH)2]}_{Ei}$	
γECS	0.04	0.038	0.053
GS	5.7×10^{-5}	4.2×10^{-5}	7.25×10^{-5}
TryS	0.007	0.03	0.04
SpdT	8.8×10^{-4}	0.015	0.016
TryR	0.98	0.97	0.99
demanda de $T(SH)_2$	-0.99	-0.99	-0.99
suministro de NADPH	0.01	0.013	0.0058
fuga de Spd	-7.9×10^{-6}	-0.01	-0.013
fuga de GSH	-4.4×10^{-6}	-0.009	-0.026
fuga de TS_2	-0.05	-0.062	-0.072

Los coeficientes negativos indican que las reacciones consumen $T(SH)_2$ o los precursores para su síntesis.

Tomando como un punto de partida que se quisiera disminuir en un 50% el flujo de la vía, el modelo predijo que era necesario inhibir a la γECS, TryS o al SpdT en un 58%, 63% y 73%, respectivamente, o en un 40% si se inhiben simultáneamente a las tres mientras que la TryR tendría que inhibirse en más de un 98% (Figura 6A) para obtener el mismo efecto lo que podría explicar el poco éxito que se ha obtenido utilizando inhibidores para esta enzima. Por otro lado, aunque la demanda de $T(SH)_2$ y la TryR controlaron la concentración de $T(SH)_2$, el modelo predijo que la γECS y la TryS también controlaban la concentración del metabolito cuando se inhiben más del 70% (Fig 6B). Otra predicción interesante fue que para inhibir la concentración de $T(SH)_2$ en un 50%, era necesario aumentar la demanda de $T(SH)_2$ (estrés oxidante) en un 200%; o bien, combinar un incremento en 60% de la demanda de $T(SH)_2$ junto con una disminución del 25% en la actividad de la TryR (Figura 6C). En contraste, solamente existe un efecto sinérgico si la demanda de $T(SH)_2$ aumenta un 200% y la γECS se inhibe más del 75% (Figura 6D) debido principalmente al menor control que tiene esta enzima sobre la concentración de $T(SH)_2$. La combinación del incremento en la demanda de $T(SH)_2$ con la inhibición de la γECS y la TryS, no tuvo ningún efecto sobre el flujo hacía $T(SH)_2$(Figura 6E y 6F).

Con esta experimentación *in silico*, en este trabajo se pudo resaltar la importancia de la aplicación del MCA y del modelado cinético para identificar a los blancos con mayor potencial terapéutico en el metabolismo del $T(SH)_2$ en *T. cruzi*, siendo la γECS ≥TryS >> SpdT los más importantes debido a su alto control en el flujo y en la concentración del metabolito. Las predicciones de este modelo nos permitirían enfocarnos en la validación experimental de estas enzimas como blancos terapéuticos utilizando inhibidores o plásmidos titulables como una perspectiva de este trabajo.

La utilidad del modelo no solamente se circunscribe a la vía de *T. cruzi*. Este modelo puede servir como base para evaluar la distribución de control de la vía para otros tripanosomátidos para lo cual se requeriría determinar menos parámetros que los que se tuvieron que determinar en este estudio. Por ejemplo, midiendo las *Vmax* de las enzimas, las concentraciones de GSH, $T(SH)_2$ y poliaminas y el flujo de

síntesis de $T(SH)_2$ y hacer la modificación de la síntesis *de novo* de Spd por la reacción de la ornitina descarboxilasa se podría determinar la distribución de control en promastigotes de *Leishmania* o tripomastigotes de *T. brucei*.

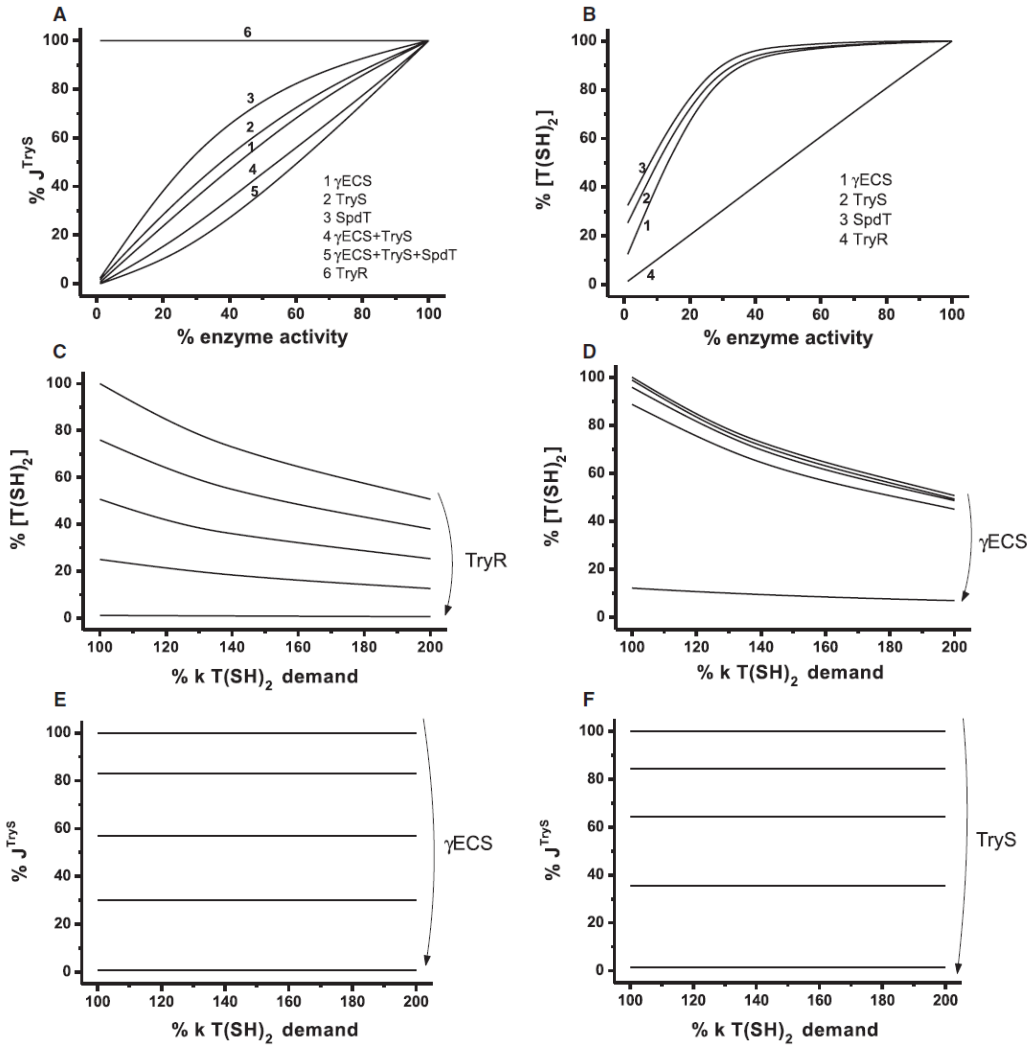

Fig. 6 Predicciones obtenidas a partir del modelo cinético construido utilizando las condiciones control

A. Efecto de la disminución en la actividad de γECS, TryS, SpdT, TryR, o de sus combinaciones sobre el flujo a través de la TryS. B. Efecto de la disminución de γECS, TryS, SpdT y TryR sobre la concentración de $T(SH)_2$. C. Efecto del incremento en la demanda de $T(SH)_2$ a diferentes actividades de TryR. D. Efecto del incremento en el bloque de demanda de $T(SH)_2$ a diferentes concentraciones de γECS. E y F. No existe efecto sinérgico sobre la concentración de $T(SH)_2$ cuando se combina la inhibición de γECS and TryS. Para C-F, las actividades en la derecha se modularon en un 100, 75, 50, 25 y 1% de su valor original de *Vmax*. Algo importante de resaltar es que el 100% de actividad es diferente para cada enzima siendo 2 órdenes de magnitud mayor para la TryR. Por lo tanto, la potencia y especificidad de los inhibidores debe ser mayor para la TryR que para la γECS y la TryS.

the FEBS Journal

Drug target validation of the trypanothione pathway enzymes through metabolic modelling

Viridiana Olin-Sandoval[1], Zahdi González-Chávez[1], Miriam Berzunza-Cruz[2], Ignacio Martínez[2], Ricardo Jasso-Chávez[1], Ingeborg Becker[2], Bertha Espinoza[3], Rafael Moreno-Sánchez[1] and Emma Saavedra[1]

1 Departamento de Bioquímica, Instituto Nacional de Cardiología Ignacio Chávez, México Distrito Federal, Mexico
2 Departamento de Medicina Experimental, Facultad de Medicina, Universidad Nacional Autónoma de México, México Distrito Federal, Mexico
3 Departamento de Inmunología, Instituto de Investigaciones Biomédicas, Universidad Nacional Autónoma de México, México Distrito Federal, Mexico

Keywords
control coefficient; drug targeting; kinetic modelling; metabolic control analysis; oxidative stress

Correspondence
E. Saavedra, Departamento de Bioquímica, Instituto Nacional de Cardiología Ignacio Chávez, Juan Badiano No. 1, Col. Sección XVI, Tlalpan, México Distrito Federal 14080, Mexico
Fax: +52(55) 5573 0994
Tel: +52(55) 5573 2911 ext. 1206
E-mail: emma_saavedra2002@yahoo.com

(Received 12 July 2011, revised 13 February 2012, accepted 1 March 2012)

doi: 10.1111/j.1742-4658.2012.08557.x

A kinetic model of trypanothione [$T(SH)_2$] metabolism in *Trypanosoma cruzi* was constructed based on enzyme kinetic parameters determined under near-physiological conditions (including glutathione synthetase), and the enzyme activities, metabolite concentrations and fluxes determined in the parasite under control and oxidizing conditions. The pathway structure is characterized by a $T(SH)_2$ synthetic module of low flux and low catalytic capacity, and another more catalytically efficient $T(SH)_2$-dependent antioxidant/regenerating module. The model allowed quantification of the contribution of each enzyme to the control of $T(SH)_2$ synthesis and concentration (flux control and concentration control coefficients, respectively). The main control of flux was exerted by γ-glutamylcysteine synthetase (γECS) and trypanothione synthetase (TryS) (control coefficients of 0.58–0.7 and 0.49–0.58, respectively), followed by spermidine (transport (0.24); negligible flux controls by trypanothione reductase (TryR) and the $T(SH)_2$-dependent antioxidant machinery were determined. The concentration of reduced $T(SH)_2$ was controlled by TryR (0.98) and oxidative stress (−0.99); however, γECS and TryS also exerted control on the cellular level of $T(SH)_2$ when they were inhibited by more than 70%. The model predicted that in order to diminish the $T(SH)_2$ synthesis flux by 50%, it is necessary to inhibit γECS or TryS by 58 or 63%, respectively, or both by 50%, whereas more than 98% inhibition was required for TryR. Hence, simultaneous and moderate inhibition of γECS and TryS appears to be a promising multi-target therapeutic strategy. In contrast, use of highly potent and specific inhibitors for TryR and the antioxidant machinery is necessary to affect the antioxidant capabilities of the parasites.

Database
The glutathione synthetase gene sequences from the Nituo and Queretaro strains have been submitted to the GenBank database under accession numbers HQ398540 and HQ398539, respectively.

Abbreviations
CumOOH, cumene hydroperoxide; γEC, γ-glutamylcysteine; γECS, γ-glutamylcysteine synthetase; nsGPxA, non-selenium glutathione peroxidase A; GSH, glutathione; GSSG, glutathione disulfide; GS, glutathione synthetase; MCA, metabolic control analysis; PAI, polyamine; Spd, spermidine; SpdT, spermidine transport; H_2O_2, hydrogen peroxide; TryR, trypanothione reductase; TryS, trypanothione synthetase; $T(SH)_2$, trypanothione; TS_2, trypanothione disulfide; TXN, tryparedoxin; TXNPx, tryparedoxin peroxidase.

Introduction

The trypanosomatid parasite *Trypanosoma cruzi* is the causal agent of American trypanosomiasis (Chagas disease), which affects 15 million people in Latin America; 28 million people in the endemic countries are at risk of being infected by the parasite [1]. In recent years, Chagas disease has become a worldwide health problem as a result of globalization, with > 300 000 infected people in the USA and > 80 000 in Europe [2]. The current drugs used for treatment of this disease are nifurtimox and benznidazole [3]. However, these compounds are highly toxic to the patient and are effective in the acute phase but not for long-term infections; the emergence of drug-resistant parasite strains is also a problem [4,5]. Thus, there is an urgent need for development of new drugs, and the search and validation of drug targets continue.

In the trypanosomatid human parasites *T. cruzi*, *Trypanosoma brucei* (which causes African trypanosomiasis) and different species of *Leishmania* (which causes several forms of leishmaniasis), the thiol peptide trypanothione ($T(SH)_2$; N^1,N^8-bis-glutathionylspermidine), together with the $T(SH)_2$-dependent antioxidant machinery (tryparedoxin, TXN; TXN-dependent peroxiredoxin, TXNPx; non-selenium glutathione peroxidase A, nsGPxA) and trypanothione reductase (TryR) replace the antioxidant functions performed by glutathione (GSH), GSH-dependent antioxidant enzymes and glutathione reductase in most cells. $T(SH)_2$ metabolism in *T. cruzi* is outlined in Fig. 1, and has been extensively reviewed elsewhere [6–9]. Because of the remarkable differences in the antioxidant physiology of these parasites, genetic strategies such as generation of conditional knockouts, gene replacement or RNA interference have been used in *T. brucei* and *Leishmania* to validate the suitability of $T(SH)_2$ pathway enzymes as drug targets (the evaluated enzymes are indicated in Fig. 1). At 80–100% down-regulation, most of the targeted enzymes were found to be essential for parasite survival, infectivity or oxidative stress management [7–9]. Similar analyses have not been reported for *T. cruzi* because genetic methodologies are under development for this parasite [10].

A drawback in the use of genetic approaches to validate drug targets in metabolic pathways is that, in general, strong down-regulation of individual enzymes in any metabolic pathway in the cell results in complete arrest of the pathway flux or cellular function. Therefore, similar phenotypic and metabolic results are expected when almost any component of trypanosomatid $T(SH)_2$ metabolism is manipulated [9]. In order to achieve similar levels of enzyme inhibition to those attained by genetic methods in parasites by pharmacological methods, high doses of specific and potent inhibitors are required, with a concomitant increase in toxic side-effects. Accordingly, genetic strategies are very useful in order to discriminate between essential/non-essential genes, but this is not the only property that determines the suitability of an enzyme as a drug target [11]. Suitable drug targets should be enzymes for which low pharmacological inhibition have a high impact on pathway function. From a metabolic regulation perspective, drug targets should be sought among those enzymes that mainly control the pathway flux and/or the concentration of a particular metabolite.

In recent years, analysis of cellular networks has been used for drug target identification instead of focusing on single enzymes/proteins [12–15]. Metabolic control analysis (MCA) is a quantitative approach in systems biology [16] that has demonstrated that control of a metabolic pathway is distributed to various degrees among all the pathway components, making it possible to establish hierarchies within the pathway components: 'leaders' are those enzymes that mainly control the pathway, whereas 'follower' enzymes are those that have over-capacity for the pathway flux. Common properties of the former are that they are not abundant in cells, are not catalytically efficient, and/or are highly regulated (allosteric enzymes), whereas the latter are generally non-allosteric, very efficient, and highly abundant in cells [12,13,17,18].

MCA quantifies the degree of control that each enzyme has over the pathway flux (flux control coefficient, $C^J_{e_i}$) and over the pathway intermediary concentrations (concentration control coefficient, $C^X_{e_i}$), where J is the pathway flux, X is an intermediary concentration, and e is the activity of pathway enzyme i in the cell [17,18]. The control coefficients are systemic properties, i.e. they cannot be deduced by analysing the kinetic properties of the single enzymes in isolation. Several experimental strategies have therefore been developed to determine the control coefficients of the individual pathway components in order to determine the control structure of a metabolic pathway [18]. One approach is kinetic modelling, which integrates the kinetic properties of the pathway enzymes determined *in vitro* under near-physiological conditions and the concentrations of pathway precursors and enzyme activities determined in cells into an interactive network that reproduces the pathway behaviour under specific cellular metabolic steady states [19,20]. It is worth emphasizing that the purpose of kinetic modelling is not just to replicate pathway behaviour, but to

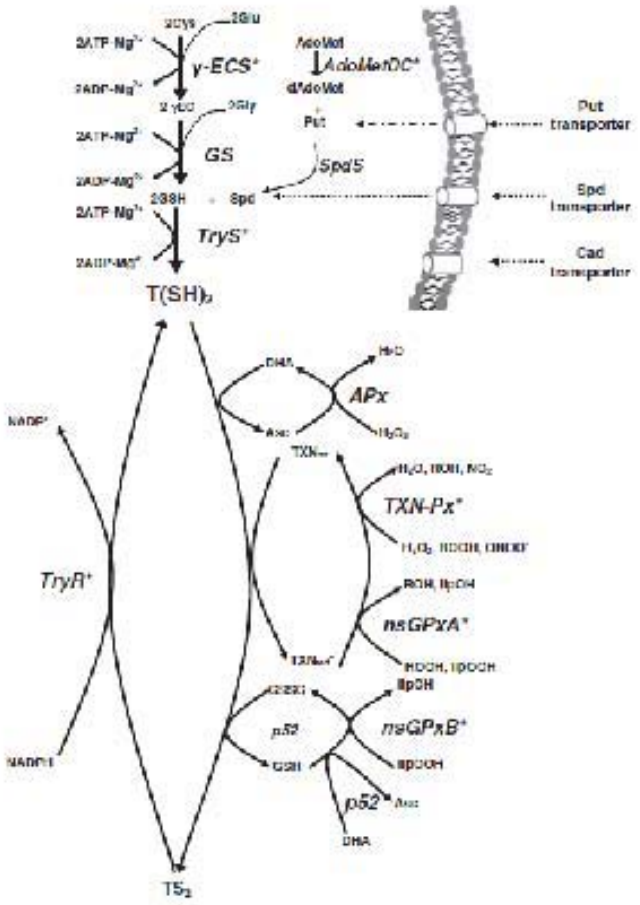

Fig. 1. $T(SH)_2$ metabolism in *T. cruzi*. $T(SH)_2$ is synthesized by trypanothione synthetase (TryS, EC 6.3.1.9) from two GSH molecules and one spermidine (Spd) molecule. In turn, GSH is synthesized by the sequential action of γ-glutamylcysteine synthetase (γ-ECS, EC 6.3.2.2), which binds glutamate (Glu) and cysteine (Cys) to produce γ-glutamylcysteine (γEC), and glutathione synthetase (GS, EC 6.3.2.3), which binds γEC and glycine (Gly) to produce GSH. Six ATP molecules are consumed per mole of $T(SH)_2$ synthesized. Spd can be *de novo* synthesized by spermidine synthase (SpdS, EC 2.5.1.16) from putrescine (Put) and decarboxylated *S*-adenosylmethionine (dAdoMet); SpdS has only been kinetically characterized in *T. brucei* [63], although the corresponding gene is found in the *T. cruzi* genome. dAdoMet is synthesized from *S*-adenosylmethionine (AdoMet) by *S*-adenosylmethionine decarboxylase (AdoMetDC, EC 4.1.1.50), an enzyme that has been characterized in the three trypanosomatid species (*T. cruzi*, *T. brucei* and *Leishmania*) [70]. In *T. brucei* and *Leishmania*, Put can be *de novo* synthesized by ornithine decarboxylase (ODC, EC 4.1.1.17) [70]; *Leishmania* can also take up Put from the medium using diamine transporters [64]. *T. cruzi* lacks ODC activity, and therefore relies on transport of Put and Spd from the extracellular environment by high affinity and catalytically efficient diamine/polyamine transporters [65–68]. For the antioxidant system, $T(SH)_2$ serves as the main electron donor for reduction of oxidized metabolites (dehydroascorbate, DHA; oxidized glutathione, GSSG) and small orthol proteins (glutaredoxins and tryparedoxin, TXN), which transfer electrons to a variety of antioxidant enzymes such as ascorbate peroxidase (Apx, EC 1.11.1.11), 2-Cys peroxiredoxins (TXNPx, EC 1.11.1.15), non-selenium glutathione peroxidase-like enzymes (nsGPxA and nsGPxB, EC 1.11.1.9) and trypanothione–glutathione thiol transferase (p52). Oxidized trypanothione (TS_2) is regenerated by trypanothione reductase (TryR, EC 1.8.1.12), consuming NADPH. For reviews, see [6–8]. Asterisks indicate enzymes that were genetically manipulated in *T. cruzi* and *Leishmania*.

identify and understand the underlying mechanisms that determine why one enzyme or transporter exerts significant or negligible pathway control [12,13,18–20].

A validated kinetic model of a metabolic pathway may help in the search for suitable drug targets by identifying the steps that exert the greatest control; it can also provide a platform to perform *in silico* experimentation to provide answers to biological questions. Using the kinetic model to assess the impact on fluxes and/or metabolite concentrations of gradual inhibition of each individual pathway component (or simultaneous inhibition of several enzymes in various combinations) allows identification of the step(s) whose inhibition has the greatest negative effect on $T(SH)_2$ pathway function. Hence, network analysis facilitates prioritization among genetically validated essential enzymes. Moreover, kinetic modelling can also be a valuable tool for drug target validation for parasites for which genetic strategies are limited, such as *T. cruzi*.

Here, we describe construction of the first kinetic model of the $T(SH)_2$ metabolism in trypanosomatid parasites using *T. cruzi* as a biological model. The kinetic model allowed identification of the enzymes and transporters that exert the greatest control on $T(SH)_2$ synthesis and concentration and allowed for elucidation of their underlying controlling mechanisms. Moreover, it provided quantitative predictions regarding the degrees of inhibition required for each pathway enzyme to affect antioxidant defence in the parasite.

Results

Due to the significant amount of detailed experimental data required to build kinetic models, only a few have been described, mostly for glycolysis in several organisms (http://jjj.biochem.sun.ac.za; [19]). Although $T(SH)_2$ metabolism has been thoroughly studied in several laboratories worldwide, the reported data are not uniform: they have been generated using different parasite species and strains, and under diverse experimental conditions. Therefore, to build the kinetic model of $T(SH)_2$ metabolism in *T. cruzi*, we obtained the majority of the experimental data under near-physiological conditions in the same strain and stage of this parasite species, and under defined metabolic steady states.

In vitro kinetic characterization of the recombinant pathway enzymes under near-physiological experimental conditions

The genes encoding γ-glutamylcysteine synthetase (γECS), trypanothione synthetase (TryS), TryR, TXN, mGPxA and tryparedoxin peroxidase (TXNPx) of *T. cruzi* Nunoa strain (MHOM/MX/1994/Nunoa) [21] were cloned, and the proteins were over-expressed in *Escherichia coli* and purified to a high degree (approximately 98%) (Fig. S1). The γECS and TryS recombinant enzymes were highly unstable under various storage conditions, but the presence of high concentrations of trehalose improved their stabilities, with 50% of the activity lost within 20 days (data not shown).

The intracellular pH of the infective trypomastigote and epimastigote stages have been determined (7.35 and 7.2, respectively [22,23]), and the optimum culture temperatures are 37 and 26 °C, respectively. Therefore, the kinetic parameters of the recombinant enzymes were all determined at pH 7.4 and 37 °C since these conditions more closely resemble the mammalian infective stage.

As previously described, γECS, TryS and TryR displayed hyperbolic kinetics for their respective substrates (data not shown), and the kinetic parameter values (Table 1) were within the range reported for several trypanosomatid parasites and other cell types. The latter were mostly determined at 25–37 °C and under optimal pH (7.5–8) (see Table S1 for data comparisons).

Glutathione synthetase (GS) has not been characterized in any trypanosomatid species. Therefore, GS genes were cloned from the *T. cruzi* Nunoa and Querétaro strains (GenBank accession HQ398240 and HQ398239, respectively), and no differences were found at the level of the amino acid translated sequences. The GS gene was over-expressed in *E. coli*, and the protein purified and kinetically characterized. To improve its poor stability, the enzyme was also stored in trehalose. The enzyme was a dimer (data not shown) that displayed hyperbolic kinetics with its three substrates (Fig. 2). The *Tc*GS V_{max} and K_m values (Table 1) were similar to those reported for GS from *Arabidopsis thaliana* and *Plasmodium falciparum* (Table S1). The enzyme was inhibited by GSH, non-competitively against Gly and ATP and uncompetitively against γ-glutamylcysteine (γEC) (Fig. 3); however, the three high K_i values (11–14 mM) (Table 1) may not have physiological significance as the GSH concentration in these parasites is one order of magnitude lower (Table 2).

Although the V_{max} and affinity constants for substrates of *Tc*TryS in the Nunoa strain were essentially the same as those of its homologue in the *T. cruzi* Silvio strain (Table S1) [24], the enzyme did not show substrate inhibition by GSH (Fig. S2), as previously reported for the *T. cruzi* Silvio strain recombinant enzyme [24], *T. brucei* [25] and *Leishmania* [26], in

Table 1. Kinetic parameters of recombinant and in the parasite trypanothione pathway enzymes. V_{max} values are units·mg protein^{-1}; $K_{m\,app}$, K_i and concentrations are mM; $k_{cat}/K_{m\,app}$ values are $M^{-1}s^{-1}$. $V_{max}/K_{m\,app}$ values are mL^{-1}·min^{-1}·mg protein^{-1}. All values were determined at pH 7.4 at 37 °C in the same buffer (see Experimental procedures). *Values are means ± SD. ** k_{cat} value in s^{-1} (0.5 for γECS, 4.25 for GS, 1.24 for TryS, 960 for TryR, 36 for TXN and 5–10 for TXNPx and nsGPXA). *** values are means ± SEM. Figures in parentheses indicate the number of independent purified protein batches assayed or the number of cytosolic extracts from parasites incubated for 10 min in NaCl/Pi + 20 mM glucose.

Enzyme	V_{max}* for purified proteins	Thiol substrate $K_{m\,app}$*	k_{cat}**/$K_{m\,app}$	Co-substrate $K_{m\,app}$*	Co-substrate/coenzyme $K_{m\,app}$*	Inhibitors	V_{max} in parasites***	$V_{max}/K_{m\,app}$
γECS	0.37 ± 0.1 (3)	Cys 0.21 ± 0.1 (3)	2.4 × 10^3	Glu 0.13 ± 0.04 (3)	ATP 0.04 ± 0.012 (3)	$K_{i\,GSH}$ 1.6 (2) $K_{i\,γEC}$ 0.43 (2) GSSG > 0.000	< 0.002^e	< 0.0006
GS	2.04 ± 0.7 (3)	γEC 0.04 ± 0.01 (3)	1.1 × 10^5	Gly 1.2 ± 0.3 (3)	ATP 0.03 ± 0.01 (3)	$K_{i\,GSH\,versus\,Gly}$ 12 ± 0.6 $K_{i\,GSH\,versus\,ATP}$ 11 ± 1 $K_{i\,GSH\,versus\,γEC}$ 14.6 ± 5.6 TS_2 > 0.005 GSSG > 0.000 Spd, Sum > 2	0.0086 ± 0.0023 (3)	0.22
TryS^a	1.04 ± 0.5 (3)	GSH 0.76 ± 0.21 (3)	1.6 × 10^3	Spd 0.66 ± 0.005 (3)	ATP 0.07 ± 0.04 (3)	GSSG > 0.000 $TS\text{-}H_2$ > 1 TS_2 > 0.005	0.0043 ± 0.0016^a (3)	0.006
TryR	531 ± 137 (3)	TS_2 0.023 ± 0.006 (3)	4.3 × 10^7		NADPH 0.000 ± 0.005 (3)	$TS\text{-}H_2$ > 1	0.264 ± 0.087 (3)	11.5
TXN	97 ± 28	$TS\text{-}H_2$ 0.0082 ± 0.002 (4)	2.9 × 10^6				0.068 (2)	7.0
TXNPx, nsGPXA	1.7–81^b	TXN^b 0.0006–0.0025	0.14–6 × 10^{6c}	CumOOH^b 0.011–0.107			0.177 ± 0.065^d (4)	6–18

^{a} Activity in µmol TSH$_2$ synthesized·min^{-1}·mg protein^{-1}. ^{b} V_{max} and K_m interval of recombinant *T. cruzi* TXNPx and nsGPXA. ^{c} Calculated using the K_m for CumOOH. ^{d} Total TXN-dependent peroxidase activity measured using CumOOH. ^{e} Below the limit of detection of the enzymatic assay. GSSG, oxidized GSH; Spm, spermine.

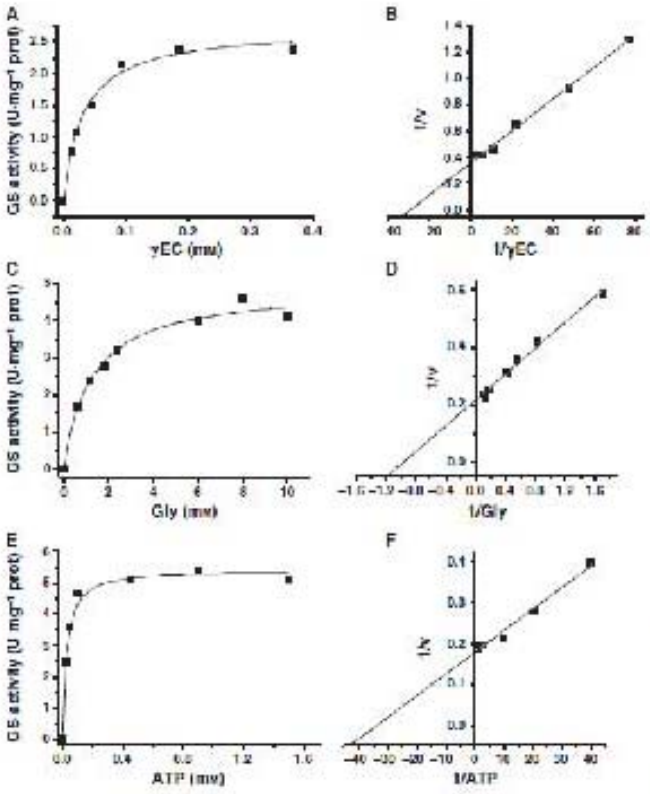

Fig. 2. Kinetic characterization of recombinant TcGS. (A,C,E) Titration curves for the three substrates. The fitting of experimental points to the Michaelis–Menten equation was performed using ORIGIN MICROCAL version 5.0 software (OriginLab, Northampton, MA, USA). The enzyme exhibits hyperbolic kinetics with the three substrates, as shown by the double reciprocal plots (B,D,F).

which inhibition at concentrations of 0.038–1.2 mM was found (Table S1). To evaluate whether the lack of GSH inhibition was an artifact of our recombinant enzyme, TryS activity was determined in parasite cytosol-enriched fractions, i.e. using the native enzyme. Activity was only detected when 6–8 mM GSH was used (10 times the K_m value) (data not shown), suggesting that this high GSH concentration is not inhibitory for *Tc*TryS from the Ninoa strain. Furthermore, as a control for our reaction assay, recombinant, His-tagged *Crithidia fasciculata* TryS was partially inhibited at 1 mM GSH. The reason for the lack of TcTryS Ninoa inhibition by GSH remains to be elucidated.

The affinity constants of TXN for $T(SH)_2$ and those of nsGPxA and TXNPx for TXN and cumene peroxide, were determined in a reconstituted system with TryR under the same conditions of pH and temperature used above; the kinetic parameters are shown in Table 1.

The purified enzymes with the lowest catalytic potential ($k_{cat}/K_{m(app)}$) regarding the thiol substrate were γECS and TryS; in contrast, efficiencies two to four orders of magnitude higher were obtained for GS, TryR, TXN, nsGPxA and TXNPx (Table 1), indicating that, under *in vitro* saturating concentrations of the thiol substrates, the first two enzymes were less catalytically efficient.

The effect of the products of the enzymatic reactions and some intermediate metabolites of trypanothione metabolism (not usually tested when working with purified enzymes) were evaluated for all the enzymes at concentrations close to those found in these parasites to determine possible regulatory mechanisms when working in the entire pathway (Table 1). γECS was competitively inhibited by GSH and non-competitively by γEC against Glu (Table 1 and Fig. S3). Trypanothione disulfide (TS_2) or $T(SH)_2$ (0.005 and 1 mM, respectively), glutathione disulfide (GSSG) (0.063 mM), spermidine (Spd) and spermine (3 mM) did not show

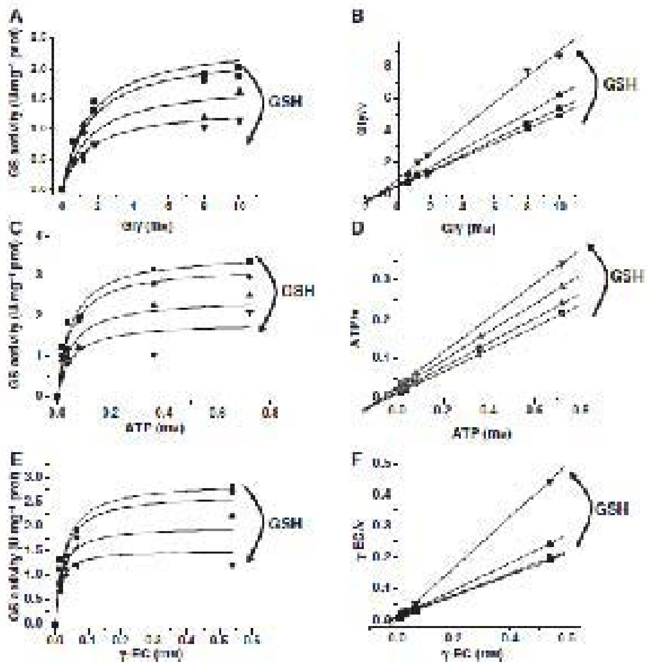

Fig. 3. TcGS inhibition by GSH. (A,C) Non-linear curve fitting to the equation for simple non-competitive inhibition $v = \left(V_{max}/(1 + I/K_i) \cdot S\right) / \left(K_s + S\right)$. (E) Non-linear curve fitting to the equation for simple uncompetitive inhibition $v = \left(V_{max}/(1 + I/K_i) \cdot S\right) / \left(K_s/(1 + I/K_i) + S\right)$ using ORIGINPRO 7.5 software (OriginLab, Northampton, MA, USA). (B,D,F) Hanes' plots corresponding to (A), (C) and (E), respectively. The inhibitor concentration varied from 0 to 10 mM GSH.

Table 2. Metabolomics of the T(SH)₂ pathway in parasites and metabolite concentrations predicted by trypanothione pathway modelling. Simulation of the model setting [a] 0, [b] 0 and [c] 50 μM H_2O_2. *The millimolar concentration was determined on the basis that 10^8 T. cruzi epimastigotes correspond to 3 μL [77]. Values are means ± SD. **Metabolites fixed in the model at the mean value of columns 2, 4 and 6. ***Fluxes (J) are in nmol·min⁻¹·mg cell protein⁻¹. NI, not included in the model. GSH_{tot} indicates the concentration of reduced plus oxidized glutathione.

Incubation time	Basal (t = 0)		Control (t = 10)		Stress (t = 10 + stress) (50 μM H_2O_2)	
Metabolite (mM)*	In vivo	Model[a]	In vivo	Model[b]	In vivo	Model[c]
Glu	8.2 ± 1.3 (3)	**	9 ± 1 (3)	**	7.7 ± 1 (3)	**
Gly	13 ± 1.6 (3)	**	9 ± 1.7 (3)	**	17 ± 4 (3)	**
Cys	0.3 ± 0.14 (3)	**	0.4 ± 0.1[d] (3)	**	0.3 ± 0.07[d,e] (3)	**
γEC	0.15 ± 0.08 (3)	0.067	0.12 ± 0.06 (3)	0.062	0.1 ± 0.04 (3)	0.06
GSH_{tot}	0.6 ± 0.28 (4)	0.65	0.77 ± 0.3 (3)	0.92	0.4 ± 0.05[d,e] (3)	0.5
TSH_2	3.8 ± 1.6 (4)	6.7	5.9 ± 2.5 (4)	7.1	4.2 ± 1.8[d] (4)	1.7
TS_2	0.5 ± 0.24 (3)	0.55	0.4 ± 0.22 (3)	0.47	0.5 ± 0.17 (3)	0.30
$NADP^+$	0.035 ± 0.02 (3)	0.026	0.025 ± 0.012[c] (3)	0.026	0.012 ± 0.004[d,f] (3)	0.025
NADPH	0.12[a]	0.08	0.084[a]	0.084	0.04[a]	0.085
Spd_{tot}	1.2 ± 0.08 (3)	0.5	0.2 ± 0.08[f] (3)	0.33	0.2 ± 0.13[g] (3)	0.35
Spd_{free}	0.0011[b]	**	0.0011[b]	**	0.0011[b]	**
ATP	4 ± 0.6 (3)	NI	4.6 ± 0.9 (3)	NI	3.4 ± 1.1 (3)	NI
J_{TryS}***		0.55	1 (2)	0.7	1.9 (2)	0.5
$\sum$ [illegible]		25.2		248		246

[a] Recalculated using a NADP⁺/NADPH ratio equal to 0.3, as reported for T. cruzi epimastigotes of CL Brener strain [79]. [b] Reported in [82]. Student's t-tests: [c] $P < 0.1$ versus $t = 0$; [d] $P < 0.05$ versus $t = 0$; [e] $P < 0.05$ versus $t = 10$; [f] $P < 0.1$ versus $t = 0$; [g] $P < 0.2$ versus $t = 0$; [h] $P < 0.2$ versus $t = 10$.

an effect on any of the tested enzymes. No other modulator has been reported to affect any of the $T(SH)_2$ metabolism enzymes at physiological concentrations. The only allosteric regulatory mechanism that appears to operate in the pathway is that of feedback competitive inhibition by GSH on γECS.

Enzyme activities, metabolite concentrations, and fluxes of $T(SH)_2$ metabolism in parasites

In vivo pathway parameters were determined in *T. cruzi* epimastigotes (insect stage) due to the experimental requirement for large amounts of biological material for reliable determination of enzyme activity or metabolite concentration. This prevented us from performing the analysis in the *T. cruzi* human stages trypomastigotes and amastigotes, for which infection of human cultured cells and further parasite purification are necessary, steps that lead to extremely low parasite yields.

The enzyme activities, metabolite concentrations and fluxes parameters described below were determined under three conditions: in non-incubated parasites (basal $t = 0$), and in parasites incubated for 10 min in NaCl/P_i supplemented with 20 mM glucose in the absence (control $t = 10$) or presence of 50 μM H_2O_2 ($t = 10+$ stress). At longer incubation times or higher peroxide concentrations (up to 100 μM), the thiol contents were abruptly depleted, preventing use of such conditions for *in vivo* steady-state experiments.

No simultaneous determination of $T(SH)_2$ pathway enzyme activities in parasites has been reported, and the V_{max} values within the cells (i.e. the content of biologically active enzyme) are the most critical kinetic parameters for building kinetic models, because the affinity parameters (K_m, K_i and K_I) and rate equations can be determined using purified enzymes. Due to the high ATPase activity in the cell extract, determination of the GS and TryS activities was performed using a stepwise and end-point assay. For each enzyme, two separate reactions were prepared, one containing the three substrates and another lacking one of the specific substrates; the latter reaction accounted for the spurious ADP generated by ATPase activities (see Experimental procedures). The number of nmoles of ADP attributable to GS and TryS activities in cytosolic parasite extracts was approximately 6–12% of the total ATPase activity measured in the complete reaction. Nevertheless, a linear dependency of the ADP produced by GS and TryS activities on the amount of protein extract used was observed (Table S2); in contrast, the number of nmoles of ADP produced by ATPase background activity increased by only 25–33% when the amount of protein added was doubled. These differences clearly show that only GS and TryS specific activities (but not ATPase activity) can be reliably determined under initial velocity conditions (linearity on the amount of protein used and saturating concentrations of the substrates). Moreover, the GS activities shown in Table 1 and Table S3 are well within the range reported for cell extracts from various organisms such as the parasites *Plasmodium berghei* (7.6 mU·mg protein^{-1} [27]) and *Setaria cervi* (11 mU·mg protein^{-1} [28]), the rat cell lines M3Z and OC/CDF2Z (3.9–7.8 mU·mg protein^{-1}) and rat kidney (39 mU·mg protein^{-1}) [29], using different experimental procedures. However, γECS activity could not be determined, most probably due to its scarcity in *T. cruzi* and other biological systems; indeed, γECS activities as low as < 2 mU·mg protein^{-1} for plants [30] and 0.8–4 mU·mg protein^{-1} for human and rat cells [29] have been reported.

On the other hand, TryR activity in cytosolic parasite extracts was determined with high reliability due to the natural high abundance of the enzyme and the high specificity of the spectrophotometric assay (Table 1). TXN and combined TXN-dependent peroxidase activities (TXNPx and nsGPxA activities) were also abundant in the parasites (Table 1). Moreover, no significant differences in the activities of GS, TryS and TryR were found between stressed and unstressed parasites and between 0 and 10 min of incubation (Table S3), indicating that a steady-state metabolic condition with no changes in enzyme activities had been attained in our experimental setting, a requirement for MCA experiments.

The V_{max} values in the parasites indicated that GS and TryS activities (and probably γECS) were two orders of magnitude lower than those of TryR and the TXN-dependent antioxidant machinery (Table 1). However, a more appropriate comparison among enzymes involves consideration of the catalytic efficiency ($V_{max}/K_{m\ subst.}$). TryS and γECS showed the lowest efficiencies, suggesting that these enzymes may limit the flux under *in vivo* conditions (Table 1). Although the Spd concentration under control conditions was close to the TryS $K_{m\ Spd}$, it decreased after the parasites were stressed (Table 2); thus TryS activity may be limited by two of its substrates.

The metabolite concentrations were determined under the three experimental conditions (Table 2). It is worth noting that some stress is generated just by subjecting the parasites to incubation, accounting for the observed changes in the $T(SH)_2$ and Spd concentrations (Table 2, columns 2 and 4). In this regard, Spd has been found to be oxidized under many types of stresses, including oxidative stress [31,32]. To diminish

this basal stress, other incubation media were tested, but similar patterns of response were obtained (data not shown). Despite this, significant additional oxidative stress was induced by adding peroxide, as indicated by the significantly diminished total GSH content as well as the decreased $T(SH)_2/TS_2$ ratios (from 15 to 7 after 10 min of incubation; Table 2, columns 4 and 6). Excretion of GSSG under oxidative stress conditions resulting in a loss of total GSH content has been reported previously for antimony-sensitive *Leishmania* [33], *Neurospora crassa* [34] and erythrocytes [35]. However, due to limitations in thiol measurement protocols, these oxidized compounds were not detected in the incubation medium of the epimastigotes.

The thiol compound contents in trypanosomatids are highly variable and depend on the strains and culture media used; however, our data for GSH and $T(SH)_2$ fall within the range reported for trypanosomatids [7], other *T. cruzi* strains, and for the strain used here cultured in two different media (Table S4). The Glu, Gly, γEC and ATP concentrations remained constant and saturating for the enzymes under the three conditions. The $NADP^+$ concentration did not change significantly (Table 2).

$T(SH)_2$ synthesis flux under the control condition was low, and increased two-fold in *T. cruzi* epimastigotes subjected to oxidative stress (Table 2, columns 4 and 6). The low flux to $T(SH)_2$ synthesis is related to the low activities and catalytic efficiencies in the synthetic pathway module (Table 1).

Kinetic model properties

The kinetic model for $T(SH)_2$ metabolism in *T. cruzi* was constructed using the metabolic simulator GEPASI/COPASI [36,37] (http://www.copasi.org) using the affinity constants for ligands of the recombinant pathway enzymes determined here under near-physiological conditions of pH and temperature (Table 1), and the V_{max} activities and precursor metabolite concentrations determined in the parasites under steady-state conditions (Tables 1 and 3). The reactions included in the model are shown in Fig. 4, and the model main features are described below. Details on its construction and rate-equation descriptions for each reaction are given in Experimental procedures and in Tables S5–S7.

All the reactions (except for the Spd, GSH and TS_2 leaks, which function as sinks) were considered reversible, including γECS, GS and TryS. The high K_{eq} values for the latter three were included in their rate equations to meet the thermodynamic constraints

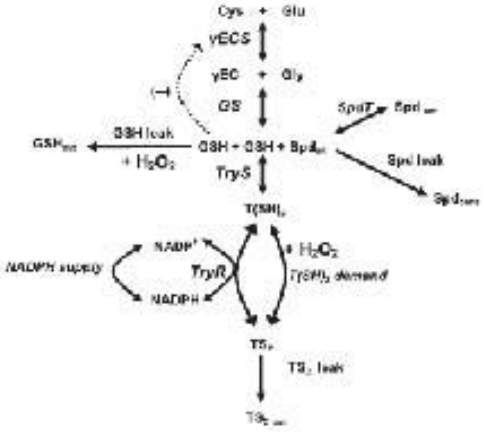

Fig. 4. Graphic rendition of the model of *T. cruzi* $T(SH)_2$ metabolism. The model included enzymes for the synthesis of GSH and Spd transport (SpdT), the synthesis of TS_2, the $T(SH)_2$ demand (oxidative stress plus the TXN-dependent peroxide detoxification system), the GSH, Spd and TS_2 leaks, the regenerating system (TryR) and the NADPH supply. As indicated, the reactions were considered reversible except for the GSH, Spd and TS_2 leaks. Feedback inhibition of γECS by GSH was also included.

imposed by ATP hydrolysis on reaction reversibility. The reversibility of the reaction steps is a necessary condition to attain a stable steady state during kinetic model predictions; it allows the transfer of information throughout all the pathway components [38]. In addition, Spd was considered to be supplied only from the extracellular environment through the polyamine transporter(s), while its synthesis from *S*-adenosylmethionine and putrescine (Put) (Fig. 1) was not included, because the contribution of the latter route to the Spd pool has been not studied. The supply of NADPH (derived from the oxidative section of the pentose phosphate pathway or by transhydrogenation) was also included to maintain the balance in the pyridine nucleotide concentration. In addition, H_2O_2 was included as a substrate of the $T(SH)_2$ demand reactions and GSH leak reactions in order to simulate stress and non-stress oxidizing conditions.

It has been previously demonstrated by MCA that the reactions that consume a pathway end-product (demand) significantly contribute to the control of flux and intermediary concentrations; for example, ATP demand for glycolysis in *Lactococcus lactis* and *Escherichia coli* [18] and GSH demand for GSH synthesis [39] (for details on supply/demand theory in MCA, see [40]). On the other hand, it has been observed that the peroxide detoxification system is abundant in

trypanosomatids [7,9]; TXN accounts for up to 3% (0.3–0.5 mM) of the total soluble protein content in *T. cruzi*, and TryR reaches 1.25 μM [41,42]; furthermore, 6% of the soluble protein in *C. fasciculata* corresponds to 2-Cys Prx (TXNPx). The TXN-dependent peroxidase activities (corresponding to mGPxA and TXNPx in Fig. 1) and TXN level determined in the epimastigotes used in this work were high (Table 1). These data indicate that the peroxide detoxification system has catalytic over-capacity compared with the $T(SH)_2$ synthetic pathway module; therefore, $T(SH)_2$-demanding processes, i.e. oxidative stress and the antioxidant machinery (TXN, TXNPx and mGPxA), were combined into a single reversible reaction ($T(SH)_2$ demand).

Due to the decrease of the total contents of Spd, GSH and $T(SH)_2$ under oxidative stress conditions (the latter two most probably in oxidized form; Table 2), it was necessary to include reactions representing leaks for these metabolites; in their absence, the model did not accurately predict the intermediary concentrations found under oxidative stress conditions. The cellular mechanisms involved in these phenomena are highly interesting but beyond the scope of this study.

Using the model, three conditions were analyzed: (a) basal non-incubated parasites, (b) parasites incubated in the absence of H_2O_2, or (c) parasites incubated in the presence of 20 μM H_2O_2. The model predictions displayed hyperbolic patterns, indicating that under all tested conditions a stable steady state was reached.

Validity and robustness of the kinetic model

Construction and validation of kinetic models are performed using different datasets. For construction, datasets for the individual enzymes were used (affinity constants for ligands and V_{max} in cells), and, for validation, datasets obtained from the complete system (i.e. intermediary concentrations and pathway fluxes measured *in vivo*) were compared with model-predicted datasets. Hence, a validated kinetic model is one that can accurately predict pathway behaviour within the biological variability of the *in vivo* parameters [19,20,43].

Under the three modelled conditions, the concentrations of the thiol molecules Spd and $NADP^+$ were within 0.36–1.85 times the average concentrations determined *in vivo* (Table 2; columns 3, 5 and 7). The predicted flux agreed with that measured *in vivo* under control conditions; however, the predicted flux under stress was 0.3 times the experimental value (Table 2). This variation was due to inclusion of the highly H_2O_2 concentration-sensitive GSH leak reaction; however, in its absence, a fourfold higher GSH concentration was predicted compared to the experimental value. To further explore these interactions, the $T(SH)_2$ synthesis flux and thiol concentrations were modelled at different rates of GSH and $T(SH)_2$ leaks (Fig. S4). A higher dependency on the GSH leak rate was observed, correlating with the observed diminution in GSH levels in the parasites in the presence of the oxidant (Table 2). For the basal condition, the rate constant (k) values for $T(SH)_2$ demand and the GSH and Spd leaks were modified to obtain the higher Spd concentration observed in the *in silico* experiment; these changes avoided GSH and $T(SH)_2$ accumulation. Overall, the kinetic model closely predicted the metabolite steady-state concentrations and fluxes in the parasites under each experimental condition.

The kinetic model also showed high robustness (Table S8); it permitted decreases or increases in the values of the affinity constants and V_{max} values of the enzymes without significantly altering the pathway control distribution, i.e. the steps that exerted the greatest control remained the same. Flux control was redistributed between γECS and TryS when their V_{max} values or the $K_{m,Glx}$ for γECS and the $K_{m,Spd}$ for TryS (Table S8) were varied by 50%. Only when the V_{max} values were decreased was the flux significantly decreased. As expected, variation of the TryR V_{max} only modified the $T(SH)_2$ concentration (< 50%) and the $T(SH)_2/TS_2$ ratio, but not the TS_2 concentration, because the latter is controlled by oxidative stress (Table S8). Remarkably, decrease of γECS and TryS activities by 50% resulted in a decreased TS_2 concentration. The model was not sufficiently robust to accurately predict the pathway behaviour at > 20 μM H_2O_2, because, at this concentration, the $T(SH)_2$ demand reaction completely depleted the $T(SH)_2$ concentration. However, at 10 μM H_2O_2, the model predicted highly similar metabolite concentrations and fluxes to those experimentally determined in parasites incubated with 50 μM H_2O_2, suggesting that, *in vivo*, the parasites were perhaps exposed to 10 μM H_2O_2, and that the rest of the added H_2O_2 reacted with the incubation medium.

Control structure of $T(SH)_2$ metabolism in *T. cruzi*

Flux control distribution

The kinetic model provided the flux control coefficients for each reaction step under the three experimentally evaluated conditions (Table 3). Under basal conditions (which reflect the culture conditions as the parasites were analysed shortly after harvest), the main flux control step was γECS, with a low but significant contribution of TryS. The rest of the pathway steps did not contribute to flux control.

Table 3. Control coefficients of the $T(SH)_2$ synthesis enzymes. The pathway flux was considered to be through the TryS reaction. The negative sign for the flux control coefficients for some steps indicates that their activities do not favour $T(SH)_2$ synthesis flux because they either consume precursors for its synthesis or regenerate them as metabolites.

Condition	Parasite	Control	Stressed
Enzyme/process (a)	C^J_a		
γECS	0.84	0.58	0.7
GS	0.001	0.5×10^{-4}	9.8×10^{-4}
TryS	0.14	0.49	0.28
SpdT	0.018	0.24	0.22
TryR	−0.0025	−0.012	−0.0095
$T(SH)_2$ demand	0.003	0.017	0.0095
NADPH supply	-3×10^{-6}	-1.6×10^{-4}	-5.5×10^{-6}
Spd leak	-1.5×10^{-4}	−0.17	−0.17
GSH leak	-9.2×10^{-4}	−0.16	−0.38
TS_2 leak	1.5×10^{-4}	7.7×10^{-4}	6.9×10^{-4}

Under unstressed control conditions, a 31% decrease in $C^J_{\gamma ECS}$ was observed whereas TryS flux control significantly increased, in parallel with increased flux control by Spd supply and the Spd and GSH leaks (Table 3). The augmented flux control by TryS is a consequence of the sixfold decrease in Spd content seen under control and stress conditions (Table 2), such that it becomes non-saturating for the enzyme; in addition, the decrease in Spd also resulted in increased control by its supply and demand reactions. The model predicted a similar flux control distribution in the stressed parasites (Table 3); the increased flux control by γECS and TryS was proportional to the increase in flux control by the GSH leak, which accounted for the large decrease in GSH concentration under these conditions (Table 2). TryR did not exhibit significant control of $T(SH)_2$ synthesis flux under any of the three modelled conditions. Unexpectedly, the $T(SH)_2$ demand also exhibited low control of the $T(SH)_2$ synthesis flux.

Remarkably, the model-predicted $T(SH)_2$ synthesis fluxes of 0.5–0.9 nmol·min^{-1}·mg protein^{-1} contrasted with the high fluxes through the TryR/$T(SH)_2$ demand/NADPH supply pathway module of approximately 548 nmol·min^{-1}·mg protein^{-1} (Table 2). Hence, kinetic modelling indicated a bi-functional modular organization of $T(SH)_2$ metabolism in the parasite.

Why do γECS and TryS control the synthesis of $T(SH)_2$?

The elasticity coefficients of the pathway enzymes and transporters help to establish the molecular mechanisms that explain why an enzyme controls, or does not control, the pathway flux. The elasticity coefficient (ε^v_x) represents the change in the rate or activity (a) of a pathway enzyme/transporter (J) relative to the change in the concentrations of its ligands X (substrates, products or modulators). The elasticity coefficients are intrinsic properties of the enzymes (in contrast to flux and concentration control coefficients, which are systemic properties), and are only determined by the particular kinetic features of each enzyme [17,18]. Moreover, the elasticity coefficients are inversely related to their flux control coefficient: the rate of an enzyme with low elasticity (ε^v_x approaching 0) cannot increase at increasing substrate concentrations, representing a constraint in the pathway flux [17,18].

γECS is competitively inhibited by GSH versus Glu, and has the lowest elasticity coefficient for the thiol molecule amongst the pathway enzymes (Table S9). To determine whether the γECS high flux control was due to low enzyme activity in the parasites or to GSH feedback inhibition at physiological concentrations of its ligands (Glu and γEC), the pathway was modelled under a wide range of $K_{i,GSH}$ values (0.1–10 times the experimentally determined value), resulting in no changes in the control distribution (data not shown). As the Glu and GSH intracellular concentrations are 5.6- and 0.5 times the K_m and K_i values, respectively, the contribution of GSH feedback inhibition to the high γECS flux control appears to be negligible. TryS showed high elasticity for its substrates (Table S9); thus, its high control can only be explained by its low activity in the cells. Within the $T(SH)_2$ synthesis module, GS exhibited the highest elasticity towards the third ligand, such that this enzyme exerted the lowest control (Table S9). TryR had a low elasticity coefficient for TS_2, but the presence of high activity in the cell resulted in negligible flux control. In conclusion, the high flux control of the $T(SH)_2$ synthesis enzymes is mainly derived from their low activities in these parasites.

Concentration control distribution

In contrast to control of the pathway flux, control of $T(SH)_2$ concentration was exerted by its demand and TryR under the three modelled conditions (Table 4). To visualize whether the synthetic pathway contributes to $T(SH)_2$ concentration control, a model was constructed from which TryR was not included (data not shown). Using this truncated model, the values for the control coefficients of the $T(SH)_2$ concentration were similar to the flux control coefficients for γECS, TryS, spermidine transport (Spd1) and the Spd leak

Table 4. Control coefficients on the $T(SH)_2$ concentration of the pathway enzymes. Negative coefficients indicate that these reactions reduce (consume) $T(SH)_2$ or consume a precursor.

Condition	Basal	Control	Stress
Enzyme/precursor (*x*)	$C^{T(SH)_2}_x$		
γECS	0.04	0.008	0.003
GS	5.7×10^{-5}	4.2×10^{-5}	7.95×10^{-5}
TryS	0.007	0.03	0.04
SpdT	8.6×10^{-4}	0.015	0.016
TryR	0.93	0.97	0.95
$T(SH)_2$ demand	−0.99	−0.99	−0.99
NADP+ supply	0.01	0.013	0.0064
Spd sink	-7.8×10^{-5}	−0.01	−0.013
GSH sink	-4.4×10^{-5}	−0.009	−0.026
$T(S_2)$ sink	−0.05	−0.062	−0.072

(Table 3), except for $T(SH)_2$ demand, whose control coefficient value remained −0.99.

Kinetic modelling for drug target identification in the $T(SH)_2$ metabolism of parasites

According to the fundamental principles of MCA, in order to inhibit the flux of a hypothetical linear pathway by 50%, an equal percentage inhibition must be attained for a pathway enzyme that has a flux control coefficient equal to 1 (a true rate-limiting step) [17,18]. Due to the branched nature of metabolic pathways and the shared control of metabolic fluxes, higher percentage inhibition is usually necessary for enzymes with lower control coefficients, and almost complete inhibition is necessary for enzymes with insignificant control.

The kinetic model described above predicted that, to inhibit the flux of $T(SH)_2$ synthesis by 50%, it is necessary to inhibit the individual activities of γECS, TryS and SpdT by 58, 62 and 73%, respectively (Fig. 5A). Furthermore, combined 50% inhibition of the first two enzymes or 40% inhibition of the three proteins resulted in the same decrease in flux. In marked contrast, 99% inhibition of TryR did not affect the synthesis of $T(SH)_2$ (Fig. 5A), as expected from its low flux control coefficient. On the other hand, due to the high TryR control coefficient on the concentration of reduced $T(SH)_2$, the kinetic model predicted that TryR inhibition causes a linear decrease in the metabolite level (Fig. 5B). However, the $T(SH)_2$ concentration is also remarkably affected by the activities of γECS, TryS or SpdT when they are inhibited by > 70% (Fig. 5B).

The model also predicted that, to decrease the $T(SH)_2$ reductive capacity of the parasites by 50%, 60% increased oxidative stress ($T(SH)_2$ demand) combined with a 25% decrease in TryR activity was required (Fig. 5C). With no TryR inhibition, a more than twofold increase in $T(SH)_2$ demand (Fig. 5C), or alternatively 50–75% inhibition of γECS (Fig. 5D), was necessary to achieve a similar decrease in $T(SH)_2$ reductive capacity. On the other hand, the decrease in $T(SH)_2$ synthesis flux brought about by inhibiting γECS and TryS was not further potentiated by increasing oxidative stress (Fig. 5E,F).

Discussion

Characteristics of $T(SH)_2$ metabolism pathway enzymes, metabolite concentrations and fluxes

The kinetic constants of the recombinant purified pathway enzymes were determined under near-physiological conditions of temperature and intracellular pH. The kinetic properties of GS from *T. cruzi* are reported for the first time for a trypanosomatid species, thus completing characterization of the GSH synthetic pathway in these parasites. The kinetic parameters of the recombinant enzymes were similar to those previously reported in the literature (Table S1), except for the lack of GSH inhibition of recombinant and native TryS. Notably, the affinity of TryS from *T. cruzi* strains for GSH is one order of magnitude lower than that for the enzymes from *T. brucei* and *Leishmania* (Table S1).

The V_{max} of most of the pathway enzymes was determined here in *T. cruzi* epimastigotes, except for γECS. These values are critical for construction of the kinetic model as they reflect the amount of active enzyme inside living cells. Estimation of the *in vivo* V_{max} from the content of protein determined by western blot was avoided because, in our experience, there is no linear correlation between the content of protein and the amount of active enzyme [44–46], resulting in miscalculated control coefficients.

Comparison of the catalytic efficiencies V_{max}/K_m of the pathway enzymes suggested that γECS ≥ TryS > > > GS, in the precursor supply module, limit $T(SH)_2$ *de novo* synthesis in the parasites. In contrast, TryR and the TXN-dependent antioxidant machinery (TXN, TXNPx and GPXA), in the $T(SH)_2$-consuming module, have over-capacity (high catalytic efficiency *in vitro* and *in vivo*, and saturation for the substrates). The low catalytic efficiencies of the enzymes of the $T(SH)_2$ supply module correlated with the low pathway fluxes determined *in vivo* (Table 2). Therefore, the most probable reason why TryR and the TXN-dependent peroxide detoxification system are abundant in

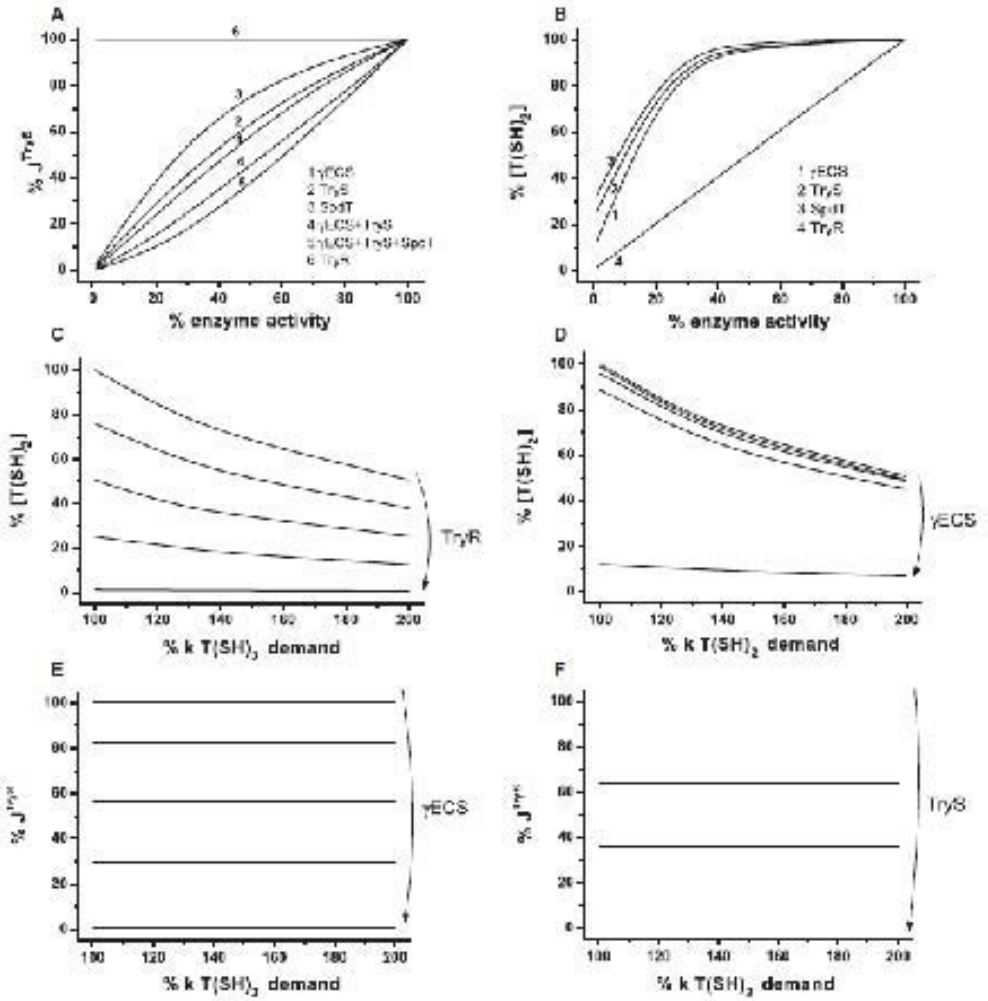

Fig. 5. Predictions using the kinetic model under control conditions. (A) Effect of decreasing the activity of γECS, Try_2S, SodT, Try_2R, and combinations thereof on the flux through Try_2S. Inhibition of the three steps that exert the greatest control affects the flux almost linearly, whereas Try_2I has no effect. (B) Effect of decreased γECS, Try_2S, SodT and Try_2I activity on $T(SH)_2$ concentration. Try_2I inhibition affects the metabolite concentration linearly, whereas γECS, Try_2S and SodT have to be inhibited by > 60% to decrease the metabolite concentration. (C) Effect of increasing the $T(SH)_2$ demand rate at various Try_2R activities. Simultaneous inhibition of Try_2R and increasing the demand module lead to synergistic $T(SH)_2$ depletion. (D) Effect of increasing the $T(SH)_2$ demand module at various concentrations of γECS. Due to the low control that γECS exerts on the $T(SH)_2$ concentration, the synergistic effect is important until γECS is inhibited by > 60%. (E,F) Increasing the rate of $T(SH)_2$ demand has no synergistic inhibitory effect on the $T(SH)_2$ concentration when combined with inhibition of γECS and Try_2S. For (C–F), the activities indicated on the right were modulated at 100, 75, 50, 25 and 7.5% of their original V_{max} values. Note that 100% activity is different for each enzyme, being two orders of magnitude higher for Try_2I than for γECS and Try_2S.

the parasites is to provide an efficient system to immediately deal with external perturbations that decrease the $T(SH)_2/TS_2$ ratio, before activation of the much slower *de novo* $T(SH)_2$ synthesis pathway under prolonged periods of oxidative stress.

Kinetic modelling of $T(SH)_2$ metabolism

Kinetic models of metabolic pathways in human parasites have been described only for glycolysis in *T. brucei* [47] and *Entamoeba histolytica* [48,49] and the glyoxalase system in *Leishmania infantum* [50]. The first kinetic model of $T(SH)_2$ metabolism in a trypanosomatid reported here facilitates understanding of the controlling mechanisms of this important pathway in these parasites.

The kinetic model predicted that $T(SH)_2$ synthesis was mainly controlled (50–70%) by γECS and TryS (Table 1), as a result of their relatively low cellular active contents and non-saturating thiol and polyamine substrates (Table S9). The negligible contribution of feedback inhibition by GSH to the high flux control coefficient of γECS was a consequence of the high $[Glu]/K_{m\ Glu}$ ratio of 59–60 and low $[GSH]/K_{i\ GSH}$ ratio of 0.25–0.5; the competing substrate predominantly binds the enzyme and blocks inhibitor binding. These results emphasize the need to abandon the dogmatic concepts of a 'rate-limiting step' or an 'allosteric or feedback-inhibited enzyme' as the only criteria to describe the controlling steps of metabolic pathways [13,17,18,46]. In contrast, an integral and dynamic network analysis of the pathway can allow precise and quantitative predictions regarding the relevance of a particular enzyme for control of the metabolic pathway, and may unveil unknown interactions among enzymes and metabolites.

The enzymes/processes that control the concentration of $T(SH)_2$ were mainly its demand (oxidative stress) and TryR. However, γECS and TryS also exert control when they are strongly inhibited or when TryR is absent or inhibited. An explanation for this behaviour is that TryR serves as a buffer enzyme to maintain a constant $T(SH)_2/TS_2$ ratio; however, the total $T(SH)_2$ concentration in the cell will only depend on the flux through the synthetic module. Thus, γECS and TryS may potentially exert significant control on the total $T(SH)_2$ concentration in these parasites. In various drug-resistant *Leishmania* strains, an increased content of the enzymes of the $T(SH)_2$ synthesis and antioxidant machinery was determined by microarrays and western blot analyses [51–54]. This indicates that enhancement of $T(SH)_2$ synthetic enzymes is also required to potentiate the antioxidant capabilities of the parasites.

Metabolic modelling also allows the identification of emergent properties of the network that cannot be identified by studying its elements in isolation or as separate pathways [15]. In this regard, the kinetic model identified $T(SH)_2$ metabolism as comprising a catalytically slow and less efficient synthetic module (γECS, GS, TryS and Spd1) and a fast and highly efficient module (the antioxidant enzymatic machinery and TryR), connected through the common metabolite $T(SH)_2$. Moreover, it indicated that excretion of oxidized thiols under oxidative stress may also have a significant effect on the antioxidant capabilities of the parasites as a result of loss of essential GSSG and TS_2 (oxidized) moieties. These pathway emergent properties were only recognized by studying the enzymes and transporters in the network.

It is worth emphasizing that the present *T. cruzi* epimastigote-based kinetic model may be used as a core model to which the particular variations of the pathway between parasite stages or different trypanosomatid species can be added once metabolomic and enzymatic (kinetomic) data become available. For example, the polyamine synthetic pathway lead by *S*-adenosyl methionine decarboxylase and ornithine decarboxyluse in *T. brucei* and *Leishmania*, Spd enzymatic synthesis in *T. cruzi* (Fig. 1), and the oxidative section of the pentose phosphate pathway, which provides NADPH for the antioxidant machinery, are pathways that are directly connected to the reactions considered in the present kinetic model. Another useful application of kinetic/mathematical models is the readiness to predict possible pathway scenarios under different physiological conditions. As discussed above, the most critical parameter for kinetic modelling is the V_{max} value determined in cells; obtaining this parameter for the steps identified here as exerting the greatest control, and measurements of relevant metabolites (GSH, $T(SH)_2$ and Spd) and pathway fluxes in the human stages of *T. cruzi*, may extend the benefits of the present kinetic model. Moreover, the robustness of the model and pathway permits the hypothesis that the steps that exert the greatest control will probably be the enzymes with the lowest activities in cells of *T. cruzi* trypomastigotes and amastigotes.

Utility of kinetic modelling for drug target validation

Kinetic modelling is a useful systems biology approach that facilitates the identification of drug targets with the highest therapeutic potential. Thus, drug design focusing on the steps that exert the greatest control in the network for multi-target inhibition emerges as a

substantiated sound and novel strategy that contrasts with the traditional approach of attempting to fully inhibit non-controlling steps or the 'rate-limiting' steps reported in biochemistry textbooks [13]. Many metabolic enzymes from parasites display substantial differences regarding their allosteric modulation compared to their human counterparts [47–49,55,56], and these differences may be exploited for species-specific targeted therapy. For these reasons, it is worthwhile to embark on a complete kinetic description of parasite enzymes and study them using network-based analysis for validation as drug targets.

Based on the model predictions (Fig. 5), we propose that simultaneous inhibition of the flux-controlling enzyme γECS and TryS will have more striking effects on $T(SH)_2$ metabolism than separate inhibition. Thus, use of combination therapies, or design of multi-target drugs for these enzymes, are interesting starting points for alternative chemotherapy against *T. cruzi* and possibly other trypanosomatids. However, the possible presence of GSH transporters in *T. cruzi*, as suggested for *T. brucei* and *Leishmania* [57,58], may diminish the flux control of γECS and increase those of TryS and SpdT. Therefore, more studies are required on GSH transport in these parasites for a complete understanding of pathway control mechanisms.

With regard to multi-target therapy, it was previously reported that the parasiticidal effects of nifurtimox and benznidazole were increased by co-treatment with buthionine sulfoximine [59,60], an irreversible inhibitor of γECS that also appears to inhibit GSH transport in *T. brucei* [57]. By inhibiting *de novo* $T(SH)_2$ synthesis using buthionine sulfoximine and increasing oxidative stress using commercial drugs, a stronger inhibitory effect on trypanothione metabolism (and growth) was achieved, suggesting that pharmacological intervention on several reactions at lower doses, rather than inhibiting individual enzymes at higher doses, is a more efficient approach to affect the pathway.

Because TryS is not present in the host and has a high flux control coefficient in the pathway, it appears to be the most relevant drug target in $T(SH)_2$ metabolism. Recently, potent non-competitive inhibitors (in the nanomolar range) against purified TryS from *T. brucei* were identified by high-throughput screening of a chemical compound library; however, their effects on growth and thiol contents were achieved in the micromolar range [61], indicating how cellular complexity can make successful drug discovery difficult [62].

On the other hand, TryR inhibition, together with oxidative stress, may favour an oxidized cellular state only when the $T(SH)_2$ synthesis pathway is not activated. Inhibition of TryR or the antioxidant machinery enzymes for therapeutic purposes will be a very challenging task because their high activity in the cell will require the design of highly specific and potent inhibitors or use of high concentrations, with probable severe side-effects for patients. Therefore, inhibition of already limiting enzymes such as γECS and TryS is therapeutically more promising than inhibition of abundant enzymes such as TryR or the peroxide detoxification machinery.

Correlations of the kinetic model predictions with experimental genetic results in other trypanosomatids

The results yielded by kinetic modelling indicated that γECS and TryS were the main controlling steps of $T(SH)_2$ synthesis flux, and probably also of the total $T(SH)_2$ concentration under prolonged stress conditions. Decreased expression (50–80%) of γECS induced by genetic means in *T. brucei* and *Leishmania* resulted in almost 50% decreased content of GSH and $T(SH)_2$ [57,58]. Moreover, treatment of *T. cruzi* with buthionine sulfoximine decreased the intracellular thiol content by 70–80% [59,60]. These results are in agreement with predictions by the present kinetic model regarding the high control that this enzyme exerts on the pathway.

TryS down-regulation in *T. brucei* (85%) promotes fourfold accumulation of GSH and a 10% increase in the amount of Spd, respectively, in addition to an 80% decrease in $T(SH)_2$ levels [63,64] versus control parasites, in agreement with the predictions of the model (Fig. 5B). Although TryS down-regulation also induced an increase in γECS and TryR activities in vivo, most probably to compensate for $T(SH)_2$ depletion, parasite resistance to oxidative stress was impaired and cellular viability was compromised.

SpdT, as the main supply of Spd, showed lower control of $T(SH)_2$ synthesis compared to γECS and TryS, due to its higher catalytic efficiency (V_{max} = 5.8 nmol·min^{-1}·mg cell protein^{-1}; $K_{m,Spd}$ = 0.81 μM) [65]. The molecular identity and kinetic characterization of an Spd transporter in *T. cruzi* has been reported (V_{max} 3.6 pmol·min^{-1} per 10^7 cells, i.e. approximately 156 pmol·min^{-1}·mg cell protein^{-1}; K_m 0.014 mM) [66]. By using these other kinetic parameters, full control by SpdT was achieved because of the extremely low catalytic efficiency (data not shown). Thus, further studies on Spd uptake kinetics are necessary. On the other hand, fast high-affinity transporters for Put/cadaverine have been well characterized in *T. cruzi*

epimastigotes [65–68]. Unfortunately, there is limited information regarding the rate of Spd synthesis from Put (Fig. 1), although it appears to be fast [69]; spermidine synthase (SpdS) from *T. cruzi* has not been characterized. This additional internal source of Spd may further decrease the control exerted by SpdT. Furthermore, *de novo* Spd synthesis from ornithine is possible in *T. brucei* and *Leishmania* [9,70]; hence, redistribution of the control coefficients is expected in these trypanosomatids.

TryR showed negligible control on the synthesis of $T(SH)_2$. In agreement with its predicted control properties, knocking down TryR in both *T. brucei* (< 10% remaining activity) and *Leishmania* did not modify the total thiol content [71,72].

Using the present kinetic model to reproduce longer oxidative stress conditions under which enzyme activities change will require re-determination of fewer experimental parameters than determined in this work, i.e. V_{max}, thiol contents, and fluxes under the new steady state.

Concluding remarks

From the perspective of the organization of intermediary metabolism, all constituent enzymes and transporters are essential for proper pathway function, because deleting any of them creates a gap in the pathway flux. However, from the perspective of the control of metabolism, not all of the pathway components have therapeutic potential, only those that exert significant pathway control. Genetic strategies can determine whether a pathway component is essential for cell function. Kinetic modelling predicts how essential each pathway component is by determining their control coefficients. Hence, kinetic modelling of $T(SH)_2$ metabolism in parasites assists in validation of drug targets with the highest therapeutic potential by identifying the enzymes with the highest control on the pathway flux and $T(SH)_2$ concentration (i.e. γECS ≥ TryS ≫ SpdT).

Experimental procedures

Reagents

ATP, γEC, trifluoroacetic acid, 5,5′-dithio-bis(2-nitrobenzoic acid), haemin, imidazole, sodium borohydride ($NaBH_4$), MES, potassium phosphate monobasic, trehalose, catalase, GSH, $MgCl_2$, EDTA, dansyl chloride, methanol, diethylenetriamine pentaacetic acid, *N*-ethylmaleimide and NADH were purchased from Sigma (St. Louis, MO, USA); glycine, MOPS, dithiothreitol and Hepes were purchased from Research Organics (Cleveland, OH, USA); acetonitrile and NaCl were purchased from Caledon (Georgetown, Ontario, Canada); triethanolamine, perchloric acid, sodium phosphate dibasic and glucose were purchased from JT Baker (Phillipsburg, NJ, USA); phosphoenolpyruvate and β-mercaptoethanol were purchased from ICN Biomedicals (Aurora, OH, USA); H_2O_2 was purchased from Laboratorios Arsenaux (Mexico City, Mexico); isopropyl-β-D-thiogalactoside was purchased from Amresco (Solon, OH, USA). Tris was purchased from IBI Scientific (Peosta, IA, USA).

Culture conditions

Epimastigotes of *T. cruzi* Querétaro strain (TBAR/MX/000-Querétaro) [21] were cultured in RPMI-1640 medium (Sigma) supplemented with 10% fetal bovine serum (PAA Laboratories, Pasching, Austria). The cultures were incubated at 26 °C as described previously [34]. Parasite cultures were started in 20 mL medium and scaled up, always maintaining a density of 2×10^6 parasites per mL, to reach 200 mL after 6 days, then harvested. For TXN and TXN-dependent peroxidase activities, the parasites were cultured in liver infusion tryptose medium (DIFCO, Detroit, MI, USA), supplemented with 10% fetal bovine serum and 25 μg·mL^{-1} haemin, and maintained at 26 °C. In this case, parasite cultures were initiated at a density of 4×10^6 parasites per mL and harvested after 5 days, reaching a density of approximately 25×10^6 parasites per mL.

Gene amplification

Genomic DNA from the *T. cruzi* Nicoa strain was isolated as previously described [34]. γECS, GS, TryS, TryR, TXN, rsGPxA and TXNPx genes were amplified by PCR using genomic DNA from this strain. The nucleotide sequences of the primers used for each gene are: γECS (sense 5′-CGTACCATGGGTCTCTTGACAACG-3′, antisense 5′-TAGCCTCGAGCTCACGGGATCTTTTTGG-3′); GS (sense 5′-CGTACATATGGAACTCTTGGGGGAC-3′, antisense 5′-TAGCGTCGACTTAAACAAGCGCCAGTGA-3′); TryS (sense 5′-CGTACCATGGGCTCTTTGGCGGTACCA-3′, antisense 5′-TAGCAAGCTTCGTTTTCAAGCCACC-3′); TryR (sense 5′-CGTACATATGATGTCAAAGATTTTTG-3′, antisense 5′-TAGCAAGCTTTTACAGAGATGCTTCTGA-3′); TXN (sense 5′-CGTACATATGTCTGGTTTGGCGAAGTAC-3′, antisense 5′-GCTAAGCTTTTAGTCGGACCAGGGGAAG-3′); rsGPxA (sense 5′-GCACATATGTTTCGTTTCGGTCAATTGCTTAG-3′, antisense 5′-GCTAAGCTTTCAAATCCTAGCACCACCAAG-3′); TXNPx (sense 5′-CGTACATATGTCCTGCGGAGACGC-3′, antisense 5′-CGATAAGCTTCTACGCGACAGCACC-3′). All sequences contain *Nde*I and *Hin*dIII restriction sites. The PCR products were cloned in the pGEM®-T easy vector (Promega, Madison, WI, USA), and their identity was confirmed by nucleotide sequencing.

Over-expression and protein purification

The genes were cloned into the *Nde*I and *Hin*dIII restriction sites of the pET28 plasmid (Novagen, Darmstadt, Germany), which was used to transform *Escherichia coli* BL21(DE3) cells in order to over-express the proteins fused to a histidine tail. The cells were grown at 30 °C in Luria Bertani medium to an attenuance at 600 nm of 0.6; then protein expression was induced by adding 0.4 mM isopropyl-β-D-thiogalactoside, and the cells were further cultured overnight at 25 °C. The cells were harvested and resuspended in 20 mL buffer containing 100 mM triethanolamine, pH 7.4, 300 mM NaCl and 2 mM imidazole, and lysed in a French press (AMINCO SLM, Rochester, NY, USA) by passing the cellular suspension three times at 20 000 psi (137.9 MPa) for TryS and TryR, four times at 20 000 psi for γECS, and four times at 16 000 psi (110.3 MPa) for GS. The protocol was optimized for each enzyme because they were highly susceptible to inactivation by sonication, high pressures and the number of passages. For analyses of TXN, GPxA and TXNPx, bacteria were lysed by sonication using a Branson Sonifier 450 (Emerson, Danbury, CT, USA) with one cycle of 30 s at 20% output, one cycle of 1 min at 10–15% output, and one cycle of 30 s at 20% output. Each cycle was followed by a 1 min incubation on ice. The bacterial lysates were centrifuged at 7818 *g* for 15 min at 4 °C. The enzymes were purified from the supernatant at room temperature by Co^{2+}-affinity chromatography using Talon resin (Clontech, Mountain View, CA, USA) as previously described [58]. The enzymes were concentrated at 0.5–2 mg·mL^{-1} for γECS and TryS, 2 mg·mL^{-1} for GS, 1–5 mg·mL^{-1} for TryR, 10 mg·mL^{-1} for TXN, 12.5 mg·mL^{-1} for nsGPxA and 6 mg·mL^{-1} for TXNPx. The enzymes were stored at −80 °C in the presence of 50% glycerol for TXN, nsGPxA, TXNPx and TryR. γECS, GS and TryS recombinant enzymes were relatively unstable under any storage conditions, such as 50% glycerol at −20 °C or 3.2 M ammonium sulfate at 4 °C; only the presence of 0.2 M trehalose for γECS and TryS and 1 M trehalose for GS and storage at 4 °C improved their stabilities.

Kinetic characterization

All the reactions and kinetic parameters were determined at 27 °C. The activities of recombinant γECS, GS and TryS were determined by coupling the ADP production to pyruvate kinase/lactate dehydrogenase (Roche, Mannheim, Germany) and following the NADH oxidation at 340 nm. The standard reaction mixture contained 40 mM Hepes/NaOH, pH 7.4, 5 mM $MgCl_2$, 1 mM EDTA, 1 mM phosphoenolpyruvate, 0.2 mM NADH, 2–20 units (monomer/min) pyruvate kinase/lactate dehydrogenase in ammonium sulfate, and 2–5 μg enzyme plus specific substrates for γECS, 1.5 mM Glu and 0.5 mM ATP, plus 2.1 mM Cys to start the reaction; for GS, 8 mM Gly and 0.9 mM ATP, plus 0.4 mM γECC to start the reaction; for TryS, 11 mM Spd and 0.7 mM ATP, plus 7.6 mM GSH to start the reaction. The K_m for each substrate was determined using saturating concentrations of the two co-substrates (as in the standard reaction). The concentrations of the substrates were varied as follows: for γECS, 0–2 mM Cys, 0–2 mM Glu and 0–1 mM ATP; for GS, 0–0.4 mM γEC, 0–10 mM Gly and 0–1.5 mM ATP; for TryS, 0–5 mM GSH, 0–11 mM Spd and 0–1 mM ATP. TryS purified from bacteria disrupted by sonication showed hysteresis, however, by starting the reaction with Spd or by disrupting bacteria using the French press, this phenomenon was not observed (data not shown).

TryR activity was determined spectrophotometrically following NADPH oxidation at 340 nm. The standard reaction mixture contained 40 mM Hepes, pH 7.4, 1 mM EDTA, 0.07–0.09 μg TryR, 0.24 mM TS_2 (Bachem, Torrance, CA, USA) and 0.2 mM NADPH. For K_m determinations, the NADPH concentration was varied from 0 to 0.2 mM (saturating with 0.24 mM TS_2) and the TS_2 concentration was varied from 0 to 0.4 mM (saturating with 0.2 mM NADPH).

For GS $K_{i(app)}$ determinations, saturation curves for each substrate were determined as described above (for the K_m determinations) in the presence of varying GSH concentrations (0–10 mM). For γECS, $K_{i(GSH)}$ and $K_{i(γEC)}$ saturation curves for Glu were determined in the presence of 0–5 mM γEC or 0–5 mM GSH.

The effect of TS_2, GSSG and $T(SH)_2$ on the three enzymes was determined using saturating concentrations of their substrates. The concentrations tested were within the physiological range of concentrations.

The TXN, nsGPxA and TXNPx activities were determined by reconstituting the antioxidant pathway in the presence of TS_2 and TryR, and spectrophotometrically monitoring NADPH oxidation at 340 nm. In all cases, it was ensured that all added TS_2 was reduced by TryR before addition of the enzyme of interest. The 0.5 mL standard reaction mixture contained 40 mM Hepes, pH 7.4, 1 mM EDTA, 0.16 mM NADPH, 0.4 mM TS_2, and the following proteins and substrates: for TXN (0.12–0.16 μM), 0.5 μM TryR, 20 μM TXNPx and 0.22 mM *tert*-butylhydroperoxide (t-butOOH); for nsGPxA (0.02–0.075 μM), 0.5 μM TryR, 22 μM TXN and 1 mM cumene hydroperoxide (CumOOH); for TXNPx (1 μM), 0.045 mM TS_2, 10 nM TryR, 1 μM TXN and 150 μM t-butOOH. The reactions were started by addition of the enzyme of interest at the indicated concentrations. The K_m for each substrate was determined by varying one of the substrates and using saturating concentrations of the co-substrate. The substrates were varied as follows: for TXN, 0–0.4 mM TS_2; for nsGPxA, 0–22 μM TXN and 0–1 mM CumOOH; for TXNPx, 0–20 μM TXN and 0–800 μM CumOOH or 0–700 μM t-butOOH. In these assays, the spurious reaction between the formed $T(SH)_2$ and the hydroperoxides was

monitored before the reaction was started, and subtracted when calculating the activity.

The thiol substrates were routinely calibrated using 5,5′-dithio-bis(2-nitrobenzoic acid), whereas ATP was calibrated using hexokinase and glucose-6-phosphate dehydrogenase. The experimental and coupling enzymes concentrations were varied to ensure that measurements were obtained under initial velocity conditions, except for TXNPx, which was measured under non-saturating conditions because of its instability under dilution.

Determination of enzyme activities in parasites under control and oxidant conditions

Forty million epimastigotes from the Queretaro strain [28] suspended in 1 mL of NaCl/P$_i$ (137 mM NaCl, 2.7 mM KCl, 10 mM Na_2HPO_4 and 2 mM KH_2PO_4, pH 7.4) supplemented with 20 mM glucose were incubated at room temperature (25–30 °C) in the absence or presence of 50 μM H_2O_2. After 10 min, catalase (10 units) was added and further incubated for 2 min, and cytosolic extracts were obtained.

The cells were harvested, resuspended in 0.1 mL lysis buffer (20 mM Hepes, pH 7.4, 1 mM EDTA, 0.15 mM KCl, 1 mM dithiothreitol and 1 mM phenylmethanesulfonyl fluoride), and lysed by freezing in liquid nitrogen and thawing at 37 °C three times. The cellular extract was centrifuged at 20 817 *g* for 10 min, and the supernatant was immediately used for enzyme activity measurements. In the case of TXN and peroxidase activity, no pre-incubation in H_2O_2 was performed, i.e. the cells were harvested, washed in NaCl/P$_i$ buffer, and lysed as described above.

γECS, GS and TryS activities in clarified cytosolic parasite extracts were determined by following ADP production in an end-point kinetic assay. Briefly, the reaction mixture contained 40 mM Hepes, pH 7.4, 10 mM $MgCl_2$, 0.1–0.5 mg cytosolic extract, and 1.3 mM Glu, 2.1 mM Cys and 2 mM ATP for γECS, 0.4 mM γEC, 8 mM Gly and 2 mM ATP for GS, and 8 mM GSH, 11 mM Spd, and 2 mM ATP for TryS. Parallel reactions were set up that lacked one of the co-substrates. After 30 min of incubation at 37 °C, the reaction was stopped by perchloric acid extraction (2% final concentration), the samples were centrifuged at 20 817 *g* for 10 min at 4 °C to eliminate the precipitated protein, and the supernatant was neutralized with 2 M KOH/0.1 M Tris. The ADP concentration was determined spectrophotometrically using a pyruvate kinase/lactate dehydrogenase-coupled assay as described previously [48]. The spurious ADP produced by ATPase activity in the clarified extracts in control reactions was always subtracted (Table S1). We ensured that the enzyme activity was linearly dependent on the amount of extract (Table S2). Longer incubation times decreased the enzyme activity. TryR activity was determined spectrophotometrically by following NADPH oxidation at 340 nm. The reaction mixture contained 40 mM Hepes, pH 7.4, approximately 50 μg extract, 0.24 mM TS_2 and 0.2 mM NADPH. The TXN and peroxidase activities in the cytosolic parasite extracts were determined by reconstituting the antioxidant pathway in the same way as for the recombinant enzyme activities. The standard reaction mixture contained 40 mM Hepes, 1 mM EDTA, 0.16 mM NADPH, 0.5 μM TryR, 0.45 mM $T(SH)_2$ and 25–35 μg of parasite extract; subsequent additions were for TXN 0.1 mM CumOOH, and the reaction was started by adding 20 μM nsGPxA; for the TXN-dependent peroxidase activities were 5 μM CumOOH, and the reaction was started by adding 20 μM TXN.

Determination of metabolites

For determination of thiol content, two protocols were used, either direct parasite mixing with perchloric acid or by preparing cytosolic extracts as described above, followed by incubation for 10 min on ice with an excess of $NaBH_4$, and further precipitation with 2% perchloric acid (final concentration). There were no differences in the results obtained using each protocol. The acid extracts were centrifuged at 20 817 *g* for 5 min at 4 °C. Twenty microlitres of the supernatant were separated by an HPLC system (Waters, Milford, MA, USA) coupled to a reversed-phase C18 column (3.5 μm particle size; Symmetry, Milford, MA, USA) previously equilibrated with a 99% trifluoroacetic acid solution (0.1% v/v in water) plus 1% acetonitrile. Thiol molecules were separated by elution with the same buffer for 10 min at a rate of 1 mL·min^{-1}; the eluates were mixed with 5,5′-dithio-bis(2-nitrobenzoic acid) and the absorbance was detected at 412 nm. The identity of each peak was determined using commercial compounds either run in parallel or mixed with the samples.

For TS_2 determination, approximately 1×10^9 parasites were incubated for 10 min in the absence or presence of H_2O_2; the parasites were then harvested and resuspended in 0.025 mL buffer containing 40 mM Hepes, pH 8.0, 4 mM diethylenetriaminepentaacetate and 6 mM *N*-ethylmaleimide. Alkylation of free thiols was performed at 70 °C for 5 min. An equal volume of 20% trichloroacetic acid in 10 mM HCl was added to the sample, which was further incubated for 30 min at 4 °C, followed by centrifugation at 20 817 *g* for 10 min at 4 °C. The unbound *N*-ethylmaleimide was extracted 10 times using water-saturated ethyl acetate, and the sample was bubbled with N_2. The acid extracts were neutralized using 3 M KOH/0.1 M Tris. The amount of TS_2 was determined in the neutralized extracts in a 1 mL reaction containing 40 mM Hepes, pH 7.4, 1 units TryR and 0.16 mM NADPH. Alternatively, alkylation of free thiols using vinylpyridine was performed. Briefly, the same amount of parasites was deproteinized with 2% sulfosalicylic acid; then 2 μL 100% vinylpyridine were added, and the pH was adjusted to 6–7 by adding triethanolamine. The alkylation was performed at room temperature over 60 min, and TS_2

in the sample was quantified as described above. Both protocols yielded comparable results.

For determination of free amino acids, parasite extracts were obtained by three cycles of freezing and thawing, and perchloric acid was added for protein precipitation. The lysates were centrifuged at 20 817 *g* for 5 min at 4 °C, the supernatant was neutralized with 3 M KOH/0.1 M Tris, and the samples were derivatized with two volumes of *ortho*-phtalaldehyde solution (7.6 mM *ortho*-phtalaldehyde, 5% ethanol, 5% β-mercaptoethanol and 9 mM 0.4 M boric acid, pH 10.4), and incubated for 5 min at room temperature. Fifty microlitres of the reaction were injected into an HPLC device coupled to a reverse-phase C18 column (Waters, Spherisorb, 5 μm particle size, 4.6 × 250 mm column size) previously equilibrated with a mixture of 90% solution A (40 mM sodium phosphate buffer, pH 7.8) plus 10% solution B (45% methanol, 45% acetonitrile, 10% water). A 90 min gradient of solution B (10–95%) was used. The amino acids were detected by fluorescence (340 nm excitation, 460 nm emission).

For polyamine determination, the deproteinized cytosolic extracts were neutralized using $NaHCO_3$ powder, and the samples were evaporated at 70 °C. The desiccated samples were resuspended in a mix containing 0.050 mL 0.05 N HCl, 0.4 mL 0.1 M $NaHCO_3$, pH 9.45, and 0.8 mL 4 mM dansyl chloride, and incubated at 70 °C for 15 min, then 1 mL methanol was added for each 0.95 mL of sample, and the sample was filtered. Twenty microlitres were injected into an HPLC device coupled to a reverse-phase C18 column (Waters, 5 μm diameter Spherisorb, 4.6 × 250 mm column) was previously equilibrated with a mixture of 60% methanol and 40% water. A 55 min gradient from 60 to 95% methanol was used to separate the samples, and the polyamines were detected by fluorescence (365 nm excitation, 510 nm emission).

For ATP determination, deproteinized and neutralized cytosolic extracts were obtained as for amino acid content analysis from 5.4×10^8 epimastigotes. ATP was determined as previously described [40]. $NADP^+$ determination was performed by spectrofluorometry as described previously [75] from 2.4×10^9 parasites. The NADPH concentration was calculated on the basis that the NADP/NADPH ratio in *T. cruzi* epimastigotes is 0.5 [76].

The metabolite concentrations were calculated by assuming that 1×10^7 parasites correspond to 3 μL, as described previously [77].

Flux determination

Aliquots of 4×10^7 parasites resuspended in 1 mL $NaCl/P_i$ supplemented with 20 mM glucose were incubated at room temperature in the absence or presence of the peroxide; the cells were harvested at various times (0, 5 and 10 min), disrupted, and the $T(SH)_2$ content was determined by HPLC as described above. Flux was calculated considering that 1×10^7 *T. cruzi* epimastigotes correspond to 0.23 ± 0.00 mg soluble protein ($n = 2$), value determined in the present study.

Rate equations used in the model

As the ATP concentration is high and constant under stress and non-stress conditions (Table 7), and is saturating (approximately 10-fold) for the three synthetic enzymes γ-ECS, GS and TryS (Table 1), their rate equations were simplified by not including the ATP concentrations. The K_{eq} values used were the K_c values for the third product (Table 1). The K_{eq} values of 55% used for the γ-ECS, GS and TryS equations were calculated as described previously [39], in which $\Delta G^{\circ\prime}$ (standard free energy change) was the difference between that of peptide bond formation (+5.2 kcal·mol^{-1}) and that of ATP hydrolysis (−7.3 kcal·mol^{-1}).

For γ-ECS, a random bi-reactant rate equation with competitive inhibition by GSH versus Glu was used [78]:

$$v = \frac{V_{max}\left(\left(\frac{A \cdot B}{K_{ia}K_b}\right) - \left(\frac{P}{K_{eq}}\right)\right)}{\left(1 + \left(\frac{A}{K_{ia}}\right) + \left(\frac{B}{K_b}\right) + \left(\frac{\alpha \cdot A \cdot B}{\alpha K_{ia}K_b}\right) + \left(\frac{P}{K_{eq}}\right) + \left(\frac{A \cdot B}{\beta K_{ia}K_b}\right)\right)}$$

where A = Cys, B = Glu, I = GSH and P is γEC. The α and β values were adjusted to reach metabolite concentrations present in the parasite (Tables S6 and S7). The α value is the factor by which binding of one substrate changes the affinity of the enzyme for the co-substrates. For γ-ECS, the α value was 1, as previously reported [8]. The β value represents the factor by which the K_{ia} for Cys is modified when GSH, which is an inhibitor, is bound to the free enzyme, competing for Glu. To our knowledge, no information on this value has been reported, thus it was adjusted to obtain the γEC concentrations in the parasite.

For GS, a random bi-reactant mechanism equation [78] was used:

$$v = \frac{V_{max}\left(\left(\frac{A \cdot B}{K_{ia}K_b}\right) - \left(\frac{P}{K_{eq}}\right)\right)}{\left(1 + \left(\frac{A}{K_{ia}}\right) + \left(\frac{B}{K_b}\right) + \left(\frac{P}{K_{eq}}\right) + \left(\frac{A \cdot B}{\alpha K_{ia}K_b}\right)\right)}$$

where A = γEC, B = Gly and P = GSH. An α value of 12 was used based on those obtained for *A. thaliana* GS [80].

*T.*Try*S* is able to use GSH and free glutathionyl spermidine as substrates to synthesize $T(SH)_2$, but only the overall reaction was considered. For this enzyme, a random tri-uni mechanism equation was used [78]:

$$v = \frac{V_{max}\left(\left(\frac{A \cdot A \cdot B}{K_{ia}K_{ia}K_b}\right) - \left(\frac{P}{K_{eq}}\right)\right)}{1 + 2 \cdot \left(\frac{A}{K_{ia}}\right) + \left(\frac{B}{K_b}\right) + 2 \cdot \left(\frac{\alpha \cdot A \cdot A}{\alpha K_{ia}K_{ia}}\right) + \left(\frac{\alpha \cdot A \cdot B}{\alpha K_{ia}K_b}\right) + \left(\frac{P}{K_{eq}}\right)}$$

where A = GSH, B = Spd and P = $T(SH)_2$. As already mentioned, the $K_{m\,GSH}$ of *T. cruzi* Try*S* is 10 times higher

than the K_m reported for the *T. brucei* and *Leishmania* enzymes (Table S1). Thus, only when the α value was adjusted to a value of 0.1 (which increases the affinity for GSH by 10-fold) could the pathway kinetic model simulate the GSH concentration found in the parasites. This suggests the presence of an unknown TryS activator in *T. cruzi*.

The kinetic mechanism of TryR has not been described, but putative bi-bi-ping-pong kinetics have been suggested, similar to glutathione reductase [81]. To avoid adjustment of all the constants affecting the kinetic parameters for such a complex equation, its rate equation was simplified to ordered bi-bi kinetics [78]:

$$v = \frac{\frac{V_{max}}{K_{iA}K_{mB}}\left(AB - \left(\frac{PQ}{K_{eq}}\right)\right)}{\left(1 + \left(\frac{A}{K_{iA}}\right) + \left(\frac{B}{K_{mB}}\right) + \left(\frac{AB}{K_{iA}K_{mB}}\right) + \left(\frac{P}{K_{iP}}\right) + \left(\frac{Q}{K_{iQ}}\right) + \left(\frac{PQ}{K_{iP}K_{iQ}}\right)\right)}$$

where A = NADPH, B = TS_2, P = $NADP^+$ and Q = $T(SH)_2$.

For SpdT, a ranmosubstrate Haldane's equation [78] was used:

$$v = \frac{\frac{V_{max}}{K_{mS}} \cdot \left(S - \left(\frac{P}{K_{eq}}\right)\right)}{1 + \left(\frac{S}{K_{mS}}\right) + \left(\frac{P}{K_{iP}}\right)}$$

where S = Spd_{in} and P = Spd_{ex}. The K_i and K_m values were adjusted given that the Spd_{in} is low in the parasites and a high K_{eq} favours the forward reaction.

For the $T(SH)_2$ demand reaction, a reversible mass action equation was used:

$$v = k_1 \prod S - k_2 \prod P$$

For the reactions of the Spd, $T(SH)_2$ and GSH leaks, irreversible mass action equations were used:

$$v = k \cdot \prod S$$

Acknowledgements

This work was supported by Consejo Nacional de Ciencia y Tecnología (CONACyT) Mexico grant numbers 83084 to E.S., and 80554 and 123636 to R.M.-S. V.O.-S. was supported by CONACyT PhD fellowship number 176866. We thank Professor Luise Krauth-Siegel Biochemistry Center, University of Heidelberg, Germany for providing $T(SH)_2$ for some experiments and accepting V.O.-S. for a short research stay at her laboratory.

References

1 World Health Organization (2007) *Reporte sobre la enfermedad de Chagas*. World Health Organization on behalf of the Special Programme for Research and Training in Tropical Diseases, Geneva, Switzerland.
2 Coura JR & Albajar-Viñas P (2010) Chagas disease: a new worldwide challenge. *Nature* **465**, S6–S7.
3 Rodrigues J & de Castro SL (2002) A critical review on Chagas disease chemotherapy. *Mem Inst Oswaldo Cruz* **97**, 3–24.
4 Clayton J (2010) Chagas disease 101. *Nature* **465**, S4–S5.
5 Wilkinson SR & Kelly JM (2009) Trypanocidal drugs: mechanisms, resistance and new targets. *Expert Rev Mol Med* **11**, e31.
6 Fairlamb AH & Cerami A (1992) Metabolism and functions of trypanothione in the Kinetoplastida. *Annu Rev Microbiol* **46**, 695–729.
7 Krauth-Siegel RL & Comini MA (2008) Redox control in trypanosomatids, parasitic protozoa with trypanothione-based thiol metabolism. *Biochim Biophys Acta* **1780**, 1236–1248.
8 Irigoín F, Cibils L, Comini MA, Wilkinson SR, Flohé L & Radi R (2008) Insights into the redox biology of *Trypanosoma cruzi*: trypanothione and oxidant detoxification. *Free Radic Biol Med* **45**, 733–742.
9 Olin-Sandoval V, Moreno-Sánchez R & Saavedra E (2010) Targeting trypanothione metabolism in trypanosomatid human parasites. *Curr Drug Targets* **11**, 1614–1640.
10 Taylor MC, Huang H & Kelly JM (2011) Genetic strategies in *Trypanosoma cruzi*. *Adv Parasitol* **75**, 231–250.
11 Krauth-Siegel L & Leroux AE (2012) Low molecular mass antioxidants in parasites. *Antioxid Redox Signal* doi:10.1089/ars.2011.4392.
12 Hornberg JJ, Bruggeman FJ, Bakker BM & Westerhoff HV (2007) Metabolic control analysis to identify optimal drug targets. *Prog Drug Res* **64**, 171, 173–189.
13 Moreno-Sanchez R, Saavedra E, Rodriguez-Enriquez S, Gallardo-Perez JC, Quezada H & Westerhoff HV (2010) Metabolic control analysis indicates a change of strategy in the treatment of cancer. *Mitochondrion* **10**, 626–639.
14 Klipp E, Wade RC & Kummer U (2010) Biochemical network-based drug-target prediction. *Curr Opin Biotechnol* **21**, 511–516.
15 Kolodkin A, Boogerd FC, Plant N, Bruggeman FJ, Goncharuk V, Lunshof J, Moreno-Sánchez R, Yilmaz N, Bakker BM, Snoep JL *et al.* (2011) Emergence of the silicon human and network targeting drugs. *Eur J Pharm Sci* doi:10.1016/j.ejps.2011.06.006.
16 Westerhoff HV & Palsson BO (2004) The evolution of molecular biology into systems biology. *Nat Biotechnol* **22**, 1249–1252.
17 Fell D (1997) *Understanding the Control of Metabolism*. Portland Press, London.
18 Moreno-Sanchez R, Saavedra E, Rodriguez-Enriquez S & Olin-Sandoval V (2008) Metabolic control analysis:

a tool for designing strategies to manipulate metabolic pathways. *J Biomed Biotechnol* **2008**, 369015.

19 Snoep JL (2005) The Silicon Cell initiative: working towards a detailed kinetic description at the cellular level. *Curr Opin Biotechnol* **16**, 336–343.

20 Westerhoff HV, Kolodkin A, Conradie R, Wilkinson SJ, Bruggeman FJ, Krab K, van Schuppen JH, Hardin H, Bakker BM, Moné MJ *et al.* (2009) Systems biology towards life *in silico*: mathematics of the control of living cells. *J Math Biol* **58**, 7–34.

21 Bosseno MF, Barnabé C, Gastélum EM, Kasten FL, Ramsey J, Espinoza B & Breniere SF (2002) Predominance of *Trypanosoma cruzi* lineage I in Mexico. *J Clin Microbiol* **40**, 627–632.

22 Vanderheyden N, Benaim G & Docampo R (1996) The role of a H^+-ATPase in the regulation of cytoplasmic pH in *Trypanosoma cruzi* epimastigotes. *Biochem J* **318**, 103–109.

23 Vanderheyden N & Docampo R (2000) Intracellular pH in mammalian stages of *Trypanosoma cruzi* is K^+-dependent and regulated by H^+-ATPases. *Mol Biochem Parasitol* **105**, 257–271.

24 Oza SL, Tetaud E, Ariyanayagam MR, Warnon SS & Fairlamb AH (2002) A single enzyme catalyses formation of trypanothione from glutathione and spermidine in *Trypanosoma cruzi*. *J Biol Chem* **277**, 35853–35861.

25 Oza SL, Ariyanayagam MR, Aitcheson N & Fairlamb AH (2003) Properties of trypanothione synthetase from *Trypanosoma cruzi*. *Mol Biochem Parasitol* **131**, 25–33.

26 Oza SL, Shaw MP, Wyllie S & Fairlamb AH (2005) Trypanothione biosynthesis in *Leishmania major*. *Mol Biochem Parasitol* **139**, 107–116.

27 Sharma SK & Bonyal HS (2011) Characterization of *Plasmodium berghei* glutathione synthetase. *Parasitol Int* **60**, 321–327.

28 Gupta S, Srivastava AK & Bamezai N (2005) Steady state kinetic studies of filarial glutathione synthetase by high performance liquid chromatography. *Exp Parasitol* **111**, 137–141.

29 Velohonsky G, Tuby ANYIL, Parat N, Wellman-Rousseau M, Visvikis A, Leroy P, Rashi S, Steinberg P & Stark AA (2002) A spectrophotometric assay of γ-glutamylcysteine synthetase and glutathione synthetase in crude extracts from tissues and cultured mammalian cells. *Chem Biol Interact* **140**, 49–63.

30 Hell R & Bergmann L (1990) γ-glutamylcysteine synthetase in higher plants: catalytic properties and subcellular localization. *Planta* **180**, 603–612.

31 Khan AU, Mei YH & Wilson T (1992) A proposed function for spermine and spermidine: protection of replicating DNA against damage by singlet oxygen. *Proc Natl Acad Sci USA* **89**, 11426–11427.

32 Hernández SM, Sánchez MS & Schwarcz de Tarlovsky MN (2006) Polyamines as a defense mechanism against lipoperoxidation in *Trypanosoma cruzi*. *Acta Trop* **98**, 94–102.

33 Wyllie S, Cunningham ML & Fairlamb AH (2004) Dual action of antimonial drugs on thiol redox metabolism in the human pathogen *Leishmania donovani*. *J Biol Chem* **279**, 39925–39932.

34 Toledo I, Noronha-Dutra AA & Hansberg W (1991) Loss of NAD(P)-reducing power and glutathione disulfide excretion at the start of induction of aerial growth in *Neurospora crassa*. *J Bacteriol* **173**, 3245–3249.

35 Sharma R, Awasthi S, Zimniak P & Awasthi YC (2000) Transport of glutathione- conjugates in human erythrocytes. *Acta Biochim Pol* **47**, 751–762.

36 Mendes P (1993) GEPASI: a software package for modeling the dynamics, steady states and control of biochemical and other systems. *Comput Appl Biosci* **9**, 563–571.

37 Hoops S, Sahle S, Gauges R, Lee C, Pahle J, Simus N, Singhal M, Xu L, Mendes P & Kummer U (2006) COPASI – a COmplex PAthway SImulator. *Bioinformatics* **22**, 3067–3074.

38 Cornish-Bowden A & Cárdenas ML (2001) Information transfer in metabolic pathways. Effects of irreversible steps in computer models. *Eur J Biochem* **268**, 6610–6624.

39 Mendoza-Cozatl D & Moreno-Sánchez R (2006) Control of glutathione and phytochelatin synthesis under cadmium stress. Pathway modeling for plants. *J Theor Biol* **238**, 919–936.

40 Hofmeyr JHS & Cornish-Bowden A (2000) Regulating the cellular economy of supply and demand. *FEBS Lett* **476**, 47–51.

41 Krauth-Siegel RL, Enders B, Henderson GB, Fairlamb AH & Schirmer RH (1987) Trypanothione reductase from *Trypanosoma cruzi*. Purification and characterization of the crystalline enzyme. *Eur J Biochem* **164**, 123–128.

42 Castro H & Tomás AM (2008) Peroxidases of trypanosomatids. *Antioxid Redox Signal* **10**, 1593–1606.

43 van Gend C, Conradie R, du Preez FB & Snoep JL (2007) Data and model integration using JWS Online. *In Silico Biol* **7**, S27–S35.

44 Rodríguez-Enríquez S, Carreño-Fuentes L, Gallardo-Pérez JC, Saavedra E, Quezada H, Vega A, Marín-Hernández A, Olín-Sandoval V, Torres-Márquez ME & Moreno-Sánchez R (2010) Oxidative phosphorylation is impaired by prolonged hypoxia in breast and possibly in cervix carcinoma. *Int J Biochem Cell Biol* **42**, 1744–1751.

45 Marín-Hernández A, Gallardo-Pérez JC, Rodríguez-Enríquez S, Encalada R, Moreno-Sánchez R & Saavedra E (2011) Modeling cancer glycolysis. *Biochim Biophys Acta* **1807**, 755–767.

46 Quezada H, Marín-Hernández A, Aguilar H, López G, Gallardo-Pérez JC, Jasso-Chávez R, González A,

Saavedra E & Moreno-Sánchez R (2011) The Lys20 homocitrate synthase isoform exerts most of the flux control over the lysine synthesis pathway in *Saccharomyces cerevisiae*. *Mol Microbiol* 82, 578–590.

47 Albert MA, Haanstra JR, Hannaert V, Van Roy J, Opperdoes FR, Bakker BM & Michels PA (2005) Experimental and *in silico* analyses of glycolytic flux control in bloodstream form *Trypanosoma brucei*. *J Biol Chem* 280, 28306–28315.

48 Saavedra E, Marín-Hernández A, Encalada R, Olivos A, Mendoza-Hernández G & Moreno-Sánchez R (2007) Kinetic modeling can describe *in vivo* glycolysis in *Entamoeba histolytica*. *FEBS J* 274, 4922–4949.

49 Moreno-Sánchez R, Encalada R, Marín-Hernández A & Saavedra E (2008) Experimental validation of metabolic pathway modeling. *FEBS J* 275, 3454–3469.

50 Sousa M, Ferreira AE, Tomás AM, Cordeiro C & Ponces A (2008) Quantitative assessment of the glyoxylate pathway in *Leishmania infantum* as a therapeutic target by modelling and computer simulation. *FEBS J* 272, 2388–2398.

51 Grondin K, Haimeur A, Mukhopadhyay R, Rosen BP & Ouellette M (1997) Co-amplification of the γ-glutamylcysteine synthetase gene *gshI* and of the ABC transporter gene *pgpA* in arsenite-resistant *Leishmania tarentolae*. *EMBO J* 16, 3057–3065.

52 Guimond C, Trudel N, Brochu C, Marquis N, El Fadili A, Peytavi R, Boisvert F, Richard D, Messier N, Papadopoulou B *et al.* (2003) Modulation of gene expression in *Leishmania* drug resistant mutants as determined by targeted DNA microarrays. *Nucleic Acids Res* 31, 5886–5896.

53 Mukherjee A, Padmanabhan PK, Singh S, Roy G, Girard I, Chatterjee M, Ouellette M & Madhubala R (2007) Role of ABC transporter MRPA, γ-glutamylcysteine synthetase and ornithine decarboxylase in natural antimony-resistant isolates of *Leishmania donovani*. *J Antimicrob Chemother* 59, 204–211.

54 Wyllie S, Mandal G, Singh N, Sundar S, Fairlamb AH & Chatterjee M (2010) Elevated levels of tryparedoxin peroxidase in antimony unresponsive *Leishmania donovani* field isolates. *Mol Biochem Parasitol* 173, 162–164.

55 Opperdoes FR & Michels PA (2001) Enzymes of carbohydrate metabolism as potential drug targets. *Int J Parasitol* 31, 482–490.

56 Saavedra E, Encalada R, Pineda E, Jasso-Chávez R & Moreno-Sánchez R (2005) Glycolysis in *Entamoeba histolytica*. Biochemical characterization of recombinant glycolytic enzymes and flux control analysis. *FEBS J* 272, 1767–1783.

57 Huynh TT, Huynh VT, Harrison MA & Phillips MA (2003) Gene knockdown of γ-glutamylcysteine synthetase by RNAi in the parasitic protozoa *Trypanosoma brucei* demonstrates that it is an essential enzyme. *J Biol Chem* 278, 39794–39800.

58 Mukherjee A, Roy G, Guimond C & Ouellette M (2009) The γ-glutamylcysteine synthetase gene of *Leishmania* is essential and involved in response to oxidants. *Mol Microbiol* 74, 914–927.

59 Faundez M, Pino L, Letelier P, Ortiz C, Lopez R, Seguel C, Ferreira J, Pavani M, Morello A & Maya JD (2006) Buthionine sulfoximine increases the toxicity of nifurtimox and benznidazole to *Trypanosoma cruzi*. *Antimicrob Agents Chemother* 49, 126–140.

60 Faundez M, Lopez-Munoz R, Torres G, Morello A, Ferreira J, Kemmerling U, Orellana M & Maya JD (2008) Buthionine sulfoximine has anti-*Trypanosoma cruzi* activity in a murine model of acute Chagas' disease and enhances the efficacy of nifurtimox. *Antimicrob Agents Chemother* 52, 1857–1859.

61 Torrie LS, Wyllie S, Spinks D, Oza SL, Thompson S, Harrison JR, Gilbert IH, Wyatt PG, Fairlamb AH & Frearson JA (2009) Chemical validation of trypanothione synthetase: a potential drug target for human trypanosomiasis. *J Med Chem* 284, 137–145.

62 Frearson JA, Wyatt PG, Gilbert IH & Fairlamb AH (2007) Target assessment for antiparasitic drug discovery. *Trends Parasitol* 23, 589–595.

63 Comini MA, Guerrero SA, Haile S, Menge U, Lünsdorf H & Flohé L (2004) Validation of *Trypanosoma brucei* trypanothione synthetase as drug target. *Free Radic Biol Med* 36, 1289–1302.

64 Ariyanayagam MR, Oza SL, Guther ML & Fairlamb AH (2005) Phenotypic analysis of trypanothione synthetase knockdown in the African trypanosome. *Biochem J* 391, 425–432.

65 Le Quesne SA & Fairlamb AH (1996) Regulation of a high-affinity diamine transport system in *Trypanosoma cruzi* epimastigotes. *Biochem J* 316, 481–486.

66 Carrillo C, Canepa GE, Algranati ID & Pereira CA (2006) Molecular and functional characterization of a spermidine transporter (TcPAT12) from *Trypanosoma cruzi*. *Biochem Biophys Res Commun* 344, 936–940.

67 Gonzalez NS, Ceriani C & Algranati ID (1992) Differential regulation of putrescine uptake in *Trypanosoma cruzi* and other trypanosomatids. *Biochem Biophys Res Commun* 188, 120–125.

68 Hasne MP, Coppens I, Soysa R & Ullman B (2010) A high-affinity putrescine–cadaverine transporter from *Trypanosoma cruzi*. *Mol Microbiol* 76, 78–91.

69 Algranati ID (2010) Polyamine metabolism in *Trypanosoma cruzi*: studies on the expression and regulation of heterologous genes involved in polyamine biosynthesis. *Amino Acids* 38, 649–651.

70 Persson L (2007) Ornithine decarboxylase and S-adenosylmethionine decarboxylase in trypanosomatids. *Biochem Soc Trans* 35, 314–317.

71 Dumas C, Ouellette M, Tovar J, Cunningham ML, Fairlamb AH, Tamar S, Olivier M & Papadopoulou B (1997) Disruption of the trypanothione reductase gene

of *Leishmania* decreases its ability to survive oxidative stress in macrophages. *EMBO J* 16, 2590–2598.

72 Krieger S, Schwarz W, Ariyanayagam MR, Fairlamb AH, Krauth-Siegel RL & Clayton C (2000) Trypanosomes lacking trypanothione reductase are avirulent and show increased sensitivity to oxidative stress. *Mol Microbiol* 35, 542–552.

73 Fernández-Presas AM, Tato P, Becker I, Solano S, Kopitin N, Berzunza M, Willms K, Hernández J & Molinari JL (2010) Specific antibodies induce apoptosis in *Trypanosoma cruzi* epimastigotes. *Parasitol Res* 106, 1327–1337.

74 Berzunza-Cruz M, Cabrera N, Crippa-Rossi M, Sosa Cabrera T, Pérez-Montfort R & Becker I (2002) Polymorphism analysis of the internal transcribed spacer and small subunit of ribosomal RNA genes of *Leishmania mexicana*. *Parasitol Res* 88, 918–925.

75 Bergmeyer HU (1985) *Methods of Enzymatic Analysis*, Vol. VI, 3rd edn. Deutsche Bibliothek, Federal Republic of Germany.

76 De Vas MG, Portal P, Alonso GD, Schlesinger M, Flawiá MM, Torres HN, Fernández-Villamil S & Paveto C (2011) The NADPH-cytochrome P450 reductase family in *Trypanosoma cruzi* is involved in the sterol biosynthesis pathway. *Int J Parasitol* 41, 99–108.

77 Rangel-Aldao R, Allende O, Triana F, Piras R, Henriquez D & Piras M (1987) Possible role of cAMP in the differentiation of *Trypanosoma cruzi*. *Mol Biochem Parasitol* 22, 39–43.

78 Segel IH (1975) *Enzyme Kinetics*. Wiley, New York.

79 Brekken DL & Phillips MA (1998) *Trypanosoma brucei* γ-glutamylcysteine synthetase. Characterization of the kinetic mechanism and the role of Cys-319 in cystamine inactivation. *J Biol Chem* 273, 26317–26322.

80 Jez JM & Cahoon RE (2004) Kinetic mechanism of glutathione synthetase from *Arabidopsis thaliana*. *J Biol Chem* 279, 42726–42731.

81 Moreno S, de Arriaga D & Soler J (1990) A study of kinetic mechanism followed by glutathione reductase from mycelium of *Phycomyces blakesleeanus*. *Arch Biochem Biophys* 278, 32–38.

82 Marton LJ, Russell DH & Levy CC (1973) Measurement of putrescine, spermidine and spermine in physiological fluids by use of an amino acid analyzer. *Clin Chem* 19, 923–926.

83 Bitonti AJ, Kelly SE & McCann PP (1984) Characterization of spermidine synthase from *Trypanosoma brucei brucei*. *Mol Biochem Parasitol* 13, 21–28.

84 Basselin M, Coombs GH & Barrett MP (2000) Putrescine and spermidine transport in *Leishmania*. *Mol Biochem Parasitol* 109, 37–46.

Supporting information

The following supplementary material is available:

Fig. S1. SDS/PAGE of the purified enzymes.

Fig. S2. Kinetics of *Tc*TryS against GSH.

Fig. S3. γECS inhibition by GSH and γEC.

Fig. S4. Dependence of flux and $T(SH)_2$ concentration on the *k* values of the leaks.

Table S1. Comparison of the kinetic parameters of the pathway enzymes with those reported in the literature.

Table S2. Determination of GS and TryS activities in parasite extracts.

Table S3. Enzyme activities in parasite extracts exposed to various conditions.

Table S4. Thiol content in various strains of *Trypanosoma cruzi* epimastigotes.

Table S5. Reactions as written in GEPASI/COPASI.

Table S6. Summary of the rate constant values used in the model.

Table S7. Summary of the affinity values used for each enzyme.

Table S8. Robustness of the model.

Table S9. Elasticity coefficients.

This supplementary material can be found in the online version of this article.

Please note: As a service to our authors and readers, this journal provides supporting information supplied by the authors. Such materials are peer-reviewed and may be re-organized for online delivery, but are not copy-edited or typeset. Technical support issues arising from supporting information (other than missing files) should be addressed to the authors.

SUPPLEMENTARY MATERIAL

Fig S1 SDS-PAGE of the purified enzymes

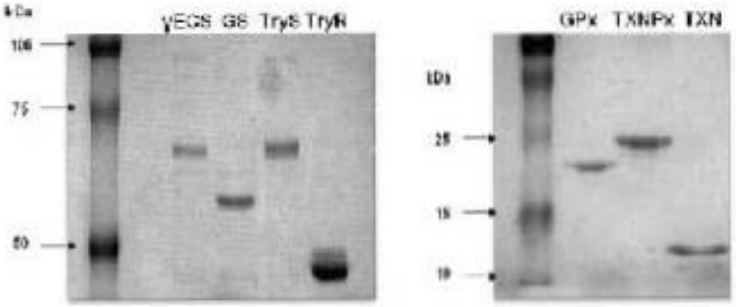

Table S1. Comparison of the kinetic parameters of the pathway enzymes as obtained in this work and those reported in the literature

Enzyme	Kinetic parameters*	*T. cruzi*	*T. brucei*	*Leishmania*	other
γGCS	*Vmax*	0.37 ± 0.1	2 - 7.6 [m]	NR	
	$Km_{apo\ Cys}$	0.21± 0.1	0.69 [a]	NR	
	$Km_{apo\ Glu}$	0.13 ± 0.04	0.24 [a] 0.93 [b]	NR	
	$Km_{apo\ ATP}$	0.04 ± 0.012	0.071-0.074 [a-c]	NR	
	$Ki_{GSH\ vs\ Glu}$	1.0	1.1 [a]	NR	
	$Ki_{GSH\ vs\ Cys}$	0.43	NR	NR	
GS	*Vmax*	2.04 ± 0.7	NR	NR	5.24 [c] 7.9 [d]
	$Km_{apo\ γEC}$	0.04 ± 0.01	NR	NR	0.039 [d]
	$Km_{apo\ Gly}$	1.2 ± 0.3	NR	NR	5 [d] 1.5 [d]
	$Km_{apo\ ATP}$	0.03 ± 0.01	NR	NR	0.059 [d] 0.02 [d]
	$Ki_{GSH\ vs\ Gly}$	12 ± 0.6 [m]	NR	NR	22.7 [m] [d]
	$Ki_{GSH\ vs\ ATP}$	11 ± 1[m]	NR	NR	35.4[m] [d]
	$Ki_{GSH\ vs\ γEC}$	14 ± 5.6[m]	NR	NR	16.6[m] [d]
TryS	*Vmax*	1.04 ± 0.5[n] 0.77 [f]	2.4 [g,k]	1.6 [h,n]	
	Km_{apoGSH}	0.76 ± 0.21 0.57 [f]	0.056 [k]	0.089 [l]	
	Km_{apoCoA}	0.80 ± 0.095 0.625 [f]	0.037 [k]	0.95 [l]	
	Km_{apoATP}	0.07 ± 0.04 0.053 [f]	0.007 [k]	0.063 [l]	
	Ki_{GSH}	No effect 1.2 [f]	0.0360 [n]	1 [n]	
TryR	*Vmax*	531 ± 137 143	91[i]	113 [i]	
	Km_{apoTS2}	0.023 ± 0.006 0.015 [f]	0.0009[i]	0.050 [k]	
	$Km_{apoNADPH}$	0.009 ± 0.005 0.005 [f]	0.00077[i]	0.020 [k]	

* *Vmax* values in U/mg protein, Km_{apo} and *Ki* in mM. **non competitive inhibition. *** uncompetitive inhibition. **** reported in this table as nmoles ADP produced/min*mg protein for comparative purposes. NR, not reported. [a] [51]; [b] for reference see [79] in main text; [c] [52]; [d] from *Plasmodium falciparum* [53]; [e] from *Arabidopsis thaliana* for reference see [80] in main text, [f] for reference see [21] in main text, [g] for reference see [25] in main text ; [h] for reference see [26] in main text. [i] [54]; [j] [55]; [k] [56]; [l]* Calculated from references [25, 26] in main text considering that $Vmax = kcat\ [enzyme_{tot}]$

Fig S2. Kinetics of *Tc*TryS against GSH

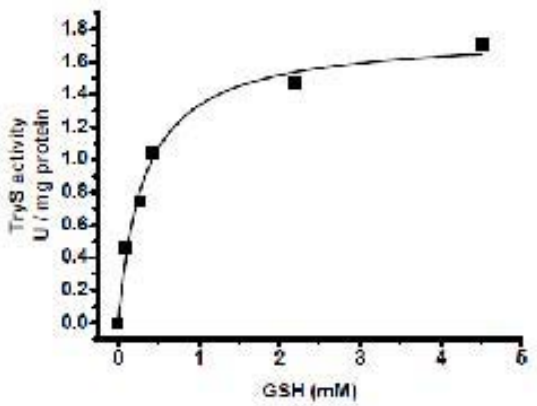

*Tc*TryS from Nmoa strain is not inhibited by its substrate GSH. The figure shows a representative plot. The data were fitted to the Michaelis-Menten equation using the OriginPro 7.5 software.

Fig S3. γECS inhibition by GSH and γEC

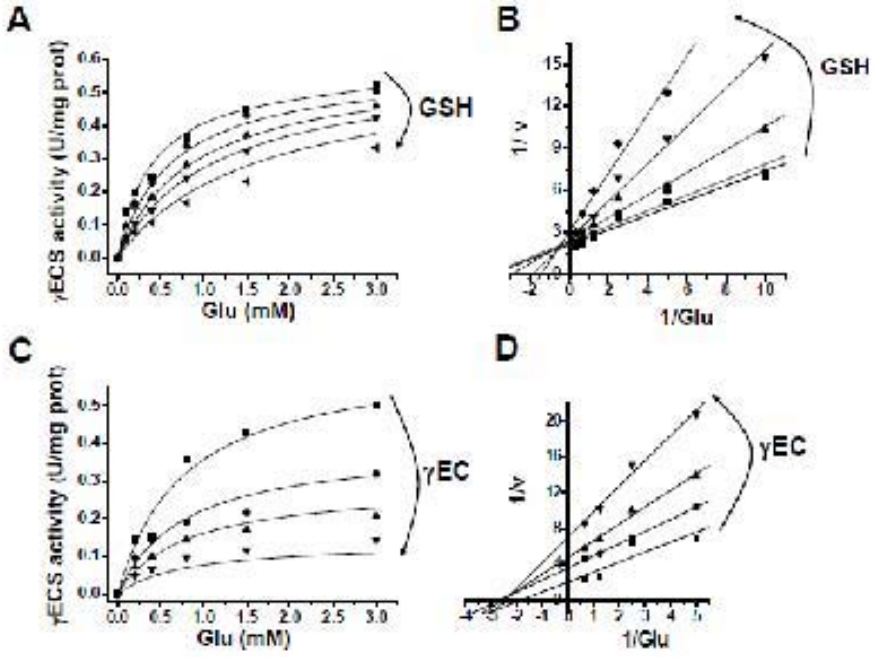

γECS is competitively inhibited by GSH and non competitively by γEC against Glu. A and C represent the global non-linear fitting to the equations of simple competitive inhibition $v = \frac{Vm * S}{Km * \left(1 + \frac{I}{Ki}\right) + S}$ and simple non competitive inhibition $v = \frac{\frac{Vm}{\left(1 + \frac{I}{Ki}\right)} * S}{Ks + S}$ using the OriginPro 7.5 software. B and D are the corresponding double reciprocal plots. The inhibitor concentrations were varied from 0-5 and 0-3 mM for GSH and γEC, respectively

5

Table S2. GS and TryS activities determination in parasite cytosolic extracts

	GS				TryS			
mg protein of cytosolic fraction	0.1		0.2		0.1		0.2	
Reaction conditions*	nmol ADP produced	total activity (mU/mg cell prot)	nmol ADP produced	total activity (mU/mg cell prot)	nmol ADP produced	total activity (mU/mg cell prot)	nmol ADP produced	total activity (mU/mg cell prot)
Addition of all substrates	410	137	528	88	506	169	708	118
Absence of one specific substrate** (ATPase activity)	385	128	480	80	461	154	617	103
nmol ADP produced by GS or TryS	25		48		45		89	
Specific enzyme activity nmol /min*mg protein	8.3		8		7.5***		7.45***	

*The reaction was stopped after 30 min incubation at 37°C. ** for GS Gly was absent whereas for TryS the reaction lacked Spd. The specific enzyme activity was calculated by dividing nmol ADP produced by GS or TryS by 30 min and multiplying by 10 (0.1 mg) or 5 (0.2 mg)); *** the specific activity is divided by two because two ATP molecules are consumed per synthesized $T(SH)_2$. mU are nmoles/min.

6

Table S3. Enzyme activities in parasite extracts exposed to different conditions

Enzyme	*Vmax* forward (U/mg cell protein)		
	0 min	10 min	10 min + H_2O_2
GS	0.0059±0.0008	0.0086*	0.007±0.0029
TryS	0.0043±0.0008	0.0043*	0.0039 ± 0.0006
TryR	0.297±0.0083	0.264*	0.274 ± 105

n =3 *Data from Table 1

Table S4. Thiol content in different strains of *Trypanosoma cruzi* epimastigotes

Thiol (mM)[a]	Strain (culture medium) Querétaro[b] (RPMI/FBS)	Querétaro[b] (LIT/FBS/H)	Silvio[c] (RTH/FCS)	Silvio[d] (RTH/FCS)	MI[e] (Diamond's medium)	Tulahuen[f] (BHI/FCS)
Cys	0.3 ± 0.14	3.1 ± 1.6	ND	0.05[g]	ND	ND
γLC	0.45 ± 0.29	1.6 ± 0.7	ND	0.05[g]	ND	ND
GSH	0.6 ± 0.26	1.8 ± 0.6	2.1[*] 0.7[**]	0.7[g]	1.3	0.23
$T(SH)_2$	3.0 ± 1.5	6.7 ± 3.6	0.04[*] 2.1[**]	0.05[g]	1.4	0.02

[a] The mM concentration was determined considering that 10^8 *T. cruzi* epimastigotes correspond to 3 µL [77]. [*] parasites grown in medium non-supplemented with Put and [**] in the presence of 100 µM Put. [b] this work ± 0. [c] This group using other medium. [d] [s7]. [e] [s8]. [f] [s9]. [g] [s10]. ND not determined. RPMI/FBS is Roswell Park Memorial Institute medium supplemented with foetal bovine serum; LIT/FBS/H is liver infusion triptose medium supplemented with foetal bovine serum and hemin; RTH medium is RPMI medium supplemented with trypticase and hemin; BHI is brain heart infusion media supplemented with foetal calf serum.

8

Table S5. Reactions as written in Gepasi/Copasi

Enzyme	Reaction
γLCS	Cys + Glu = gEC
GS	gEC + Gly = GSH
SpdT	Spdext = Spdint
TryS	GSH + Spdint = TSH
T(SH)$_2$ demand	TSH + H2O2 = TS2
TryR	NADPH + TS2 = NADP + TSH
NADPH supply	NADP = NADPH
Spd leak	Spdint -> Spd_{out}
GSH leak	GSH + H2O2 -> GSH_{out}
TS2 leak	TS2 -> $TS2_{out}$

9

Table S6. Summary of the rate constant values used in the model for the three simulated conditions

Enzyme	*Vmax* forward			*Vmax* reverse	*Keq*
	0 min	10 min	10 min + H_2O_2		
γECS		0.0017***		NA	5597 [a]
GS		0.0086*		NA	5597 [a]
TryS		0.0043*		NA	5597 [a]
TryR		0.264*		NA	$35x10^{6}$ [b]
SpdT		0.0058[c]		ND	1000**
$T(SH)_2$ demand	k_f=15**	k_f = 7**		k_r = $1x10^{-3}$ **	NA
NADPH supply		k_f = 10**		k_r = 0.1**	NA
Spd leak	k= $1x10^{-4}$ **	k=$5x10^{-3}$ **		NA	NA
GSH leak	k= $5x10^{-4}$ **	k= 0.05 **		NA	NA
TS_2 leak		k= $1.5x10^{-3}$ **		NA	NA

* Vm in U/mg soluble protein from Table 1 of main text. ** adjusted. *** Vm from plants [30]. NA, not applicable; ND, not determined

[a] calculated from data reported in [39],

[b] calculated from the Haldane equation $Keq = \left(\frac{Vf}{Vr}\right)^{2} * \left(\frac{Km_p Km_q}{Km_r Km_s}\right)$ [7,8]

[c] recalculated of 1.34 nmol/ min * 10^8 cells reported in [55] of main text and considering that 10^8 cells = 0.23 mg

10

Table S7 Summary of the affinity values used for each enzyme

	γECS	GS	TryS	TryR	SpdT
Km_A	0.21 (Cys)	0.01 (γEC)	0.76 (GSH)	0.0095 (NADPH)	0.0003* (Spd_{ac})
Km_B	0.13 (Glu)	1.2 (Gly)	0.86 (Spd_{ac})	0.023 (TS_2)	-
Km_P	0.43 (γEC)	12.0 (GSH)	10* (TSH)	0.011[b] NADP	10* (Spd_{ac})
Km_Q	-	-	-	10* (TSH)	-
Ki	1.6 (GSH)	-	-	-	-
α	1*	12[c,d]	0.1*		
β	0.03[c]				

Km, *Ki* in mM. *Adjusted
[a] reported in [65]
[b] from *T. congolense* TryR [s11]
[c] Adjusted considering the α and β values reported in [79]
[d] Adjusted considering the α value reported in [80]

Fig. S4. Flux and $T(SH)_2$ concentration dependency on the *k* values of the leaks

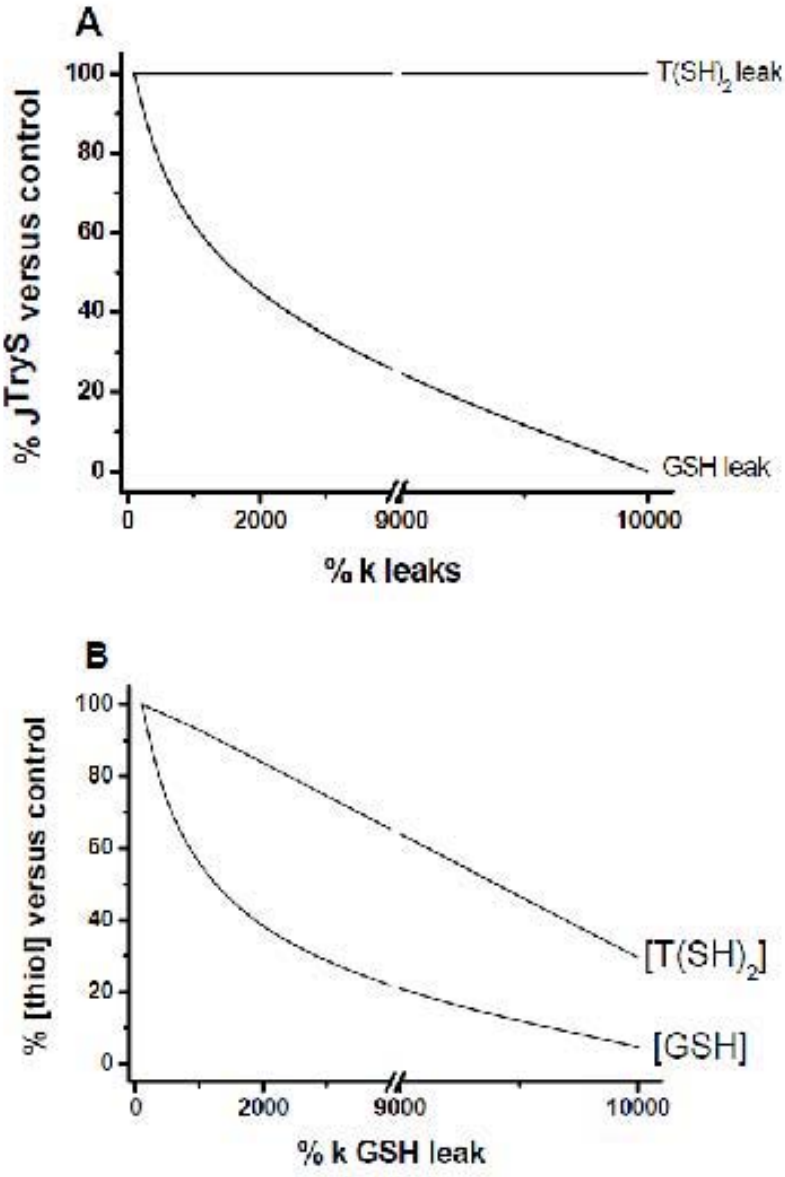

The effect of the GSH or TS_2 leaks on the flux and thiol concentrations was simulated in the model by increasing their *k* values. The GSH leak had more effect on the flux and on GSH and $T(SH)_2$ concentrations than the TS_2 leak.

Table S8. Robustness of the model

		γECS							
	folds	$C^{J}_{\gamma ECS}$	C^{J}_{TryS}	$C^{[mM]}_{TryS}$	$C^{[mM]}_{dem}$	J^{TryS}_{γ}	$[(SH)_4]$	$[TS_2]$	$[(SH)_2]/[TS_2]$
γECS									
Vmax	0.5x	0.89	0.26	0.96	0.98	0.1	6.8	0.27	25
	1x	0.58	0.49	0.97	0.97	0.7	7.1	0.47	15.1
	1.5x	0.33	0.65	0.97	-0.99	0.04	7.2	0.56	12.9
$Km_{\gamma ECS}$	0.5x	0.46	0.67	0.97	0.99	0.75	7.1	0.51	13.9
	1x	0.58	0.49	0.97	-0.97	0.7	7.1	0.47	15.1
	1.5x	0.68	0.42	0.97	0.99	0.64	7	0.43	16.3
Km_{TryS}	0.5x	0.58	0.49	0.97	0.99	0.73	7.1	0.49	14.5
	1x	0.58	0.49	0.97	-0.97	0.7	7.1	0.47	15.1
	1.5x	0.58	0.49	0.97	-0.99	0.67	7.1	0.45	15.8
TryS									
Vmax	0.5x	0.33	0.75	0.96	-0.99	0.45	6.85	0.3	22.8
	1x	0.58	0.49	0.97	-0.97	0.7	7.1	0.47	15.1
	1.5x	0.75	0.31	0.97	0.99	0.02	7.15	0.55	13
Km_{TryS}	0.5x	0.55	0.46	0.97	0.99	0.9	7.1	0.53	13.4
	1x	0.58	0.49	0.97	-0.97	0.7	7.1	0.47	15.1
	1.5x	0.61	0.51	0.97	-0.99	0.63	7.03	0.42	16.74
Km_{NADP}	0.5x	0.75	0.33	0.97	-0.99	0.8	7.1	0.53	13.4
	1x	0.58	0.49	0.97	0.97	0.7	7.1	0.47	15.1
	1.5x	0.44	0.61	0.97	-0.99	0.61	7.02	0.41	17.12
TryR									
Vmax	0.5x	0.57	0.49	0.99	-0.99	0.7	3.6	0.47	7.6
	1x	0.58	0.49	0.97	-0.97	0.7	7.1	0.47	15.1
	1.5x	0.59	0.45	0.94	0.07	0.7	10.1	0.46	22.7
Km_{TryR}	0.5x	0.58	0.49	0.96	-0.99	0.7	7.3	0.47	15.5
	1x	0.58	0.49	0.97	-0.97	0.7	7.1	0.47	15.1
	1.5x	0.58	0.49	0.96	-0.98	0.7	6.9	0.47	14.7
Km $_{NADP}$	0.5x	0.58	0.49	0.98	-0.99	0.7	7.1	0.47	15.1
	1x	0.58	0.49	0.97	-0.97	0.7	7.1	0.47	15.1
	1.5x	0.58	0.49	0.96	-0.98	0.7	7.02	0.47	14.9

The *Vmax* and *Km* values were varied for each enzyme within the experimental dispersion of the data (~50%). * Flux in nmol/min mg protein, ** mM

Table S9. Elasticity coefficients

Enzyme/condition	$\varepsilon^{v}_{substrate}$			$\varepsilon^{v}_{coenzyme}$			$\varepsilon^{v}_{product}$		
	0	10	10+ H_2O_2	0	10	10+ H_2O_2	0	10	10+ H_2O_2
γECS		Cys			Glu			γEC; Inhibitor (GSH)	
	0.37	0.29	0.32	0.12	0.17	0.1	-0.0009, -0.11	-0.0008, -0.15	-0.00095, -0.09
GS		γEC			Gly			GSH	
	0.73	0.72	0.7	0.25	0.26	0.27	-0.005	-0.005	-0.003
TryS		GSH			Spd_{ox}			$T(SH)_2$	
	0.65	0.48	0.7	0.32	0.59	0.48	-0.021	-0.026	-0.017
SpdT		Spd_{ox}						Spd_{ox}	
	0.1	0.05	0.09		NA		-2.7	-0.13	-0.18
$T(SH)_2$ demand		$T(SH)_2$			H_2O_2			TS_2	
	1	1	1	1	1	1	$-2x10^{-5}$	$-1.5x10^{-5}$	$-1.4x10^{-5}$
TryR		TS_2			NADPH			$T(SH)_2$; NADP	
	0.05	0.06	0.07	0.01	0.02	0.01	-0.01; 0.0066	-0.01; 0.008	-0.001; 0.005
NADPH supply		NADP						NADPH	
	1.03	1.03	1.03		NA		-0.03	-0.03	-0.03
Spd leak		Spd_{ox}							
	1	1	1		NA			NA	
GSH leak		GSH			H_2O_2				
	1	1	1	1	1	1		NA	
TS_2 leak		TS_2							
	1	1	1		NA			NA	

NA Not applicable

References for supplementary material

[s1] Lueder DV, Phillips MA (1996) Characterization of *Trypanosoma brucei* gamma-glutamylcysteine synthetase, an essential enzyme in the biosynthesis of trypanothione (diglutathionylspermidine). *J Biol Chem* **271**, 17485-17490.

[s2] Abbott JJ, Ford JL, Phillips M (2002) Substrate binding determinants of *Trypanosoma brucei* γ-glutamylcysteine synthetase. *Biochemistry* **41**, 2741-2750.

[s3] Meierjohann S, Walter RD, Muller S (2002) Glutathione synthetase from *Plasmodium falciparum*. *Biochem J* **363**, 833-838.

[s4] Jockers-Scherubl MC, Schirmer RH, Krauth-Siegel RL (1989) Trypanothione reductase from *Trypanosoma cruzi*. Catalytic properties of the enzyme and inhibition studies with trypanocidal compounds. *Eur J Biochem* **180**, 267-272.

[s5] Jones DC, Ariza A, Chow WH, Oza SL, Fairlamb AH (2010) Comparative structural, kinetic and inhibitor studies of *Trypanosoma brucei* trypanothione reductase with *T. cruzi*. *Mol Biochem Parasitol* **169**, 12-19.

[s6] Mittal MK, Misra S, Owais M, Goyal N (2005) Expression, purification, and characterization of *Leishmania donovani* trypanothione reductase in *Escherichia coli*. *Protein Expr Purif* **40**, 279-286.

[s7] Ariyanayagam MR and Fairlamb AH (2001) Ovothiol and trypanothione as antioxidants in trypanosomatids. *Mol Biochem Parasitol* **115**, 189-198.

[s8] Ariyanayagam MR, Oza SL, Mehlert A, Fairlamb AH (2003) Bis(glutathionyl)spermine and other novel trypanothione analogues in *Trypanosoma cruzi*. *J Biol Chem* **278**, 27612-27619.

[s9] Maya JD, Repetto Y, Agosin M, Ojeda JM, Téllez R, Gaulo C, Morello A (1997) Effects of nifurtimox and benznidazole upon glutathione and trypanothione content in epimastigote, trypomastigote and amastigote forms of *Trypanosoma cruzi*. *Mol Biochem Parasitol* **86**, 101-106.

[s10] Thomson L, Denicola A, Radi R (2003) The trypanothione - thiol system in *Trypanosoma cruzi* as a key antioxidant mechanism against peroxynitrite – mediated cytotoxic. *Arch Biochem Biophys* **412**, 55-64.

[s11] Zhong R, Conas N, Blanchard JS (1995) Catalytic and potentiometric characterization of E201D and E201Q mutants of *Trypanosoma congolense* trypanothione reductase. *Biochemistry* **34**, 12697-12703.

8.2 RESULTADOS Y DISCUSIÓN DE LOS DATOS NO PUBLICADOS

A continuación se describen y discuten los resultados de los experimentos que no se incluyeron en el artículo (Olin-Sandoval *et al*, 2012)

8.2.1 Determinación de la actividad de GS y TryS en extractos del parásito utilizando inhibidores de ATPasas

Como se discutió en el artículo publicado, la actividad de GS y TryS en el extracto de epimastigotes fue muy difícil de determinar debido a la presencia de una actividad contaminante de ATPasa muy alta por lo que las actividades calculadas de dichas enzimas correspondían aproximadamente al 8-11% del consumo de ATP total en la mezcla de reacción. La manera en que se validó el método fue que la actividad específica de la GS y TryS tuviera un comportamiento lineal con respecto a la cantidad de proteína utilizada en el ensayo (lo que no ocurre con la actividad de ATPasa) y además de que hubiera una menor producción de ADP en ausencia de uno de los sustratos específicos de la TryS o GS. Ambos controles son indispensables incluso cuando se determina la actividad de una enzima purificada. Sin embargo, para validar aún más el método, se decidió explorar el uso de una mezcla de inhibidores para F y P ATPasas que incluía azida, oligomicina, molibdato y vanadato con el objetivo de que la actividad contaminante de ATPasa disminuyera y por lo tanto, las actividades de la GS y TryS representaran más del 11% de la actividad ATPasa total en la reacción haciendo más confiable la medición.

La presencia de los inhibidores promovió una disminución del 30-60% de la actividad contaminante de la ATPasa a los diferentes tiempos (Tabla 5). Esto hizo que la actividad correspondiente a la enzima de interés pasara de ser del 6-8% a ser del 10-20% del consumo total de ATP en la reacción, lo que le dio más confiabilidad al método. En el caso de la TryS, utilizando el doble de la proteína se obtuvo el doble de la actividad de la enzima solamente en el tiempo de 30 min de reacción. A menores tiempos no se pudo obtener una correlación lineal con la proteína utilizada. Por otro lado, la reacción de GS sólo se pudo detectar incubando 30 minutos.

A pesar de que los valores de actividad que se presentan en la Tabla 5 no varían en presencia de los inhibidores, en algunas repeticiones experimentales, los compuestos parecen ejercer un efecto inhibitorio sobre las enzimas que se quieren medir lo cual podría depender del proceso de obtención del extracto clarificado. Debido a lo anterior, lo más conveniente es que las actividades de estas enzimas se sigan determinando en ausencia de la mezcla de inhibidores de actividad de ATPasas. Sin embargo estos experimentos nos permitieron validar más la técnica desarrollada para medir estas enzimas en extractos del parásito.

Tabla 5. Actividades de GS y TryS en extractos de epimastigotes de *T. cruzi* en ausencia y presencia de inhibidores de ATPasas

Condicion experimental	**GS**				**TryS**							
incubación (min)	30				15				30			
mg prot extracto	0.1		0.2		0.1		0.2		0.1		0.2	
mezcla de Inhibidores	**-**	**+**	**-**	**+**	**-**	**+**	**-**	**+**	**-**	**+**	**-**	**+**
	nmoles de ADP producido											
Reacción con todos los sustratos	200	78	282	109	119	82	204	124	182	99	224	121
Reacción en ausencia de uno de los sustratos	203	84	265	97	120	84	194	110	181	87	231	97
Reacción específica de GS o TryS	NR	NR	**17**	**12**	NR	NR	**11**	**14**	1.5	**12**	NR	**24**
	Actividad específica											
mU/mg de proteína	NR	NR	**2.8**	**2**	NR	NR	**1.8***	**2.3***	NR	**1.95***	NR	**2***

NR, No hubo reacción. La actividad específica se obtuvo dividiendo los nmoles de ADP producidos entre el tiempo y la cantidad de proteína. * Para TryS las U equivalen a nmol de $T(SH)_2$ producido/min y se utilizan 2 moléculas de ATP por $T(SH)_2$ producido.

Un aspecto muy importante es el hecho de que con este protocolo de determinación de la actividad de GS se obtienen valores en el mismo intervalo de actividad que los reportados por otras metodologías para otros modelos biológicos tal como se discute en el artículo. Por lo tanto, a pesar de la dificultad en medir estas actividades, se obtuvieron algunos valores que pudieron utilizarse para construir el modelo de la vía metabólica.

8.2.2 Polimorfismos del gen de la GS en diferentes cepas de Trypanosoma cruzi

Como parte de la realización de este proyecto de tesis, se tuvo que caracterizar tanto genéticamente como cinéticamente a la GS de *T. cruzi* debido a que no habían reportes en ningún tripanosomátido. Considerando que la cepa CL Brener la cual es la que se secuenció su genoma tiene dos marcos de lectura abiertos (ORF, por las siglas en inglés de open reading frame) que codifican para GS, la caracterización genética en las cepas mexicanas que utilizamos permitiría determinar si la actividad de GS presente en los parásitos correspondía al producto de uno o dos genes. Por otro lado, la caracterización cinética aportaría los parámetros cinéticos necesarios para la construcción del modelado cinético. Los resultados de este trabajo se prepararon en un artículo que tenía como título “Glutathione synthetase and antioxidant metabolism in *Trypanosoma cruzi*”. Este trabajo no se publicó debido a que los revisores del artículo publicado en *FEBS J* (sección 8.1) demandaron la inclusión de todos los datos bioquímicos de la GS en este último. Es por ello que los resultados de los polimorfismos del gen que codifica para esta enzima no se incluyeron en este artículo por quedar fuera del objetivo principal del trabajo. Estos resultados, se describen a continuación.

Los dos marcos de lectura que codifican para GS en la cepa de referencia CL Brener de *T. cruzi* (Tc00.1047053508865.10, GS1 ORF; Tc00.1047053506659.30, GS2 ORF) comparten una identidad del 97.9% y del 98.5% a nivel de nucleótidos y de secuencia de aminoácidos, respectivamente. Algo importante de resaltar fue que uno de los genes (GS1) contenía dos sitios de reconocimiento para la enzima de restricción *Hind* III en los nucleótidos 262 y 677 mientras que el gen GS2 carecía de éstos.

Para determinar la posible presencia de estos polimorfismos en las cepas de origen mexicano Ninoa y Querétaro (Bosseno *et al*, 2002), se diseñaron cebadores basados en la secuencia idéntica del extremo 5' y 3' de ambos ORFs reportados para CL Brener. Al amplificar el gen de GS a partir del DNA genómico de las dos cepas nacionales, se obtuvo solamente un producto de PCR de 1600 bp. Posteriormente, este gen amplificado se digirió con la enzima *Hind* III obteniéndose únicamente dos bandas de ~ 900 y 700 bp (Figura 7A). Por otro lado cuando se realizó el mismo análisis utilizando DNA genómico de la cepa CL Brener se obtuvo el patrón de restricción correspondiente a la presencia de ambos ORFs (1600, 900 y 700 bp). Esto sugirió que las cepas Ninoa y Querétaro presentaban un gen único que codificaba para la GS el cual presentaba un solo sitio de corte para *Hind* III.

Posteriormente, los genes de GS de las cepas Ninoa y Querétaro se clonaron en el vector pGEM T-Easy y se secuenciaron. La secuencia demostró que los genes de GS de estas dos cepas presentaban un 99.9% y 100% de identidad en las secuencias de nucleótidos y aminoácidos, respectivamente. Además, se encontró que ambos genes carecían de un codón que codificaba para alanina en la posición 372 la cual está presente en ambos ORFs de CL Brener (datos no mostrados). No se ha reportado alguna función catalítica o de unión de sustratos de la Ala-372 por lo que, hasta el momento, no podemos saber si la carencia de este amino ácido en las cepas Ninoa y Querétaro puede tener un efecto sobre la actividad enzimática.

Por otro lado, para determinar si existían más copias de genes de GS en la cepa Querétaro (en la cual se determinaron los parámetros *in vivo* para el modelo), se realizó un análisis tipo Southern blot utilizando como sonda el gen de GS clonado y el DNA genómico digerido con *Hind* III (Figura 7B). El resultado de este análisis mostró dos bandas de hibridación con un peso molecular alto lo que sugería la presencia de un solo gen para GS en esta cepa. Se demostró la especificidad de la hibridación hacia el gen de GS al digerir el DNA genómico con *Pst* I, el cual contenía 4 sitios de restricción en el gen. El patrón de hibridación mostró bandas con tamaños de ~730, 400 y 300 bp y una de peso molecular muy alto, las cuales correspondían al patrón de restricción esperado para un gen de copia única a pesar de que la banda que correspondía al extremo 3' del gen no apareció probablemente debido al tamaño

tan pequeño. Esta información fue suficiente para corroborar que el gen se encontraba en copia única en el genoma. Considerando que *T. cruzi* es diploide, es necesario corroborar la presencia de este gen en uno o ambos alelos.

Para determinar la expresión de el/los genes de GS en las 3 cepas, se aisló RNA total de las tres cepas crecidas en ausencia de estrés oxidante, se sintetizó el cDNA y se amplificó el cDNA de la GS. Posteriormente, el producto de PCR se digirió con *Hind* III. Estos resultados demostraron que las cepas Querétaro y Ninoa expresaban un solo gen de GS y que la cepa CL Brener expresaba los dos ORFs reportados en el proyecto del genoma (Figura 7C).

La conclusión de este análisis fue que las cepas Ninoa y Querétaro contienen un solo gen para la GS el cual es transcripcionalmente activo en condiciones no oxidantes mientras que la cepa CL Brener posee dos genes que codifican para la GS los cuales también se expresan en condiciones de no estrés.

Las diferencias en la organización de los genes de GS en estas tres cepas también se han observado para proteínas de respuesta a estrés por calor (SHSP16). Esto se debe principalmente a que la cepa CL Brener es un híbrido de al menos dos grupos de cepas de *T. cruzi* (Brisse *et al*, 1998). Esto se ha demostrado mediante diferentes análisis en donde se pudieron detectar en la cepa CL Brener dos isoformas de la fosfoglucosa isomerasa, fosfoglucomutasa y de la glutamato deshidrogenasa dependiente de $NADP^+$ mientras que en otras cepas solo se encuentra una isoforma.

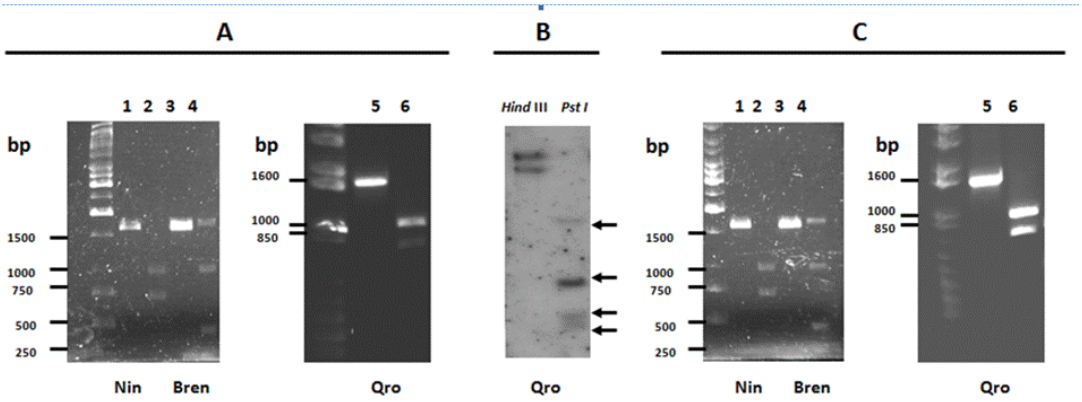

Figura 7. Polimorfismos del gen de la GS en diferentes cepas de *T. cruzi*

A) Los genes de *gs* de *T. cruzi* se amplificaron a partir de DNA genómico de las cepas Ninoa (Nin), CL Brener (Bren) y Querétaro (Qro) (Carriles 1,3 y 5). Con el objetivo de confirmar la presencia de los polimorfismos, los productos de amplificación se cortaron con *Hind* III (Carriles 2,4 y 6).

B) Southern Blot of *T. cruzi* cepa Qro. El DNA genómico se digirió con *Hind* III y *Pst* I. Posteriormente los fragmentos se separaron por electroforesis en geles de agarosa y se hibridaron con el gen de la GS de la cepa Ninoa.

C) Transcritos de *gs* en las diferentes cepas de *T. cruzi*. Se aisló el RNA de los parásitos y posteriormente se sintetizó el cDNA. Los cDNAs de GS se amplificaron (Carriles 1,3 y 5) y se cortaron con *Hind* III (Carriles 2,4 y 6).

9. DISCUSIÓN GENERAL

El MCA permite determinar la proporción en la que cada una de las enzimas de una vía controla el flujo de síntesis así como la concentración de sus intermediarios. Por otro lado, el objetivo de la biología de sistemas es construir modelos matemáticos con la capacidad de predecir el comportamiento de una vía metabólica de un organismo. El enfoque “bottom up” en biología de sistemas pretende crear modelos a partir de las propiedades básicas (características cinéticas) de sus elementos más fundamentales que son las enzimas (Westerhoff, 2011). La combinación del modelado metabólico y MCA nos permite conocer los mecanismos de control de una vía metabólica y puede ser una herramienta poderosa muy útil para la identificación de blancos terapéuticos (Hornberg, 2007). Por lo tanto, la construcción de este primer modelo cinético del metabolismo del $T(SH)_2$ pudo ayudar a categorizar de entre las enzimas esenciales aquellas que pudieran tener el mayor potencial terapéutico de acuerdo a sus capacidades de control de la vía metabólica.

A diferencia de otros modelos cinéticos del metabolismo de los tioles en los cuales los parámetros utilizados para su construcción se tomaron de distintos reportes científicos en donde se determinaron en distintas condiciones experimentales (pH, temperatura, cepas, estadio, etc.) (Mendoza-Cózatl y Moreno-Sánchez, 2006), el trabajo experimental que se realizó en esta tesis involucró la obtención de la base de datos completa. Éstos incluyen la obtención de las enzimas recombinantes de la misma especie; los parámetros cinéticos determinados bajo las mismas condiciones de pH y temperatura las cuales fueron cercanas a las fisiológicas; las actividades enzimáticas, las concentraciones de metabolitos y los flujos hacia $T(SH)_2$ determinados *in vivo* en epimastigotes de *T. cruzi* de la misma cepa. Así mismo, la determinación de todos estos parámetros se llevó a cabo en tres condiciones experimentales. Esto nos permitió construir un modelo cinético validado con una alta capacidad predictiva, ya que puede modelar el comportamiento de la vía en diversas condiciones experimentales.

Los resultados del modelo permitieron identificar que el control del metabolismo del $T(SH)_2$ se encuentra repartido entre varias enzimas y que no existe una única

etapa limitante en esta vía. El control de la síntesis de $T(SH)_2$ está distribuido principalmente entre la γECS, la TryS y SpdT en las tres condiciones estudiadas aunque en distintas proporciones. La razón de su alto control de flujo se debe principalmente a que son las enzimas con las menores eficiencias catalíticas (*Vm*/*Km*) en el parásito las cuales a su vez se deben a que sus actividades enzimáticas son bajas en los parásitos y a que las concentraciones de sus sustratos en la célula se encuentran alrededor de su valor de *Km*, lo que limita mucho su actividad y por lo tanto el flujo total de la vía. Algo importante de resaltar es que el control que ejerce la γECS no es debido a la retro-inhibición competitiva ejercida por el GSH respecto al glutamato (Grifith y Mulcahy, 1999) ya que las concentraciones tan altas del sustrato glutamato contrarrestan el efecto del inhibidor. Lo anterior resalta la importancia de eliminar el concepto de "paso limitante" así como el de que las enzimas que controlan una vía metabólica son únicamente aquellas que son moduladas alostéricamente (enfoques de la bioquímica clásica), ya que su actividad dependerá de las concentraciones de sustratos, productos y efectores presentes en la célula (Moreno-Sánchez *et al*, 2008). Lo anterior fue uno de los motivos por los que se desarrolló el MCA (Westerhoff, 2004) que hace un análisis integral de la vía lo que resalta la importancia de la biología de sistemas para entender los mecanismos de control, regulación y organización subcelular.

Por otro lado, las enzimas que controlan la concentración de $T(SH)_2$ son el bloque de enzimas que lo demandan así como la TryR. Sin embargo, cuando las actividades de la γECS y TryS se inhiben más de un 70% o en ausencia de la TryR (modelo sin TryR), estas enzimas también controlan la concentración del metabolito reducido. Estos experimentos virtuales de inhibición sugieren que la TryR parece ser la enzima en la primera línea de defensa ante un estímulo antioxidante inicial, sin embargo, en periodos prolongados de estrés cuando ya se requiere de una mayor concentración de $T(SH)_2$, la γECS y TryS tendrán mayor relevancia. Además, considerando que el bloque de enzimas de demanda de $T(SH)_2$ así como la TryR tienen una concentración intracelular y actividades mayores que las enzimas del bloque de síntesis, presenta limitaciones para considerarlas buenos blancos terapéuticos ya que, por ejemplo, inhibir en un 50% a una enzima abundante en la célula requiere de mayores concentraciones de inhibidor que inhibir en la misma

proporción a una enzima poco abundante o catalíticamente poco eficiente (como se analizó en la revisión y en el artículo experimental de esta tesis). Esta información es importante ya que la enzima a la cual se le han diseñado mayor número de inhibidores es a la TryR (Austin SE *et al*, 1999; Martyn *et al*, 2007; Holloway *et al*, 2007; Holloway *et al*, 2009; Duyzend MH *et al*, 2011; Patterson *et al*, 2011)

Lo anterior demuestra que considerar solamente las características cinéticas de las enzimas, su esencialidad en el parásito, o la ausencia de ésta en el hospedero como únicos criterios para proponer un blanco terapéutico es una aproximación incompleta debido a que solo se está considerando a la enzima de manera individual excluyéndose el análisis de la enzima como parte de un sistema. Esto puede ser una de las razones por las que no han tenido éxito clínico muchos inhibidores (Wyatt *et al*, 2011) y resalta la importancia de también aplicar enfoques integrales como el SB para la identificación de blancos terapéuticos.

Una de las ventajas más importantes de los modelos matemáticos es que permiten realizar experimentación *in silico* con el cual se puede predecir el comportamiento de una vía bajo diferentes condiciones. Esto es muy útil en la identificación y validación de blancos terapéuticos debido a que se pueden sugerir estrategias terapéuticas. Con el modelo del $T(SH)_2$ que se obtuvo en este proyecto de tesis se pudo determinar que es más efectivo inhibir simultáneamente a la γECS y TryS para poder inhibir el flujo de la vía y que incluso la inhibición de la TryR puede ser una estrategia terapéutica siempre y cuando se aplique una terapia multisitio.

Un inconveniente que puede surgir de proponer a la γECS como un blanco terapéutico es su presencia en el hospedero. Cabe resaltar que, aunque la vía metabólica sea muy parecida en ambos organismos, la distribución del control en el hospedero puede ser diferente (como se observó en los diferentes modelos de glucólisis en diferentes organismos) por lo se requerirían concentraciones distintas de inhibidor para afectar a ambas enzimas. Otra manera de hacer más específica la inhibición sería estudiando las diferencias sutiles entre la γECS de los parásitos y del hospedero. Por ejemplo, el fármaco difluorometilornitina (DFMO) tiene un efecto tóxico mayor para *T. brucei* porque su enzima blanco, la ornitina descarboxilasa tiene una vida media mayor que la de las células humanas (Heby and Persson, 1990;

Carrillo *et al*, 2000); o también el diseño de un fármaco que se active por mecanismos específicos del parásito (Lüscher *et al*, 2007).

A diferencia de la enzima anterior, la TryS puede ser considerada como el mejor blanco terapéutico debido a que, además de tener un control importante sobre el flujo y la concentración de $T(SH)_2$, debido a su poca abundancia y eficiencia catalítica, ésta no se encuentra presente en el hospedero y se ha demostrado que es esencial para el parásito (Olin-Sandoval *et al*, 2010). Considerando esto, el inhibidor que se diseñe para esta enzima será específico y se requerirán bajas concentraciones de éste para afectar a la vía de síntesis de $T(SH)_2$, lo que disminuirá los efectos secundarios sobre el hospedero.

Por otro lado, otra utilidad de este modelo es que puede ser utilizado como base para predecir la distribución de control de esta vía en otros estados estacionarios o para otros modelos biológicos como tripomastigotes de *T. cruzi*, o para *T. brucei* y *Leishmania* para los cuales se requeriría solamente determinar concentración de metabolitos y actividades enzimáticas presentes en esas nuevas condiciones o en esos parásitos. Los resultados que se pueden esperar en estos casos son que las enzimas con mayor control de flujo y de concentración de $T(SH)_2$ sean las mismas, y que la única diferencia radique en la proporción en la que controlan. Así, integrando estos estudios con lo que se ha observado por ensayos de inhibición genética en *T. brucei* y *Leishmania spp* en donde se demuestra que la γECS y la TryS son esenciales para el parásito (Olin-Sandoval *et al*, 2010), estas enzimas podrían estar cumpliendo uno de los requisitos propuestos por Wyatt *et al* (2011) para proponerlas como blancos para el diseño de fármacos clínicamente exitosos.

Por último, uno de los mayores impactos que tiene el trabajo es haber identificado los blancos con mayor potencial terapéutico para un tripanosomátido en el que las herramientas de manipulación genética son limitadas comparado con las que se cuentan para *T. brucei* y *Leishmania*

Una perspectiva importante de este trabajo es validar experimentalmente los resultados obtenidos del modelo para así corroborar la potencialidad como blanco terapéutico de las enzimas que controlan de manera importante el flujo de la vía.

Considerando esto, otros grupos de investigación han comenzado a validar químicamente como blanco a la TryS en *T. brucei* (Torrie *et al*, 2009). En ese trabajo utilizaron un inhibidor no competitivo de la TryS identificado a partir de una biblioteca de fármacos. Este inhibidor logró disminuir la concentración de $T(SH)_2$ intracelular y el crecimiento del parásito pero en concentraciones micromolares, las cuales aún son muy altas desde el punto de vista terapéutico. Sin embargo, considerando los resultados obtenidos en esta tesis podemos sugerir que para mejorar la efectividad de ese inhibidor, se podría combinar con la inhibición de la γECS. De hecho, ya se ha reportado que combinar el uso de un inhibidor de la γECS (butionina sulfoximina; BSO) con NFX o BNZ, promueve una disminución en los valores de IC_{50} de éstos últimos ensayados en cultivos de epimastigotes y tripomastigotes, disminuyendo también las concentraciones intracelulares de GSH y $T(SH)_2$ en los tres estadios del parásito (Fáundez *et al*, 2005). Por lo tanto, aunque el diseño de inhibidores es difícil incluso para las enzimas que tienen mayor potencial terapéutico, aplicar varios criterios, incluyendo de manera importante el enfoque metabólico (utilizado en este trabajo) y de biología de sistemas, facilitará el diseño de fármacos para los mejores blancos así como de estrategias terapéuticas.

.

10. CONCLUSIONES

- La síntesis de $T(SH)_2$ está controlada principalmente por la γECS > TryS > SpdT.
- La concentración de $T(SH)_2$ está determinada principalmente por la demanda de $T(SH)_2$ y la TryR; sin embargo la γECS y TryS también controlan cuando se disminuye su actividad más del 70%.
- La enzima con mayor potencial terapéutico es la TryS debido a su baja actividad, a su alto control en el flujo así como a su ausencia en el hospedero.
- Una terapia multi-sitio tendrá mayores efectos sobre la vía de síntesis de $T(SH)_2$.
- El uso de inhibidores de la TryR sólo será útil siempre y cuando se combine con la intervención farmacológica de otros procesos celulares [p ej síntesis de $T(SH)_2$] o generación de estrés oxidante.

11. PERSPECTIVAS

- Validar experimentalmente los resultados obtenidos por el modelo cinético utilizando inhibidores de las enzimas que tienen un mayor control sobre la vía.
- Determinar si la distribución de control de esta vía recae en las mismas enzimas en parásitos sometidos a exposiciones prolongadas de estrés en donde el parásito tiene la oportunidad de sintetizar proteínas para contrarrestar el estrés y por lo tanto cabe la posibilidad de que la cantidad de enzima activa cambie. Así las enzimas que controlan podrían validarse como blancos terapéuticos.
- Determinar la distribución de control en los estadios de *T. cruzi* que afectan al humano. Enfocándose en determinar los parámetros experimentales más esenciales del modelo requerirá menor material biológico de estos estadios.
- Aumentar la complejidad del modelo integrando la cinética de cada una de las reacciones del sistema enzimático de desintoxicación de peróxidos así como las vías de síntesis *de novo* de Spd y del suministro de NADPH para determinar el aporte que tienen al control de la síntesis y concentración de $T(SH)_2$.
- Determinar por otras estrategias experimentales la distribución del control de la vía, por ejemplo utilizando inhibidores específicos para algunas de las enzimas.

12. REFERENCIAS

Albert MA, Haanstra JR, Hannaert V, Van Roy J, Opperdoes FR, Bakker BM, Michels PA (2005) Experimental and *in Silico* analyses of glycolytic fllux control in bloodstream form *Trypanosoma brucei*. *J Biol Chem* 280 (31), 28306-28315.

Andrade LO, Andrews NW (2005) The Trypanosoma cruzi – host – cell interplay: location, invasion, retention. *Nat Rev Microbiol*3, 819-823.

Austin SE, Khan MO, Douglas KT (1999) Rational drug design using trypanothione reductase as a target for anti-trypanosomal and anti-leishmanial drug leads. *Drug.Des.Discov.* 16(1), 5-23.

Bakker BM, Michels PA, Opperdoes FR, Westerhoff HV (1999) What control glycolisis in bloodstream form *Trypanosoma brucei*. *J Biol Chem* 274(21), 14551-14559.

Bakker BM, Krauth-Siegel RL, Clayton C, Mathews K, Girolami M, Westerhoff HV, Michels PA, Breitling R, Barrett MP (2010) The Silicon trypanosome.*Parasitol* 137 (9) 1333-1341.

Berzunza-Cruz M, CabreraN, Crippa-Rossi M, Sosa Cabrera T, Pérez-Montfort R, Becker I (2002) Polymorphism analysis of the internal transcribed spacer and small subunit of ribosomal RNA genes of *Leishmania mexicana*. *Parasitol. Res*. 88 918-925.

Bosseno M, Barnabe C, Magallon E, Gastélum E, Lozano-Kasten F, Ramsey J, Espinoza B, Brenière SF (2002) Predominance of *Trypanosoma cruzi* lineage I in Mexico. J. Clin. Microbiol. 40, 627-632

Brisse S, Barnabe C, Bañuls AL, Sidibé I, Noël S, Tibayrenc M (1998) A phylogenetic analysis of the *Trypanosoma cruzi* genome project CL Brener reference strain by multilocus enzyme electrophoresis and multiprimer random amplified polymorphic DNA fingerprinting, *Mol. Biochem. Parasitol*. 92, 253-263

Bruggeman FJ, Hornberg JJ, Boogerd FC, Westerhoff HV (2007) Introduction to systems biology. *Plant Syst Biol* (97) Experientia supplementum, 1-19

Carrillo C, Cejas S, Cortés M, Ceriani C, Huber A, González NS, Algranati ID (2000) Sensitivity of trypanosomatid protozoa to DFMO and metabolc turnover of ornitine decarboxylase. *Biochem Biophys Res Comm* 279, 663-668.

Cascante M, Boros LG, Comin-Andiux B, de Atauri P, Centelles JJ, Lee PWN (2002) Metabolic control analysis in drug discovery and disease. *Nature Biotech* 20, 243-249.

Clayton J (2010) Chagas disease 101, *Nature* 465, S4-S5.

Cornish-Bowden A, Hofmeyr JHS (1991) Metamodel: a program for modelling and control analysis of metabolic pathways on the IBM PC and compatibles. *Comp Appl Biosc* 7 (1), 89-93.

De Souza W (2002) Basic cell biology of *Trypanosoma cruzi*.*Curr Pharm Des* 8, 269-285.

De Souza W (2009) Structural organization of *Trypanosoma cruzi*.*Mem Inst Orwaldo Cruz*104 (1), 89-100.

Duyzend MH, Clark CT, Simmons SL, Johnson WB, Larson AM, Leconte AM, Wills AW, Ginder-Vogel M, Wilhelm AK, Czechowicz JA, Alberg DG (2011) Synthesis and

evaluation of substrate analogue inhibitors of trypanothione reductase. *J. Enz.Inhib.Med. Chem.*doi 10.3109/14756366.2011.604319.

Epting CL, Coates BM, Engman DM (2010) Molecular mechanism of host cell invasion by *Trypanosoma cruzi*.*Exp Parasitol* 126, 283-291.

Estani S, Colantonio L, Segura EL (2012) Therapy of Chagas Disease: Implications for levels of prevention. *J Trop Med* 2012, 10 pages

Fairlamb AH, Blackburn P, Ulrich P, Chait BT, Cerami A (1985) Trypanothione: a novel bis(glutathionyl)spermidine cofactor for glutathione reductase in trypanosomatids. *Science* 227 (4693) 1485-1487.

Fairlamb AH, Cerami A (1992) Metabolism and functions of trypanothione in the Kinetoplastida. *Annu Rev Microbio*l 46, 695-729

Fáundez M, Pino L, Letelier P, Ortiz C, López R, Seguel C, Ferreira J, Pavani M, Morello A, Maya JD (2005) Butionine sulfoximine increases the toxicity of nifurtimox and benznidazol to *Trypanosoma cruzi. Antimicrob Agents Chemother* 49, 126-130.

Fell D (1997) *Understanding the control of metabolism*. London, Portland Press.

Ferreira A, Morello A (2007) Mode of action of natural and synthetic drugs against *Trypanosoma cruzi* and their interaction with the mammalian host.*Comp Biochem Physiol* 146 (Part A), 601-620.

Flisser A, Pérez Tamayo R (2006) Aprendizaje de la parasitología basado en problemas. México, ETM.

Grifith OW, Mulcahy RT (1999) The enzymes of glutathione synthesis: g-glutamylcysteine synthetase. *Adv Enzimol Rel Areas Mol Biol* 73, 209-263.

Gu X (2010) Systems biology approaches to the computational modelling of trypanothione metabolism in *Trypanosoma brucei*. PhD thesis, University of Glasgow.http://theses.gla.ac.uk/1618

Guzmán-Bracho C (2001) Epidemiology of Chagas disease in Mexico: an update. *Trends In Parasitol* 17 (8) 372-376.

Hall BS, Bot C, Wilkinson SR (2011) Nifurtimox activation by Trypanosomal type I nitroreductases generates cytotoxic nitrile metabolites. *J Biol Chem* 286 (15) 13088-13095.

Hall BS, Wilkinson SR (2012) Activation of benznidazole by Trypanosomal ttype I nitroreductases results in Glyoxal formation.*Agents Chemother* 56 (1) 115 doi: 10.1128/AAC.05135-11.

Heby O, Persson L (1990) Molecular genetics of polyamine synthesis in eukaryotic cells. *Trends Biochem* 15, 153-158.

Holloway GA, Baell JB, Fairlamb AH, Novello PM, Parisot JP, Richardson J, Watson KG, Street IP (2007) Discovery of 2-iminobenzimidazoles as a new class of trypanothione reductase inhibitor by high throughput screening. *Bioorg Med Chem Lett* 17 (5) 1422-1427.

Holloway GA, Charman WN, Fairlamb AH, Brun R, Kaiser M, Kostewicz E, Novello PM, Parisot JP, Richardson J, Street IP, Watson KG, Baell JB (2009) Trypanothione reductase highthrouhput screening campaign identifies novel classes of inhibitors with antiparasitic activity. *Antimicrob Agent Chemother* 53 (7) 2824-2833.

Hoops S, Sahle S, Gauges R, Lee C, Pahle J, Simus N, SInghal M, Xu L, Mendes P, Kummer U (2006) COPASI- a COmplex PAthway SImulator. *Bioinformatics* 22, 3067-3074.

Hornberg JJ, Bruggeman FJ, Bakker BM, Westerhoff HV (2007) Metabolic control analysis to identify optimal drug targets. *Prog Drug Res* 64 (171), 173-189.

Kolodkin A, Boogerd FC, Plant N, Bruggeman FJ, Goncharuk V, Lunshof J, Moreno-Sánchez R, Yilmaz N, Bakker BM, Snoep JL, Balling R, Westerhohh HV (2011) Emergence of the silicon human and network targeting drugs. *Eur J Pharm Sci* In press. doi:10.1016/j.ejps.2011.06.006

Krauth-Siegel RL, Comini MA (2008) Redox control in trypanosomatids, parasitic protozoa with trypanothione –based thiol metabolism. *Biochim Biophys Acta* 1780, 1236-1248.

Lüscher A, de Koning HP, Mäser P (2007) Chemotherapeutic strategies against *Trypanosoma brucei*: drug target vs drug targeting. *Curr Pharm Des* 13 (6) 555-567.

Mansour TE (2002) *Chemotherapeutic Targets in Parasites*. Cambridge, Cambridge University Press, 90-101.

Marín-Hernández A, Gallardo-Pérez JC, Rodríguez-Enríquez S, Encalada R, Moreno-Sánchez R, Saavedra E (2011) Modeling cancer glycolysis. *Biochim Biophys Acta* 1807(6):755-767.

Martyn DC, Jones DC, Fairlamb AH, Clardy J (2007) High-throughput screening afford novel and selective trypanothione reductase inhibitors with anti- trypanosomal activity. *Bioorg Med Chem* 17 (5) 1280-1283.

Maya JD, Cassels BK, Iturriaga-Vásquez P, Ferreira J, Fáudez M, Galanti N, Ferreira A, Morello A (2007) Mode of action of natural ans synthetic drugs against *Trypanosoma cruzi* and their interaction with the mammallian host. *Comp Biochem Physiol* 146 (Part A), 601-620.

Mendes P (1993) GEPASI: a software package for modeling the dynamics, steady states and control of biochemical and other systems. *Comput Appl Biosci* 9, 563-571.

Mendoza-Cózatl D, Moreno-Sánchez R (2006) Control of glutatione and phytochelatin synthesis under cadmium stress. Pathway modeling for plants. *J Theor Biol* 238, 919-936.

Montrichard F, Le Guen F, Laval-Martin DL, Davioud-Charvet E (1999) Evidence for the co-existence of glutathione reductase and trypanothione reductase in the non-trypanosomatid *Euglenozoa*: *Euglena gracilis Z*.*FEBS Lett* 442, 29-33.

Moreno-Sanchez R, Saavedra E, Rodriguez-Enriquez S, Olin-Sandoval V (2008) Metabolic control analysis: a tool for designing strategies to manipulate metabolic pathways. *J Biomed Biotechnol* 2008: 597913.

Muñoz MJ, Murcia L, Segovia M. (2011) The urgent need to develop new drugs and tools for the treatment of Chagas´disease. *Expert Rev Anti Infect Ther* 9(1), 5-7)

Olivier BG, RohwerJM, Hofmeyr JHS (2005) Modelling cellular systems with PySCes.*Bioinformatics* 21 (4) 560-561.

Palma-Gutiérrez HN, Rodríguez-Zavala JS, Jasso-Chávez R,. Moreno-Sanchez R, Saavedra E (2008) Gene cloning and biochemical characterization of an alcohol dehydrogenase from *Euglena gracilis*.*J. Eukaryot. Microbiol* 55 554-561

Patterson S, Alphey MS, Jones DC, Shanks EJ, Street IP, Frearson JA, Wyatt PG, Gilbert IH, Fairlamb AH (2011) Dihydroquinazolines as a novel class of Trypanosoma brucei trypanothione reductase inhibitors: discovery, synthesis and characterization of their binding mode by protein rystallography. *J. Med. Chem.* 54(19), 6514-30.

Rodrigues-Coura J, L de Castro S (2002) A critical review on Chagas disease chemotherapy. *Mem Inst Oswaldo Cruz* 97 (1), 3-24.

Rodrigues-Coura J (2009) Present situation and new strategies for Chagas disease chemotherapy- a proposal. Mem Inst Oswaldo Cruz 104 (4), 549-554

Rodrígues-Coura J, Borges-Pereira J (2010) Chagas disease: 100 years after its discovery. A systemic review. *Acta Tropica* 115, 5-13.

Saavedra E, Marín-Hernández A, Encalada R, Olivos A, Mendoza-Hernández G, Moreno-Sánchez R (2007) Kinetic modeling can describe *in vivo* glycolysis in *Entamoeba histolytica*. *FEBS J* 274, 4922-4949.

Saavedra E, Rodríguez-Enríquez S, Quezada H, Jasso-Chávez R, Moreno-Sánchez R (2011) Rational design of strategies base on metabolic control analysis. In: Murray Moo-Young (ed.) *Comprehensive Biotechnology*, Second edition, volume 1, 511-524 pp. Elsevier.

Salazar-Schettino PM, Marín y Lopez RA (2006) Manual para el diagnóstico de la infección por *Trypanosoma cruzi.* Universidad Nacional Autónoma de México y Centro Nacional de la Transfusión sanguínea

Salazar-Schettino PM, Cabrera M, Bucio M, de Haro I (2011) Diagnóstico morfológico de las parasitosis. Méndez Editores 3ª ed. 6-12 pp

Sauro HM (1993) SCAMP: a general purpose simulator and metabolic control analysis program, *Comp Appl Biosc* 9 (4) 441-450.

Snoep JL (2005) The Silicon Cell initiative: working towards a detailed kinetic description at the cellular level. *Curr Op Biotechnol* 16, 336-343.

Sousa M, Ferreira AE, Tomás AM, Cordeiro C, Ponces A (2005) Quantitative assessment of the glyoxylase pathway in *Leishmania infantum* as a therapeutic target by modelling and computer simulation. *FEBS J* 272, 2388-2398.

Tamayo EM, Iturbe A, Hernández E, Hurtado G, Gutiérrez-X ML, Rosales JL, Woolery M, Ondarza RN (2005) Trypanothione reductase from the human parasite *Entamoeba histolytica*: a new drug target. *Biotechnol Appl Biochem*. 41, 105-115.

Torrie LS, Wyllie S, Spinks D, Oza SL, Thompson S, Harrison JR, Gilbert IH, Wyatt PG, Fairlamb AH,, Frearson JA (2009) Chemical validation of trypanothione synthetase: a potential drug target for human trypanosomiasis. *J Biol Chem* 284, 137-145.

Wildermuth MC (2000) Metabolic control analysis: biological applications and insights. *Genome Biology* 1(6), 103.1-103.5.

Westerhoff HV, Palsson BO (2004) The evolution of molecular biology into systems biology. *Nature Biotechnol* 22(10), 1249-1252.

Westerhoff HV (2007) Mathematical and theoretical biology for systems biology, and then… viceversa.*J Math Biol* 54, 147-150.

Westerhoff HV, Verma M, Nardelli M, Adamczyk M, van Eunen K, Simeonidis E, Bakker BM (2010) Systems biochemistry in practice: experimenting with modelling and undesrtanding with regulation and control. *Biochem Soc Trans* 38, 1189-1196.

Westerhoff, HV (2011) Systems biology left and right.*Meth Enzymol* 500, 3-11.

World Health Organization (2007) Reporte sobre la enfermedad de Chagas, World Health Organization on behalf of the special programme for research and training in tropical diseases , 1-96.

Wyatt PG, Gilbert IH, Read KD, Fairlamb AH (2011) Target validation: Linking target and chemical properties to desired product profile*. Curr Top Med Chem* 11, 1275-1283.

13. ANEXO

Hindawi Publishing Corporation
Journal of Biomedicine and Biotechnology
Volume 2008, Article ID 597913, 30 pages
doi:10.1155/2008/597913

Review Article

Metabolic Control Analysis: A Tool for Designing Strategies to Manipulate Metabolic Pathways

Rafael Moreno-Sánchez, Emma Saavedra, Sara Rodríguez-Enríquez, and Viridiana Olín-Sandoval

Departamento de Bioquímica, Instituto Nacional de Cardiología, Juan Badiano no. 1, Colonia Sección 16, Tlalpan, México DF 14080, Mexico

Correspondence should be addressed to Rafael Moreno-Sánchez, rafael.moreno@cardiologia.org.mx

Received 1 October 2007; Revised 16 January 2008; Accepted 26 March 2008

Recommended by Daniel Howard

The traditional experimental approaches used for changing the flux or the concentration of a particular metabolite of a metabolic pathway have been mostly based on the inhibition or over-expression of the presumed rate-limiting step. However, the attempts to manipulate a metabolic pathway by following such approach have proved to be unsuccessful. Metabolic Control Analysis (MCA) establishes how to determine, quantitatively, the degree of control that a given enzyme exerts on flux and on the concentration of metabolites, thus substituting the intuitive, qualitative concept of rate limiting step. Moreover, MCA helps to understand (i) the underlying mechanisms by which a given enzyme exerts high or low control and (ii) why the control of the pathway is shared by several pathway enzymes and transporters. By applying MCA it is possible to identify the steps that should be modified to achieve a successful alteration of flux or metabolite concentration in pathways of biotechnological (e.g., large scale metabolite production) or clinical relevance (e.g., drug therapy). The different MCA experimental approaches developed for the determination of the flux-control distribution in several pathways are described. Full understanding of the pathway properties when is working under a variety of conditions can help to attain a successful manipulation of flux and metabolite concentration.

1. INTRODUCTION

Is an effort to manipulate the metabolism of an organism worthy and reasonable, knowing that this cellular process has been continuously modified and refined through evolution and natural selection for adapting, in the most convenient manner, to the ongoing environmental conditions? The answer to this question seems obvious when three broad areas of research and development are identified in which manipulation of metabolic pathways is relevant: (a) drug design to treat diseases, (b) genetic engineering of organisms of biotechnological interest, and (c) genetic syndromes therapy.

Historically, drug design was the first area in which modification of metabolism was tried: the primary goal of drug administration is the inhibition of essential metabolic pathways, for example, in a parasite or a tumor cell. Thus, any metabolic pathway can be a potential therapeutic target. In the absence of a solid theoretical background that may build a strategy for the rational design of drugs, the pharmaceutical industry has applied the knowledge of inorganic and organic chemistry for the arbitrary and rather randomized modification of metabolic intermediaries by replacing hydrogen atoms in a model molecule with any other element or compound. This approach has been successful in the battle against many diseases. However, in many other instances such an approach has been unsuccessful.

The era of rational drug design probably started in the 50s when Hans Krebs proposed that, after having an exact description of a metabolic pathway, the "pacemaker" enzyme or "rate-limiting step" had to be identified. This approach certainly decreased the amount of intermediaries to be chemically modified, focusing only on the substrates, products, and allosteric effectors of the "rate-limiting step," instead of dispersing efforts on all the metabolic pathway intermediates. The experimental approaches used in the

identification of the pacemaker, key enzymes, "bottlenecks." limiting steps, or regulatory enzymes [1, 2] were

(i) inspection of the metabolic pathway architecture: due to cell economy and for reaching the highest efficiency, pathway control must reside in the enzymes localized at the beginning of a pathway or after a branch (teleological approach);

(ii) determination of nonequilibrium reactions: those reactions in which the quotient between the mass action ratio (Γ) and its equilibrium constant (Keq) is low, $\Gamma/\text{Keq} \ll 1$ (thermodynamic approach);

(iii) identification of the steps with the lowest maximal rates (V_{max}) in cellular extracts: the key enzyme of the pathway is the one that has the lowest rate (kinetic approach);

(iv) enzymes with sigmoidal kinetics: steps that are susceptible to alteration in their kinetic properties by compounds different from substrates and products and which may coordinate the entire metabolism (NADH/NAD^+; NADPH/$NADP^+$, ATP/ADP; acetyl CoA/CoA; Ca^{2+}/Mg^{2+}; high pH/low pH) or at least two metabolic pathways (citrate, Pi, AMP, malonyl-CoA);

(v) crossover theorem. Comparing the intermediary concentrations between a basal and an active steady-state pathway flux, the rate-limiting step in the basal condition will be that for which its substrate concentration diminishes and its product concentration increases when the system changes from the basal to the active state or vice versa (crossover point on a histogram of each intermediary versus its normalized variation in concentration);

(vi) the shape of the metabolic flux inhibition curve: a sigmoidal curve on a plot of inhibitor concentration versus flux shows that the sensitive step to the inhibitor exerts no control, that is, there is not proportionality between enzyme activity inhibition and pathway flux inhibition because there is an "excess" of enzyme. On the other hand, a hyperbolic curve indicates that the enzyme susceptible to the inhibitor controls the flux.

2. CONTROLLING SITES IN A METABOLIC PATHWAY

Once a site in a metabolic pathway has been identified with at least one of the criteria described above as "the rate-limiting step," researchers have frequently concluded that such enzyme or transporter is the only limiting step of the metabolic flux and extend this conclusion to all cell types and to all conditions.

For example, inspection of the glycolytic pathway (teleological approach) suggests that hexokinase (HK) and phosphofructokinase-1 (PFK-1) (which are at the beginning and after a branch of the pathway) are the key steps of glycolysis. However, all studies on glycolysis in the 60s, 70s, and 80s were performed by taking into account only the intracellular reactions from HK to LDH (i.e., without including the glucose transport reaction through the plasma membrane) and by considering glycolysis as a linear pathway without branches. To this regard, it is recalled that the glucose transporter (GLUT) includes a family of proteins and genes that are susceptible of regulation. Thus, if the extracellular glucose is considered as the initial glycolytic substrate, then another potential key step would be GLUT. Hence, if all the branches of the pathway are considered (Figure 1), then according to the teleological approach there will be additional potential rate-limiting sites.

Application of the thermodynamic and kinetic approaches to glycolysis reveals that HK, PFK-1, and pyruvate kinase (PYK) are the rate-limiting steps because in the living cell they catalyze reactions that are far away from equilibrium ($\Gamma/\text{Keq} = 10^{-3}$–$10^{-4}$), and they are also the slowest enzymes in the pathway by at least one order of magnitude (they have the lowest V_{max} values).

The use of the enzyme cooperativity approach has established that the regulatory steps of glycolysis are (i) PFK-1 and PYK because they are allosteric enzymes and (ii) HK because it is inhibited by its products (G6P and ADP, or AMP as an ADP-analogue). The application of the crossover theorem (approach no. v) to glycolysis has shown a consistent variation in the PFK-1 substrate (F6P) and product (F1,6BP). Up to now, there are few studies on control of glycolysis using the shape of the inhibitor titrating curve (approach no. vi), due to the lack of specific inhibitors for any of the three presumed key steps. An exception is iodoacetate which is indeed a potent inhibitor of GAPDH, but also of other highly reactive cysteine-containing enzymes [3–5]. By using iodoacetate as specific inhibitor, both GAPDH activity and flux showed identical titration curves, leading to the conclusion that GAPDH was the rate-limiting step of glycolysis in *Streptococcus lactis* and *S. cremoris* [6] (see, however, Section 3.2; Glycolysis in lactobacteria below).

All together, these results constitute the main reason why many intermediary metabolism researchers, including the authors of biochemistry text books, have proposed HK, PFK-1, and PYK as the rate-limiting steps of glycolysis. In consequence, to vary the glycolytic flux, one of these enzymes has to be modified.

Although the above-described experimental approaches are qualitative, full control has been automatically assigned to the "key" steps because the concept of the rate-limiting step assumes that there is only one single enzyme controlling the metabolic pathway flux (and the concentration of the final product of the pathway) and, in consequence, assigns values of zero to the control exerted by the other enzymes and transporters. However, as analyzed for glycolysis, researchers have commonly "identified" more than one limiting step. In the case of oxidative phosphorylation (OXPHOS), in the 70s and 80s some researchers considered cytochrome c oxidase as the rate-limiting step, whereas others preferred the ATP/ADP translocator or the Krebs cycle Ca^{2+}-sensitive dehydrogenases (for a review, see [7]).

Rephrasing the initial question, which could be the aim of manipulating a metabolic pathway such as glycolysis,

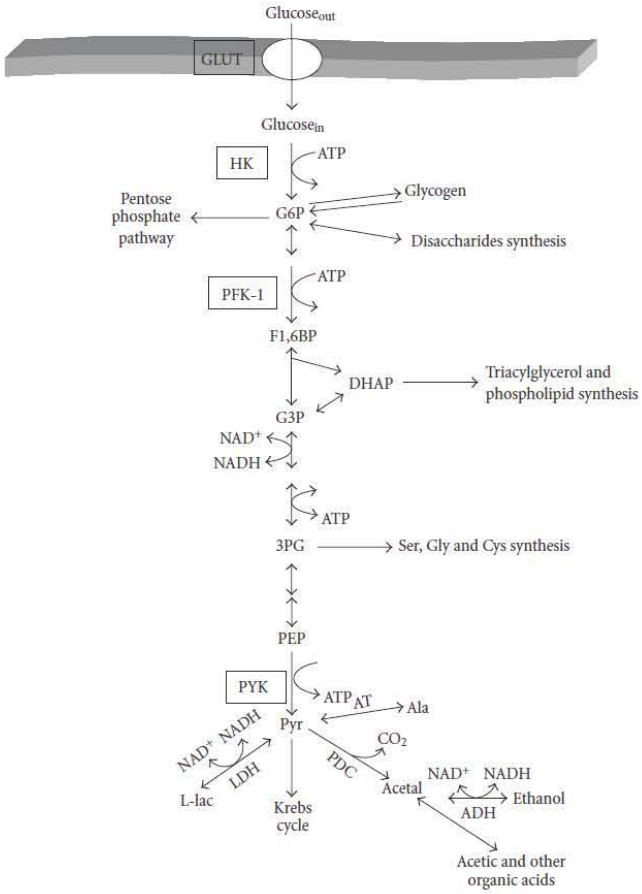

Figure 1: Glycolytic pathway and principal branches. GLUT, glucose transporter; HK, hexokinase; PFK-1, phosphofructokinase-1; G6P, glucose-6-phosphate; F1,6BP, fructose 1,6 bisphosphate; DHAP, dihydroxyacetone phosphate; G3P, glyceraldehyde-3-phosphate; 3PG, 3-phosphoglycerate; PEP, phosphoenolpyruvate; pyr, pyruvate; PYK, pyruvate kinase; L-lac, L-lactate; acetal, acetaldehyde; AT, alanine transaminase. *S. cerevisiae* lacks the LDH gene.

knowing its universal distribution in the living organisms? From a clinical standpoint, the inhibition of glycolysis is relevant for the treatment of human parasitic or pathological diseases such as cancer. The glycolytic reactions are almost identical in all organisms; in addition, the enzymes catalyzing these reactions are highly conserved throughout the evolutionary scale (their amino acid sequences are highly similar). In mammals, the genes of the 12 glycolytic enzymes are scattered throughout the genome, generally in different chromosomes, whereas in bacteria many of the glycolytic enzymes are clustered in operons [8]. However, there are organisms (like some human parasites) that contain enzymes with remarkable differences in their biochemical properties (substrate selectivity, catalytic capacity, stability, and oligomeric structure), or in genetic expression regulation in comparison to the human enzymes, which could be considered as drug targets.

Furthermore, some glycolytic products are of commercial interest such as ethanol for wine, beer, and other alcoholic beverages; CO_2 for bread manufacturing; and lactic acid and other organic acids for cheese production. Thus, from a biotechnological standpoint, it is convenient to accelerate the pathway flux to diminish the processing time and it is also desirable to increase the concentration of the metabolite to obtain robust commercial products. Here, it is important to emphasize that the metabolic pathways are designed to attain changes in flux with minimal disturbances in the intermediary concentrations. For example, the glycolytic flux in skeletal muscle can increase from rest to an active state by 100 fold, without large changes in

Table 1: Overexpression of glycolytic enzymes in different cell types.

Cell type	Enzyme	Activity (overexpression fold)	Flux (% Control)	Reference
Saccharomyces cerevisiae	HK	13.9	107	[12]
	PFK-1	3.5, 3.7,5	102	[9, 10, 12]
	PYK	8.6	107	[12]
	PDC	3.7	85	[13]
	ADH	4.8	89	[12]
	PFK-1 + PYK	5.6 + 1.3	107	[12]
	GAPDH + PGK + PGAM + ENO + PYK + PDC + ADH	1.4 + 1.7 + 16 + 4 + 10.4 + 1.08 + 1.4	121	[12]
	GAPDH + PGK + PGAM + ENO + PYK + PDC + ADH	1.5 + 1.4 + 3.4 + 1.5 + 2.5 + 1.1 + 1.2	94	[11, 14]
Escherichia coli	PFK	8.7	72	[15]
	PYK	2.9, 4.2	91,95	[16]
Lactococcus lactis	GAPDH	14-210	100	[17]
Aspergillus niger	PFK	3	100	[18]
	PYK	5	100	
Chinese hamster ovary	PFK	2.2, 3.4, 3.7	100	[19]

Flux to ethanol was for *S. cerevisiae* and *E. coli*; flux to citrate was for *A. niger*; and flux to L-lactate was for hamster.

metabolites. Then, it is physiologically more common to change a metabolic flux and the production of the final metabolite in the pathway than varying the intermediary concentrations [2]. However, we will see that, by using a suitable approach of metabolic control analysis, it is possible to design strategies to manipulate not only fluxes but also metabolic intermediary concentrations.

3. IN VIVO OVEREXPRESSION EXPERIMENTS OF ENZYMES

3.1. Glycolysis in yeasts

When the yeast *Saccharomyces cerevisiae* is exposed to high glucose (>2%; 0.11 M), the genes of all glycolytic enzymes are induced (PDC and ENO increase their expression by 20 fold; PGK, PYK, and ADH, 3–10 times; and the others, 2 fold in average) [8–11]. However, when the methodological development of genetic engineering allowed modulating the expression of enzymes within cells, researchers turned to the rate-limiting step concept to manipulate a metabolic pathway to increase flux and/or its intermediates, hypothesizing that the overexpression of only one, or of a few key glycolytic genes, should increase the flux.

Historically, Heinisch [9] in Germany was the first author to obtain a 3.5 fold overexpression of PFK-1 in *S. cerevisiae*, but surprisingly he observed that the rate of ethanol production was not modified. Subsequent experiments for increasing the ethanol production rate by overexpressing either each of the presumed limiting steps, or in combination with other glycolytic enzymes (Table 1), have been unsuccessful and, even in some cases, a slight decrease in flux has been attained. For instance, the simultaneous overexpression of seven enzymes of the final section of glycolysis induced only a 21% increase in ethanol production after 2 hours of culture (Table 1) [11]. This was accompanied by a 10–20% decrease in PFK-1 expression, which might have attenuated the flux increase.

In yeasts, HK is not product inhibited by G6P or ADP; instead, it is strongly feedback inhibited by trehalose-6-phosphate (Tre6P). This metabolite is synthesized from G1P by Tre6P synthase and Tre6P phosphatase. Deletion of the Tre6P synthase gene does not bring about an increased ethanol production, but it rather induces a defective cellular growth on glucose and fructose and a lowered ethanol production, as a result of a highly active HK that leads to hyperaccumulation of hexose phosphate metabolites (particularly F1,6BP) and fast depletion of ATP, Pi, and downstream metabolites. The explanation for this event is that, in the Tre6P synthase mutants, the rate of glucose phosphorylation exceeds the rate of glycolytic ATP synthesis (named "turbo effect"). Heterologous expression of a Tre6P-insensitive HK does not recover completely the wild-type phenotype. Furthermore, deletion of the Tre6P synthase gene in the Tre6P-insensitive HK strain did affect growth, suggesting other interactions and functions of Tre6P synthase in the control of sugar metabolism, at least in *Schizosaccharomyces pombe* [20].

Davies and Brindle [10] obtained a 5-fold overexpression of PFK-1 in *S. cerevisiae*, but the increase in ethanol production was not attained under anaerobic conditions. There was a slight increase in ethanol production in resting cells in aerobic conditions, under which the mitochondrial metabolism contributes to the ATP supply. In all these works,

it may be noted that enzyme overexpression indeed affects the concentration of several intermediaries, but this effect has not been further examined.

It is worth noting that the experiments described in Table 1 do not rigorously reproduce the physiological situation, in which overexpression of all the enzymes should be carried out in the proportions found in the organisms. The rationale behind this observation is that overexpression of only one "limiting" step leads to a flux control redistribution, a condition at which other steps now become rate limiting. Thus, the concept of "rate-limiting step" offers no simple answer to the question of increasing the yeast glycolytic flux, and it rather makes this problem to appear as a difficult task to solve. In contrast, it seems that all relevant controlling steps have to be overexpressed, thus reproducing what natural selection has already successfully accomplished.

In addition to *S. cerevisiae*, overexpression of glycolytic enzymes in other organisms such as *E. coli* [15, 16], lactobacteria [17], tomato [21], potato [22], and hamster ovary cells [19] has been accomplished, although without increasing flux (Table 1). It is somewhat surprising to note that in the glycolytic enzyme overexpression experiments, the strong inhibitory effect of G6P (or Tre6P in *S. cerevisiae*), and citrate on HK and PFK-1, respectively, have been neglected. This regulatory mechanism does not disappear in the cells overexpressing the enzymes but, on the contrary, it is exacerbated. Then, what would be the aim of overexpressing HK, PFK-1 or any other allosteric, or strongly product-inhibited enzyme if they will be more inhibited?

A successful experiment of increasing the glycolytic flux was performed in primary cultures of rat hepatocytes [23]. HK and glucokinase (GK) were overexpressed by using adenovirus as carrier. The transformed hepatocytes showed higher activity of 18.7- and 7.1-times for HK and GK, respectively, at 3 mM glucose, and of 6.3- and 7.1-times at 20 mM glucose. However, at 20 mM glucose, the flux to lactate was not modified in HK-transformed cells, just like the experiments described above (Table 1). In contrast, with GK overexpression, a 3-fold increase in flux was achieved. The mechanistic difference is the HK inhibition by G6P (10 mM G6P inhibits HK activity by 90%), whereas GK is not product inhibited.

3.2. Glycolysis in lactobacteria

Lactococcus lactis is used in cheese production. For this purpose, *L. lactis* ferments lactose to lactic acid by glycolysis. The end products, lactate and H^+, are expelled and acidify the external medium which contributes to cheese flavor and texture and inhibits the growth of other bacteria. Similarly to yeast, the lack of carbon source in lactobacteria promotes a metabolic change that leads to the production of formic and acetic acids, ethanol, and, in a lower proportion, L-lactic acid, altering the product quality. Thus, from a commercial point of view, it does not seem important to know what controls the flux to lactate (because its rate of production is adequate), but what controls the branching flux.

To understand the process, and to eventually inhibit the production of secondary acids, Andersen et al. [24] constructed LDH mutants, using a synthetic promoter library for tuning the gene expression. In mutants lacking this enzyme, most of the pyruvate was transformed into acetic and formic acids (Figure 1). In turn, flux to lactate was affected in mutants expressing only 10% or less of wild-type LDH levels, which indicated that LDH exerts no control of the glycolytic flux in wild-type bacteria. Only with a normal content of this enzyme (100%), flux toward secondary acids was prevented. Therefore, the flux to formic and acetic acids is negatively controlled by LDH, and positively by PYK [17, 25]. As in *S. cerevisiae*, overexpression of PFK-1, PYK, or GAPDH in lactobacteria did not increase the flux to L-lactic acid [17, 25]. Similarly to *E. coli* glycolysis [26], glycolysis in *L. lactis* was controlled by the ATP demand when working below its maximum capacity [27, 28], whereas, under high-rate conditions, the glucose and lactate transporters exerted the main flux control [28]. Furthermore, this kind of observations indicates that the flux control may reside outside the pathway [27–29], and it also supports the proposal by Hofmeyr and Cornish-Bowden [30] that the end-product demand (which is usually overlooked in studies of metabolism because these metabolites are frequently not considered as part of the pathway) might be essential in flux control.

3.3. Glutathione and phytochelatin synthesis in plants

Glutathione (γ-Glu-Cys-Gly; GSH) is the most abundant nonproteinaceous thiol compound (1–10 mM) in almost all living cells. GSH is involved in the oxidative stress processing, xenobiotic detoxification, and, in some plants and yeasts, in the inactivation of toxic heavy metals (for a recent revision see [31]). GSH is synthesized by two enzymes: γ-glutamylcysteine synthetase (γ-ECS) and glutathione synthetase (GS) (Figure 2), which catalyze reactions with high-equilibrium constants (Keq > 1000). Under a low GSH demand (unstressed conditions), the producing block of enzymes has to receive information from the last part of the pathway to (i) avoid the excessive and toxic accumulation of the intermediary γ-EC and (ii) reach a stable steady state [32]. This information transfer is mediated by GSH, which exerts strong competitive inhibition of γ-ECS [33] (Figure 2). GSH and Cys also exert inhibition on the ATP-sulfurylase (ATPS) and on sulfate transporters (Figure 2) (for a review, see [31]). The feedback inhibition of γ-ECS has led several researchers to propose that this enzyme is the rate-limiting step of GSH synthesis [33–35]. Although there are no studies about the pathway's behavior under stressed conditions, which means under a high GSH demand, the proposal that γ-ECS is the key enzyme has been automatically extended to any environmental condition such as heavy metal exposure.

By assuming that γ-ECS is the rate-limiting step, many research groups have tried to increase, in plants and yeasts, the rate of synthesis and the concentration of GSH and phytochelatins (PCs) with the aim of fortifying their heavy metal resistance and storage capacity, mainly toward Cd^{2+}. The development of organisms able to grow in soils and water systems contaminated with heavy metals, which may

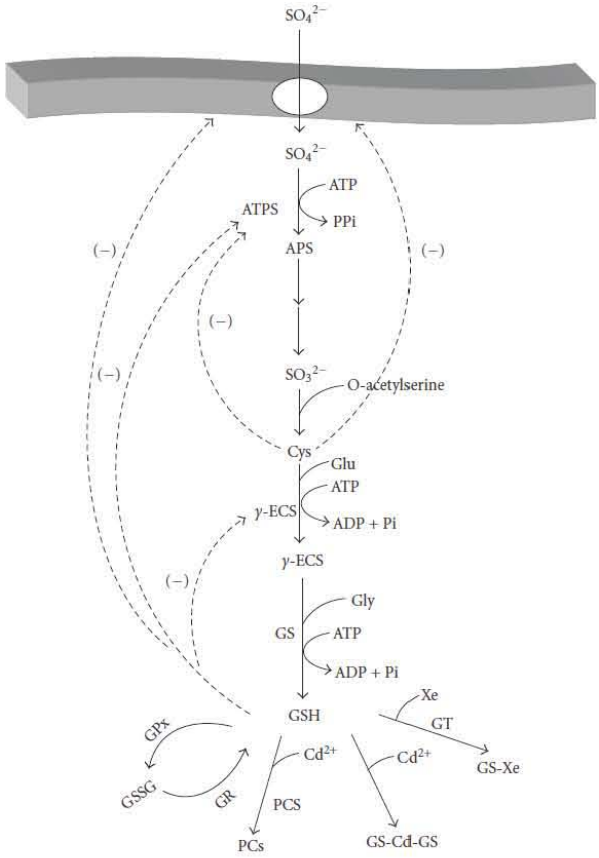

Figure 2: Sulfur assimilation and glutathione and phytochelatins synthesis in plants ATPS, ATP sulfurylase; APS, adenosine 5′ phosphosulphate; γ-ECS, γ-glutamyl cysteine synthetase; γ-EC, γ-glutamyl cysteine; GS, glutathione synthetase; GSH, reduced glutathione; GSSG, oxidized glutathione; GPx, GSH peroxidase; GR, GSH reductase; PCS, phytochelatin synthase; PCs, phytochelatins; GT, GSH-S-transferases; Xe, xenobiotic; GS-Xe, glutathione-xenobiotic complex. The reactions are not shown stochiometrically. GR uses the cofactor NADPH. The Cd^{2+}-GSH complex formation (cadmium bis-glutathionate) is fast and spontaneous and does not require enzyme catalysis. Modified from [31].

have the ability of accumulating toxic metal ions, is of biotechnological interest for bioremediation strategies.

With this goal in mind, researchers have then over-expressed γ-ECS and other pathway enzymes, including phytochelatin synthase (PCS) (Table 2). Some of these experiments have been partially successful in increasing GSH levels, although this has been rather marginal with no correlation between enzyme levels and GSH concentration. Unfortunately, these overexpression experiments have not been accompanied by determinations of fluxes or other relevant metabolite concentrations such as PCs or Cys. On the other hand, the overexpression of PCS has surprisingly induced oxidative stress and necrosis instead of increasing Cd^{2+} accumulation and resistance [36]. This result suggests that, under high GSH demand (i.e., for PCs synthesis and for direct heavy metal sequestration by GSH), the GSH concentration does not suffice for maintaining the other essential GSH functions such as oxidative stress management and xenobiotic detoxification.

Another problem in the study of GSH biosynthesis for its eventual manipulation is that the pathway has been analyzed considering only the GSH-synthetic reactions without taking into account the GSH-consuming reactions (Figure 2), [31]. The analysis of an incomplete pathway leads to misleading conclusions about the control of flux. Metabolic modeling has shown that only with the incorporation of the consuming reactions of the pathway end products, a true steady state can be established [30]. In conclusion, without a solid theoretical

Table 2: GSH and phytochelatin synthesis enzymes overexpression in plants and yeasts.

Overexpressed enzyme (activity fold)	Organism (experimental condition)	Metabolite (increment fold)	Reference
ATP sulfurylase (2.1)	*Brassica juncea*	2.1 [GSH]	[37]
ATP sulfurylase (4.8)	Tobacco (unstressed)	1.3 [SO_4^{2-}]	[38]
O-acetyl-serine thiol-lyase (2.5)	Tobacco (unstressed)	2 [Cys] 0 [GSH]	[39]
Serine acetyl transferase (>10)	Potato chloroplasts (unstressed)	2 [Cys] 0 [GSH]	[40]
E. coli GS (90)	*Populus tremula* (unstressed)	0 [GSH]	[34]
GS (3)	*S. cerevisiae* (unstressed)	0 [GSH]	[41]
E. coli γ-ECS (>2)	*Brassica juncea* (unstressed)	0 [GSH]	[35]
	B. juncea (+100 μM Cd^{2+})	4 [GSH][(a)]	
γ-ECS (2.1)	*S. cerevisiae* (unstressed))	1.3 [GSH]	[42]
E. coli γ-ECS (50)	*Populus tremula* (unstressed)	4.6 [GSH]	[34]
E. coli γ-ECS (4.9)	*Brassica juncea* (unstressed) *B. juncea* (+200 μM Cd^{2+})	3.5 [GSH][(b)] 1.5 [GSH][(b)]	[43]
E. coli γ-ECS (40)	Tobacco (unstressed)	>4 [GSH]	[44]
γ-ECS (9.1) + GS (18)	*S. cerevisiae* (unstressed)	1.8 [GSH]	[45]
PCS (>2)	*Arabidopsis thaliana* (+85 μM Cd^{2+})	0 [GSH]	[36]
Vacuolar transporter of PC-Cd complexes (>2)	*S. pombe*	Higher Cd^{2+} resistance	[46]

[(a)]The increase was only in roots with no effect on shoots. [(b)]The increase was only in shoots with no effect on roots.

framework, the overexpression of only one enzyme (the "rate-limiting step"), or of many arbitrarily selected enzymes (Tables 1 and 2), the problem of increasing the flux or metabolite concentrations cannot be solved.

3.4. Overexpression of proteins from other metabolic pathways

There are some successful examples of the genetic engineering approach to manipulate metabolism:

(i) overexpression (approx. 23 fold) of the five genes of the tryptophan synthesis pathway in *S. cerevisiae*, to increase (9-fold) flux [47];

(ii) increase in amino acids (Trp, Ile, Lys, Val, Thr) and trehalose production in *Corynebacterium glutamicum*, in which some proteins of each metabolic pathway are simultaneously overexpressed, but some of them with mutations that confer insensitivity to feedback inhibition [48–53]. In these transformed bacteria, the end products are indeed overproduced and their excretion is accelerated;

(iii) overexpression of PFK and PyK to increase ethanol production by 35% in *E. coli*, although lactic acid formation was not modified [16];

(iv) mannitol 1-phosphate dehydrogenase and mannitol 1-phosphatase overexpression to increase mannitol production by 27–50% in LDH-deficient *Lactococcus lactis* [54];

(v) increase in sorbitol production (5 fold) in LDH-deficient *Lactobacillus plantarum* through the overexpression of sorbitol 6-phosphate dehydrogenase (activity up to 250 fold in mutants *versus* wild type) [55];

(vi) overexpression of PFK (14 fold) or LDH (3.5 times) to increase 2-3 times the homolactic fermentation flux in *Lactococcus lactis* growing on maltose, and in parallel decrease fluxes toward secondary acids and ethanol [56].

4. DOWNREGULATION OF ENZYMES TO MANIPULATE METABOLISM

4.1. Glycolysis in tumor cells

Glycolysis is enhanced in human and animal cancer cells (reviewed in [57]). Several glycolytic enzymes are overexpressed in at least 70% of human cancers [58]. Except for glucose transporter 1 (GLUT-1), the other 11 glycolytic enzymes (HK to LDH) are overexpressed in brain and nervous system cancers. Prostate and lymphatic nodule cancers (Hodgkin and non-Hodgkin lymphomas; myelomas) overexpress 10 glycolytic enzymes (except for HK; in prostate cancer GLUT1

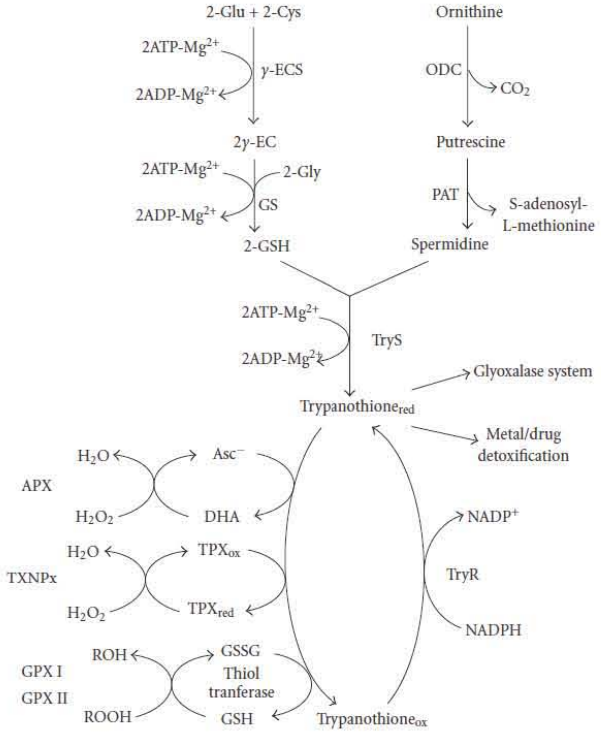

Figure 3: Trypanothione synthesis in trypanosomatids. The trypanothione producing enzymes are γ-ECS, GS, ODC, aminopropyl transferase (PAT), and TryS. The trypanothione consuming enzymes are ascorbate peroxidase (APX); tryparedoxin peroxidases (TXNPx); trypanothione-glutathione thiol transferase (thiol transferase); and glutathione peroxidases I (GPX I) and II (GPX II). The regenerating enzyme is TryR. APX, thiol transferase, and GPX II have only been described in *T. cruzi*. This last parasite lacks ODC activity, but it has developed high-affinity transporters for putrescine, cadaverine, and spermidine [71].

is also overexpressed). There is a second group of cancers that overexpresses 6–8 glycolytic genes (skin, kidney, stomach, testicles, lung, liver, placenta, pancreas, uterus, ovary, eye, head and neck, and mammary gland). A third group includes those cancers overexpressing 1 or 2 glycolytic genes (bone, bone marrow, cervix, and cartilage) [58].

In animals, gene expression of glycolytic enzymes is regulated (both coordinately and individually) under hypoxic conditions by hypoxia-responsive transcription factors such as HIF-1α (hypoxia-inducible factor 1α), SP family factors, AP-1, and possibly MRE (metal response elements) [8, 59–61]. HIF-1α is probably the principal coordinator in gene induction. There are binding sites (consensus sequence ACGT) for HIF-1α in the promoters of genes for HK [62], PFK-1, ALDO, GAPDH, PGK, ENO, PYK, and LDH (reviewed in [8]). TPI and perhaps HPI and PGAM are also induced by hypoxia, but it is not clear whether HIF-1α mediates this induction [8], and whether this factor regulates other metabolic pathways associated with glucose catabolism. For example, although glycogen phosphorylase is overexpressed under hypoxia in human tissues [63], the role of HIF-1 has not been demonstrated.

If direct manipulation of pathway genes becomes difficult, then the overexpression or repression of transcription factors such as HIF-1α, AP1, and MREs might solve the problem of changing flux, although overexpression of transcription factors may also be difficult due to the numerous upstream and downstream factors involved.

4.2. Glycolysis in Trypanosoma brucei

The kinetoplastid parasites *Trypanosoma cruzi, Trypanosoma brucei, and Leishmania* are the causative agents of Chagas disease, African trypanosomiasis, and leishmaniasis, respectively. The available drugs to treat these diseases are highly toxic for humans. Moreover, the parasites may become resistant, and hence the search for new drugs and drug targets is relevant for solving these public health problems.

In these parasites, the metabolism is organized in a peculiar way; they have a subcellular structure called glycosome

in which several metabolic pathways take place: gluconeogenesis, reactions of the pentose phosphate pathway, purine salvage and pyrimidine biosynthesis, β-oxidation of fatty acids, fatty acid elongation, biosynthesis of ether lipids, and the first seven steps of glycolysis. In fact, approximately 90% of glycosome enzyme content corresponds to glycolytic enzymes [64]. Glycosomal glycolytic enzymes have unique structural, kinetic, and regulatory features not found in their human counterparts, and therefore have been the subject of extensive biochemical studies to use them as drug targets [65]. The rationale behind this is to synthesize inhibitors that affect mainly the parasitic enzymes with relatively low effect on the human enzymes since the infective parasite stages rely mostly on glycolysis for ATP supply.

There are reports on the design of presumed specific inhibitors for some of the *T. brucei* glycolytic enzymes: GLUT (bromoacetyl-2-glucose) [66], HK, HPI, PFK, ALDO, TPI, GAPDH, PGK, PYK, and glycerol-3-phosphate dehydrogenase [67]. Although the purified enzymes display very low *Ki* values for these inhibitors and some of them inhibit parasite growth or infective capabilities, their effect on inhibiting the glycolytic flux has not been explored. Therefore, it is not yet possible to directly ascribe the effects seen in parasite culture with the in vitro effects on the isolated enzymes. To identify the best drug targets, determination of the flux control steps of glycolysis in *T. brucei* has been recently initiated [68].

4.3. Trypanothione synthesis in kinetoplastid parasites

Trypanothione (TSH_2) is a reducing agent present in trypanosomatids that is synthesized from one spermidine and two GSH molecules by TSH_2 synthetase (TryS) (Figure 3). This metabolite and its reducing enzyme, TSH_2 reductase (TryR), replace the antioxidant and metabolic functions of the more common GSH/GSH reductase system present in mammals. In fact, most of the antioxidant metabolism of these parasites depend on TSH_2 (Figure 3) [69, 70]. Thus, the enzymes of this metabolic pathway have been proposed as drug targets for killing the parasites.

Several studies have focused in assessing TryR as drug target. Diminution in its gene transcription yields a loss of activity between 56–90%, depending on the genetic technique [72–75]. In knockdown *T. brucei* cells (i.e., when TryR activity has diminished to less than 10% of the wild-type level), the parasites show growth diminution and higher sensitivity to H_2O_2 in culture and loss of infectiveness in mice. However, TSH_2 and thiol compound contents were not affected [75]. TryR downregulation by >85% in *Leishmania* species causes inability to survive under oxidative stress inside macrophages [72–74]. In contrast, when TryR is 14- and 10 fold overexpressed in *Leishmania* and *T. cruzi*, respectively, there are no significant differences in H_2O_2 susceptibility between control and transfected cells; both types of cells are also equally resistant to the oxidative stress-inducers gentian violet, and nitrofurans [76]. Intriguingly, the cellular levels of TSH_2, GSH, and glutathionylspermidine, determined in both types of experiments (TryR suppression and overexpression) were similar in control and transformed cells.

Other studies have proposed TryS as an alternative drug target. Knockdown of TryS by siRNA in procyclic *T. brucei* causes (i) viability impairment and arrest of proliferation when TSH_2 levels decrease to 15% of the wild-type level, (ii) increased sensitivity to H_2O_2 and alkyl hydroperoxides, (iii) damage to the plasma membrane, and (iv) diminution of the TSH_2 content and accumulation of GSH and glutathionyl-spermidine [77]. A similar metabolite variation (lower TSH_2; higher GSH) was attained with a TryS knockdown induced by siRNA in the bloodstream form of *T. brucei* [78]. This TryS knockdown also induced an increased sensitivity to different compounds that affect TSH_2 metabolism such as arsenicals, melarsen oxide, trivalent antimonials, and nifurtimox [78]. Indeed, western blot analysis showed, in addition to the expected (10-fold) decrease in TryS protein, a 2-3-folds increase in γ-ECS and TryR. The changes in expression of other enzymes suggest unveiled compensatory or pleiotropic effects on TSH_2 metabolism.

Other researchers have selected γ-glutamylcysteine synthetase (γ-ECS), the presumed rate-limiting step of GSH synthesis, as an alternative drug target of TSH_2 synthesis in *T. brucei* (Figure 3). Knockdown of γ-ECS gene in the parasite induces cell death and depletion of GSH and TSH_2 only after 80% decrease in the enzyme content [79]. The γ-ECS knockdown cells are rescued from death by adding external GSH, which elevates the cellular GSH and TSH_2 levels [79].

Glutathione synthetase (GS) has not been manipulated in trypanosomatids, or in any other organism, perhaps because it has been considered as a nonrate-limiting step of GSH and TSH_2 biosynthesis. However, DNA microarray analysis of antimonite-resistant *Leishmania tarentolae* shows increased transcription of γ-ECS, GS, and P-glycoprotein A RNAs [80]. Although it was not evaluated whether increase in gene transcription correlated with an increase in enzyme activity, it may be possible that under high GSH demand (i.e., under oxidative stress conditions) GS might exert control of TSH_2 synthesis. On the other hand, ornithine decarboxylase (ODC) overexpression in *T. brucei* (the presumed limiting step of spermidine synthesis) causes no change in TSH_2 levels [81]. Therefore, ODC does not seem to be a controlling step of TSH_2 synthesis.

Although almost full inhibition (>80%) of gene transcription or activity of any of these enzymes results in parasite death, the question remains of how TSH_2 metabolism is affected when the enzymes are less inhibited. For example, in the therapeutic treatment of patients it is certain that drugs have to be administered for long periods of time. If the parasites are not completely cleared from the patient, disease recurrence and generation of drug-resistant parasites are possible. The results described above indicate that each enzyme by itself has low control on TSH_2 synthesis and concentration; therefore, highly specific and very potent inhibitors have to be designed in order to attain the required full activity blockade to affect TSH_2 metabolism in these parasites.

5. THEORY OF METABOLIC CONTROL ANALYSIS

The metabolic control analysis (MCA) was initially developed by Kacser and Burns in Scotland [82, 83] and by Heinrich and Rapoport in East Germany [84, 85]. This analysis establishes a theoretical framework that explains the results observed with the enzyme overexpression and downregulation experiments. In addition, it helps to identify and design experimental strategies for the manipulation of a given process in an organism (heavy metal hyperaccumulation; increased production of ethanol, CO_2, lactate or acetate; or inhibition of a metabolic pathway flux with therapeutic purposes). MCA rationalizes the quantitative determination of the degree of control that a given enzyme exerts on flux and on the concentration of metabolites. Different experimental approaches have been developed to detect and direct what has to be done and measured, in order to identify and understand why an enzyme exerts a significant or a negligible control on flux and metabolite concentration in a metabolic pathway. Thus, the application of this analysis avoids the "trial and error" experiments for identifying and manipulating the conceptually wrong "rate-limiting step."

To understand how a metabolic pathway is controlled and could be manipulated, its control structure has to be evaluated. The control structure of a pathway is constituted by the flux control coefficient (C^J_{vi}), which is the degree of control that the rate (v) of a given enzyme i exerts on flux J; the concentration control coefficient (C^X_{vi}), which is the degree of control that a given enzyme i exerts on the concentration of a metabolite (X); and the elasticity coefficients. The control coefficients are systemic properties of the pathway that are mechanistically determined by the elasticity coefficients (ε^{vi}_X), which are defined as the degree of sensitivity of a given enzyme v_i (i.e., the enzyme's ability to change its rate) when any of its ligands (X: substrate, products or allosteric modulators) is varied.

The flux control coefficient is defined as

$$C^J_{v_i} = \frac{dJ}{dv_i} \bullet \frac{v_{io}}{J_o}, \tag{1}$$

in which the expression dJ/dv_i describes the variation in flux (J) when an infinitesimal change is done in the enzyme i concentration or activity. In practice, the infinitesimal changes in v_i are undetectable, and hence measurable noninfinitesimal changes are undertaken. If a small change in v_i promotes a significant variation in J, then this enzyme exerts an elevated flux control (Figure 4, position 1). In contrast, if a rather small or negligible change in flux is observed when v_i is greatly varied, then the enzyme does not exert significant flux control (Figure 4, position 2). To obtain dimensionless and normalized values of C^J_{vi} the scaling factor v_{io}/J_o is applied, which represents the ratio between the initial values from which the slope dJ/dv_i is calculated. If all C^J_{vi} of the pathway enzymes and transporters are added up, the sum comes to one (summation theorem).

The MCA clearly distinguishes between the control exerted by a given enzyme on flux (flux control coefficient) and on the metabolite concentration (concentration control coefficient). Thus, an enzyme can have significant control on a metabolite concentration but not on the pathway flux. This distinction is important for biotechnology purposes. On one hand, the use of the rate-limiting step concept for manipulating metabolic pathways does not make such differentiation, which probably has contributed to the many unsuccessful experiments reported in the literature; on the other hand, it should be clearly defined whether the aim of the project is to increase flux and/or a metabolite concentration since MCA establishes for each aim a different experimental design.

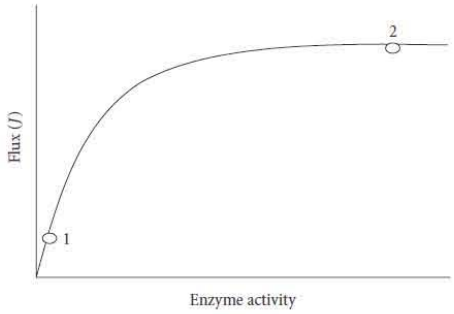

FIGURE 4: Experimental determination of flux control coefficient.

To determine the flux control coefficient of a given enzyme, small variations in the enzyme content, or preferentially, in activity are required, without altering the rest of the pathway, and then the changes in flux are determined. The experimental points are plotted as shown in Figure 4 to calculate the slope at the reference point v_{io}/J_o. This experiment, apparently easy to perform, has demanded great intellectual and experimental effort. Several experimental strategies have been developed to determine C^J_{vi}:

(i) formation of heterokarionts and heterocygots (classical genetics),

(ii) titration of flux with specific inhibitors,

(iii) elasticity analysis,

(iv) mathematical modeling (in silico biology),

(v) in vitro reconstitution of metabolic pathways,

(vi) genetic engineering to manipulate in vivo protein levels.

5.1. *Classical mendelian genetics*

The arginine biosynthesis in *Neurospora crassa* was the first metabolic pathway in which flux control coefficients were experimentally determined by Kacser's laboratory [86]. This fungus forms multinucleated mycelia that facilitate the generation of polyploid cells. By mixing different ratios of spores containing genes encoding wild (active) and mutant (inactive) enzymes of this pathway, it was possible to generate heterokaryont mycelia with different content, and activity, of four pathway enzymes. The authors built plots of

enzyme activity versus flux (see Figure 4) for acetyl-ornithine aminotransferase, ornithine transcarbamoylase, arginine-succinate synthetase, and arginine-succinate lyase. All the experimental points of these heterokaryonts localized near to position 2 of Figure 4 with $C_{vi}^{J\,\mathrm{arg}} = 0.02$–$0.2$ (flux control by these enzymes was only 2–20%), which indicated that none of these enzymes exerted significant control on arginine synthesis. The authors did not determine the remaining flux control (75%), which might reside in carbamoyl-phosphate synthetase I (this mitochondrial ammonium-dependent isoform can be bound to the mitochondrial inner membrane or form complexes with ornithine transcarbamoylase [87, 88]) and in mitochondrial citruline/ornithine transporter, both of which have been proposed as limiting steps, or might be in the arginine demand for protein synthesis.

Organisms with many alleles of one enzyme may form homo-and heterozygotes expressing different activity levels. *Drosophila melanogaster* has three ADH alleles encoding for isoforms with different $V_{\max}$. When three natural homozygotes, a null mutant, and some heterozygotes were generated, different ADH activities were attained but the ethanol consuming rate did not change (Figure 4, position 2). It was concluded that the ADH flux control was near zero [89].

5.2. Titration of flux with inhibitors (control of oxidative phosphorylation)

Oxidative phosphorylation (OXPHOS) is the only pathway for which specific and potent inhibitors for many enzymes and transporters are available. OXPHOS is divided in two segments (Figure 5): the oxidative system (OS) formed by substrate transporters (pyruvate, 2-oxoglutarate, glutamate, glutamate/aspartate, dicarboxylates), Krebs cycle enzymes, and the respiratory chain complexes; and the phosphorylating system (PS) constituted by the ATP/ADP (ANT) and Pi (PiT) transporters, and ATP synthase. The proton electrochemical gradient ($\Delta\mu^{-}{}_{\mathrm{H}}{}^{+}$) connects the two systems.

When the flux (ATP synthesis) is titrated by adding increasing concentrations of each specific inhibitor, plots are generated in which the enzyme activity is progressively diminished by increasing inhibitor concentration. Hence, the C_{vi}^{J} value depends on the type of inhibitor used

(a) for irreversible inhibition,

$$C_{v_i}^{J} = \left(\frac{-I_{\max}}{J_o}\right)\left(\frac{dJ}{dI}\right)_{[I]\to 0}, \tag{2}$$

(b) for simple noncompetitive inhibition,

$$C_{v_i}^{J} = \left(\frac{-Ki}{J_o}\right)\left(\frac{dJ}{dI}\right)_{[I]\to 0}, \tag{3}$$

(c) for simple competitive inhibition,

$$C_{v_i}^{J} = \left(\frac{-Ki[(1+S)/Km]}{J_o}\right)\left(\frac{dJ}{dI}\right)_{[I]\to 0}, \tag{4}$$

where J_o is the pathway flux in the absence of inhibitor; $I_{\max}$, minimal inhibitor concentration to reach maximal flux inhibition; Ki, inhibition constant; S, substrate concentration; Km, Michaelis-Menten constant; and dJ/dI, initial slope ($[I] = 0$) of inhibition titration curve.

To estimate flux control coefficients from inhibitor titration of ADP-stimulated (state 3) respiratory rates (i.e., mitochondrial O_2 consumption coupled to ATP synthesis), (2) for irreversible inhibitors was used because researchers assumed that mitochondrial inhibitors such as rotenone, antimycin, carboxyatractyloside, and oligomycin were "pseudoirreversible," due to the enzyme's high affinity for them. However, under this assumption flux control coefficients were usually overestimated [90, 91]. To solve this problem, Gellerich et al. [92] developed (5) for noncompetitive tightly-bound inhibitors and, by using nonlinear regression analysis, it was possible to include all experimental points from the titration curve thus increasing accuracy in calculating C_{vi}^{J}:

$$J = \left[\frac{n(J_o - J_i)^2 \bullet E^n}{C_o \bullet J_o \bullet E_o{}^n[(n - C_o)\bullet J_o - (n \bullet J_i)\bullet E^n]}\right] + J_i$$
$$E^2 + (Kd + I - E_o)\bullet E - Kd \bullet E_o = 0, \tag{5}$$

in which J_o and J_i are the respiration fluxes in the noninhibited ($E = E_o$) and inhibited ($E = 0$) states; Kd is the dissociation constant of the enzyme-inhibitor complex, and n is an empirical component that expresses the relationship between substrate concentration and the reaction catalyzed by the enzyme E.

The analysis of data in Table 3 shows that OXPHOS is not controlled by only one limiting step, but the flux control is rather distributed among several enzymes and transporters. It is worth noting that the value of the flux control coefficient depends on the content of enzyme or transporter, which varies from tissue to tissue. Perhaps the ATP/ADP translocase in AS-30D hepatoma mitochondria might reach the status of being the "OXPHOS limiting step" with a $C_{\mathrm{ANT}}^{\mathrm{JOxPhos}} = 0.70$, or the Pi transporter in kidney mitochondria [93], or the ATP/ADP translocase and the respiratory chain complex 3 in liver mitochondria [94], but it should be noted that other steps also exert significant control (Table 3). Although the distribution of control varies between tissues, the flux control mainly resides in the PS of organs with high ATP demand such as the heart ($C_{\mathrm{PT+ANT+ATPsynthase}}^{\mathrm{JOxPhos}} = C_{\mathrm{PS}}^{\mathrm{JOxPhos}} = 0.73$), kidney ($C_{\mathrm{PS}}^{\mathrm{JOxPhos}} = 0.75$; $C_{\mathrm{OS}}^{\mathrm{JOxPhos}} = 0.31$), and fast-growing tumors ($C_{\mathrm{PS}}^{\mathrm{JOxPhos}} = 0.98$). In contrast, in the liver ($C_{\mathrm{OS}}^{\mathrm{JOxPhos}} = 0.80$; $C_{\mathrm{PS}}^{\mathrm{JOxPhos}} = 0.65$) and brain ($C_{\mathrm{OS}}^{\mathrm{JOxPhos}} = 0.35$; $C_{\mathrm{PS}}^{\mathrm{JOxPhos}} = 0.41$), the control is shared by both systems.

The situation in skeletal muscle appears controversial. Wisniewski et al. [97] determined that the OXPHOS control was shared by the PS ($C_{\mathrm{PS}}^{\mathrm{JOxPhos}} = 0.62$) and the ATP demand (purified ATPase). In turn, Rossignol et al. [95] concluded that the OS exerted the main control ($C_{\mathrm{OS}}^{\mathrm{JOxPhos}} = 0.68$), but these authors apparently used low-quality mitochondria (low respiratory control values that lead to low rates of ATP synthesis associated with high rates of respiration) that were

Table 3: Control distribution of oxidative phosphorylation.

Enzyme	C_{vi}^{JATP}	Rat organ mitochondria	Specific inhibitor	Inhibition mechanism	Reference
NADH-CoQ-oxidoreductase (Site 1 of energy conservation or Complex I of respiratory chain)	0.15	Heart (0.5 mM pyr + 0.2 μM Ca^{2+})	Rotenone	Noncompetitive tightly bound	[93]
	0.26	Heart (10 mM pyr + 10 mM mal)			[95]
	0.31	Kidney (0.5 mM pyr + 0.2 μM Ca^{2+})			[93]
	0.06	Kidney (10 mM pyr + 10 mM mal)			[95]
	0.06–0.10	Brain (0.05 mM pyr + 0.4 μM Ca^{2+})			[91]
	0.25	Brain (10 mM pyr + 10 mM mal)			[95]
	0	Tumor (10 mM glut + 3 mM mal)			[96]
	0.27	Liver (10 mM pyr + 10 mM mal)			[95]
	0.13	Skeletal muscle (10 mM pyr + 10 mM mal)			[95]
CoQ.cytochrome c oxidoreductase (Site 2 of energy conservation or Complex III of respiratory chain)	0.01	Heart	Antimycin	Noncompetitive tightly bound	[93]
	0.19	Heart			[95]
	0.02	Kidney			[95]
	0.05–0.11	Brain			[91]
	0.02	Brain			[95]
	0	Tumor			[96]
	0.43	Liver (5 mM Succ + 1 μM Ca^{2+})			[94]
	0.07	Liver			[95]
	0.22	Skeletal muscle			[95]
Cytochrome c oxidase (Site 3 of energy conservation or Complex IV of respiratory chain)	0.11	Heart	Cyanide or azide	Noncompetitive simple	[93]
	0.13	Heart			[95]
	0.04	Kidney			[95]
	0.02–0.07	Brain			[91]
	0.02	Brain			[95]
	0.04	Tumor			[96]
	0.23	Liver			[94]
	0.03	Liver			[95]
	0.20	Skeletal muscle			[95]
ATP/ADP transporter (adenine-nucleotides or ATP/ADP transporter, carrier or exchanger)	0.24	Heart	Carboxy-atractyloside (CAT)	Noncompetitive tightly bound	[93]
	0.04	Heart			[95]
	0	Kidney			[93]
	0.07	Kidney			[95]
	0.08	Brain			[91]
	0.08	Brain			[95]
	0.60–0.70	Tumor			[96]
	0.48	Liver			[93]
	0.01	Liver			[93]
	0.37	Skeletal muscle (10 mM Glut + 3 mM mal)			[97]
	0.08	Skeletal muscle			[95]

Table 3: Continued.

Enzyme	C_{vi}^{JATP}	Rat organ mitochondria	Specific inhibitor	Inhibition mechanism	Reference
ATP synthase	0.34	Heart	Oligomycin	Noncompetitive tightly bound	[93]
	0.12	Heart			[95]
	0.32	Kidney			[93]
	0.27	Kidney			[95]
	0.09–0.20	Brain			[91]
	0.26	Brain			[95]
	0.28	Tumor			[96]
	0.05	Liver			[94]
	0.20	Liver			[95]
	0.10	Skeletal muscle			[97]
	0.10	Skeletal muscle			[95]
Pi transporter	0.15	Heart	Mersalyl	Noncompetitive simple	[93]
	0.14	Heart			[95]
	0.43	Kidney			[93]
	0.28	Kidney			[95]
	0.13	Brain			[91]
	0.26	Brain			[95]
	0	Tumor			[96]
	0.05–0.12	Liver			[94]
	0.26	Liver			[95]
	0.15	Skeletal muscle			[97]
	0.08	Skeletal muscle			[95]
Pyruvate transporter	0.15	Heart	α-cyano-4-hydroxy-cinnamate	Noncompetitive simple	[95]
	0.03	Kidney			[95]
	0.08	Brain			[91]
	0.26	Brain			[95]
	0.21	Liver			[95]
	0.20	Skeletal muscle			[95]
Dicarboxylates transporter	0.05–0.14	Liver	Malate or butyl-malonate	Competitive simple	[94]
External ATPase	0.40	Skeletal muscle	Purified ATPase addition		[94]

not incubated under near physiological conditions (10 mM pyruvate, 10 mM malate, 10 mM Pi, pH 7.4 in Tris buffer), and the authors incorrectly assumed that rotenone and antimycin were irreversible inhibitors. It is notorious that in all works shown in Table 3 at least one of these mistakes is evident.

There are some inhibitors for enzymes and transporters from other pathways, but they are not quite specific and may affect other sites. Due to the fact that there are no inhibitors for every step in these pathways, only one flux control coefficient has been determined by inhibitor titration. Examples of these inhibitors are 6-chloro-6-deoxyglucose for glucose transporters in bacteria, 2-deoxyglucose for HPI, iodoacetate for GAPDH [6], 1,4-dideoxy-1,4-imino-D-arabinitol for glycogen phosphorylase [98], oxalate and oxamate for LDH, 6-amino nicotinamide for the phosphate pentose pathway [99], amino-oxyacetate for aminotransferases and kirureninase (tryptophan synthesis), norvaline for ornithine transcarbamylase, mercaptopycolinate for PEP carboxykinase, acetazolamide for carbonic anhydrase, and isobutyramide for ADH (compiled by Fell [2]).

Potential uses of the experimental approach

Mitochondrial pathologies are a heterogeneous group of metabolic perturbations characterized by morphological abnormalities and/or OXPHOS dysfunction [100]. Mitochondrial DNA analysis has revealed specific mutations for some mitochondriopathies. Although the specific OXPHOS mutations causing the disease may appear in all tissues, the functioning of only some of them is altered. The organ's sensitivity might be related to the different flux

control coefficients of the mutated enzyme in the different tissues (Table 3) and to their ATP supply dependence from OXPHOS versus glycolysis.

MCA allows for the analysis of a metabolic flux or intermediate concentration by focusing either on one step or by grouping enzymes in blocks or in pathways. Thus, a comparative analysis of OXPHOS control distribution reveals that heart, kidney, some fast growing tumors (rat AS-30D hepatoma, mouse fibrosarcoma, human breast, lung, thyroid carcinoma, melanoma) [101], and perhaps skeletal muscle are more susceptible to mitochondrial mutations in ATP synthase, which is the only PS site with subunits encoded in the mitochondrial genome. On the other side, liver and brain might be more susceptible to mitochondrial mutations of the respiratory chain enzymes (see Table 3). Considering that the brain is a fully aerobic organ [102], whereas the liver depends on both OXPHOS (70–80%) and glycolysis (20–30%) for ATP supply [103], then it can be postulated that the brain is more sensitive to mutations in the mitochondrial genome than the liver because subunits of complexes I, III, and IV are encoded by the mitochondrial genome.

Titration of flux with specific inhibitors to determine the flux control coefficients of OXPHOS has been applied to intact tumor cells [90]. The results showed that the flux control resided mainly in site 1 of the respiratory chain ($C_{\text{Sitel}}^{\text{JOxPhos}} = 0.30$), whereas the other evaluated sites exerted a marginal control [90]. This observation could have therapeutic application if site 1 does not exert control in healthy cells, leading to less severe side effects.

The use of inhibitors in intact cells to determine control coefficients might pose two problems: hydrophilic inhibitors such as carboxyatractyloside (for ANT) and α-cyano-4-hydroxy-cinammate (for pyruvate transporter) cannot readily enter the cell due to the presence of the plasma membrane barrier; the other problem is that hydrophobic but slow inhibitors, such as oligomycin, require long incubation times to ensure the interaction with the specific sites. These problems can be solved by incubating the cells for long periods of time and taking care of cell viability, for instance, AS-30D hepatoma cells are fairly resistant to this mechanical manipulation as they maintain high viability after a lengthy incubation under smooth orbital agitation of 1 h at 37°C [90].

5.3. Elasticity analysis

MCA defines the elasticity coefficients as

$$\varepsilon_X^{v_i} = \frac{dvi}{dX} \bullet \frac{X_o}{v_{io}}, \tag{6}$$

which is a dimensionless number that show the rate variation v of a given enzyme or transporter i when the concentration of a ligand X (substrate S, product P or allosteric modulator) is varied in infinitesimal proportions. The elasticity coefficients are positive for those metabolites that increase the enzyme or transporter rate (substrate or activator), and they are negative for the metabolites that decrease the enzyme or transporter rates (product or inhibitor). An enzyme working, under a steady-state metabolic flux, at saturating conditions of S or P, is no longer sensitive to changes in these metabolites. Thus, its elasticity is close to zero (Figure 6, $\varepsilon_X^{v_i} = 0$). In turn, an enzyme working at S or P concentrations well below the Michaelis constant (Km_S or Km_P) is expected to be highly sensitive to small variations in these metabolites (Figure 6, $\varepsilon_X^{v_i} = 1$).

The elasticities are intrinsically linked to the actual enzyme kinetics. If the kinetic parameters of an enzyme are known (Vm_f, Vm_r, Km_S, and Km_P), then the enzyme elasticity for any given metabolite concentration may be calculated as shown in the following equations.

For substrate,

$$\varepsilon_s^{v_i} = \frac{-S/Km_s}{1 + S/Km_s + P/Km_p} + \frac{1}{1 - \Gamma/\text{Keq}}, \tag{7}$$

and for product,

$$\varepsilon_p^{v_i} = \frac{-P/Km_P}{1 + S/Km_s + P/Km_P} - \frac{\Gamma/\text{Keq}}{1 - \Gamma/\text{Keq}}, \tag{8}$$

in which Γ is the mass action ratio, and Keq is the equilibrium constant preferentially determined under physiological conditions.

An enzyme with low elasticity cannot increase (or decrease) its rate despite large variations in S (or P) concentration; in consequence, such enzyme exerts a high flux control. In turn, an enzyme with a high elasticity can adjust its rate to the variation in S or P concentrations, and thus it does not interfere with the metabolic flux, exerting a low flux control. This inverse relationship between the elasticity and the flux control coefficients is expressed in a formal equation denominated connectivity theorem. A metabolic pathway can be divided in two blocks around an intermediary X: the producing (synthetic, supply) and the consuming (demand) enzyme blocks of X are i_1 and i_2, respectively. Thus, the connectivity theorem for this two-block system is

$$\frac{C_{v1}^J}{C_{v2}^J} = -\frac{\varepsilon_X^{v2}}{\varepsilon_X^{v1}}. \tag{9}$$

The negative sign of the right part of the equation cancels with $\varepsilon_X^{v_{i1}}$, which is negative because X is a product of enzyme block i_1 (Figure 6).

To obtain the flux control coefficients, this approach requires experimental determination of the elasticity coefficients. How can this be done? Many strategies have been designed [90, 103–108], but the most used and probably more trustworthy is that in which the initial pathway metabolite (S_o) concentration is varied to increase the X concentration (any intermediary in the pathway), and measuring in parallel the variation in flux. Under steady-state conditions, the flux rate is equal to the rate of end-product formation (i.e., lactate or alcohol for glycolysis; oxygen consumption for OXPHOS) and to the rate of any partial reaction. Then, plots of X versus flux (Figure 7) are generated. The slope, calculated at the reference coordinate

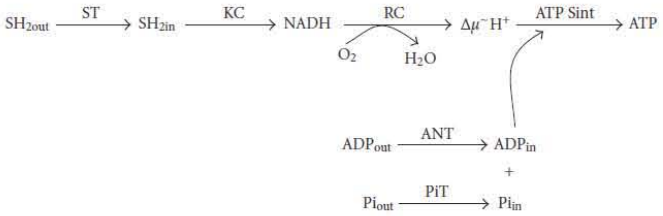

FIGURE 5: Mitochondrial oxidative phosphorylation. ST, oxidizable substrate transporter; KC, Krebs cycle; RC, respiratory chain; ($\Delta\mu^-{}_{H^+}$), proton electrochemical gradient; ANT, adenine nucleotide translocator; PiT, phosphate transporter; ATP Sint, ATP synthase.

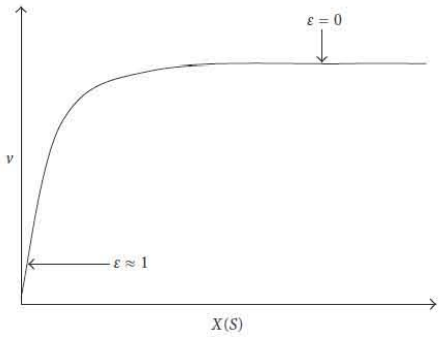

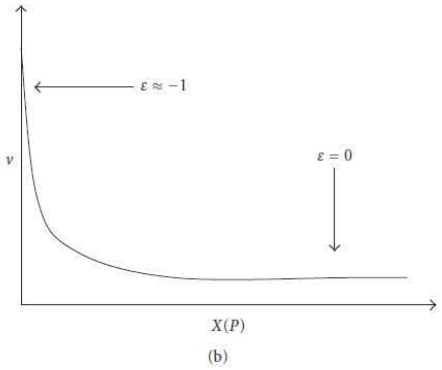

FIGURE 6: Elasticity coefficients.

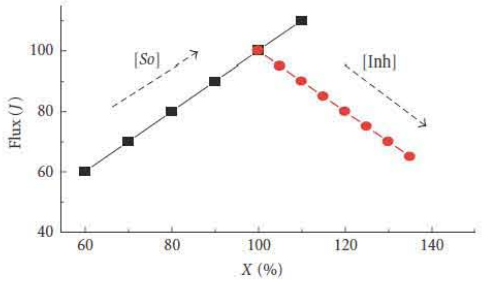

FIGURE 7: Experimental determination of the elasticity coefficients for substrates and products.

(X_o, J_o) that is equivalent to (S_o, v_{io}), yields the elasticity coefficient of the consuming block of X. In another set of experiments, an inhibitor is added to block one or more enzymes after X. The X concentration and flux are determined and plotted as shown in Figure 7, from which the elasticity coefficient of the producing block is calculated.

The flux control coefficients are determined by using the connectivity theorem and considering that the sum of the control coefficients comes to 1, $C_1 + C_2 = 1$ (summation theorem):

$$C^J_{v1} = \frac{\varepsilon^{v2}_X}{\varepsilon^{v2}_X - \varepsilon^{v1}_X},$$
$$C^J_{v2} = -\frac{\varepsilon^{v1}_X}{\varepsilon^{v2}_X - \varepsilon^{v1}_X}. \quad (10)$$

This method for determining $C^J_{v_i}$ using the elasticities of the two blocks was called double modulation by Kacser and Burns [83]. Years later, Brand and his group [103, 104] renamed this method as top-down approach. By applying the procedure shown in Figure 7 and using (10) for different metabolites along the metabolic pathway, it is possible to identify those sites that exert a higher control (which may be the sites for therapeutic use or biotechnological manipulation) and those that exert a negligible control under a given physiological or pathological situation.

Elasticity analysis has been used to evaluate the OXPHOS control distribution in tumor cells [90]. Almost all studies on this subject have been carried out with isolated mitochondria incubated in sucrose-based medium at 25 or 30°C or with the more physiological KCl-based medium but still at 30°C (Table 3). Furthermore, these studies did not consider that the product, ATP, never accumulates in the living cells, which does occur in experiments with isolated mitochondria. Under such a condition, a steady state in ATP production can never be reached as in living cells. In other words, the

distribution of control in mitochondria (Table 3) has been determined in the absence of an ATP-consuming system. A remarkable exception to this incomplete experimental design was the work done by Wanders et al. [105], in which isolated liver mitochondria were incubated with two different ATP-consuming systems (or ADP-regenerating systems): HK + glucose and creatine kinase (CK) + creatine. Under this more physiological setting, the OXPHOS flux control distributed between ANT and the ATP-consuming system; however, flux control by the other pathway components was not examined. Therefore, to accurately evaluate OXPHOS control distribution, mitochondria should be incubated in the presence of an ATP-consuming system or in their natural environment (i.e., inside the cell).

The rate of OXPHOS in intact cells is determined from the rate of oligomycin-sensitive respiration: in the steady state, the enzyme rates are the same and constant; in branched pathways the sum of the branched fluxes equals the flux that supplies the branches. The global elasticity of the ATP-consuming processes (e.g., synthesis of protein, nucleic acid, and other biomolecules, as well as ion ATPases to maintain the ionic gradients, mechanical activity such as muscular contraction or flagellum and cilium movement, and secretion of hormones, digestive enzymes and neurotransmitters) is estimated by inhibiting flux with low concentrations of oligomycin or a respiratory chain inhibitor. To determine the elasticity of the ATP-producing block, flux, and [ATP] are varied with streptomycin, an inhibitor of protein synthesis (Figure 7). The elasticity coefficients are calculated from the initial coordinate slopes (without inhibitors) of each titration. With this procedure, it has been determined that the ATP-consuming block exerts a significant flux control of 34% [90]. Remarkably, this flux control value obtained in cells is quite similar to the flux control coefficients of the ATP-consuming system (HK or CK) reported by Wanders et al. [105] with isolated mitochondria.

Elasticity analysis by enzyme blocks allows the inclusion of the end-product demand as another pathway block. The conclusions obtained from this analysis have formulated the supply-demand theory [30], which proposes that when flux is controlled by one block (demand), the concentration of the end-product is determined by the other block (supply). The ratio of elasticities determines the distribution of flux control between supply and demand blocks. For instance, if $\varepsilon_X^{\text{Supply}} > \varepsilon_X^{\text{Demand}}$ (i.e., demand becomes saturated by the end-product X, and hence its elasticity is near zero), then the demand block exerts the main flux control. For concentration control, at larger $\varepsilon_X^{\text{Demand}} - \varepsilon_X^{\text{Supply}}$, smaller absolute values of both C^X_{Supply} and C^X_{Demand} are attained; hence, under demand saturation, the supply elasticity fully governs the magnitude of the variation in the end-product concentration. On the other hand, when demand increases, it loses flux control and induces a diminution in the end-product concentration. In turn, supply gains flux control and loses concentration control. In the presence of feedback inhibition, the system can maintain the end-product concentration orders of magnitude away from equilibrium (at a concentration around the $K_{0.5}$ of the allosteric enzyme).

As mentioned before, the demand is not usually included in the pathway because it is erroneously thought that it is not part of it. But then, is it valid to analyze the control of a metabolite synthesis if its demand is not considered? When the demand block is not included, it is assumed that the metabolic pathway produces a metabolite at the same rate regardless whether the metabolite demand is high or low. This reasoning is incorrect because a metabolic pathway indeed responds to changes in the metabolite demand and, more importantly, a pathway without end-products consumption reactions is unable to reach a steady state.

Therefore, a metabolic pathway can be divided in supply and demand blocks. The intermediary X linking the two blocks is one of the end-products of the producing block (e.g., pyruvate or lactate or ethanol, and ATP for glycolysis). The variation in rate of the two blocks in response to a variation in X can be theoretical or experimentally determined (Figure 8(a)). It is worth noting that, for this supply-demand approach, it is not necessary to know the kinetics of each pathway enzyme because the rate response of each block reflects the global kinetics of all participating enzymes. When the X concentration is increased, the rate of the supply block decreases (i) because X is its product and (ii) because usually an enzyme within this block receives information from the final part of the pathway, decreasing its rate through feedback inhibition. In turn, the rate of the demand block increases as X is its substrate.

To better visualize the effect of large rate changes, the kinetics of both blocks are plotted in a logarithmic scale. Figure 8(b) shows the kinetics described in Figure 8(a) converted to natural logarithm. The intersection point between kinetic curves, at which the supply and demand rates are identical, represents the pathway steady-state flux (in the Y axis) and end-product concentration (in the X axis). Since the elasticity is also defined as $\varepsilon_X^{v_i} = d\ln v_i / d\ln X$, the slope at the intersection point represents the elasticity of each block towards the intermediary X. Here, the use of the scalar factor is not necessary because it is included in the logarithmic equation. With the elasticity coefficients calculated from plots like those shown in Figure 8, and the connectivity theorem, the flux control coefficient of each block is determined. The example in Figure 8(b) shows that the demand exerts a high flux control (and has low elasticity) and the supply block exerts low control (and has high elasticity).

The fact that the demand may exert a high flux control in metabolite pathways has at least three important implications: (a) the supply block responds to variations in the demand (high elasticity); (b) the demand block has information transfer mechanisms towards the supply block that avoid the unrestricted intermediary accumulation under a low demand, particularly when the supply block has reactions with large Keq (>100; $\Delta G^{\circ\prime} > 3\,\text{Kcal mol}^{-1}$ at 37°C); and (c) if the main flux control resides in the demand block, then the supply block may only exert control on the intermediary concentration but not on the flux [30, 32]. This last conclusion explains why it is incorrect to consider that an enzyme that controls flux must also control the intermediary concentration.

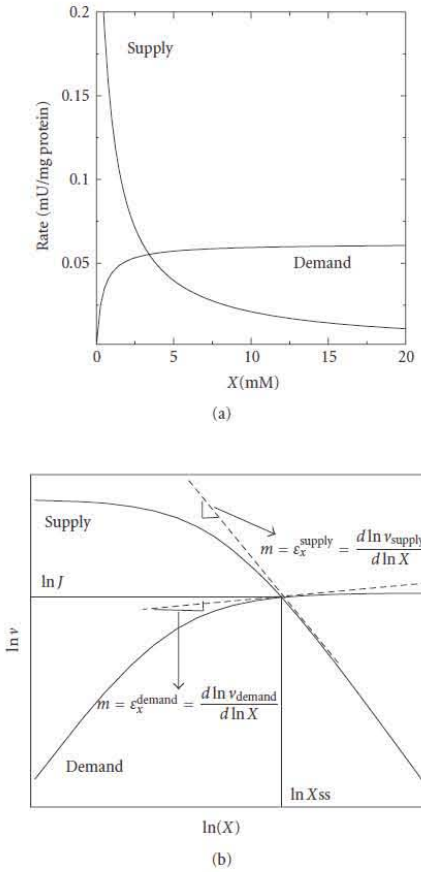

FIGURE 8: (a) Kinetics of the synthesis (supply) and consuming (demand) blocks of the intermediary X. The kinetic parameters are from enzymes in tobacco glutathione (GSH) synthesis. X represents the intermediary concentration, in this case GSH. (b) Rate plots of the supply and demand blocks in a natural logarithmic scale.

Regulatory mechanisms of enzyme activity are modulation of protein concentration by synthesis and degradation, as well as covalent modification and variation in the substrate or product concentrations (which are components of the pathway). In addition, another regulatory mechanism is the modulation by molecules that are not part of the pathway, that is, through allosteric interaction with cooperative (sigmoidal kinetics) or noncooperative enzymes (hyperbolic kinetics) (e.g., Ca^{2+} activates some Krebs cycle dehydrogenases; citrate inhibits PFK-1; malonyl-CoA inhibits the mitochondrial transporter of acyl-carnitine/carnitine; or the initial substrate of a pathway that has not entered the system). For these last cases, Kacser and Burns [83] proposed the use of the response coefficient R which is defined by the following expression:

$$R_M^J = C_{v_i}^J \bullet \varepsilon_M^{v_i}, \tag{11}$$

where M is the external modulator of the i enzyme. The response coefficient is $dJ/dM \bullet M_0/J_0$. If the elasticity of the sensitive enzyme toward the external effector is also determined, then it is possible to calculate $C_{v_i}^J$ by using (11). Unfortunately, due to the experimental complexity for determining the elasticity coefficient, this coefficient is often calculated in a theoretical way by using the respective rate equation (Michaelis-Menten or Hill equations) and the kinetic parameters Km and $V_{\max}$ determined by someone else under optimal assay conditions, which are commonly far away from the physiological ones. Therefore, for this theoretical determination of elasticity only the value of the external modulator concentration is required. It is convenient to emphasize that the determination of the flux control coefficients becomes more reliable when they are calculated from several experimental points (Figure 7), instead of only one, as occurs with the theoretical elasticity analysis.

Groen et al. [106] determined the flux control distribution of gluconeogenesis from lactate in hepatocytes by using both theoretical and experimental elasticity analysis and the response coefficient. These authors concluded that gluconeogenesis stimulated by glucagon was controlled by the pyruvate carboxylase ($C_{\text{PC}}^{J_{\text{glucose}}} = 0.83$); in the absence of this hormone, the control was shared by PC, PYK, ENO-PGK segment, and TPI-fructose-1,6-biphosphatase segment [106].

Elasticity analysis has been applied to elucidate the flux control of ATP-producing pathways in fast-growing tumor cells. For OXPHOS, this approach showed that respiratory chain complex I and the ATP-consuming pathways were the enzymes with higher control ($C_{v_i}^J = 0.7$) [90]. For glycolysis, the main flux control ($C_{v_i}^J = 0.71$) resided in GLUT + HK reactions because HK is strongly inhibited by its product G6P despite extensive enzyme overexpression [107]. Examples of elasticity analysis on other pathways are photosynthesis [108], ketogenesis [109], serine [110] and threonine synthesis in *E. coli* [111], glycolysis in yeast [112], glucose transport in yeast [113], DNA supercoiling [114], glycogen synthesis in muscle [115], and galactose synthesis in yeast [116].

In conclusion, the elasticity analysis is the most frequently used method for determining flux control coefficients because it does not need a group of specific inhibitors for all the enzymes and transporters of the pathway, neither does it require knowledge of the inhibitory mechanisms or kinetic constants. It is only necessary to produce a variation in the intermediary concentration X by using an inhibitor of either block or by directly varying the X concentration.

5.4. *Pathway modeling*

In agreement with Fell [2], it seems impossible for a researcher to analyze one by one the rate equation of each

enzyme in a metabolic pathway to predict and explain the system behavior as a whole. To deal with this problem, in the last three decades some scientists have constructed mathematical models for some metabolic pathways using several software programs. Thus, the specific variation of a single enzyme activity without altering the rest of the pathway (Figure 4), which has been an experimentally difficult task for applying MCA, becomes easier to achieve with reliable computing models. The term "in silico biology" has been coined for this approach.

There are two basic types of modeling: (a) structural modeling and (b) kinetic modeling. The former is related to the pathway chemical reaction structure and does not involve kinetic information. The use of reactions is based on their stoichiometries. The information obtained with structural modeling is the description of the following:

(i) the exact determination of which reactions and metabolites interact among them;

(ii) the conservation reactions. There are metabolites for which their sum is always constant or conserved (e.g., NADH + NAD^+; NADPH + $NADP^+$; ubiquinol + ubiquinone; ATP + ADP + AMP; CoA + acetyl-CoA). The identification of conserved metabolites might not be obvious;

(iii) enzyme groups catalyzing reactions in a given relationship with another group of enzymes;

(iv) elemental modules, which are defined as the minimal number of enzymes required to reach a steady state, which can be isolated from the system (for a review about structural modeling; see [117]).

Kinetic modeling is more frequently used. In addition to an appropriate computing program, this approach requires the knowledge of the stoichiometries, rate equations, and Keq values of each reaction in the pathway (or the V_{max} in the forward and reverse reactions), as well as the intermediary concentrations reached under a given steady state. Some currently used softwares are Copasi (http://www.copasi.org/tiki-index.php) based on Gepasi (http://www.gepasi.org/; [118]); Metamodel [119]; WinScamp [120] and Jarnac [121] (both available at http://www.sys-bio.org/); and PySCeS (http://pysces.sourcesforge.net/; [122]). For other programs and links, go to http://sbml.org/index.psp. To reach a steady-state flux, it is necessary to fix the initial metabolite concentration to a constant value and the irreversible and constant removal of the end products. Except for the final reactions in which their products have to be removed from the system, all pathway reactions have to be considered as reversible, notwithstanding whether they have large Keq (if there is an irreversible reaction under physiological conditions, then a reversible rate equation that includes the Keq suffices to maintain the reaction as practically irreversible). Care should be taken to include the enzyme's sensitivity toward its products because this property is related with the enzyme elasticity and hence with its flux control; omission of this parameter may very likely lead to erroneous conclusions.

It should be pointed out that the purpose of kinetic modeling is not merely to replicate experimental data but also to explain them [117]. Thus, pathway modeling is a powerful tool that allows for (i) the detection of those properties of the pathway that are not so obvious to visualize when the individual kinetic characteristics of the participating enzymes are examined; and (ii) the understanding of the biochemical mechanisms involved in flux and intermediary concentration control. Modeling requires the consideration of all reported experimental data and interactions that have been described for the components of a specific pathway, thus allowing for the integration of disperse data, discarding irrelevant facts [84]. Although all models are oversimplifications of complex cellular processes, they are useful for the deduction of essential relationships, for the design of experimental strategies that evaluate the control of a metabolic pathway, and for the detection of incompatibilities in the kinetic parameters of the participating enzymes and transporters, which may prompt the experimental revision of the most critical uncertainties.

With the model initially constructed, the simulation results do not usually concur with the experimental results; in consequence, the model normally requires refinement, a point at which the researcher's thinking and knowledge of biology plays a fundamental role in modifying the structure and parameters of the model. The discrepancies observed between modeling and experimentation unequivocally pinpoint what elements or factors have to be re-evaluated or incorporated so that the model approximates more closely reality (i.e., experimental data). The comparison of the experimentally obtained intermediary concentrations and fluxes with those obtained by simulation is an appropriate validating index of the model; this index indicates whether the model approximation to the physiological situation is acceptable or whether re-evaluation of the kinetic properties of some enzymes and transporters and/or incorporation of other reactions or factors is required.

A reason to why the results obtained by modeling may substantially differ from the experimental results is that the kinetic parameters of the pathway enzyme and transporters and the Keq values used were determined by different research groups, under different experimental conditions and in different cell types. Moreover, enzyme kinetic assays are carried out at low, diluted enzyme concentrations (thus discarding or ignoring relevant protein-protein interactions), and at optimal (but not physiological) pH and "room temperature" (which may be far away from the physiological values). In addition, no experimental information is usually available regarding the reactions reversibility and the product inhibition of the enzymes and transporters (particularly for physiological irreversible reactions, i.e., reactions with large Keq). With worrisome frequency, the researcher has to adjust the experimentally determined Vm and Km values to achieve a model behavior that acceptably resembles that observed in the biological system. Apparently, this type of limitations as well as the sometimes overwhelming amount of kinetic data necessary for the construction of a kinetic model has restricted the number of reliable models that can be used for the prediction of the pathway control structure.

Once the kinetic model stability, robustness, structural and dynamic properties have been evaluated, and experimentally validated, the model may become a virtual laboratory in which any parameter or component can be modified or replaced and any aspect of the pathway behavior can be explored within a wide diversity of circumstances or limits [117]. At this stage, the model is suitable for examining the pathway regulatory properties and control structure.

Glycolysis in *S. bayanus, S. cerevisiae* [113, 123, 124], and *Trypanosoma brucei* [125, 126] is the metabolic pathway that has been more extensively modeled. Both cell types have a very active glycolysis and are fully dependent on this metabolic pathway for ATP supply, under anaerobiosis and aerobiosis, respectively. One advantage of modeling glycolysis in these cell types is that most of the kinetic parameters used have been experimentally determined by the same groups under the same experimental conditions. However, the kinetics of the reverse reactions has not been determined and thus these authors used Km_P and Keq values reported by others and obtained in other cell types under rather different experimental conditions, or they were adjusted to improve model fitting.

Nevertheless, the simulation results yielded relevant information on the control of the glycolytic flux. In both cases, the enzymes traditionally considered the rate-limiting steps, HK, ATP-PFK-1, and PYK did not contribute to the flux control, whereas the main control resided in GLUT (54% in the parasite and 85–100% in yeast). Under some conditions, HK may exert some control (15%) in *S. cerevisiae* and some nonallosteric enzymes such as ALDO, GAPDH, and PGK may also exert some flux control in *T. brucei*.

MCA through kinetic modeling has been applied to several pathways:

(i) glycolysis in erythrocytes [84] in which flux control distributes between HK (71%) and PFK-1 (29%);

(ii) carbohydrate metabolism during differentiation in *Dictyostelium discoideum* [127] with cellulose synthase (86%) as the main controlling step;

(iii) sucrose accumulation in sugar cane with HK, invertase, fructose uptake, glucose uptake, and vacuolar sucrose transporter having the most significant flux control [128];

(iv) glycerol synthesis in *S. cerevisiae* with GAPDH (85%) as the main control step [129];

(v) penicillin synthesis in *Penicillium chrysogenum* controlled (75–98%) either by d-(a-aminoadipyl) cysteinylvaline synthetase (short incubation times <30 hour) or isopenicillin N. synthetase (long incubation times > 100 h) [130];

(vi) Calvin cycle [131] controlled by GAPDH (50%) and sedoheptulose-1,7-bisphosphatase (50%);

(vii) threonine synthesis in *E. coli* controlled by homoserine dehydrogenase (46%), aspartate kinase (28%), and aspartate semialdehyde dehydrogenase (25%) [111];

(viii) lysine production in *Corynebacterium glutamicum* mainly controlled by aspartate kinase and permease [132];

(ix) nonoxidative pentose pathway in erythrocytes mainly controlled by transketolase (74%) [133];

(x) EGF-induced MAPK signaling in tumor cells controlled by Ras-activation by EGF (21%), Ras dephosphorylation (43%), ERK phosphorylation by MEK (44%), and MEK phosphorylation by RAS (143%) [13];

(xi) *Aspergillus niger* arabinose utilization with flux control shared by arabinose reductase (68%), arabitol dehydrogenase (17%), and xylulose reductase (14%) [134];

(xii) glycolysis in *L. lactis* in which several end products are generated (lactate, organic acids, ethanol, acetoin) [135]. Model predictions indicated that flux toward diacetyl and acetoin (important flavor compounds) was mainly controlled by LDH but not by acetolactate synthetase, the first enzyme of this branch.

We modeled the GSH and PCs biosynthesis (Figure 2) to determine and understand the control structure of the pathway and thus be able to identify potential sites for genetic engineering manipulation that might lead to the generation of improved species in heavy metal resistance and accumulation. Two models were constructed, one for higher plants and the other for yeast, both exposed to high concentrations of Cd^{2+} [136]. Due to the similarity in the results, only the plant results are analyzed below.

An interesting conclusion from the GSH-PCs synthesis modeling is that control of flux (and GSH concentration) is shared between the GSH supply and demand under both unstressed and Cd^{2+} exposure conditions (Table 4). This observation strongly differs from the idea that γ-ECS is the rate-limiting step [33–35]. For many researchers, the concept of γ-ECS being the key controlling step has seemed to be correct because (a) γ-ECS receives information from the final part of the pathway, as it is potently inhibited by GSH, the pathway end-product; and (b) γ-ECS is localized in the first part of the pathway (Figure 2). In addition, GS is usually more abundant and efficient than γ-ECS [137].

However, in most of the studies on the control of GSH synthesis, the GSH demand has not been considered. The GSH synthesis modeling shows that under a physiological feedback inhibition of γ-ECS by GSH a small increase in demand increases flux because the GSH concentration decreases and the γ-ECS inhibition attenuates. In contrast, if the demand remains constant, then an increase in γ-ECS activity or content (by overexpression) does not increase flux because the GSH inhibition is still there and operates on both new and old enzymes. The same pattern is also observed when HK is overexpressed to increase glycolytic flux since it is still inhibited by G6P (see Section 3). On the other hand, γ-ECS indeed exerts significant concentration control on GSH, which means that a γ-ECS increase results in higher GSH concentration (Table 4). This last observation demonstrates

Table 4: Control of GSH and PC synthesis in plants exposed to Cd^{2+}.

Enzyme	1x γ-ECS + PCS				2.5x γ-ECS + PCS			
	C_{vi}^{JGSH}	C_{vi}^{JPC}	C_{vi}^{GSH}	C_{vi}^{PC}	C_{vi}^{JGSH}	C_{vi}^{JPC}	C_{vi}^{GSH}	C_{vi}^{PC}
γ-ECS	0.58	0.60	0.68	0.76	0.45	0.61	0.70	0.60
GS	<0.01	<0.01	0.01	0.01	0.19	<0.01	<0.01	0.97
GS-transferase	0.01	−0.06	−0.07	−0.07	<0.01	<0.01	< −0.01	−0.05
PCS	0.40	0.44	−0.63	−0.56	0.33	0.44	−0.62	0.57
vacuole PC-Cd transporter	<0.01	<0.01	<0.01	−1.2	<0.01	<0.01	<0.01	−2.1

C_{vi}^{JGSH}, control coefficient of enzyme i in GSH synthesis; C_{vi}^{JPC}, control coefficient of enzyme Ei on PCs synthesis; C_{vi}^{GSH}, control coefficient of enzyme i on GSH concentration; C_{vi}^{PC}, control coefficient of enzyme i on PCs concentration. An enzyme with a negative flux control indicates that it is localized in a branch, turning aside the principal flux; an enzyme with a negative concentration control indicates that an increase in its activity decreases metabolite concentration.

that an enzyme controlling a metabolite concentration does not necessarily control the flux.

Cd^{2+} exposure promotes a high GSH demand because significant oxidative stress surges, thus causing oxidation of GSH through GSH peroxidases, and because GSH and PCs are used for sequestering the toxic metal ion; hence, a higher GSH consuming rate sets up. Under this condition, modeling predicted that control was almost equally shared between the supply and demand blocks, but particularly between γ-ECS and PCS (see Figure 2). Modeling was also able to explain why PCS overexpression can have toxic effects on the cell [36]. An increase in the GSH demand (PCS overexpression) under high-demand conditions (Cd^{2+} stress) leads to GSH depletion that severely compromises other processes such as the oxidative stress control and xenobiotic detoxification.

The conclusions drawn by this model led us to propose that, to significantly increase the Cd^{2+} resistance and accumulation, γ-ECS and PCS should be simultaneously overexpressed (Table 4; Figure 9). This particular manipulation promotes an increase in the rate of GSH and PCs synthesis (determined by the high-to-low transition of their flux control coefficients) and in the GSH and PCs concentrations (determined by their high concentration control coefficients). The model predicts that a 2-fold increase in the simultaneous overexpression of γ-ECS and PCS brings about a 1.9–2.4-fold increase in flux to GSH (J_{GS}) and PCs (J_{PCS}) and in PCs concentration (Figure 9); a 5-fold overexpression further increases by 4.5–8.1 times the fluxes and PCs concentration.

This proposed enzyme overexpression should not exceed the GS and the complex PC-Cd (or GS-Cd-GS) vacuolar transporters' maximal activities, in order to keep the cell away from a severe oxidative stress caused by GSH depletion or γ-EC accumulation. Indeed, the concentration of GSH was maintained high and constant although γ-EC accumulated with the simultaneous overexpression (Figure 9). Furthermore, this enzyme manipulation should avoid the increase of the PC-Cd and GS-Cd-GS complexes in cytosol to toxic levels. In other words, excessive enzyme overexpression should be avoided, unless this is accompanied by compensating overexpression of consuming enzymes (GS for γ-ECS overexpression and PCs vacuolar transporters for that of PCS). In yeasts and plants, Cd^{2+} is ultimately inactivated by the additional interaction with S^{2-} and the subsequent

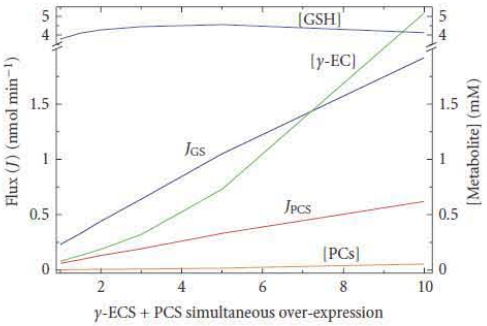

Figure 9: Modeled simultaneous overexpression of two controlling enzymes, one in the supply (γ-glutamylcisteine synthetase, γ-ECS) and the other in the demand branch (phytochelatin synthase, PCS), of the glutathione and phytochelatins synthesis pathway in plants.

formation of stable high molecular weight complexes with PCs, Cd^{2+}, S^{2-}, and GSH [138, 139]. In parallel to the γ-ECS and PCS overexpression, moderate repression of GSH-S-transferases, which compete for the available GSH (Figure 2), may also promote an increase in GSH concentration and PCs formation flux [136].

MCA is based on infinitesimal changes in an enzyme or metabolite concentration. In contrast, gene overexpression induces large changes in activity; hence, further theoretical background has been developed for predicting the effect on flux and metabolite concentrations induced by large enzyme changes. Such a theoretical background was initially developed by Small and Kacser [140], who depicted (12) based on the flux control coefficients to predict the effect promoted by large changes in enzyme activity:

$$f_{E_{j\to m}^r}^J = \frac{1}{1 - \sum_{i=j}^{m} \left(C_{v_{i0}}^{J_o} \bullet (r_i - 1)/r_i\right)}, \tag{12}$$

in which f is the amplification factor (the flux increase), and r represents how many times the enzyme is overexpressed. To predict the flux changes, promoted by identical

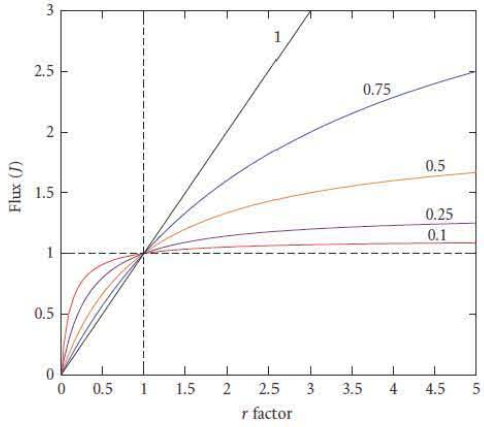

FIGURE 10: Effect on flux when one or more enzymatic activities with different control coefficients are varied. This figure represents an enzyme or group of enzymes in which their $C^J_{v_i}$ sum is indicated in parenthesis and is modified by the same r factor. Number 1 represents the reference control, thus if $r < 1$, there is suppression, whereas $r > 1$ represents overexpression.

overexpression of two enzymes (same r value) with different $C^J_{v_i}$, the equation is

$$f^J_{E^r_{j-m}} = \frac{1}{1 - (C^J_i + C^J_j) \bullet ((r-1)/r)}. \quad (13)$$

Figure 10 shows the effect on flux when one or more enzymes with different $C^J_{v_i}$ are changed by the same r factor. If the sum of $C^J_{v_i}$ of one or more enzymes is less than 0.25, the impact on flux is discrete when the expression increases 5 folds (which is the most common variation in the overexpression experiments analyzed in Section 2). But for a 3-fold overexpression of a group of enzymes, for which their sum of $C^J_{v_i}$ is more than 0.5, then a significant flux change is achieved. If the sum of $C^J_{v_i}$ is 1, the flux varies in a linear proportion with the degree of overexpression. It has to be remarked, however, that the predicted change in flux (Figure 10) will be valid until certain degree, the limits of which being determined by the other pathway enzymes that should stay as noncontrolling steps.

Figure 10 also shows the effect on flux of decreasing an enzyme activity (third quadrant). This segment plot is useful when inhibition of pathway flux is being pursued for therapeutic purposes or for understanding the molecular basis of the genetic dominance and recessivity. Like in the enzyme overexpression experiment, only a significant effect on flux is achieved when the enzymes with high $C^J_{v_i}$ values are inhibited. For an enzyme or group of enzymes with $C^J_{v_i}$ of 0.25, greater than 80% inhibition has to be attained to decrease 50% the pathway flux. In this context, it seems feasible to explain why knockdown of enzymes involved in TSH_2 synthesis has to be almost total to detect an effect on TSH_2 content or to alter functional or pathogenic properties of the parasites (Section 4.3). The knockdown or knockout experiments in trypanosomatids suggest that γ-ECS, TryS, and TryR most probably have low flux control and concentration-control coefficients since their contents or activities have to be reduced >80% of the normal levels to reach changes in intermediary levels or in oxidative stress handling.

Contrary to the several unsuccessful overexpression experiments carried out to increase the flux or metabolites of a metabolic pathway, modeling may allow for a more focused and appropriate design of experimental strategies of genetic engineering to increase flux or a given metabolite, and for selecting drug targets to decrease flux or metabolite concentration. For these predictions, modeling considers that overexpression of a controlling enzyme or transporter may promote flux or metabolite control redistributions. Thus, a low-control step may become a controlling point when overexpressing another step and, in consequence, the prediction shown in Figure 10 based on (11) and (12) may be inaccurate. By considering the whole pathway components, modeling is also a powerful tool for predicting the effects on flux and metabolite concentration of varying an enzyme activity (by overexpression or drug inhibition).

Model predictions to inhibit a pathway flux

Kinetic modeling has been used to identify the flux controlling steps in *Trypanosoma brucei* glycolysis for drug targeting purposes. Interestingly, modeling has predicted controlling steps for the parasite pathway different from those described for glycolysis in human host cells [125, 126].

Entamoeba histolytica is the causal agent of human amebiasis. The parasite lacks functional mitochondria and has neither Krebs cycle nor OXPHOS enzyme activities. Therefore, substrate level phosphorylation by glycolysis is the only way to generate ATP for cellular work [141]. An important difference in amebal glycolysis in comparison to glycolysis in human cells is that it contains the pyrophosphate (PPi)-dependent enzymes phosphofructokinase (PPi-PFK) and pyruvate phosphate dikinase (PPDK), which replace the highly modulated ATP-PFK and PYK present in human cells. Moreover, both have been proposed as drug targets by using PPi analogues (bisphosphonates) [141].

We recently described the construction of a kinetic model of *E. histolytica* glycolysis to determine the control distribution of this energetically important pathway in the parasite [142]. The model was constructed using the Gepasi software and was based on the kinetic parameters determined in the purified recombinant enzymes [143], as well as the enzyme activities, fluxes, and metabolite concentrations found in the parasite. The results of the metabolic control analysis indicated that HK and PGAM are the main flux control steps of the pathway (73 and 65%, resp.) and perhaps GLUT. In contrast, the PPi-PFK and PPDK displayed low flux control (13 and 0.1%, resp.) because they have overcapacity over the glycolytic flux [142]. The amebal model allowed evaluating the effect on flux of "inhibiting" the pathway enzymes. The model predicted that

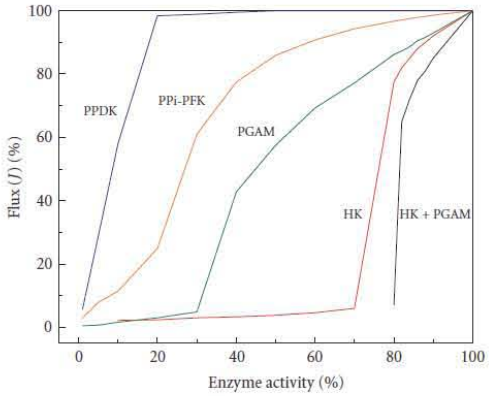

FIGURE 11: Modeled flux behavior when inhibiting pathway enzymes. The predicted flux when varying the enzyme activity was obtained using the kinetic model for *Entamoeba histolytica* glycolysis [142]. In this case, 100% enzyme activity is the enzyme activity present in amebal extracts, and 100% flux is the ethanol flux displayed by amoebae incubated with glucose. PPi-PFK, PPi-dependent phosphofructokinase; PPDK, pyruvate phosphate dikinase; PGAM, 2,3 bisphosphoglycerate independent 3-phosphoglycerate mutase.

in order to diminish by 50% the glycolytic flux (and the ATP concentration; data not shown), HK and PGAM should be inhibited by 24 and 55%, respectively, or both enzymes by 18% (Figure 11). In contrast, to attain the same reduction in flux by inhibiting PPi-PFK and PPDK, they should be decreased >70% (Figure 11). Therefore, the kinetic model results indicate that HK can be an appropriate drug target because its specific inhibition can compromise the energy levels in the parasite. They also indicate that although PPi-PFK and PPDK remain as promising drug targets because of their divergence from the human glycolytic enzymes, highly potent and very specific inhibitors should be designed for these enzymes in order to affect the parasite's energy metabolism.

5.5. *In vitro reconstitution of metabolic pathways*

Another experimental approach for determining the enzyme control coefficients is the in vitro reconstitution of segments of metabolic pathways. It is recalled that for determining the flux control coefficient exerted by a given step on a metabolic pathway the enzyme activity has to be varied, without altering the other components in the system, and the flux variations are to be measured (Figure 4). Such an experiment can be readily made if a pathway is reconstituted with purified enzymes. Some advantages of this approach are that the pathway structure is known, in which the components concentration may be manipulated and analyzed separately, and the enzyme effectors can be assayed. As the system composition is strictly controlled, the results may be highly reproducible. The main disadvantage is that the enzyme concentrations in the assays are diluted and thus the enzyme interactions are not favored. If this interaction is important for activity, the in vitro reconstitution may limit the extrapolation to the metabolic pathway inside the cell.

There are not many studies describing this type of experiments, most probably due to the fact that for applying MCA the pathway must be working under steady-state conditions. In a reconstituted system, only a quasi steady state may be reached because there is net substrate, and cofactors consumption, as well as product accumulation, since it is difficult to attain a constant substrate supply and release of products.

One of the first experimental reports on control coefficient determination in a reconstituted system was carried out for the upper glycolytic segment with the commercially available rabbit muscle HK, HPI, PFK-1, ALDO, and TPI [144]. Each enzyme was separately titrated and the flux variation to glycerol-3-phosphate (by coupling the reconstituted system to an excess of α-GPDH) was measured in the presence of CK to maintain the ATP concentration constant. The flux control coefficients were determined as described in Figure 4. The results showed that PFK-1 and HK exerted the main flux control (65% and 20%, resp.), whereas the remaining 15% resided in the other enzymes. These authors observed that the addition of F1,6BP, a PFK-1 activator slightly diminished the flux control exerted by PFK-1 and increases that of HK. The validation of the summation theorem was also demonstrated in this work [144].

The lower glycolytic segment has also been reconstituted with commercial enzymes for determining the flux control coefficients [145]. The results showed that flux was mainly controlled by PYK (60–100%), although under some conditions control was shared with PGAM; ENO did not contribute to the flux control.

Another important limitation of the reconstitution experiments is that the commercial availability of the purified enzymes from the same organism is restricted or inexistent. However, by using the information from the genome sequence projects and the recombinant DNA technology, it is now possible to access all the enzyme genes from a metabolic pathway in the same organism, thus facilitating their cloning, overexpression, and purification. With this strategy, we cloned, overexpressed, and purified the 10 glycolytic enzymes of *Entamoeba histolytica* [143] for studying the flux control distribution in this organism by using kinetic modeling [142] and pathway reconstitution.

The reconstitution experiments of the lower amebal glycolytic segment, under near physiological conditions of pH, temperature, and enzyme activity (Figure 12) showed that PGAM and, to a lesser extent, PPDK exert the main flux control (these amebal enzymes are genetically and kinetically different from their human counterparts) with ENO exhibiting negligible control [143]. In turn, reconstitution of the upper amebal glycolytic segment has revealed that HK and, to a much lesser extent HPI, PPi-PFK, and ALD, exerted the main flux control, with TPI having negligible control [146]. These results strongly correlate with the enzyme catalytic efficiencies previously reported [143], in which HK is highly sensitive to AMP inhibition, ALD, and PGAM

have the lowest catalytic efficiencies among the glycolytic enzymes, leading to high flux control coefficients and thus becoming suitable candidates for therapeutic intervention. The reconstitution results also agree with the pathway modeling predictions previously analyzed (Section 5.4), in which HK and PGAM are two of the main controlling steps [142].

The in vitro reconstitution experiments are also useful for studying the effect on control redistribution of an enzyme modulation that is particularly difficult to manage in vivo; the main controlling steps identified with the reconstitution experiments should be further analyzed with other experimental strategies such as elasticity analysis in the in vivo systems.

5.6. Genetic engineering to manipulate the in vivo protein levels

This experimental approach for determining the control coefficients could be part of the genetic approach analyzed in Section 5.1, but it was separated due to its recent methodological development and because it actually belongs to the molecular genetics rather than to the Mendelian genetics.

5.6.1. Repression of gene expression

This approach is based on the in vivo modulation of the enzyme levels using the RNA antisense technology. There are at least three strategies to inhibit gene expression: (a) the use of single stranded antisense oligonucleotides, which form a double stranded RNA that might be degraded by RNAse H; (b) target RNA degradation with catalytically active oligonucleotides, known as ribozymes that bind to their specific RNA; and (c) RNA degradation using siRNAs (21–23 nucleotides) [147].

The RNA antisense technology was applied for control coefficient determination of the ribulose-bisphosphate-carboxylase (Rubisco) that fixes CO_2 in the plant Calvin cycle. This enzyme considered the rate-limiting step of the Calvin cycle and of the whole photosynthetic process, despite its high concentration (4 mM) in the chloroplasts stroma that compensates its low catalytic efficiency.

Attempts to make Rubisco a nonlimiting step, either by modifying its catalytic efficiency or by overexpressing it, have been unsuccessful. Stitt et al. [148] determined the $C^{J\text{photosynthesis}}_{\text{rubisco}}$ of tobacco plants by decreasing its activity with DNA antisense. The plants were transformed with DNA antisense against the mRNA of the enzyme's small subunit, thus promoting its degradation. For Calvin cycle enzymes, the pleiotropic effects were minimal. The results showed that Rubisco may indeed be the photosynthesis limiting step with a $C^{J\text{photosynthesis}}_{\text{rubisco}} = 0.69$–$0.83$ when plants are exposed to high illumination ($1050\,\mu$mol quanta $m^{-2}s^{-1}$), high humidity (85%), and low CO_2 concentrations (25 Pa). However, this flux control decreases to 0.05–0.12 under moderate illumination or high CO_2 levels [148]. Unfortunately, the authors did not determine the control coefficients of the other pathway enzymes or the branches fluxes which may be significant.

As described in Section 5.4, the results of the *T. brucei* glycolysis modeling indicated that GLUT was the main flux control step ($C^{J}_{\text{GLUT}} \sim 50\%$), [125, 126]. This model predicted a large overcapacity for HK, PFK-1, ALDO, GAPDH, PGAM, ENO, and PYK over the glycolytic flux leading to low flux control coefficients [125, 126]. To validate the modeling results, the concentrations of HK, PFK-1, PGAM, ENO, and PYK were changed with siRNAs in growing parasites [149]. These knockdown expression experiments showed overcapacity of HK and PYK over the flux, although at lower levels than predicted by the model. A good correlation for PGAM and ENO was obtained between model predictions and experimental results. However, a large difference (9 folds) was obtained for PFK-1. This discrepancy is perhaps related to pleiotropic effects of PFK-1 downregulation, as these mutants also displayed diminution in the activities of other enzymes (HK, ENO, and PYK). The combination of these two approaches, in silico modeling and in vivo experimentation, is complementary: on one hand, modeling identifies the enzymes (out of 19 that contain the model) that display the highest flux control coefficients, whereas in vivo experimentation validates the accuracy of the model to establish predictions about the pathway's behavior.

5.6.2. Fine tuning of cellular protein expression

The knockdown experiments described above usually yield only two experimental points of the plot shown in Figure 4: the wild-type and the knockdown strain protein levels or enzyme activities. Thus, with such an approach high levels of inhibition (>80%) are mostly analyzed, whereas intermediate levels of downregulation (if obtained) are generally overlooked. Therefore, knockdown experiments are not very useful to obtain the complete set of experimental data (above and below the wild-type levels of enzyme activity with the corresponding flux) for determining reliable control coefficients.

A strategy to determine flux control coefficients from several protein levels has been developed by using adenovirus-mediated glucose-6-phosphatase (G6Pase) overexpression under the control of the cytomegalovirus promoter in rat hepatocytes. A 2-fold G6Pase overexpression did not alter $C^{\text{Glycolysis}}_{\text{G6Pase}}$ or $C^{\text{Glycolysis}}_{\text{GK}}$ (GK, glucokinase). However, if G6Pase is overexpressed by 4 folds, then $C^{\text{Glycogen-synthesis}}_{\text{GK}}$ diminished from 2.8 to 1.8 and there was a 35% lowering in glycogen synthesis [150]. However, this approach allows titration of flux only above the basal enzyme activities found in the cell, but not below.

These experimental inconveniences have been circumvented by using inducible gene expression systems based in the *lac*, Lambda, nisin, GAL, tetracycline, and other inducible promoters, in bacteria and yeast [151, 152]. However, a problem frequently encountered with inducible promoters is that a steady-state of protein expression is difficult to attain [151, 152].

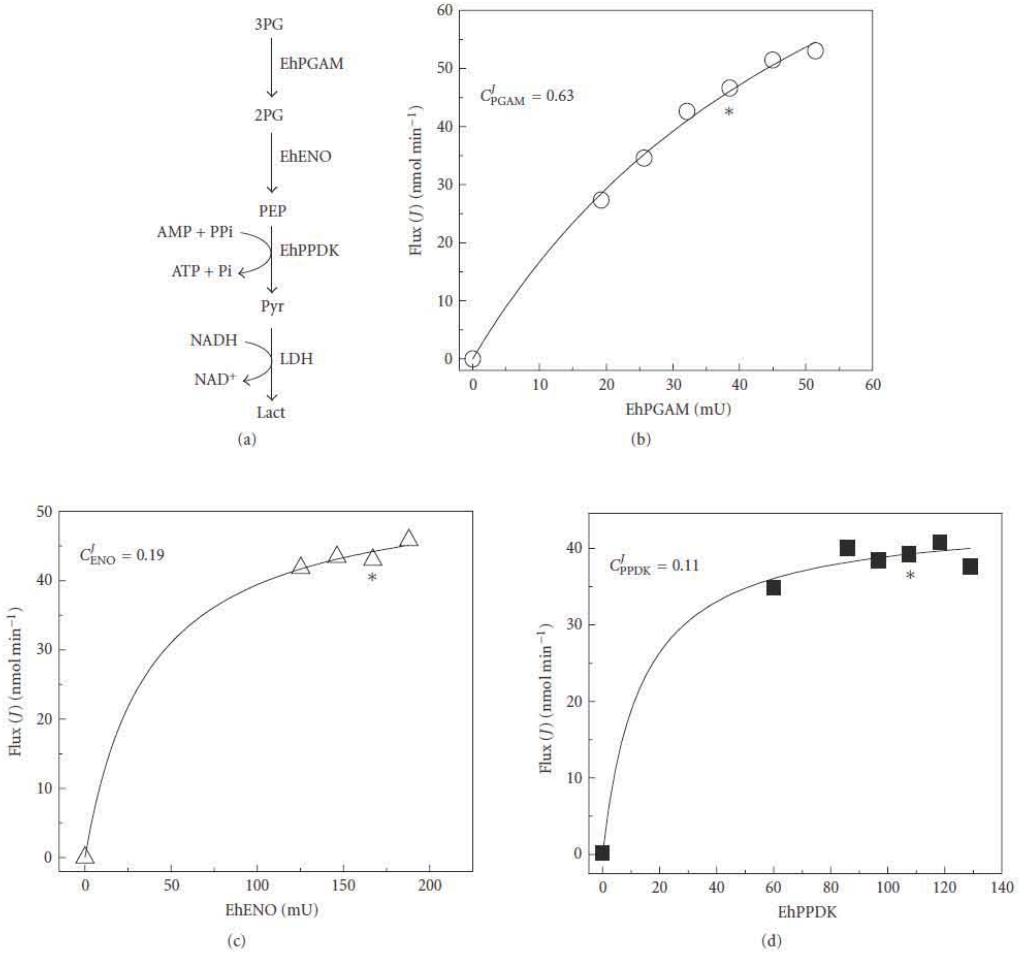

Figure 12: Determination of flux control coefficients in an in vitro reconstitution of the final section of *Entamoeba histolytica* glycolysis. Enzymatic assay with the three recombinant enzymes from the ameba: EhPGAM, EhENO, and EhPPDK. LDH, commercial lactate dehydrogenase. The flux control coefficient was determined at the *marked position. 2PG, 2-phosphoglycerate; 3PG, 3-phosphoglycerate. Modified from [143].

Recently, Jensen and Hammer described the design of synthetic promoter libraries (SPL), in particular for *L. lactis* metabolic optimization [153]. These promoters maintain constant the array of the known consensus sequences for *L. lactis* gene transcription (−10 and −35 boxes), while the nucleotide sequence between these boxes (a spacer sequence of 17 ± 1 bp) is randomized, thus producing a set of promoters with different transcriptional strength. These promoter libraries allow the transcription and protein expression several folds above and below the wild-type levels of enzyme activity [153], thus enhancing the usefulness of this approach for MCA studies.

The control distribution of glycolysis in *E. coli* and *L. lactis*, as discussed in Section 3.2 [17, 24, 27, 151], has been determined by using the SPL technology. SPL for yeast, mammalian and plant cells are also under development [151, 152]. Certainly, the advances in genetic engineering in combination with MCA allow better experimental designs for metabolic optimization of micro-organisms of biotechnological interest.

Concluding remarks

(1) The frequently recurred idea of manipulating the key enzyme or rate-limiting step (a concept based on a qualitative and rather intuitive background) to change metabolism is incorrect. As MCA has demonstrated, flux control is shared by multiple steps and it is not usually localized in only one step. MCA determines quantitatively the control that a given enzyme exerts on the flux and on intermediary concentration and helps to explain why an enzyme does or does not exert control.

(2) A metabolic pathway is manipulated to change the rate of the end-product formation (i.e., the flux) or the concentration of a relevant intermediary. As it is demonstrated in many unsuccessful experiments, it is not enough to overexpress one enzyme (the rate-limiting step) or many arbitrarily selected sites of the pathway. MCA proposes an initial experimental analysis that determines the structural control of the pathway and identifies the sites (enzymes and transporters) with higher control coefficients values (i.e., targets to be manipulated). For example, if there is a system composed of six enzymes and three of them have flux control coefficients with values of 0.2 or higher and the other three with values of 0.1 or lower, the three enzymes with high control coefficients must be overexpressed (if a flux increase is desired) or repressed (if flux inhibition is the objective) and not only one of them. If one of the selected enzymes is strongly inhibited by its product or has allosteric inhibition, the overexpression of this enzyme might not be enough to increase the flux, as it may also be necessary to moderately vary the product and allosteric modulator consuming enzymes.

(3) If the aim of the researcher is a metabolite concentration increase, which is not the end product of the pathway, MCA suggests the overexpression of those enzymes or transporters in the supply block with the highest control coefficients and/or the repression of those enzymes in the demand block with the highest control coefficients. These manipulations may become complicated if the metabolite of interest has allosteric interactions with enzymes and transporters (inhibition and activation) of both the supply and demand blocks. It is recalled that ethanol production in yeast and lactate and acetate production in lactobacteria do not increase by overexpressing PFK-1, an allosteric enzyme and the presumed rate-limiting step of glycolysis. In fact, the flux was diminished with an excessive PFK-1 overexpression. However, the analysis of these results reveals that the F1,6BP concentration is indeed increased many times over the control level. Another strategy for eliminating the feedback inhibition might be the introduction of mutations on the enzymes that are closer to the metabolite of interest.

ABBREVIATIONS

ADH:	alcohol dehydrogenase
CK:	creatine kinase
ENO:	enolase
GAPDH:	glyceraldehyde-3 phosphate dehydrogenase
HPI:	hexose phosphate isomerase
LDH:	lactate dehydrogenase
PDC:	pyruvate decarboxylase
PGK:	phosphoglucokinase
PGAM:	phosphoglycerate mutase
TPI:	triose phosphate isomerase
PPi-PFK:	pyrophosphate-dependent phosphofructokinase
α-GPDH:	α-glycerophosphate dehydrogenase
F6B:	fructose-6-phosphate
F1,6BP:	fructose-1,6-bisphosphate
G1P:	glucose-1-phosphate
G6P:	glucose-6-phosphate
GSH:	reduced glutathione
γ-EC:	γ-glutamylcysteine
MCA:	metabolic control analysis
siRNA:	small interfering RNA.

ACKNOWLEDGMENT

The present work was partially supported by CONACyT-Mexico Grants no. 60517 to RMS and 46719-Q to ES.

REFERENCES

[1] E. A. Newsholme and C. Start, *Regulation of Metabolism*, John Wiley & Sons, London, UK, 1973.

[2] D. Fell, *Understanding the Control of Metabolism*, Portland Press, London, UK, 1997.

[3] M. David, I. R. Rasched, and H. Sund, "Studies of glutamate dehydrogenase. Methionine-169: the preferentially carboxymethylated residue," *European Journal of Biochemistry*, vol. 74, no. 2, pp. 379–385, 1977.

[4] H. Teng, E. Segura, and C. Grubmeyer, "Conserved cysteine residues of histidinol dehydrogenase are not involved in catalysis. Novel chemistry required for enzymatic aldehyde oxidation," *Journal of Biological Chemistry*, vol. 268, no. 19, pp. 14182–14188, 1993.

[5] T. N. C. Wells, M. A. Payton, and A. E. Proudfoot, "Inhibition of phosphomannose isomerase by mercury ions," *Biochemistry*, vol. 33, no. 24, pp. 7641–7646, 1994.

[6] B. Poolman, B. Bosman, J. Kiers, and W. N. Konings, "Control of glycolysis by glyceraldehyde-3-phosphate dehydrogenase in *Streptococcus cremoris* and *Streptococcus lactis*," *Journal of Bacteriology*, vol. 169, no. 12, pp. 5887–5890, 1987.

[7] R. Moreno-Sánchez and M. E. Torres-Márquez, "Control of oxidative phosphorylation in mitochondria, cells and tissues," *International Journal of Biochemistry*, vol. 23, no. 11, pp. 1163–1174, 1991.

[8] K. A. Webster, "Evolution of the coordinate regulation of glycolytic enzyme genes by hypoxia," *Journal of Experimental Biology*, vol. 206, no. 17, pp. 2911–2922, 2003.

[9] J. Heinisch, "Isolation and characterization of the two structural genes coding for phosphofructokinase in yeast,"

Molecular and General Genetics, vol. 202, no. 1, pp. 75–82, 1986.

[10] S. E. C. Davies and K. M. Brindle, "Effects of overexpression of phosphofructokinase on glycolysis in the yeast *Saccharomyces cerevisiae*," *Biochemistry*, vol. 31, no. 19, pp. 4729–4735, 1992.

[11] J. Hauf, F. K. Zimmermann, and S. Müller, "Simultaneous genomic overexpression of seven glycolytic enzymes in the yeast *Saccharomyces cerevisiae*," *Enzyme and Microbial Technology*, vol. 26, no. 9-10, pp. 688–698, 2000.

[12] I. Schaaff, J. Heinisch, and F. K. Zimmermann, "Overproduction of glycolytic enzymes in yeast," *Yeast*, vol. 5, no. 4, pp. 285–290, 1989.

[13] J. J. Hornberg, B. Binder, F. J. Bruggeman, B. Schoeberl, R. Heinrich, and H. V. Westerhoff, "Control of MAPK signalling: from complexity to what really matters," *Oncogene*, vol. 24, no. 36, pp. 5533–5542, 2005.

[14] H. P. Smits, J. Hauf, S. Müller, et al., "Simultaneous overexpression of enzymes of the lower part of glycolysis can enhance the fermentative capacity of *Saccharomyces cerevisiae*," *Yeast*, vol. 16, no. 14, pp. 1325–1334, 2000.

[15] M. Emmerling, J. E. Bailey, and U. Sauer, "Glucose catabolism of *Escherichia coli* strains with increased activity and altered regulation of key glycolytic enzymes," *Metabolic Engineering*, vol. 1, no. 2, pp. 117–127, 1999.

[16] M. Emmerling, J. E. Bailey, and U. Sauer, "Altered regulation of pyruvate kinase or co-overexpression of phosphofructokinase increases glycolytic fluxes in resting *Escherichia coli*," *Biotechnology and Bioengineering*, vol. 67, no. 5, pp. 623–627, 2000.

[17] C. Solem, B. J. Koebmann, and P. R. Jensen, "Glyceraldehyde-3-phosphate dehydrogenase has no control over glycolytic flux in *Lactococcus lactis* MG1363," *Journal of Bacteriology*, vol. 185, no. 5, pp. 1564–1571, 2003.

[18] G. J. G. Ruijter, H. Panneman, and J. Visser, "Overexpression of phosphofructokinase and pyruvate kinase in citric acid-producing *Aspergillus niger*," *Biochimica et Biophysica Acta*, vol. 1334, no. 2-3, pp. 317–326, 1997.

[19] A. M. Urbano, H. Gillham, Y. Groner, and K. M. Brindle, "Effects of overexpression of the liver subunit of 6-phosphofructo-1-kinase on the metabolism of a cultured mammalian cell line," *Biochemical Journal*, vol. 352, part 3, pp. 921–927, 2000.

[20] B. M. Bonini, P. Van Dijck, and J. M. Thevelein, "Uncoupling of the glucose growth defect and the deregulation of glycolysis in *Saccharomyces cerevisiae tps1* mutants expressing trehalose-6-phosphate-insensitive hexokinase from *Schizosaccharomyces pombe*," *Biochimica et Biophysica Acta*, vol. 1606, no. 1–3, pp. 83–93, 2003.

[21] J. Rivoal and A. D. Hanson, "Metabolic control of anaerobic glycolysis. Overexpression of lactate dehydrogenase in transgenic tomato roots supports the Davies-Roberts hypothesis and points to a critical role for lactate secretion," *Plant Physiology*, vol. 106, no. 3, pp. 1179–1185, 1994.

[22] S. Thomas, P. J. F. Mooney, M. M. Burrell, and D. A. Fell, "Metabolic control analysis of glycolysis in tuber tissue of potato (*Solanum tuberosum*): explanation for the low control coefficient of phosphofructokinase over respiratory flux," *Biochemical Journal*, vol. 322, part 1, pp. 119–127, 1997.

[23] R. M. O'Doherty, D. L. Lehman, J. Seoane, A.M. Gómez-Foix, J. J. Guinovart, and C. B. Newgard, "Differential metabolic effects of adenovirus-mediated glucokinase and hexokinase I overexpression in rat primary hepatocytes," *Journal of Biological Chemistry*, vol. 271, no. 34, pp. 20524–20530, 1996.

[24] H. W. Andersen, M. B. Pedersen, K. Hammer, and P. R. Jensen, "Lactate dehydrogenase has no control on lactate production but has a strong negative control on formate production in *Lactococcus lactis*," *European Journal of Biochemistry*, vol. 268, no. 24, pp. 6379–6389, 2001.

[25] B. J. Koebmann, C. Solem, and P. R. Jensen, "Control analysis as a tool to understand the formation of the *las* operon in *Lactococcus lactis*," *FEBS Journal*, vol. 272, no. 9, pp. 2292–2303, 2005.

[26] B. J. Koebmann, H. V. Westerhoff, J. L. Snoep, D. Nilsson, and P. R. Jensen, "The glycolytic flux in *Escherichia coli* is controlled by the demand for ATP," *Journal of Bacteriology*, vol. 184, no. 14, pp. 3909–3916, 2002.

[27] B. J. Koebmann, H. W. Andersen, C. Solem, and P. R. Jensen, "Experimental determination of control of glycolysis in *Lactococcus lactis*," *Antonie van Leeuwenhoek*, vol. 82, no. 1–4, pp. 237–248, 2002.

[28] B. J. Koebmann, C. Solem, M. B. Pedersen, D. Nilsson, and P. R. Jensen, "Expression of genes encoding F_1-ATPase results in uncoupling of glycolysis from biomass production in *Lactococcus lactis*," *Applied and Environmental Microbiology*, vol. 68, no. 9, pp. 4274–4282, 2002.

[29] S. Thomas and D. A. Fell, "A control analysis exploration of the role of ATP utilisation in glycolytic-flux control and glycolytic-metabolite-concentration regulation," *European Journal of Biochemistry*, vol. 258, no. 3, pp. 956–967, 1998.

[30] J.-H. S. Hofmeyr and A. Cornish-Bowden, "Regulating the cellular economy of supply and demand," *FEBS Letters*, vol. 476, no. 1-2, pp. 47–51, 2000.

[31] D. Mendoza-Cózatl, H. Loza-Tavera, A. Hernández-Navarro, and R. Moreno-Sánchez, "Sulfur assimilation and glutathione metabolism under cadmium stress in yeast, protists and plants," *FEMS Microbiology Reviews*, vol. 29, no. 4, pp. 653–671, 2005.

[32] A. Cornish-Bowden and M. L. Cárdenas, "Information transfer in metabolic pathways. Effects of irreversible steps in computer models," *European Journal of Biochemistry*, vol. 268, no. 24, pp. 6616–6624, 2001.

[33] A. Meister, "Glutathione metabolism," *Methods in Enzymology*, vol. 251, pp. 3–7, 1995.

[34] G. Noctor, A.-C. M. Arisi, L. Jouanin, and C. H. Foyer, "Manipulation of glutathione and amino acid biosynthesis in the chloroplast," *Plant Physiology*, vol. 118, no. 2, pp. 471–482, 1998.

[35] Y. L. Zhu, E. A. H. Pilon-Smits, A. S. Tarun, S. U. Weber, L. Jouanin, and N. Terry, "Cadmium tolerance and accumulation in Indian mustard is enhanced by overexpressing γ-glutamylcysteine synthetase," *Plant Physiology*, vol. 121, no. 4, pp. 1169–1177, 1999.

[36] S. Lee, J. S. Moon, T.-S. Ko, D. Petros, P. B. Goldsbrough, and S. S. Korban, "Overexpression of Arabidopsis phytochelatin synthase paradoxically leads to hypersensitivity to cadmium stress," *Plant Physiology*, vol. 131, no. 2, pp. 656–663, 2003.

[37] E. A. H. Pilon-Smits, S. Hwang, C. Mel Lytle, et al., "Overexpression of ATP sulfurylase in Indian mustard leads to increased selenate uptake, reduction, and tolerance," *Plant Physiology*, vol. 119, no. 1, pp. 123–132, 1999.

[38] Y. Hatzfeld, N. Cathala, C. Grignon, and J.-C. Davidian, "Effect of ATP sulfurylase overexpression in bright yellow 2 tobacco cells: regulation of ATP sulfurylase and So_4^{2-} transport activities," *Plant Physiology*, vol. 116, no. 4, pp. 1307–1313, 1998.

[39] K. Saito, M. Kurosawa, K. Tatsuguchi, Y. Takagi, and I. Murakoshi, "Modulation of cysteine biosynthesis in chloroplasts of transgenic tobacco overexpressing cysteine synthase [*O*-acetylserine(thiol)-lyase]," *Plant Physiology*, vol. 106, no. 3, pp. 887–895, 1994.

[40] K. Harms, P. von Ballmoos, C. Brunold, R. Höfgen, and H. Hesse, "Expression of a bacterial serine acetyltransferase in transgenic potato plants leads to increased levels of cysteine and glutathione," *The Plant Journal*, vol. 22, no. 4, pp. 335–343, 2000.

[41] Y. Inoue, K.-I. Sugiyama, S. Izawa, and A. Kimura, "Molecular identification of glutathione synthetase (*GSH2*) gene from *Saccharomyces cerevisiae*," *Biochimica et Biophysica Acta*, vol. 1395, no. 3, pp. 315–320, 1998.

[42] S.-J. Kim, Y. H. Shin, K. Kim, E.-H. Park, J.-H. Sa, and C.-J. Lim, "Regulation of the gene encoding glutathione synthetase from the fission yeast," *Journal of Biochemistry and Molecular Biology*, vol. 36, no. 3, pp. 326–331, 2003.

[43] Y. L. Zhu, E. A. H. Pilon-Smits, L. Jouanin, and N. Terry, "Overexpression of glutathione synthetase in Indian mustard enhances cadmium accumulation and tolerance," *Plant Physiology*, vol. 119, no. 1, pp. 73–79, 1999.

[44] G. Creissen, J. Firmin, M. Fryer, et al., "Elevated glutathione biosynthetic capacity in the chloroplasts of transgenic tobacco plants paradoxically causes increased oxidative stress," *The Plant Cell*, vol. 11, no. 7, pp. 1277–1291, 1999.

[45] C. M. Grant, F. H. MacIver, and I. W. Dawes, "Glutathione synthetase is dispensable for growth under both normal and oxidative stress conditions in the yeast *Saccharomyces cerevisiae* due to an accumulation of the dipeptide γ-glutamylcysteine," *Molecular Biology of the Cell*, vol. 8, no. 9, pp. 1699–1707, 1997.

[46] D. F. Ortiz, T. Ruscitti, K. F. McCue, and D. W. Ow, "Transport of metal-binding peptides by HMT1, a fission yeast ABC-type vacuolar membrane protein," *Journal of Biological Chemistry*, vol. 270, no. 9, pp. 4721–4728, 1995.

[47] P. Niederberger, R. Prasad, G. Miozzari, and H. Kacser, "A strategy for increasing an in vivo flux by genetic manipulations: the tryptophan system of yeast," *Biochemical Journal*, vol. 287, part 2, pp. 473–479, 1992.

[48] R. Katsumata and M. Ikeda, "Hyperproduction of tryptophan in *Corynebacterium glutamicum* by pathway engineering," *Nature Biotechnology*, vol. 11, no. 8, pp. 921–925, 1993.

[49] S. Morbach, H. Sahm, and L. Eggeling, "Use of feedback-resistant threonine dehydratases of *Corynebacterium glutamicum* to increase carbon flux towards L-isoleucine," *Applied and Environmental Microbiology*, vol. 61, no. 12, pp. 4315–4320, 1995.

[50] M. A. G. Koffas, G. Y. Jung, J. C. Aon, and G. Stephanopoulos, "Effect of pyruvate carboxylase overexpression on the physiology of *Corynebacterium glutamicum*," *Applied and Environmental Microbiology*, vol. 68, no. 11, pp. 5422–5428, 2002.

[51] L. Padilla, R. Krämer, G. Stephanopoulos, and E. Agosin, "Overproduction of trehalose: heterologous expression of *Escherichia coli* trehalose-6-phosphate synthase and trehalose-6-phosphate phosphatase in *Corynebacterium glutamicum*," *Applied and Environmental Microbiology*, vol. 70, no. 1, pp. 370–376, 2004.

[52] E. Radmacher, A. Vaitsikova, U. Burger, K. Krumbach, H. Sahm, and L. Eggeling, "Linking central metabolism with increased pathway flux: L-valine accumulation by *Corynebacterium glutamicum*," *Applied and Environmental Microbiology*, vol. 68, no. 5, pp. 2246–2250, 2002.

[53] P. Simic, J. Willuhn, H. Sahm, and L. Eggeling, "Identification of *glyA* (encoding serine hydroxymethyltransferase) and its use together with the exporter ThrE to increase L-threonine accumulation by *Corynebacterium glutamicum*," *Applied and Environmental Microbiology*, vol. 68, no. 7, pp. 3321–3327, 2002.

[54] H. W. Wisselink, A. P. H. A. Moers, A. E. Mars, M. H. N. Hoefnagel, W. M. de Vos, and J. Hugenholtz, "Overproduction of heterologous mannitol 1-phosphatase: a key factor for engineering mannitol production by *Lactococcus lactis*," *Applied and Environmental Microbiology*, vol. 71, no. 3, pp. 1507–1514, 2005.

[55] V. Ladero, A. Ramos, A. Wiersma, et al., "High-level production of the low-calorie sugar sorbitol by *Lactobacillus plantarum* through metabolic engineering," *Applied and Environmental Microbiology*, vol. 73, no. 6, pp. 1864–1872, 2007.

[56] C. Solem, B. J. Koebmann, F. Yang, and P. R. Jensen, "The *las* enzymes control pyruvate metabolism in *Lactococcus lactis* during growth on maltose," *Journal of Bacteriology*, vol. 189, no. 18, pp. 6727–6730, 2007.

[57] R. Moreno-Sánchez, S. Rodríguez-Enríquez, A. Marín-Hernández, and E. Saavedra, "Energy metabolism in tumor cells," *FEBS Journal*, vol. 274, no. 6, pp. 1393–1418, 2007.

[58] B. Altenberg and K. O. Greulich, "Genes of glycolysis are ubiquitously overexpressed in 24 cancer classes," *Genomics*, vol. 84, no. 6, pp. 1014–1020, 2004.

[59] D. J. Discher, N. H. Bishopric, X. Wu, C. A. Peterson, and K. A. Webster, "Hypoxia regulates β-enolase and pyruvate kinase-M promoters by modulating Sp1/Sp3 binding to a conserved GC element," *Journal of Biological Chemistry*, vol. 273, no. 40, pp. 26087–26093, 1998.

[60] M. Egea, I. Metón, and I. V. Baanante, "Sp1 and Sp3 regulate glucokinase gene transcription in the liver of gilthead sea bream (*Sparus aurata*)," *Journal of Molecular Endocrinology*, vol. 38, no. 3-4, pp. 481–492, 2007.

[61] B. J. Murphy, G. K. Andrews, D. Bittel, et al., "Activation of metallothionein gene expression by hypoxia involves metal response elements and metal transcription factor-1," *Cancer Research*, vol. 59, no. 6, pp. 1315–1322, 1999.

[62] S. R. Riddle, A. Ahmad, S. Ahmad, et al., "Hypoxia induces hexokinase II gene expression in human lung cell line A549," *American Journal of Physiology*, vol. 278, no. 2, pp. L407–L416, 2000.

[63] M. L. Parolin, L. L. Spriet, E. Hultman, M. G. Hollidge-Horvat, N. L. Jones, and G. J. F. Heigenhauser, "Regulation of glycogen phosphorylase and PDH during exercise in human skeletal muscle during hypoxia," *American Journal of Physiology*, vol. 278, no. 3, pp. E522–E534, 2000.

[64] P. A. M. Michels, F. Bringaud, M. Herman, and V. Hannaert, "Metabolic functions of glycosomes in trypanosomatids," *Biochimica et Biophysica Acta*, vol. 1763, no. 12, pp. 1463–1477, 2006.

[65] F. R. Opperdoes and P. A. M. Michels, "Enzymes of carbohydrate metabolism as potential drug targets," *International Journal for Parasitology*, vol. 31, no. 5-6, pp. 481–489, 2001.

[66] L. Azema, S. Claustre, I. Alric, et al., "Interaction of substituted hexose analogues with the *Trypanosoma brucei* hexose transporter," *Biochemical Pharmacology*, vol. 67, no. 3, pp. 459–467, 2004.

[67] F. Lakhdar-Ghazal, C. Blonski, M. Willson, P. Michels, and J. Perie, "Glycolysis and proteases as targets for the design of new anti-trypanosome drugs," *Current Topics in Medicinal Chemistry*, vol. 2, no. 5, pp. 439–456, 2002.

[68] B. M. Bakker, H. V. Westerhoff, F. R. Opperdoes, and P. A. M. Michels, "Metabolic control analysis of glycolysis in trypanosomes as an approach to improve selectivity and effectiveness of drugs," *Molecular and Biochemical Parasitology*, vol. 106, no. **1**, pp. 1–10, 2000.

[69] A. H. Fairlamb and A. Cerami, "Metabolism and functions of trypanothione in the Kinetoplastida," *Annual Review of Microbiology*, vol. 46, pp. 695–729, 1992.

[70] S. Müller, E. Liebau, R. D. Walter, and R. L. Krauth-Siegel, "Thiol-based redox metabolism of protozoan parasites," *Trends in Parasitology*, vol. 19, no. 7, pp. 320–328, 2003.

[71] S. A. Le Quesne and A. H. Fairlamb, "Regulation of a high-affinity diamine transport system in *Trypanosoma cruzi* epimastigotes," *Biochemical Journal*, vol. 316, part 2, pp. 481–486, 1996.

[72] C. Dumas, M. Ouellette, J. Tovar, et al., "Disruption of the trypanothione reductase gene of *Leishmania* decreases its ability to survive oxidative stress in macrophages," *The EMBO Journal*, vol. 16, no. 10, pp. 2590–2598, 1997.

[73] J. Tovar, M. L. Cunningham, A. C. Smith, S. L. Croft, and A. H. Fairlamb, "Down-regulation of *Leishmania donovani* trypanothione reductase by heterologous expression of a trans-dominant mutant homologue: effect on parasite intracellular survival," *Proceedings of the National Academy of Sciences of the United States of America*, vol. 95, no. 9, pp. 5311–5316, 1998.

[74] J. Tovar, S. Wilkinson, J. C. Mottram, and A. H. Fairlamb, "Evidence that trypanothione reductase is an essential enzyme in *Leishmania* by targeted replacement of the *tryA* gene locus," *Molecular Microbiology*, vol. 29, no. 2, pp. 653–660, 1998.

[75] S. Krieger, W. Schwarz, M. R. Arlyanayagam, A. H. Fairlamb, R. L. Krauth-Siegel, and C. Clayton, "Trypanosomes lacking trypanothione reductase are avirulent and show increased sensitivity to oxidative stress," *Molecular Microbiology*, vol. 35, no. 3, pp. 542–552, 2000.

[76] J. M. Kelly, M. C. Taylor, K. Smith, K. J. Hunter, and A. H. Fairlamb, "Phenotype of recombinant *Leishmania donovani* and *Trypanosoma cruzi* which over-express trypanothione reductase. Sensitivity towards agents that are thought to induce oxidative stress," *European Journal of Biochemistry*, vol. 218, no. 1, pp. 29–37, 1993.

[77] M. A. Comini, S. A. Guerrero, S. Haile, U. Menge, H. Lünsdorf, and L. Flohé, "Validation of *Trypanosoma brucei* trypanothione synthetase as drug target," *Free Radical Biology and Medicine*, vol. 36, no. 10, pp. 1289–1302, 2004.

[78] M. R. Ariyanayagam, S. L. Oza, M. L. Guther, and A. H. Fairlamb, "Phenotypic analysis of trypanothione synthetase knockdown in the African trypanosome," *Biochemical Journal*, vol. 391, part 2, pp. 425–432, 2005.

[79] T. T. Huynh, V. T. Huynh, M. A. Harmon, and M. A. Phillips, "Gene knockdown of γ-glutamylcysteine synthetase by RNA_i in the parasitic protozoa *Trypanosoma brucei* demonstrates that it is an essential enzyme," *Journal of Biological Chemistry*, vol. 278, no. 41, pp. 39794–39800, 2003.

[80] C. Guimond, N. Trudel, C. Brochu, et al., "Modulation of gene expression in *Leishmania* drug resistant mutants as determined by targeted DNA microarrays," *Nucleic Acids Research*, vol. 31, no. 20, pp. 5886–5896, 2003.

[81] S. K. Shahi, R. L. Krauth-Siegel, and C. E. Clayton, "Overexpression of the putative thiol conjugate transporter *Tb*MRPA causes melarsoprol resistance in *Trypanosoma brucei*," *Molecular Microbiology*, vol. 43, no. 5, pp. 1129–1138, 2002.

[82] H. Kacser and J. A. Burns, "The control of flux," *Symposia of the Society for Experimental Biology*, vol. 27, pp. 65–104, 1973.

[83] H. Kacser and J. A. Burns, "Molecular democracy: who shares the controls?" *Biochemical Society Transactions*, vol. 7, no. 5, pp. 1149–1160, 1979.

[84] R. Heinrich, S. M. Rapoport, and T. A. Rapoport, "Metabolic regulation and mathematical models," *Progress in Biophysics and Molecular Biology*, vol. 32, pp. 1–82, 1978.

[85] T. A. Rapoport, R. Heinrich, G. Jacobasch, and S. Rapoport, "A linear steady state treatment of enzymatic chains. A mathematical model of glycolysis of human erythrocytes," *European Journal of Biochemistry*, vol. 42, no. 1, pp. 107–120, 1974.

[86] H. J. Flint, R. W. Tateson, I. B. Barthelmess, D. J. Porteous, W. D. Donachie, and H. Kacser, "Control of the flux in the arginine pathway of *Neurospora crassa*. Modulations of enzyme activity and concentration," *Biochemical Journal*, vol. 200, no. 2, pp. 231–246, 1981.

[87] N. S. Cohen, C.-W. Cheung, E. Sijuwade, and L. Raijman, "Kinetic properties of carbamoyl-phosphate synthase (ammonia) and ornithine carbamoyltransferase in permeabilized mitochondria," *Biochemical Journal*, vol. 282, part 1, pp. 173–180, 1992.

[88] S. G. Powers-Lee, R. A. Mastico, and M. Bendayan, "The interaction of rat liver carbamoyl phosphate synthetase and ornithine transcarbamoylase with inner mitochondrial membranes," *Journal of Biological Chemistry*, vol. 262, no. 32, pp. 15683–15688, 1987.

[89] R. J. Middleton and H. Kacser, "Enzyme variation, metabolic flux and fitness: alcohol dehydrogenase in *Drosophila melanogaster*," *Genetics*, vol. 105, no. 3, pp. 633–650, 1983.

[90] S. Rodríguez-Enríquez, M. E. Torres-Márquez, and R. Moreno-Sánchez, "Substrate oxidation and ATP sypply in AS-30D hepatoma cells," *Archives of Biochemistry and Biophysics*, vol. 375, no. 1, pp. 21–30, 2000.

[91] C. Garcia, J. P. Pardo, and R. Moreno-Sánchez, "Control of oxidative phosphorylation supported by NAD-linked substrates in rat brain mitochondria," *Biochemical Archives*, vol. 12, no. 3, pp. 157–176, 1996.

[92] F. N. Gellerich, W. S. Kunz, and R. Bohnensack, "Estimation of flux control coefficients from inhibitor titrations by non-linear regression," *FEBS Letters*, vol. 274, no. 1-2, pp. 167–170, 1990.

[93] R. Moreno-Sánchez, S. Devars, F. López-Gómez, A. Uribe, and N. Corona, "Distribution of control of oxidative phosphorylation in mitochondria oxidizing NAD-linked substrates," *Biochimica et Biophysica Acta*, vol. 1060, no. 3, pp. 284–292, 1991.

[94] R. Moreno-Sánchez, "Contribution of the translocator of adenine nucleotides and the ATP synthase to the control of oxidative phosphorylation and arsenylation in liver mitochondria," *Journal of Biological Chemistry*, vol. 260, no. 23, pp. 12554–12560, 1985.

[95] R. Rossignol, T. Letellier, M. Malgat, C. Rocher, and J.-P. Mazat, "Tissue variation in the control of oxidative phosphorylation: implication for mitochondrial diseases," *Biochemical Journal*, vol. 347, part 1, pp. 45–53, 2000.

[96] F. J. López-Gómez, M. E. Torres-Márquez, and R. Moreno-Sánchez, "Control of oxidative phosphorylation in AS-30D hepatoma mitochondria," *International Journal of Biochemistry*, vol. 25, no. 3, pp. 373–377, 1993.

[97] E. Wisniewski, W. S. Kunz, and F. N. Gellerich, "Phosphate affects the distribution of flux control among the enzymes of oxidative phosphorylation in rat skeletal muscle

mitochondria," *Journal of Biological Chemistry*, vol. 268, no. 13, pp. 9343–9346, 1993.

[98] T. Latsis, B. Andersen, and L. Agius, "Diverse effects of two allosteric inhibitors on the phosphorylation state of glycogen phosphorylase in hepatocytes," *Biochemical Journal*, vol. 368, part 1, pp. 309–316, 2002.

[99] S. A. Gupte, M. Arshad, S. Viola, et al., "Pentose phosphate pathway coordinates multiple redox-controlled relaxing mechanisms in bovine coronary arteries," *American Journal of Physiology*, vol. 285, no. 6, pp. H2316–H2326, 2003.

[100] D. C. Wallace, "Mitochondrial diseases in man and mouse," *Science*, vol. 283, no. 5407, pp. 1482–1488, 1999.

[101] X. L. Zu and M. Guppy, "Cancer metabolismml: facts, fantasy, and fiction," *Biochemical and Biophysical Research Communications*, vol. 313, no. 3, pp. 459–465, 2004.

[102] M. Erecinska and F. Dagani, "Relationships between the neuronal sodium/potassium pump and energy metabolism. Effects of K^+, Na^+, and adenosine triphosphate in isolated brain synaptosomes," *Journal of General Physiology*, vol. 95, no. 4, pp. 591–616, 1990.

[103] G. C. Brown, P. L. Lakin-Thomas, and M. D. Brand, "Control of respiration and oxidative phosphorylation in isolated rat liver cells," *European Journal of Biochemistry*, vol. 192, no. 2, pp. 355–362, 1990.

[104] R. P. Hafner, G. C. Brown, and M. D. Brand, "Analysis of the control of respiration rate, phosphorylation rate, proton leak rate and protonmotive force in isolated mitochondria using the 'top-down' approach of metabolic control theory," *European Journal of Biochemistry*, vol. 188, no. 2, pp. 313–319, 1990.

[105] R. J. Wanders, A. K. Groen, C. W. van Roermund, and J. M. Tager, "Factors determining the relative contribution of the adenine-nucleotide translocator and the ADP-regenerating system to the control of oxidative phosphorylation in isolated rat-liver mitochondria," *European Journal of Biochemistry*, vol. 142, no. 2, pp. 417–424, 1984.

[106] A. K. Groen, C. W. T. van Roermund, R. C. Vervoorn, and J. M. Tager, "Control of gluconeogenesis in rat liver cells. Flux control coefficients of the enzymes in the gluconeogenic pathway in the absence and presence of glucagon," *Biochemical Journal*, vol. 237, part 2, pp. 379–389, 1986.

[107] A. Marín-Hernández, S. Rodríguez-Enríquez, P. A. Vital-González, et al., "Determining and understanding the control of glycolysis in fast-growth tumor cells: flux control by an over-expressed but strongly product-inhibited hexokinase," *FEBS Journal*, vol. 273, no. 9, pp. 1975–1988, 2006.

[108] A. L. Kruckeberg, H. E. Neuhaus, R. Feil, L. D. Gottlieb, and M. Stitt, "Decreased-activity mutants of phosphoglucose isomerase in the cytosol and chloroplast of *Clarkia xantiana*. Impact on mass-action ratios and fluxes to sucrose and starch, and estimation of flux control coefficients and elasticity coefficients," *Biochemical Journal*, vol. 261, part 2, pp. 457–467, 1989.

[109] P. A. Quant, D. Robin, P. Robin, J. Girard, and M. D. Brand, "A top-down control analysis in isolated rat liver mitochondria: can the 3-hydroxy-3-methylglutaryl-CoA pathway be rate-controlling for ketogenesis?" *Biochimica et Biophysica Acta*, vol. 1156, no. 2, pp. 135–143, 1993.

[110] D. A. Fell and K. Snell, "Control analysis of mammalian serine biosynthesis. Feedback inhibition of the final step," *Biochemical Journal*, vol. 256, part 1, pp. 97–101, 1988.

[111] C. Chassagnole, D. A. Fell, B. Rais, B. Kudla, and J.-P. Mazat, "Control of the threonine-synthesis pathway in *Escherichia coli*: a theoretical and experimental approach," *Biochemical Journal*, vol. 356, part 2, pp. 433–444, 2001.

[112] J. L. Galazzo and J. E. Bailey, "Fermentation pathway kinetics and metabolic flux control in suspended and immobilized *Saccharomyces cerevisiae*," *Enzyme and Microbial Technology*, vol. 12, no. 3, pp. 162–172, 1990.

[113] J. A. Diderich, B. Teusink, J. Valkier, et al., "Strategies to determine the extent of control exerted by glucose transport on glycolytic flux in the yeast *Saccharomyces bayanus*," *Microbiology*, vol. 145, no. 12, pp. 3447–3454, 1999.

[114] H. V. Westerhoff and D. Kahn, "Control involving metabolism and gene expression: the square-matrix method for modular decomposition," *Acta Biotheoretica*, vol. 41, no. 1-2, pp. 75–83, 1993.

[115] J. R. Chase, D. L. Rothman, and R. G. Shulman, "Flux control in the rat gastrocnemius glycogen synthesis pathway by in vivo 13C/31P NMR spectroscopy," *American Journal of Physiology*, vol. 280, no. 4, pp. E598–E607, 2001.

[116] P. De Atauri, D. Orrell, S. Ramsey, and H. Bolouri, "Is the regulation of galactose 1-phosphate tuned against gene expression noise?" *Biochemical Journal*, vol. 387, part 1, pp. 77–84, 2005.

[117] M. G. Poolman, H. E. Assmus, and D. A. Fell, "Applications of metabolic modelling to plant metabolism," *Journal of Experimental Botany*, vol. 55, no. 400, pp. 1177–1186, 2004.

[118] P. Mendes, "GEPASI: a software package for modelling the dynamics, steady states and control of biochemical and other systems," *Computer Applications in the Biosciences*, vol. 9, no. 5, pp. 563–571, 1993.

[119] A. Cornish-Bowden and J.-H. S. Hofmeyr, "MetaModel: a program for modelling and control analysis of metabolic pathways on the IBM PC and compatibles," *Computer Applications in the Biosciences*, vol. 7, no. 1, pp. 89–93, 1991.

[120] H. M. Sauro, "SCAMP: a general-purpose simulator and metabolic control analysis program," *Computer Applications in the Biosciences*, vol. 9, no. 4, pp. 441–450, 1993.

[121] H. M. Sauro, "JARNAC: a system for interactive metabolic analysis," in *Animating the Cellular Map*, J.-H. S. Hofmeyr, J. M. Rohwer, and J. L. Snoep, Eds., pp. 221–228, Stellenbosch University Press, Stellenbosch, South Africa, 2000.

[122] B. G. Olivier, J. M. Rohwer, and J.-H. S. Hofmeyr, "Modelling cellular systems with PySCeS," *Bioinformatics*, vol. 21, no. 4, pp. 560–561, 2005.

[123] B. Teusink, J. Passarge, C. A. Reijenga, et al., "Can yeast glycolysis be understood terms of vitro kinetics of the constituent enzymes? Testing biochemistry," *European Journal of Biochemistry*, vol. 267, no. 17, pp. 5313–5329, 2000.

[124] L. Pritchard and D. B. Kell, "Schemes of flux control in a model of *Saccharomyces cerevisiae* glycolysis," *European Journal of Biochemistry*, vol. 269, no. 16, pp. 3894–3904, 2002.

[125] B. M. Bakker, P. A. M. Michels, F. R. Opperdoes, and H. V. Westerhoff, "Glycolysis in bloodstream form *Trypanosoma brucei* can be understood in terms of the kinetics of the glycolytic enzymes," *Journal of Biological Chemistry*, vol. 272, no. 6, pp. 3207–3215, 1997.

[126] B. M. Bakker, P. A. M. Michels, F. R. Opperdoes, and H. V. Westerhoff, "What controls glycolysis in bloodstream form *Trypanosoma brucei*?" *Journal of Biological Chemistry*, vol. 274, no. 21, pp. 14551–14559, 1999.

[127] K. R. Albe and B. E. Wright, "Carbohydrate metabolism in *dictyostelium discoideumml*: II. Systems' analysis," *Journal of Theoretical Biology*, vol. 169, no. 3, pp. 243–251, 1994.

[128] J. M. Rohwer and F. C. Botha, "Analysis of sucrose accumulation in the sugar cane culm on the basis of in vitro

kinetic data," *Biochemical Journal*, vol. 358, part 2, pp. 437–445, 2001.

[129] G. R. Cronwright, J. M. Rohwer, and B. A. Prior, "Metabolic control analysis of glycerol synthesis in *Saccharomyces cerevisiae*," *Applied and Environmental Microbiology*, vol. 68, no. 9, pp. 4448–4456, 2002.

[130] J. Nielsen and H. S. Jorgensen, "Metabolic control analysis of the penicillin biosynthetic pathway in a high-yielding strain of *Penicillium chrysogenum*," *Biotechnology Progress*, vol. 11, no. 3, pp. 299–305, 1995.

[131] M. G. Poolman, D. A. Fell, and S. Thomas, "Modelling photosynthesis and its control," *Journal of Experimental Botany*, vol. 51, pp. 319–328, 2000.

[132] Q. Hua, C. Yang, and K. Shimizu, "Metabolic control analysis for lysine synthesis using *Corynebacterium glutamicum* and experimental verification," *Journal of Bioscience and Bioengineering*, vol. 90, no. 2, pp. 184–192, 2000.

[133] H. A. Berthon, P. W. Kuchel, and P. F. Nixon, "High control coefficient of transketolase in the nonoxidative pentose phosphate pathway of human erythrocytes: NMR, antibody, and computer simulation studies," *Biochemistry*, vol. 31, no. 51, pp. 12792–12798, 1992.

[134] M. J. L. de Groot, W. Prathumpai, J. Visser, and G. J. G. Ruijter, "Metabolic control analysis of *Aspergillus niger* L-arabinose catabolism," *Biotechnology Progress*, vol. 21, no. 6, pp. 1610–1616, 2005.

[135] M. H. N. Hoefnagel, M. J. C. Starrenburg, D. E. Martens, et al., "Metabolic engineering of lactic acid bacteria, the combined approach: kinetic modelling, metabolic control and experimental analysis," *Microbiology*, vol. 148, no. 4, pp. 1003–1013, 2002.

[136] D. G. Mendoza-Cózatl and R. Moreno-Sánchez, "Control of glutathione and phytochelatin synthesis under cadmium stress. Pathway modeling for plants," *Journal of Theoretical Biology*, vol. 238, no. 4, pp. 919–936, 2006.

[137] A. Meister, "Glutathione synthesis," in *The Enzymes*, P. D. Boyer, Ed., vol. 10, pp. 671–697, Academic Press, New York, NY, USA, 1994.

[138] D. M. Speiser, S. L. Abrahamson, G. Banuelos, and D. W. Ow, "*Brassica juncea* produces a phytochelatin-cadmium-sulfide complex," *Plant Physiology*, vol. 99, no. 3, pp. 817–821, 1992.

[139] W. J. G. Vande and D. W. Ow, "Accumulation of metal-binding peptides in fission yeast requires *hmt2*$^{+}$," *Molecular Microbiology*, vol. 42, no. 1, pp. 29–36, 2001.

[140] J. R. Small and H. Kacser, "Responses of metabolic systems to large changes in enzyme activities and effectors. 1. The linear treatment of unbranched chains," *European Journal of Biochemistry*, vol. 213, no. 1, pp. 613–624, 1993.

[141] R. E. Reeves, "Metabolism of *Entamoeba histolytica* Schaudinn, 1903," *Advances in Parasitology*, vol. 23, pp. 105–142, 1984.

[142] E. Saavedra, A. Marín-Hernández, R. Encalada, A. Olivos, G. Mendoza-Hernández, and R. Moreno-Sánchez, "Kinetic modeling can describe in vivo glycolysis in *Entamoeba histolytica*," *FEBS Journal*, vol. 274, no. 18, pp. 4922–4940, 2007.

[143] E. Saavedra, R. Encalada, E. Pineda, R. Jasso-Chávez, and R. Moreno-Sánchez, "Glycolysis in *Entamoeba histolytica*: biochemical characterization of recombinant glycolytic enzymes and flux control analysis," *FEBS Journal*, vol. 272, no. 7, pp. 1767–1783, 2005.

[144] N. V. Torres, R. Souto, and E. Meléndez-Hevia, "Study of the flux and transition time control coefficient profiles in a metabolic system in vitro and the effect of an external stimulator," *Biochemical Journal*, vol. 260, part 3, pp. 763–769, 1989.

[145] C. Giersch, "Determining elasticities from multiple measurements of flux rates and metabolite concentrations. Application of the multiple modulation mehod to a reconstituted pathway," *European Journal of Biochemistry*, vol. 227, no. 1-2, pp. 194–201, 1995.

[146] R. Moreno-Sánchez, R. Encalada, A. Marín-Hernández, and E. Saavedra, "Experimental validation of metabolic pathway modeling. An illustration with glycolytic segments from *Entamoeba histolytica*," *FEBS Journal*, vol. 275, no. 13, pp. 3454–3469, 2008.

[147] J. Kurreck, "Antisense technologies: improvement through novel chemical modifications," *European Journal of Biochemistry*, vol. 270, no. 8, pp. 1628–1644, 2003.

[148] M. Stitt, W. P. Quick, U. Schurr, E.-D. Schulze, S. R. Rodermel, and L. Bogorad, "Decreased ribulose-1,5-bisphosphate carboxylase-oxygenase in transgenic tobacco transformed with 'antisense' *rbcS* II. Flux-control coefficients for photosynthesis in varying light, Co_2, and air humidity," *Planta*, vol. 183, no. 4, pp. 555–566, 1991.

[149] M.-A. Albert, J. R. Haanstra, V. Hannaert, et al., "Experimental and *in silico* analyses of glycolytic flux control in bloodstream form *Trypanosoma brucei*," *Journal of Biological Chemistry*, vol. 280, no. 31, pp. 28306–28315, 2005.

[150] S. Aiston, K. Y. Trinh, A. J. Lange, C. B. Newgard, and L. Agius, "Glucose-6-phosphatase overexpression lowers glucose 6-phosphate and inhibits glycogen synthesis and glycolysis in hepatocytes without affecting glucokinase translocation," *Journal of Biological Chemistry*, vol. 274, no. 35, pp. 24559–24566, 1999.

[151] B. J. Koebmann, J. Tornøe, B. Johansson, and P. R. Jensen, "Experimental modulation of gene expression," in *Metabolic Engineering in the Post Genomic Era*, B. N. Kholodenko and H. V. Westerhoff, Eds., pp. 155–179, Horizon Bioscience, Norfolk, UK, 2004.

[152] K. Hammer, I. Mijakovic, and P. R. Jensen, "Synthetic promoter libraries—tuning of gene expression," *Trends in Biotechnology*, vol. 24, no. 2, pp. 53–55, 2006.

[153] P. R. Jensen and K. Hammer, "The sequence of spacers between the consensus sequences modulates the strength of prokaryotic promoters," *Applied and Environmental Microbiology*, vol. 64, no. 1, pp. 82–87, 1998.

The International Journal of Biochemistry & Cell Biology 42 (2010) 1744–1751

Contents lists available at ScienceDirect

The International Journal of Biochemistry & Cell Biology

journal homepage: www.elsevier.com/locate/biocel

Oxidative phosphorylation is impaired by prolonged hypoxia in breast and possibly in cervix carcinoma

Sara Rodríguez-Enríquez[a,*], Liliana Carreño-Fuentes[a], Juan Carlos Gallardo-Pérez[a], Emma Saavedra[a], Héctor Quezada[a], Alicia Vega[b], Alvaro Marín-Hernández[a], Viridiana Olín-Sandoval[a], M. Eugenia Torres-Márquez[b], Rafael Moreno-Sánchez[a]

[a] Departamento de Bioquímica, Instituto Nacional de Cardiología Ignacio Chávez, México D.F. 14080, Mexico
[b] Departamento de Bioquímica, Facultad de Medicina, UNAM, México D.F. 04510, Mexico

ARTICLE INFO

Article history:
Received 26 March 2010
Received in revised form 18 June 2010
Accepted 12 July 2010
Available online 21 July 2010

Keywords:
Glycolysis
Hypoxia
Mitochondria
Oxidative phosphorylation
Breast cancer

ABSTRACT

It has been assumed that oxidative phosphorylation (OxPhos) in solid tumors is severely reduced due to cytochrome *c* oxidase substrate restriction, although the measured extracellular oxygen concentration in hypoxic areas seems not limiting for this activity. To identify alternative hypoxia-induced OxPhos depressing mechanisms, an integral analysis of transcription, translation, enzyme activities and pathway fluxes was performed on glycolysis and OxPhos in HeLa and MCF-7 carcinomas. In both neoplasias exposed to hypoxia, an early transcriptional response was observed after 8 h (two times increased glycolysis-related mRNA synthesis promoted by increased HIF-1α levels). However, major metabolic remodeling was observed only after 24 h hypoxia: increased glycolytic protein content (1–5-times), enzyme activities (2-times) and fluxes (4–6-times). Interestingly, in MCF-7 cells, 24 h hypoxia decreased OxPhos flux (4–6-fold), and 2-oxoglutarate dehydrogenase and glutaminase activities (3-fold), with no changes in respiratory complexes I and IV activities. In contrast, 24 h hypoxia did not significantly affect HeLa OxPhos flux; neither mitochondria related mRNAs, protein contents or enzyme activities, although the enhanced glycolysis became the main ATP supplier. Thus, prolonged hypoxia (a) targeted some mitochondrial enzymes in MCF-7 but not in HeLa cells, and (b) induced a transition from mitochondrial towards a glycolytic-dependent energy metabolism in both MCF-7 and HeLa carcinomas.

1. Introduction

For growth, solid tumors have developed strategies to maintain the carbon source and oxygen supplies. Thus, tumors exhibit an active angiogenesis which, however, is highly inefficient generating chaotic networks, with unorganized, fragile, and leaky new vessels (reviewed by Nagy et al., 2009). In consequence, the dynamics of the blood flow is affected, leading to hypoxic regions at 100–200 μm away from a functional blood supply (Vaupel et al., 1989; Helmlinger et al., 1997; Nagy et al., 2009).

It has been determined that the oxygen concentration inside well-oxygenated areas of several carcinomas ranges from 30 to 80 mm Hg whereas in their hypoxic regions, it may reach a value of 2.5–10 mm Hg (equivalent to 3–13 μM O_2, calculated by Horan and Koch, 2001) (Kallinowski et al., 1989; Vaupel et al., 1991; Hunjan et al., 1998; Erickson et al., 2003). The development of hypoxic regions in solid tumors is a typical characteristic linked to malignant phenotype, metastasis, chemo-, immuno- and radio-therapy resistance, high genetic instability and apoptosis tolerance (Graeber et al., 1996; Bristow and Hill, 2008). Some of these processes are modulated by HIF-1α, a key transcriptional factor that regulates the gene transcription of proteins involved in angiogenesis, cellular proliferation, erythropoietic and vascularization pathways (Weidemann and Johnson, 2008), allowing tissues to adjust to scarce oxygen availability. At metabolic level, HIF-1α increases the gene transcription of specific isoenzymes of almost all glycolytic enzymes and transporters (reviewed in Marín-Hernández et al., 2009); in consequence, the glycolytic flux increases by at least 2-times in the majority of neoplasias (Altenberg and Greulich, 2004; Walenta et al., 2004).

In spite of the hypoxic-glycolytic activation, the tumor intracellular ATP pool drastically diminishes (30–60%) whereas phosphate augments (Mueller-Klieser et al., 1990; Heerlein et al., 2005;

Abbreviations: COX, cytochrome c oxidase; HIF-1α, hypoxia-inducible factor 1α; HK, hexokinase; GA, glutaminase; OxPhos, oxidative phosphorylation; PDH, pyruvate dehydrogenase complex; PDK1, pyruvate dehydrogenase kinase-1; 2-OGDH, 2-oxoglutarate dehydrogenase.

* Corresponding author at: Departamento de Bioquímica, Instituto Nacional de Cardiología, Juan Badiano No. 1, Col. Sección 16, Tlalpan, México D.F. 14080, Mexico. Tel.: +52 55 55 73 29 11.
E-mail address: saren960104@hotmail.com (S. Rodríguez-Enríquez).

1357-2725/$ – see front matter © 2010 Elsevier Ltd. All rights reserved.
doi:10.1016/j.biocel.2010.07.010

Journal of Hazardous Materials 193 (2011) 216–224

Contents lists available at ScienceDirect

Journal of Hazardous Materials

journal homepage: www.elsevier.com/locate/jhazmat

Removal, accumulation and resistance to chromium in heterotrophic *Euglena gracilis*

Elizabeth Lira-Silva, Itzumi S. Ramírez-Lima, Viridiana Olín-Sandoval, Jorge D. García-García, Rodolfo García-Contreras, Rafael Moreno-Sánchez, Ricardo Jasso-Chávez*

Departamento de Bioquímica, Instituto Nacional de Cardiología, Juan Badiano # 1, Sección XVI, Tlalpan, México D.F. 14080, Mexico

ARTICLE INFO

Article history:
Received 25 January 2011
Received in revised form 16 June 2011
Accepted 13 July 2011
Available online 23 July 2011

Keywords:
Chromium transport and accumulation
Malate secretion
Chromate reductase
Cr(III) toxicity
Thiol-molecules

ABSTRACT

The removal, uptake and toxicity of chromium in *Euglena gracilis* cultured in absence and presence of malate with Cr(VI) or Cr(III) was evaluated. The malate extrusion and the extra- and intracellular Cr(VI) reduction capacity were determined and the contents of molecules with thiol group and ascorbate were also evaluated. Absence of malate in the medium decreased cell growth, increased Cr(III) toxicity, induced faster Cr(VI) disappearance from medium, and increased intracellular and intramitochondrial chromium accumulation. Both chromium species induced soluble and particulate ascorbate-dependent chromate reductase activities. Cells also secreted large amounts of malate and increased intracellular contents of thiol-molecules to bind extracellular and intracellular Cr(III), respectively. The former process was supported by significant increase in malate-producing enzyme activities and the assessment of the Cr-complexes indicated the *in situ* formation with thiol-molecules. The present results establish new paradigms regarding chromium stress on algae-like microorganisms: (i) Cr(III) may be more toxic than Cr(VI), depending on the culture (or environmental) conditions; (ii) several simultaneous mechanisms are turned on to inactivate chromium species and their toxic effects. These mechanisms, now well understood may further optimize, by genetically modifying *E. gracilis*, and facilitate the development of strategies for using this protist as potential bio-remediator of chromium-polluted water systems.

1. Introduction

It is well documented that most organisms are susceptible to heavy metals exposure, affecting their growth, development, and morphology [1]. However, some plants, bacteria and microalgae species are able to survive in heavy metal polluted environments by means of internal and/or external detoxification mechanisms such as: (1) diminished uptake; (2) internal binding; (3) biotransformation; (4) compartmentalization; and (5) external chelation [2,3]. Nevertheless, during acute insult or long time exposure, these mechanisms may not suffice to avoid or neutralize the toxic effects of heavy metals.

Cr(III) and Cr(VI) discharges in wastewaters mainly originates from metal and tanning/painting industries, respectively [1,4]. In Mexico, the total chromium concentration reported in waste and ground water bodies near to industrial, mining and tannery industrial activities ranges from 1–5 μM up to 1 mM [5,6], values that are much higher than permissible. In consequence, at these elevated chromium levels, high toxicity in algae [7] and zooplankton [8] is observed.

Conventional methods for treatment of toxic chromium waste require large amounts of chemicals and energy and are unsuitable for small-scale leather, dye, and electroplating units [9]. Therefore, biotransformation of Cr(VI) to the putative less-toxic Cr(III) by biological agents offers a viable alternative, in particular for developing processes for Cr(VI) polluted water detoxification with bacterial strains [10,11], which has been considered economical, safe and sustainable [12].

The free-living flagellated protist *Euglena gracilis* belongs to a select group of organisms with a proven capacity to resist and accumulate heavy metals [3]. Indeed, *E. gracilis* is able to tolerate high concentrations of cadmium, zinc, lead, mercury and chromium. Cadmium is accumulated and compartmentalized into chloroplasts and mitochondria [13–16]. The increased synthesis of heavy metal-chelating molecules with thiol groups such as Cys, γEC, GSH and phytochelatins, together with the metal compartmentalization into

Abbreviations: AAS, atomic absorption spectrometry; BSA, bovine serum albumin; Cys, cysteine; DFC, diphenyl-carbazide; DTNB, 5,5′-dithiobis(2-nitrobenzoic acid; γEC, γ-glutamyl-cysteine; GSH, glutathione; NAD^+-LDH, soluble lactate dehydrogenase; MDH, NAD^+-malate dehydrogenase; ME, $NADP^+$-malic enzyme; MS, malate synthase; PCA, perchloric acid; $Trp(SH_2)$, reduced trypanothione.

* Corresponding author. Tel.: +52 55 5573 2911; fax: +52 55 5573 0994.
E-mail address: rjass_cardiol@yahoo.com.mx (R. Jasso-Chávez).

0304-3894/$ – see front matter © 2011 Elsevier B.V. All rights reserved.
doi:10.1016/j.jhazmat.2011.07.056